WAVE-INDUCED TORQUE INSIDE THE SURF ZONE

BY

SERGIO ALEJANDRO SCHMIDT

A DISSERTATION PRESENTED TO THE GRADUATE SCHOOL
OF THE UNIVERSITY OF FLORIDA
IN PARTIAL FULFILLMENT OF THE REQUIREMENTS FOR
THE DEGREE OF DOCTOR OF PHILOSOPHY

UNIVERSITY OF FLORIDA

1985

Dedicated with love and gratitude
to my wife, Marisa, for her
continued faith and encouragement
over the years and to all members
of my family for always setting
higher standards in life.

ACKNOWLEDGEMENTS

The author would like to thank Dr. Robert G. Dean for his continued guidance and encouragement and for many stimulating discussions relative to this dissertation.

The author also wishes to express his thanks to the Consejo Nacional de Investigaciones Científicas y Técnicas de la República Argentina and the University of Florida for funding his studies.

Finally, the author thanks his friend, Claudio, for his encouragement and friendship.

TABLE OF CONTENTS

	Page
ACKNOWLEDGEMENTS	iii
LIST OF TABLES	vii
LIST OF FIGURES	xxviii
NOTATIONS	xxxiii
ABSTRACT	xl
CHAPTERS	
1 INTRODUCTION	1
2 GOVERNING EQUATIONS	5
Depth Integrated and Time Averaged Momentum and Continuity Equations	7
Vertical Vorticity Distribution	10
Comparison between the Applied Longshore Thrust and Applied Torque Inside the Surf Zone	11
3 MODEL DESIGN	14
4 DATA AQUISITION	20
Introduction	20
Wave Height Measurements	21
Vorticity Measurements	23
Mean Current Measurements	27
5 DATA ANALYSIS AND DISCUSSION	31
Wave Height	31
Introduction	31
Wave Stabilization Time	32
Wave Height Distribution	32

Page

Vorticity 39

Introduction 39
General Description of the Data, Types of Curves, Classification and Associated Forces 44
Mean Vorticity 47
Diffusion of Vorticity Inside the Breaker Zone 58
Estimation of Vorticity Inside the Water Surface 68

Total Wave-Applied Torque Computed from Early Measurements of the Angle of Rotation of the Mill 74
Mean Currents 75

Introduction 75
Characteristics of the Mean Current Pattern 80

Total Frictional Torque Applied to the Bottom Computed from Mean Current Measurements 80
Comparison Between the Steady State Vorticity Computed from Early Measurements of the Angle of Rotation, θ_m, of the Mill, and the Steady State Vorticity Computed from Measurements of the Mean Currents 92

6 COMPARISON WITH THEORY 95

Introduction 95
Analytical Representation of the Bathymetry 95
Refraction 96
Theoretical Wave-Applied Torque Inside the Surf Zone 100
Wave Set-Up Distribution 108
Computed and Predicted Friction Coefficient 115

7 CONCLUSIONS AND RECOMMENDATIONS 117

APPENDICES

A WAVE HEIGHT DATA 124

B VORTICITY DATA 128

Page

C MEAN CURRENT DATA ..... [illegible]

D "VORTICITY METER".STATIC AND DYNAMICAL CONSIDERATIONS· EXPERIMENTS AND THEORY ..... [illegible]

Introduction . ..... [illegible]
Net Rotation of the Mill under a Static Load An Experiment 333
Some Dynamical Considerations about the Mill 339
Estimation of the Angle of Rotation of the Mill under a Wave Field 341
Theoretical Considerations 348

BIBLIOGRAPHY 363

BIOGRAPHICAL SKETCH 365

LIST OF TABLES

[illegible]	Bathymetry of the Model	17
5-1	Wave Stabilization Time (ts)	32
5-2	Types of Curves: Frequency of Occurrence	46
5-3	Angle of Rotation θ_m Measurement Runs	58
5-4	Mean Vorticity Analysis Results; Period - 1.0 s	61
5-5	Mean Vorticity Analysis Results; Period = 1.5 s	62
5-6	Mean Vorticity Analysis Results; Period = 1.9 s	63
5-7	Values of the Torque, Ti, and the Viscosity, ν, Determined from Measurements of the Time-Dependent Angle of Rotation θ_m	69
5-8	Measurements of the Angle of Rotation θ_m at the Water Surface: Location and Number of Runs per Experiment	72
5-9	Results of Experiment A: Vorticity at the Water Surface (ω_s) and at the Bottom (ω_b) for x = 2.74 m, y = 0.61 m	73
5-10	Results of Experiment B: Vorticity at the Water Surface (ω_s) and at the Bottom (ω_b) for x = 3.35 m, y = 0.46 m	73
5-11	Values of the Total Wave-Applied Torque, $(WT)_m$, from Measurements of the Angle of Rotation, θ_m, of the Mill	75
5-12	Mean Currents. Run and Number of Disks per Run	79

Table		Page
5-13	Values of ψ_o Obtained from Current Measurements Shown in Figure 5-20; Period = 1.5 s; L_x = 3.69 m and L_y = 1.52 m	89
5-14	Values of ψ_o Obtained from Current Measurements Shown in Figure 5-21; Period = 1.9 s; L_x = 3.36 m and L_y = 1.52 m	90
5-15	Values of the Total Frictional Torque Applied to the Bottom, FT, Calculated from Current Measurements	92
5-16	Values of the Steady State Mean Vorticities, $\bar{\omega}_s$, $\bar{\omega}_f$ and $\bar{\omega}_y$ for Those Runs Where the Friction Coefficient, A_3, Was Calculated	94
6-1	Idealized Bathymetry	96
6-2	Values of $(WT)_m$, FT and $(WT)_p$ for the Periods Considered	108
A-1	Wave Height Distribution in cm; Wave Period = 1.0 s	124
A-2	Wave Height Distribution in cm; Wave Period = 1.5 s	125
A-3	Wave Height Distribution in cm, Wave Period = 1.9 s	126
B-1	Angle of Rotation θ_m Versus Time; Run No. 40; Depth = 2.5 cm; Period = 1.0 s, Location: x = 2.29 m; y = 0.30 m	128
B-2	Angle of Rotation θ_m Versus Time, Run No. 41, Depth = 2.5 cm, Period = 1.0 s; Location: x = 2.29 m; y = 0.76 m	129
B-3	Angle of Rotation θ_m Versus Time; Run No. 44; Depth = 2.9 cm; Period = 1.0 s, Location: x = 2.59 m, y = 0.15 m	130
B-4	Angle of Rotation θ_m Versus Time; Run No. 43, Depth = 3.0 cm; Period = 1.0 s; Location: x = 2.59 m; y = 0.46 m	131

Table | Page

B-5 Angle of Rotation θ_m Versus Time; Run No. 42; Depth = 3.2 cm; Period = 1.0 s; Location: x = 2.59 m; y = 0.76 m 132

B-6 Angle of Rotation θ_m Versus Time; Run No. 45; Depth = 3.0 cm; Period = 1.0 s; Location: x = 2.90 m; y = 0.15 m 133

B-7 Angle of Rotation θ_m Versus Time; Run No. 47; Depth = 3.7 cm; Period = 1.0 s; Location: x = 2.90 m; y = 0.15 m 134

B-8 Angle of Rotation θ_m Versus Time; Run No. 49; Depth = 4.1 cm; Period = 1.0 s; Location: x = 2.90 m; y = 1.37 m 135

B-9 Angle of Rotation θ_m Versus Time; Run No. 54; Depth = 4.1 cm; Period = 1.0 s; Location: x = 3.20 m; y = 0.15 m 136

B-10 Angle of Rotation θ_m Versus Time; Run No. 53; Depth = 3.5 cm; Period = 1.0 s; Location: x = 3.20 m; y = 0.46 m 137

B-11 Angle of Rotation θ_m Versus Time; Run No. 52; Depth = 3.5 cm; Period = 1.0 s; Location: x = 3.20 m; y = 0.76 m 138

B-12 Angle of Rotation θ_m Versus Time. Run No. 51; Depth = 4.6 cm; Period = 1.0 s; Location: x = 3.20 m; y = 1.07 m 139

B-13 Angle of Rotation θ_m Versus Time; Run No. 55; Depth = 3.1 cm; Period = 1.0 s; Location: x = 3.51 m; y = 0.15 m 140

B-14 Angle of Rotation θ_m Versus Time; Run No. 55b; Depth = 3.7 cm; Period = 1.0 s; Location: x = 3.51 m; y = 0.46 m 141

B-15 Angle of Rotation θ_m Versus Time; Run No. 56; Depth = 4.5 cm; Period = 1.0 s; Location: x = 3.51 m; y = 0.76 m 142

B-16 Angle of Rotation θ_m Versus Time; Run No. 56; Depth = 3.7 cm; Period = 1.0 s; Location: x = 3.81 m; y = 0.15 m 143

B-17 Angle of Rotation θ_m Versus Time; Run No. 92; Depth = 4.3 cm; Period = 1.0 s; Location: x = 3.81 m; y = 0.46 m 144

Table		Page
B-18	Angle of Rotation θ_m Versus Time; Run No. 93; Depth = 5.2 cm; Period = 1.0 s; Location: x = 3.81 m; y = 0.76 m	145
B-19	Angle of Rotation θ_m Versus Time; Run No. 57; Depth = 4.7 cm; Period = 1.0 s; Location: x = 4.11 m; y = 0.15 m	146
B-20	Angle of Rotation θ_m Versus Time; Run No. 90; Depth = 5.3 cm; Period = 1.0 s; Location: x = 4.11 m; y = 0.46 m	147
B-21	Angle of Rotation θ_m Versus Time; Run No. 89; Depth = 6.3 cm; Period = 1.0 s; Location: x = 4.42 m; y = 0.46 m	148
B-22	Angle of Rotation θ_m Versus Time; Run No. 33; Depth = 2.5 cm; Period = 1.5 s; Location: x = 2.29 m; y = 0.30 m	149
B-23	Angle of Rotation θ_m Versus Time; Run No. 15; Depth = 3.0 cm; Period = 1.5 s; Location: x = 2.59 m; y = 0.15 m	150
B-24	Angle of Rotation θ_m Versus Time; Run No. 12; Depth = 3.0 cm; Period = 1.5 s; Location: x = 2.59 m; y = 0.46 m	151
B-25	Angle of Rotation θ_m Versus Time; Run No. 14; Depth = 3.2 cm; Period = 1.5 s; Location: x = 2.59 m; y = 0.69 m	152
B-26	Angle of Rotation θ_m Versus Time; Run No. 162; Depth = 3.3 cm; Period = 1.5 s; Location: x = 2.59 m; y = 1.37 m	153
B-27	Angle of Rotation θ_m Versus Time; Run No. 1; Depth = 3.7 cm; Period = 1.5 s; Location: x = 2.82 m, y = 0.76 m	154
B-28	Angle of Rotation θ_m Versus Time. Run No. 16; Depth = 2.9 cm; Period = 1.5 s; Location: x = 2.82 m; y = 0.15 m	155
B-29	Angle of Rotation θ_m Versus Time. Run No. 11; Depth = 3.3 cm. Period = 1.5 s. Location: x = 2.90 m. y = 0.38 m	156
B-30	Angle of Rotation θ_m Versus Time. Run No. 30; Depth = 4.0 cm; Period = 1.5 s; Location. x = 2.90 m, y = 1.07 m	157

Table		Page
B-31	Angle of Rotation θ_m Versus Time; Run No. 22; Depth = 3.1 cm; Period = 1.5 s; Location: x = 3.20 m; y = 0.23 m	159
B-32	Angle of Rotation θ_m Versus Time. Run No. 13; Depth = 3.5 cm; Period = 1.5 s. Location: x = 3.20 m; y = 0.46 m	160
B-33	Angle of Rotation θ_m Versus Time; Run No. 160; Depth = 4.1 cm; Period = 1.5 s; Location: x = 3.20 m; y = 0.76 m	161
B-34	Angle of Rotation θ_m Versus Time; Run No. 2. Depth = 3.1 cm; Period = 1.5 s; Location: x = 3.43 m; y = 0.15 m	162
B-35	Angle of Rotation θ_m Versus Time. Run No. 157; Depth = 3.7 cm, Period = 1.5 s; Location: x = 3.51 m; y = 0.46 m	163
B-36	Angle of Rotation θ_m Versus Time; Run No. 156. Depth = 3.7 cm; Period = 1.5 s; Location: x = 3.51 m; y = 0.15 m	164
B-37	Angle of Rotation θ_m Versus Time; Run No. 200; Depth = 2.9 cm; Period = 1.9 s. Location: x = 2.59 m; y = 0.15 m	165
B-38	Angle of Rotation θ_m Versus Time; Run No. 201; Depth = 3.0 cm; Period = 1.9 s; Location: x = 2.59 m; y = 0.46 m	166
B-39	Angle of Rotation θ_m Versus Time; Run No. 209; Depth = 3.0 cm; Period = 1.9 s; Location: x = 2.90 m. y = 0.15 m	167
B-40	Angle of Rotation θ_m Versus Time; Run No. 208; Depth = 3.3 cm; Period = 1.9 s; Location: x = 2.90 m; y = 0.46 m	168
B-41	Angle of Rotation θ_m Versus Time; Run No. 210; Depth = 3.1 cm; Period = 1.9 s; Location: x = 3.20 m; y = 0.15 m	169
B-42	Angle of Rotation θ_m Versus Time; Run No. 219; Depth = 3.1 cm; Period = 1.9 s; Location: x = 3.51 m; y = 0.15 m	170

Table		Page
C-1	Mean Current Measurements by Floating Disk Trajectories, Run No. 41/01; Wave Period = 1.0 s; Wavemaker Starting Time = 10.5 s	172
C-2	Mean Current Measurements by Floating Disk Trajectories; Run No. 41/02; Wave Period = 1.0 s; Wavemaker Starting Time = 10.5 s	173
C-3	Mean Current Measurements by Floating Disk Trajectories; Run No. 41/03; Wave Period = 1.0 s; Wavemaker Starting Time = 10.5 s	174
C-4	Mean Current Measurements by Floating Disk Trajectories; Run No. 42/01; Wave Period = 1.0 s; Wavemaker Starting Time = 23.0 s	175
C-5	Mean Current Measurements by Floating Disk Trajectories; Run No. 42/02; Wave Period = 1.0 s; Wavemaker Starting Time = 23.0 s	176
C-6	Mean Current Measurements by Floating Disk Trajectories; Run No. 42/03; Wave Period = 1.0 s; Wavemaker Starting Time = 23.0 s	177
C-7	Mean Current Measurements by Floating Disk Trajectories; Run No. 43/01; Wave Period = 1.0 s; Wavemaker Starting Time = 16.2 s	178
C-8	Mean Current Measurements by Floating Disk Trajectories; Run No. 43/02; Wave Period = 1.0 s; Wavemaker Starting Time = 16.2 s	179
C-9	Mean Current Measurements by Floating Disk Trajectories; Run No. 43/03; Wave Period = 1.0 s; Wavemaker Starting Time = 16.2 s	180
C-10	Mean Current Measurements by Floating Disk Trajectories; Run No. 43/04; Wave Period = 1.0 s; Wavemaker Starting Time = 16.2 s	181

Table | Page

C-11 Mean Current Measurements by Floating Disk Trajectories; Run No. 43/05; Wave Period = 1.0 s; Wavemaker Starting Time = 16.2 s 182

C-12 Mean Current Measurements by Floating Disk Trajectories; Run No. 43/06; Wave Period = 1.0 s; Wavemaker Starting Time = 16.2 s 183

C-13 Mean Current Measurements by Floating Disk Trajectories, Run No. 44/01; Wave Period = 1.0 s, Wavemaker Starting Time = 29.5 s 184

C-14 Mean Current Measurements by Floating Disk Trajectories, Run No. 44/02; Wave Period = 1.0 s, Wavemaker Starting Time = 29.5 s 185

C-15 Mean Current Measurements by Floating Disk Trajectories; Run No. 44/03; Wave Period = 1.0 s, Wavemaker Starting Time = 29.5 s 186

C-16 Mean Current Measurements by Floating Disk Trajectories, Run No. 44/04; Wave Period = 1.0 s; Wavemaker Starting Time = 29.5 s 187

C-17 Mean Current Measurements by Floating Disk Trajectories; Run No. 44/05; Wave Period = 1.0 s; Wavemaker Starting Time = 29.5 s 188

C-18 Mean Current Measurements by Floating Disk Trajectories; Run No. 44/06; Wave Period = 1.0 s; Wavemaker Starting Time = 29.5 s 189

C-19 Mean Current Measurements by Floating Disk Trajectories; Run No. 45/01; Wave Period = 1.0 s; Wavemaker Starting Time = 15.4 s 190

C-20 Mean Current Measurements by Floating Disk Trajectories; Run No. 45/02, Wave Period = 1.0 s; Wavemaker Starting Time = 15.4 s 191

Table | Page

C-21 Mean Current Measuremeuts by Floating Disk Trajectories, Run No. 45/03, Wave Period = 1.0 s, Wavemaker Starting Time = 15.4 s 192

C-22 Mean Current Measurements by Floatiug Disk Trajectories· Ruu No. 45/04; Wave Period = i.0 s; Wavemaker Startiug Time - 15.4 s 193

C-23 Mean Current Measurements by Floatiug Disk Trajectories, Run No. 45/05; Wave Period = i.0 s; Wavemaker Starting Time = 15.4 s 194

C-24 Mean Current Measurements by Floating Disk Trajectories; Run No. 45/06; Wave Period = 1.0 s; Wavemaker Startiug Tiee = 15.4 s 195

C-25 Mean Current Measursments by Floatiug Disk Trajectories; Ruu No. 45/07; Wave Period = i.0 s; Wavemaker Startiug Time = i5.4 s 196

C-26 Mean Current Measurements by Floating Disk Trajectories; Run No. 45/08; Wave Period = i.0 s, Wavemaker Starting Time = 15.4 s 197

C-27 Mean Current Measurements by Floating Disk Trajectories; Ruu No. 30/0i; Wave Period = i.5 s; Wavemaker Startiug Tiee = 23.2 s 198

C-28 Meau Curreut Measurements by Floatiug Disk Trajectories; Ruu No. 30/02; Wave Period = i.5 s; Wavemaker Starting Time = 23.2 s 199

C-29 Mean Current Measurements by Floating Disk Trajectories; Run No. 30/03; Wave Period = 1.5 s; Wavemaker Starting Tiee = 23.2 s 200

C-30 Meau Currsnt Measurements by Floating Disk Trajectories, Ruu No. 30/04; Wave Period - 1.5 s; Wavemaker Startiug Time = 23.2 s 20i

Figure

Page

C-31 Mean Current Measurements by Floating Disk Trajectories; Run No. 30/05; Wave Period = 1.5 s; Wavemaker Starting Time = 23.2 s 203

C-32 Mean Current Measurements by Floating Disk Trajectories; Run No. 30/06; Wave Period = 1.5 s; Wavemaker Starting Time = 23.2 s 204

C-33 Mean Current Measurements by Floating Disk Trajectories, Run No. 30/07. Wave Period = 1.5 s; Wavemaker Starting Time = 23.2 s 205

C-34 Mean Current Measurements by Floating Disk Trajectories. Run No. 31/01; Wave Period = 1.5 s; Wavemaker Starting Time = 28.4 s 206

C-35 Mean Current Measurements by Floating Disk Trajectories; Run No. 31/02; Wave Period = 1.5 s; Wavemaker Starting Time = 28.4 s 208

C-36 Mean Current Measurements by Floating Disk Trajectories; Run No. 31/03. Wave Period = 1.5 s; Wavemaker Starting Time = 28.4 s 210

C-37 Mean Current Measurements by Floating Disk Trajectories; Run No. 31/04; Wave Period = 1.5 s; Wavemaker Starting Time = 28.4 s 212

C-38 Mean Current Measurements by Floating Disk Trajectories; Run No. 31/05; Wave Period = 1.5 s; Wavemaker Starting Time = 28.4 s 213

C-39 Mean Current Measurements by Floating Disk Trajectories, Run No. 31/06, Wave Period = 1.5 s; Wavemaker Starting Time = 28.4 s 215

C-40 Mean Current Measurements by Floating Disk Trajectories; Run No. 31/07; Wave Period = 1.5 s; Wavemaker Starting Time = 28.4 s 216

Table | Page

C-41 Mean Current Measurements by Floating Disk Trajectories, Run No. 32/01; Wave Period = 1.5 s; Wavemaker Starting Time = 22.0 s 217

C-42 Mean Current Measurements by Floating Disk Trajectories; Run No. 32/02; Wave Period = 1.5 s; Wavemaker Starting Time = 22.0 s 218

C-43 Mean Current Measurements by Floating Disk Trajectories; Run No. 32/03; Wave Period = 1.5 s; Wavemaker Starting Time = 22.0 s 219

C-44 Mean Current Measurements by Floating Disk Trajectories; Run No. 32/04; Wave Period = 1.5 s; Wavemaker Starting Time = 22.0 s 220

C-45 Mean Current Measurements by Floating Disk Trajectories; Run No. 32/05, Wave Period = 1.5 s, Wavemaker Starting Time = 22.0 s 221

C-46 Mean Current Measurements by Floating Disk Trajectories; Run No. 32/06; Wave Period = 1.5 s; Wavemaker Starting Time = 22.0 s 222

C-47 Mean Current Measurements by Floating Disk Trajectories; Run No. 32/07, Wave Period = 1.5 s; Wavemaker Starting Time = 22.0 s 223

C-48 Mean Current Measurements by Floating Disk Trajectories; Run No. 32/08; Wave Period = 1.5 s; Wavemaker Starting Time = 22.0 s 224

C-49 Mean Current Measurements by Floating Disk Trajectories; Run No. 33/01; Wave Period = 1.5 s; Wavemaker Starting Time = 24.0 s 225

C-50 Mean Current Measurements by Floating Disk Trajectories; Run No. 33/02; Wave Period = 1.5 s, Wavemaker Starting Time = 24.0 s 226

Page

C-51 Mean Current Measurements by Floating Disk Trajectories, Run No. 33/03; Wave Period = 1.5 s; Wavemaker Starting Time = 24.0 s 227

C-52 Mean Current Measurements by Floating Disk Trajectories; Run No. 33/04, Wave Period = 1.5 s, Wavemaker Starting Time = 24.0 s 228

C-53 Mean Current Measurements by Floating Disk Trajectories, Run No. 33/05; Wave Period = 1.5 s; Wavemaker Starting Time = 24.0 s 229

C-54 Mean Current Measurements by Floating Disk Trajectories; Run No. 33/06; Wave Period = 1.5 s; Wavemaker Starting Time = 24.0 s 230

C-55 Mean Current Measurements by Floating Disk Trajectories; Run No. 33/07; Wave Period = 1.5 s; Wavemaker Starting Time = 24.0 s 231

C-56 Mean Current Measurements by Floating Disk Trajectories; Run No. 33/08; Wave Period = 1.5 s; Wavemaker Starting Time = 24.0 s 232

C-57 Mean Current Measurements by Floating Disk Trajectories; Run No. 33/09; Wave Period = 1.5 s; Wavemaker Starting Time = 24.0 s 233

C-58 Mean Current Measurements by Floating Disk Trajectories; Run No. 34/01; Wave Period = 1.5 s; Wavemaker Starting Time = 25.8 s 234

C-59 Mean Current Measurements by Floating Disk Trajectories, Run No. 34/02; Wave Period = 1.5 s; Wavemaker Starting Time = 25.8 s 236

C-60 Mean Current Measurements by Floating Disk Trajectories; Run No. 34/03; Wave Period = 1.5 s; Wavemaker Starting Time = 25.8 s 237

Table		Page
C-61	Mean Current Measurements by Floating Disk Trajectories; Run No. 34/04; Wave Period = 1.5 s; Wavemaker Starting Time = 25.8 s	238
C-62	Mean Current Measurements by Floating Disk Trajectories; Run No. 34/05, Wave Period = 1.5 s; Wavemaker Starting Time = 25.8 s	239
C-63	Mean Current Measurements by Floating Disk Trajectories; Run No. 34/06; Wave Period = 1.5 s, Wavemaker Starting Time = 25.8 s	240
C-64	Mean Current Measurements by Floating Disk Trajectories; Run No. 34/07; Wave Period = 1.5 s, Wavemaker Starting Time = 25.8 s	241
C-65	Mean Current Measurements by Floating Disk Trajectories; Run No. 34/08; Wave Period = 1.5 s; Wavemaker Starting Time = 25.8 s	242
C-66	Mean Current Measurements by Floating Disk Trajectories; Run No. 34/09; Wave Period = 1.5 s; Wavemaker Starting Time = 25.8 s	243
C-67	Mean Current Measurements by Floating Disk Trajectories; Run No. 35/01, Wave Period = 1.5 s; Wavemaker Starting Time = 31.4 s	244
C-68	Mean Current Measurements by Floating Disk Trajectories; Run No. 35/02; Wave Period = 1.5 s; Wavemaker Starting Time = 31.4 s	245
C-69	Mean Current Measurements by Floating Disk Trajectories; Run No. 35/03; Wave Period = 1.5 s; Wavemaker Starting Time = 31.4 s	246
C-70	Mean Current Measurements by Floating Disk Trajectories; Run No. 35/04; Wave Period = 1.5 s; Wavemaker Starting Time = 31.4 s	247

Page

C-71 Mean Current Measurements by Floating Disk Trajectories, Run No. 35/05; Wave Period = 1.5 s; Wavemaker Starting Time = 31.4 s 248

C-72 Mean Current Measurements by Floating Disk Trajectories; Run No. 35/06; Wave Period = 1.5 s; Wavemaker Starting Time = 31.4 s 249

C-73 Mean Current Measurements by Floating Disk Trajectories; Run No. 01/01; Wave Period = 1.9 s; Wavemaker Starting Time = 20.9 s 250

C-74 Mean Current Measurements by Floating Disk Trajectories; Run No. 01/02; Wave Period = 1.9 s; Wavemaker Starting Time = 20.9 s 251

C-75 Mean Current Measurements by Floating Disk Trajectories; Run No. 01/03; Wave Period = 1.9 s; Wavemaker Starting Time = 20.9 s 253

C-76 Mean Current Measurements by Floating Disk Trajectories; Run No. 01/04; Wave Period = 1.9 s; Wavemaker Starting Time = 20.9 s 255

C-77 Mean Current Measurements by Floating Disk Trajectories; Run No. 01/05; Wave Period = 1.9 s; Wavemaker Starting Time = 20.9 s 256

C-78 Mean Current Measurements by Floating Disk Trajectories; Run No. 01/06; Wave Period = 1.9 s; Wavemaker Starting Time = 20.9 s 257

C-79 Mean Current Measurements by Floating Disk Trajectories; Run No. 01/07; Wave Period = 1.9 s; Wavemaker Starting Time = 20.9 s 258

C-80 Mean Current Measurements by Floating Disk Trajectories; Run No. 02/01; Wave Period = 1.9 s; Wavemaker Starting Time = 7.4 s 259

Table		Page
C-81	Mean Current Measurements by Floating Disk Trajectories, Run No. 02/02; Wave Period = 1.9 s; Wavemaker Starting Time = 7.4 s	260
C-82	Mean Current Measurements by Floating Disk Trajectories; Run No. 02/03; Wave Period = 1.9 s; Wavemaker Starting Time = 7.4 s	261
C-83	Mean Current Measurements by Floating Disk Trajectories, Run No. 02/04; Wave Period = 1.9 s; Wavemaker Starting Time = 7.4 s	262
C-84	Mean Current Measurements by Floating Disk Trajectories, Run No. 02/05, Wave Period = 1.9 s; Wavemaker Starting Time = 7.4 s	263
C-85	Mean Current Measurements by Floating Disk Trajectories; Run No. 02/06; Wave Period = 1.9 s; Wavemaker Starting Time = 7.4 s	264
C-86	Mean Current Measurements by Floating Disk Trajectories; Run No. 03/01; Wave Period = 1.9 s, Wavemaker Starting Time = 11.0 s	265
C-87	Mean Current Measurements by Floating Disk Trajectories; Run No. 03/02; Wave Period = 1.9 s; Wavemaker Starting Time = 11.0 s	266
C-88	Mean Current Measurements by Floating Disk Trajectories; Run No. 03/03; Wave Period = 1.9 s; Wavemaker Starting Time = 11.0 s	267
C-89	Mean Current Measurements by Floating Disk Trajectories; Run No. 03/04; Wave Period = 1.9 s, Wavemaker Starting Time = 11.0 s	268
C-90	Mean Current Measurements by Floating Disk Trajectories; Run No. 03/05; Wave Period = 1.9 s; Wavemaker Starting Time = 11.0 s	269

Table | Page

C-91 Mean Current Measurements by Floating Disk Trajectories; Run No. 03/06; Wave Period = 1.9 s; Wavemaker Starting Time = 11.0 s 270

C-92 Mean Current Measurements by Floating Disk Trajectories; Run No. 04/01; Wave Period = 1.9 s, Wavemaker Starting Time = 12.9 s 271

C-93 Mean Current Measurements by Floating Disk Trajectories, Run No. 04/02; Wave Period = 1.9 s, Wavemaker Starting Time = 12.9 s 272

C-94 Mean Current Measurements by Floating Disk Trajectories; Run No. 04/03; Wave Period = 1.9 s; Wavemaker Starting Time = 12.9 s 273

C-95 Mean Current Measurements by Floating Disk Trajectories; Run No. 04/04, Wave Period = 1.9 s, Wavemaker Starting Time = 12.9 s 274

C-96 Mean Current Measurements by Floating Disk Trajectories, Run No. 04/05; Wave Period = 1.9 s; Wavemaker Starting Time = 12.9 s 275

C-97 Mean Current Measurements by Floating Disk Trajectories; Run No. 04/06, Wave Period = 1.9 s; Wavemaker Starting Time = 12.9 s 276

C-98 Mean Current Measurements by Floating Disk Trajectories; Run No. 04/07; Wave Period = 1.9 s Wavemaker Starting Time = 12.9 s 277

C-99 Mean Current Measurements by Floating Disk Trajectories, Run No. 05/01; Wave Period = 1.9 s, Wavemaker Starting Time = 10.5 s 278

C-100 Mean Current Measurements by Floating Disk Trajectories; Run No. 05/02, Wave Period = 1.9 s, Wavemaker Starting Time = 10.5 s 279

Table		Page
C-101	Mean Current Measurements by Floating Disk Trajectories, Run No. 05/03; Wave Period = 1.9 s; Wavemaker Starting Time = 10.5 s	280
C-102	Mean Current Measurements by Floating Disk Trajectories; Run No. 05/04, Wave Period = 1.9 s, Wavemaker Starting Time = 10.5 s	281
C-103	Mean Current Measurements by Floating Disk Trajectories; Run No. 05/05; Wave Period = 1.9 s; Wavemaker Starting Time = 10.5 s	282
C-104	Mean Current Measurements by Floating Disk Trajectories; Run No. 05/06; Wave Period = 1.9 s; Wavemaker Starting Time = 10.5 s	284
C-105	Mean Current Measurements by Floating Disk Trajectories, Run No. 06/01; Wave Period = 1.9 s, Wavemaker Starting Time = 19.1 s	285
C-106	Mean Current Measurements by Floating Disk Trajectories; Run No. 06/02; Wave Period = 1.9 s; Wavemaker Starting Time = 19.1 s	286
C-107	Mean Current Measurements by Floating Disk Trajectories; Run No. 06/03; Wave Period = 1.9 s; Wavemaker Starting Time = 19.1 s	287
C-108	Mean Current Measurements by Floating Disk Trajectories, Run No. 06/04; Wave Period = 1.9 s; Wavemaker Starting Time = 19.1 s	288
C-109	Mean Current Measurements by Floating Disk Trajectories; Run No. 06/05, Wave Period = 1.9 s; Wavemaker Starting Time = 19.1 s	289
C-110	Mean Current Measurements by Floating Disk Trajectories; Run No. 06/06, Wave Period = 1.9 s; Wavemaker Starting Time = 19.1 s	290

Table | Page

C-111 Mean Current Measurements by Floating Disk Trajectories; Run No. 06/07; Wave Period = 1.9 s; Wavemaker Starting Time = 19.1 s 291

C-112 Mean Current Measurements by Floating Disk Trajectories, Run No. 06/08; Wave Period = 1.9 s; Wavemaker Starting Time = 19.1 s 292

C-113 Mean Current Measurements by Floating Disk Trajectories; Run No. 06/09; Wave Period = 1.9 s; Wavemaker Starting Time = 19.1 s 293

C-114 Mean Current Measurements by Floating Disk Trajectories; Run No. 07/01; Wave Period = 1.9 s; Wavemaker Starting Time = 25.8 s 294

C-115 Mean Current Measurements by Floating Disk Trajectories, Run No. 07/02; Wave Period = 1.9 s, Wavemaker Starting Time = 25.8 s 295

C-116 Mean Current Measurements by Floating Disk Trajectories, Run No. 07/03; Wave Period = 1.9 s; Wavemaker Starting Time = 25.8 s 296

C-117 Mean Current Measurements by Floating Disk Trajectories; Run No. 07/04, Wave Period = 1.9 s; Wavemaker Starting Time = 25.8 s 297

C-118 Mean Current Measurements by Floating Disk Trajectories; Run No. 07/05; Wave Period = 1.9 s; Wavemaker Starting Time = 25.8 s 298

C-119 Mean Current Measurements by Floating Disk Trajectories; Run No. 07/06; Wave Period = 1.9 s; Wavemaker Starting Time = 25.8 s 299

C-120 Mean Current Measurements by Floating Disk Trajectories, Run No. 07/07, Wave Period = 1.9 s, Wavemaker Starting Time = 25.8 s 300

Table		Page
C-121	Mean Current Measurements by Floating Disk Trajectories; Run No. 08/01; Wave Period = 1.9 s; Wavemaker Starting Time = 21.8 s	301
C-122	Mean Current Measurements by Floating Disk Trajectories; Run No. 08/02; Wave Period = 1.9 s; Wavemaker Starting Time = 21.8 s	302
C-123	Mean Current Measurements by Floating Disk Trajectories; Run No. 08/03; Wave Period = 1.9 s; Wavemaker Starting Time = 21.8 s	304
C-124	Mean Current Measurements by Floating Disk Trajectories; Run No. 08/04; Wave Period = 1.9 s; Wavemaker Starting Time = 21.8 s	306
C-125	Mean Current Measurements by Floating Disk Trajectories; Run No. 08/05; Wave Period = 1.9 s; Wavemaker Starting Time = 21.8 s	307
C-126	Mean Current Measurements by Floating Disk Trajectories; Run No. 09/01; Wave Period = 1.9 s; Wavemaker Starting Time = 15.7 s	308
C-127	Mean Current Measurements by Floating Disk Trajectories; Run No. 09/02; Wave Period = 1.9 s; Wavemaker Starting Time = 15.7 s	309
C-128	Mean Current Measurements by Floating Disk Trajectories; Run No. 09/03; Wave Period = 1.9 s; Wavemaker Starting Time = 15.7 s	310
C-129	Mean Current Measurements by Floating Disk Trajectories; Run No. 09/04; Wave Period = 1.9 s; Wavemaker Starting Time = 15.7 s	311
C-130	Mean Current Measurements by Floating Disk Trajectories; Run No. 09/05; Wave Period = 1.9 s; Wavemaker Starting Time = 15.7 s	312

Table | Page

C-131 Mean Current Measurements by Floating Disk Trajectories; Run No. 09/06; Wave Period = 1.9 s; Wavemaker Starting Time = 15.7 s 313

C-132 Mean Current Measurements by Floating Disk Trajectories; Run No. 09/07; Wave Period = 1.9 s; Wavemaker Starting Time = 15.7 s 314

C-133 Mean Current Measurements by Floating Disk Trajectories; Run No. 10/01; Wave Period = 1.9 s; Wavemaker Starting Time = 8.1 s 315

C-134 Mean Current Measurements by Floating Disk Trajectories, Run No. 10/02, Wave Period = 1.9 s; Wavemaker Starting Time = 8.1 s 316

C-135 Mean Current Measurements by Floating Disk Trajectories; Run No. 10/03; Wave Period = 1.9 s; Wavemaker Starting Time = 8.1 s 317

C-136 Mean Current Measurements by Floating Disk Trajectories; Run No. 10/04; Wave Period = 1.9 s; Wavemaker Starting Time = 8.1 s 318

C-137 Mean Current Measurements by Floating Disk Trajectories; Run No. 10/05; Wave Period = 1.9 s, Wavemaker Starting Time = 8.1 s 319

C-138 Mean Current Measurements by Floating Disk Trajectories, Run No. 11/01; Wave Period = 1.9 s, Wavemaker Starting Time = 8.1 s 320

C-139 Mean Current Measurements by Floating Disk Trajectories; Run No. 11/02; Wave Period = 1.9 s; Wavemaker Starting Time = 15.5 s 321

C-140 Mean Current Measurements by Floating Disk Trajectories; Run No. 11/03; Wave Period = 1.9 s; Wavemaker Starting Time = 15.5 s 322

Table | Page

C-141 Mean Current Measurements by Floating Disk Trajectories, Run No. 11/04; Wave Period = 1.9 s; Wavemaker Starting Time = 15.5 s 323

C-142 Mean Current Measurements by Floating Disk Trajectories; Run No. 12/01; Wave Period = 1.9 s, Wavemaker Starting Time = 11.0 s 324

C-143 Mean Current Measurements by Floating Disk Trajectories, Run No. 12/02; Wave Period = 1.9 s; Wavemaker Starting Time = 11.0 s 325

C-144 Mean Current Measurements by Floating Disk Trajectories; Run No. 12/03; Wave Period = 1.9 s; Wavemaker Starting Time = 11.0 s 326

C-145 Mean Current Measurements by Floating Disk Trajectories, Run No. 12/04, Wave Period = 1.9 s; Wavemaker Starting Time = 11.0 s 327

C-146 Mean Current Measurements by Floating Disk Trajectories; Run No. 12/05; Wave Period = 1.9 s; Wavemaker Starting Time = 11.0 s 328

C-147 Mean Current Measurements by Dye Release; Period = 1.5 s 329

C-148 Mean Current Measurements by Dye Release; Period = 1.9 s 330

D-1 Net Rotation of the Mill under a Static Load 337

D-2 Values of Ws/Pa and Mo 338

D-3 Angle of Rotation of the Mill θ_ℓ Versus Time As It Recovers Its Natural Position of Equilibrium 339

D-4 Angle of Rotation of the Mill θ under a Wave Field; Water Depth = 48.0 cm 342

D-5 Angle of Rotation of the Mill θ Versus Time Test No. 1 343

Table | Page

D-6 Angle of Rotation of the Mill θ Versus Time Test No. 3 343

D-7 Angle of Rotation of the Mill θ Versus Time Test No. 10 345

D-8 Angle of Rotation of the Mill θ Versus Time Test No. 13 345

D-9 Wave-Induced Torque for Cases Where No Continuous Rotation of the Mill Was Observed 347

LIST OF FIGURES

Figure		Page
2-1	Coordinate System	6
3-1	Lateral (a) and Top (b) View of the Model; Units in m	16
3-2	Bathymetry of the Model: Contours of Equal Depth in cm	19
4-1	"Capacitance Type" Wave Gage and Tripod	22
4-2	Lateral View of the Mill	24
4-3	Top View of the Mill	25
4-4	Video Camera, Tripod and Mill	26
4-5	Television Screen View During Reading Procedure	28
4-6	Top and Lateral View of the Disks Used to Measure Mean Currents	29
5-1	Wave Stabilization Time (ts): Example of the Calculation (a) Wave Record and (b) Wave Height Versus Time	34
5-2	Wave Stabilization Time (ts): Period - 1.0 s (a) Actual Record and (b) Wave Height Versus Time; Upper: Measurement No. 1 (x - 5.03 m, y - 0 m) ts - 6.0 s; Lower: Measurement No. 2 (x = 5.03 m, y = 0 m), ts = 5.5 s	35
5-3	Wave Stabilization Time (ts). Period - 1.5 s; (a) Actual Record and (b) Wave Height Versus Time; Upper: Measurement No. 1 (x - 5.03 m, y - 0 m), ts - 3.5 s; Lower. Measurement No. 2 (x - 5.03 m, y = 0 m), ts - 3.0 s	37

Figure Page

5-4 Wave Stabilization Time (ts): Period = 1.0 s; (a) Actual Record and (b) Wave Height Versus Time; Upper: Measurement No. 1 (x = 3.81 m, y = 1.07 m), ts = 3.8 s; Lower: Measurement No. 2 (x = 4.11 m, y = 0 m), ts = 2.8 s 38

5-5 Wave Height Measurements: Period = 1.0 s, Actual (•), H = γh (o) for γ = 0.78 40

5-6 Wave Height Measurements; Period = 1.5 s, Actual (•), H = γh (o) for γ = 0.78 41

5-7 Wave Height Measurements, Period = 1.9 s, Actual (•), H = γh (o) for γ = 0.78 42

5-8 Measure Wave Height (H) Versus Local Water (h) Depth Inside the Surf Zone 43

5-9 Angle of Rotation, θ_m, Versus Time. Types of Curves. (a) Type A: Run No. 99; Period = 1.0 s; Location: x = 4.42 m, y = 0.46 m; (b) Type B: Run No. 2; Period = 1.5 s; Location: x = 3.43 m, y = 0.15 m; (c) Type C: Run No. 15; Period = 1.9 s; Location: x = 2.59 m, y = 0.15 m 45

5-10 Angle of Rotation, θ_m, of the Mill Versus Time Corresponding to Run No. 13; Period = 1.5 s; Location: x = 3.20 m, y = 0.46 m; ta Indicates the Arrival Time of the First Broken Wave and ts is the Wave Stabilization Time 54

5-11 The Forcing Term, A_2, Versus Time and the Corresponding Mean Quadratic Error for Data Corresponding to Run No. 13; Period = 1.5 s; Location: x = 3.20 m, y = 0.46 m 55

5-12 Angle of Rotation, θ_m, of the Mill Measurement Stations: (a) Period = 1.0 s, (b) Period = 1.5 s and (c) Period = 1.9 s Inside the Figures the Run Numbers Are Indicated 60

5-13 Diffusion of Vorticity Inside the Surf Zone: Boundary Value Problem Sketch 65

Figure		Page
5-14	Nondimensional Vorticity Distribution over Depth Inside the Surf Zone	67
5-15	Correlation between the Mean Wave-Applied Torque, A_2, and the Wave-Applied Torque at the Water Surface, T1	70
5-16	Measurements of the Angle of Rotation, (a) Relative Position of the "Free" Mill (b) "Free" Mill Trajectory Inside the Surf Zone	71
5-17	Mean Current Measurements: Initial Locations of the Floating Disks; Period = 1.0 s; Each Run Includes All Disks with Common Symbol	76
5-18	Mean Current Measurements: Initial Locations of the Floating Disks; Period = 1.5 s, Run Includes All Disks with Each Common Symbol	77
5-19	Mean Current Measurements: Initial Locations of the Floating Disks; Period = 1.9 s; Each Run Includes All Disks with Common Symbol	78
5-20	Mean Current Measurements: Circulation Pattern: Period = 1.5 s; Floating Disk Trajectories (——) and Dye Release (---)	82
5-21	Mean Current Measurements: Circulation Pattern; Period = 1.9 s; Floating Disk Trajectories (——) and Dye Release (---)	84
5-22	Nondimensional Transport Stream Function, ψ/ψ_0	85
5-23	Mean Velocity Profile (x-component) at x = 2.67 m for a Period = 1.5 s: (——) Theory Based on Equation (5-24) for $\psi_0 = 1.04 \times 10^3$ cm^3/s and Measurement (o)	91
6-1	Idealized (——) and Actual (---) Bathymetry, Contours of Equal Depth in cm	97
6-2	Theoretical Local Wave Angle of Incidence α in Degrees	100

Figure | Page

6-3 Values Inside the Figures Indicate I and III Assuming Breaking Wave Conditions. Upper: Distribution of I Given by Equation (6-16) in $1/s^2$; Lower: Distribution (6-18) in $1/s^2$ 104

6-4 Values Inside the Figures Indicate IV and V Assuming Breaking Wave Conditions; Upper: Distribution of IV Given by Equation (6-19) in $1/s^2$; Lower: Distribution (6-20) in $1/s^2$ 105

6-5 Values Inside the Figures Indicate VI and VII Assuming Breaking Wave Conditions; Upper: Distribution of VI Given by Equation (6-21) in $1/s^2$; Lower: Distribution (6-22) in $1/s^2$ 106

6-6 Distribution of the Wave-Applied Torque (I + II + III + IV + V + VII) or Equation (6-23); Values Inside Indicate A_2 in $1/s^2$, Assuming Breaking Wave Condition 107

6-7 Wave Set-Up Distributions: A Qualitative Description; the Superscript (1) Indicates First Order Set-Up, Only a Function of x; the Superscript (2) Indicates the Contribution Due to the Bottom Undulations; Values of the Set-Up in m 114

D-1 Sketch of the Mill Inside the Glass Water Tank 334

D-2 Mill in Its Natural (No Extra Load) Position of Equilibrium; P Represents the Net Weight of the Mill 335

D-3 Mill in Its Equilibrium Position When Loaded with a Weight We 336

D-4 Angle of Rotation, θ_z, Versus Time as the Mill Recovers Its Position of Equilibrium 340

D-5 Angle of Rotation of the Mill, θ_m, Versus Time under the Effect of a Wave Field; Test No. 1; Wave Height = 4.0 cm; Period = 1.3 s; Depth = 48.0 cm; Depth of Measure = -15.0 cm 344

Figure

D-6 Angle of Rotation of the Mill, θ_m, Versus Time under the Effect of a Wave Field; Test No 3; Wave Height = 5 5 cm; Period = 1.0 s; Depth = 48.0 cm; Depth of Measure = -15.0 cm; Test No. 13; Wave Height = 12.0 cm; Period = 1.1 s, Depth = 48.0 cm, Depth of Measure = -36.0 cm 346

D-7 Position on the Mill Inside the Wave Tank and Coordinate System Adopted 349

D-8 Wave Orbital Velocities and Drag Forces Applied on the Mill 351

D-9 Nondimensional Wave-Applied Torque on the Mill under the Crest of the Wave as a Function of (h/L), for $s_o/h = 0.688$ 356

D-10 Wave Orbital Velocities at the Extremes of the Vanes Versus Time 361

NOTATIONS

A_1	Angle of rotation of the "mill" at t
A_2	Mean wave-applied torque
A_3	Dimensional friction factor
b	Width of the vane
C	Wave celerity
C_D	Drag coefficient
C_g	Wave group velocity
E	Total wave energy
$\bar{f}$	Darcy frictional coefficient
f_1	Nondimensional local vorticity
f_2	Nondimensional local angle of rotation
f_3	Function proportional to sin
f_4	Function proportional to the second order mean water level
Fdn	Instantaneous total drag force
Fun	Instantaneous horizontal net drag force
Fwn	Instantaneous vertical net drag force
Fu_+	Instantaneous horizontal drag force on the upper vane
Fu_-	Instantaneous horizontal drag force on the lower vane
Fw_+	Instantaneous vertical drag force on the left vane

[illegible]	Instant[illegible] [illegible]al drag force on the right van[illegible]
FT	Total frictional torque applied to the bottom computed from mean current measurements
g	Gravitational acceleration
h	Local water depth
$h^{(1)}$	First order water depth
$h^{(2)}$	Second order water depth
hb	Water depth at the breaking point
h_1	Proportional to the theoretical water depth
h_2	Proportional to the theoretical water depth, characteristic to the bottom undulations
h_o	Water depth at $x = x_3$
H	Wave height
k	Vector wave number
L_b	Length of the "bar area"
L	Wavelength
Lb	Bottom undulations wavelength
L_x	x-side of the area of integration of the wave-induced torque
L_y	y-side of the area of integration of the wave-induced torque
m	A parameter related with the theoretical bathymetry
Mo	Potential imbalance moment of the mill
MF	Moment of the net weight F respect to the line Fs-F
MWs	Moment of the Weight Ws respect to the line Fs-F

n	C_g/C
N	Number of points considered in the analysis of the angle of rotation data
p	Total pressure
p_1, p_2, p_3 p_4, p_5, p_6	Parameters related with the theoretical representation of the local wave angle of incidence
P	Net weight of the mill
P_n	Indicates the position of the vanes
r	Distance from the center of the mill
R	Radius of the mill
R_e	Reynolds number
R_x, R_y	Components of the bottom shear stress vector
$R_x^{(1)}$, $R_y^{(1)}$	First order components of the bottom shear stress vector
$R_x^{(2)}$, $R_y^{(2)}$	Second order components of the bottom shear stress vector
s	$(z + h)$ vertical coordinate
s_o	Vertical location of the "mill" inside the wave tank
s_m	Vertical location of measurement
$S_{i,j}$	Components of the radiation stress tensor
$S_{i,j}^{(1)}$	First order components of the radiation stress tensor
$S_{i,j}^{(2)}$	Second order components of the radiation stress tensor
t	time
t_a	Arrival time of the first broken wave

t_s	Wave stabilization time
T	Wave period
T_1	Wave-applied torque at the water surface
T_q	Wave-induced torque on the mill calculated from measurements of θ inside the wave tank
T_x, T_y	Components of the driving force vector
$T_x^{(1)}$, $T_y^{(1)}$	First order components of the driving force vector
$T_x^{(2)}$, $T_y^{(2)}$	Second order components of the driving force vector
u	Horizontal x-component of the velocity
u_c	Horizontal x-component wave orbital velocity at $s = s_m$
u_1	Horizontal x-component wave orbital velocity at the top of the upper vane
u_2	Horizontal x-component wave orbital velocity at the bottom of the lower vane
u_+	Horizontal x-component wave orbital velocity on the upper vane
u_-	Horizontal x-component wave orbital velocity on the lower vane
U	Horizontal x-component of the mean velocity
U_1	First order horizontal x-component wave orbital velocity coefficient
U_2	Second order horizontal x-component wave orbital velocity coefficient
v	Horizontal y-component wave orbital velocity
V	Horizontal y-component of the mean velocity
w	Vertical z-component wave orbital velocity
w_c	Vertical z-component wave orbital velocity at $s = s_m$

w_1	Vertical z-component wave orbital velocity at the extreme of the right vane
w_2	Vertical z-component wave orbital velocity at the extreme of the left vane
w_+	Vertical z-component wave orbital velocity on the left vane
w_-	Vertical z-component wave orbital velocity on the right vane
W_1	First order vertical z-component wave orbital velocity coefficient
W_2	Second order vertical z-component wave orbital velocity coefficient
W_α	Weight used to calculate the potential imbalance moment of the mill
$(WT)_m$	Total wave-applied torque computed from early measurements of the angle of rotation,
$(WT)_p$	Total wave-applied torque restricted by theory
x	Horizontal coordinate
x_o	Landside extreme of the area of integration of the wave-induced torque
x_1	Location of the shoreline
x_2	Landside extreme of the "bar area"
x_3	Seaside extreme of the "bar area"
X	Normalized x-coordinate
y	Horizontal coordinate
z	Vertical coordinate
z_m	Vertical location of measurement
α	Local wave angle of incidence
β	A constant related with the mean water level
β_E	Angle of rotation of the mill for experiments conducted in the water glass tank

β_ℓ	Angle of rotation of the mill as it recovers its position of equilibrium
β_N	Angle of rotation of the vane n when loaded with a weight W
γ	Proportionality factor between the wave height and the local depth inside the breaker zone
$\overline{\epsilon^2}$	Mean quadratic error
$\bar{\eta}$	Mean water level
$\bar{\eta}^{(1)}$	First order mean water level
$\bar{\eta}^{(2)}$	Second order mean water level
$\bar{\eta}_o$	Constant of integration
Θ	Constant of integration
θ	Angle of rotation of the mill for experiments inside the wave tank
θ_m	Measured angle of rotation of the mill
μ	Dimensionless parameter characteristic to the bottom undulations
ν	Kinematic viscosity
ρ	Water density
σ	Wave angular frequency
$\tau_{i,j}$	Shear stress tensor components
ψ	Transport stream function
ψ_o	Maximum transport stream function
ω	Local vorticity
ω_b	Vorticity at the bottom
ω_I	Vorticity inside the surf zone
ω_m	Vorticity at $s = s_m$

ω_e Vorticity at the water surface

$\bar{\omega}$ Mean vorticity

$\bar{\omega}_f$ Steady state mean vorticity computed from early measurements of the angle of rotation of the mill based on the mean vorticity equation

$\bar{\omega}_g$ Steady state mean vorticity computed from measurements of the angle of rotation of the mill based on the relationship between vorticity and angle of rotation

$\bar{\omega}_o$ Mean vorticity at t - ta

$\bar{\omega}_s$ Steady state mean vorticity computed from mean current measurements

Abstract of Dissertation Presented to the Graduate School of the University of Florida in Partial Fulfillment of the Requirements for the Degree of Doctor of Philosophy

WAVE-INDUCED TORQUE INSIDE
THE SURF ZONE

By

Sergio Alejandro Schmidt

December 1986

Chairman: Robert G. Dean
Major Department: Engineering Sciences

Sandy shorelines are frequently characterized by bars which trend perpendicularly or at a large angle to the beach. These bars are characterized by wide ranges of lengths, amplitudes, spacings and sediment characteristics. Rather than addressing the bar properties, the present study is concerned with a wave-induced hydrodynamics associated with a pre-existing bar geometry.

Measurements of mean currents and waves are performed over one particular bathymetry simulating a so-called transversal bar which represents a periodic form with a crest normal to the coast superimposed on a regular offshore sloping bottom. Also, a simple device is designed to sense the rotation of the water column, during the initiation of the circulatory motion.

The circulation cells characteristic of these bars depend on the wave-applied torque inside the breaker zone, mathematically represented by the curl of the wave-induced force vector which is a function of the radiation stress tensor components. This study presents a comparison between the total (integrated over the surf zone) wave-applied torque calculated from two independent data sources and that predicted by theory. The results indicate that the values of the total wave-applied torque computed from independent data sources differ by a factor of two, but predicted values are five to ten times smaller than those obtained from measurements.

Values of the dimensional friction coefficient calculated from measurements of the rotation of the water column are in agreement with the predicted values for the Reynolds Number characteristic of the model and bottom texture.

The mechanics of the device used to measure the rotation of the water column are examined theoretically and experimentally.

CHAPTER 1
INTRODUCTION

This study addresses the problem of nearshore circulation as a function of incident waves and topographic characteristics. It is well known that wave breaking induces a change in the mean sea level and eventually currents, as waves approach a shoreline obliquely.

The distribution of the wave height and associated set-up are responsible for the strength and direction of the currents, higher breaking waves induce a larger set-up driving the flow to areas of lower wave height and smaller set-up.

Qualitative descriptions of wave-induced nearshore circulation have been developed in the last few decades; however, theoretical descriptions have become available only over the late sixties and early seventies. The driving force for nearshore circulation is related to the distribution of the gradients of the radiation stress tensor components inside the surf zone (Longuet-Higgins and Stewart, 1962, 1964; Bowen, 1967). Bowen (1969b) introduced one of the first theoretical studies associated with nearshore circulation considering a longshore variation of the wave height as the driving mechanism for the development of rip currents on a plane beach. Field measurements

(Sonu, 1972), indicated that the streamlines were narrow in the outflow and broad in the inflow probably due to non-linear mechanisms. Also, Sonu observed that the circulation was pulsational and that the mean surface slopes agreed with the trajectories of drogues placed in the circulation cells. Some laboratory observations (Komar, 1971) and numerical studies (Noda, 1974) were introduced later to investigate these flows.

Mei and Liu (1977) presented a linear analytical approach to the nearshore circulation driven by periodic topographical effects along the shore, based on Bowen's (1969b) paper. They found that the position of the return flows depend on the surf zone width and on the on-offshore variation of depth.

Several experimental studies have been carried out to investigate wave transformation over three dimensional bathymetries, such as Whalin (1971) and Walker (1974). Whalin conducted a series of tests for nonbreaking waves over a bottom topography with parallel circular contours. He found negligible the reflection due to the bathymetry, small the energy dissipated over the entire area of measurement and large the amount of energy involved in diffraction along the wave crest. Walker conducted a series of tests for breaking and nonbreaking waves over a bathymetry simulating an idealized recreational surfing shoal. He found that measured wave heights at the breaking point were larger than predicted by Airy theory, also the use of this

theory in prediction of wave celerity produces a cumulative error in predicting the refraction for waves of finite height.

Ebersole and Dalrymple [1979] developed and applied a numerical model to longshore periodic features of the type investigated here. This model included convective accelerations, horizontal mixing and a quadratic bottom friction term and was applied to different beach shapes. The authors concluded that the nonlinear and lateral mixing terms are important in nearshore circulation processes, particularly for irregular bathymetries.

This study comprises the results of an experimental investigation to examine transformation and breaking of normally incident waves over one particular bathymetry and the resulting wave-applied torque inside the surf zone. The bathymetry simulates the so-called transversal bars and represents a periodic form parallel to the coast superimposed on a regular offshore sloping bottom.

Primary emphasis is focused on the hydrodynamics of the bar-wave induced circulation rather than the resulting sediment transport; however, a few conclusions can be drawn, particularly with regard to the maintenance of the bars.

This work highlights the wave-induced force or torque applied to the water column inside the surf zone. This force is responsible for the currents inside and, by continuity, outside the breakers. Some measurements of this force have been performed and compared with theory.

The measurements conducted include wave height distribution, mean currents and time dependent vorticity in such a way that the driving force can be estimated.

CHAPTER 2
GOVERNING EQUATIONS

Consider a Cartesian system of coordinates as shown in Figure (2-1) where the y-axis is parallel to the coast, the x-axis is directed seaward and the z-axis has its origin at the water surface pointing upwards. The still water shoreline is located at $x = x_1$. The Cauchy's equations in the x, y and z directions and continuity for an incompressible fluid are as follows:

$$\frac{\partial u}{\partial t} + u\frac{\partial u}{\partial x} + v\frac{\partial u}{\partial y} + w\frac{\partial u}{\partial z} = -\frac{1}{\rho}\frac{\partial p}{\partial x} + \frac{1}{\rho}\left(\frac{\partial \tau_{xx}}{\partial x} + \frac{\partial \tau_{yx}}{\partial y} + \frac{\partial \tau_{zx}}{\partial z}\right) \tag{2-1}$$

$$\frac{\partial v}{\partial t} + u\frac{\partial v}{\partial x} + v\frac{\partial v}{\partial y} + w\frac{\partial v}{\partial z} = -\frac{1}{\rho}\frac{\partial p}{\partial y} + \frac{1}{\rho}\left(\frac{\partial \tau_{xy}}{\partial x} + \frac{\partial \tau_{yy}}{\partial y} + \frac{\partial \tau_{zy}}{\partial z}\right) \tag{2-2}$$

$$\frac{\partial w}{\partial t} + u\frac{\partial w}{\partial x} + v\frac{\partial w}{\partial y} + w\frac{\partial w}{\partial z} = -\frac{1}{\rho}\frac{\partial p}{\partial z} + \frac{1}{\rho}\left(\frac{\partial \tau_{xz}}{\partial x} + \frac{\partial \tau_{yz}}{\partial y} + \frac{\partial \tau_{zz}}{\partial z}\right) - g \tag{2-3}$$

$$\frac{\partial u}{\partial x} + \frac{\partial v}{\partial y} + \frac{\partial w}{\partial z} = 0 \tag{2-4}$$

where (u, v, w) are the velocity components, p is the pressure, ρ the water density, g the gravity and

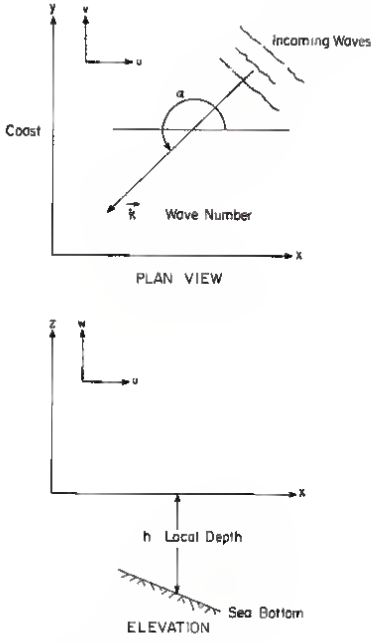

Figure 2-1 Coordinate System

$\tau_{i,j}$ $(i = x, y, z; j = x, y, z)$ are the shear stress tensor components.

Now consider a two-dimensional wave train of height H, frequency, σ, and vector wave number, $\vec{k}$, approaching the coast. The diraction of wave propagation is inclined at an angle of incidence α with the normal to the shoreline as shown in Figure 2-1. Since $\vec{k}$ and α change with x and y it is convenient to introduce here the refraction equation based on the irrotationality of the wave number vector.

$$\vec{\nabla} \times \vec{k} = 0 \tag{2-5}$$

where

$$\vec{\nabla} = \frac{\partial}{\partial x}, \frac{\partial}{\partial y} \tag{2-6}$$

and

$$\vec{k} = \vec{k}(\cos \alpha, \sin \alpha) \tag{2-7}$$

the presence of currents has been neglected in Equation (2-5).

Depth Integrated and Time Averaged Momentum and Continuity Equations

In order to overcome some of the difficulties involved in the description of the nearshore hydrodynamics the depth integrated and time averaged equations are used These equations deal with mean quantities and reduce the problem from three dimensions to two in the horizontal plane.

The time average (over one wave period) removes the wave-related fluctuations in time. The averaging procedure and further information about these equations can be found in Phillips (1966). The x and y momentum equations are

$$\frac{\partial U}{\partial t} + U\frac{\partial U}{\partial x} + V\frac{\partial U}{\partial y} = -g\frac{\partial \bar{\eta}}{\partial x} + R_x + T_x \qquad (2\text{-}8)$$

$$\frac{\partial V}{\partial t} + U\frac{\partial V}{\partial x} + V\frac{\partial V}{\partial y} = -g\frac{\partial \bar{\eta}}{\partial y} + R_y + T_y \qquad (2\text{-}9)$$

and the depth-integrated and time averaged continuity equation is

$$\frac{\partial \bar{\eta}}{\partial t} + \frac{\partial}{\partial x}\left[U(\bar{\eta} + h)\right] + \frac{\partial}{\partial y}\left[V(\bar{\eta} + h)\right] = 0 \qquad (2\text{-}10)$$

Here (U, V) are the mean horizontal velocity components, $\bar{\eta}$ the mean water level, h the location depth and (R_x, R_y) are the bottom shear stress components. The driving force components (T_x, T_y) are expressed in terms of the radiation stress tensor components $S_{i,j}(i = x, y;\ j = x, y)$

$$T_x = -\frac{1}{\rho(\bar{\eta} + h)}\left(\frac{\partial S_{xx}}{\partial x} + \frac{\partial S_{xy}}{\partial y}\right)$$

$$T_y = -\frac{1}{\rho(\bar{\eta} + h)}\left(\frac{\partial S_{yy}}{\partial y} + \frac{\partial S_{xy}}{\partial x}\right) \qquad (2\text{-}11)$$

where the radiation stress tensor components are

$$S_{xx} = E\,[(2n - 1/2)\cos^2\alpha + (n - 1/2)\sin^2\alpha]$$

$$S_{xy} = E\,n\cos\alpha\sin\alpha \qquad (2\text{-}12)$$

$$S_{yy} = E\,[(2n - 1/2)\sin^2\alpha + (n - 1/2)\cos^2\alpha]$$

here E is the total wave energy and n the ratio between the group velocity C_g and the celerity of the wave C

$$E = \frac{\rho g}{8} H^2 \qquad (2\text{-}13)$$

$$n = \frac{C_g}{C} \qquad (2\text{-}14)$$

$$C_g = \frac{C}{2}\left[1 + \frac{2kh}{\sinh(2kh)}\right] \qquad (2\text{-}15)$$

$$C = \left[\frac{g}{k}\,\mathrm{th}(kh)\right]^{1/2} \qquad (2\text{-}16)$$

All of the equations above have been derived using linear wave theory.

The selection of a linear bottom shear stress model is based on the fact that all data have been collected under low Reynolds number experiments, and, in spite of the fact that the quadratic form provides a more realistic representation to the actual stresses, the mathematical complexities are increased greatly. In later chapters it will be shown that typical mean velocities and kinematic viscosities are about 10 cm/s and 1 cm^2/s, respectively, and considering a length scale of 100 cm, a Reynolds number of about

Oil results. The linear representation for the bottom shear stress is

$$R_x = -A_3 \frac{U}{(\bar{\eta} + h)}$$
$$R_y = -A_3 \frac{V}{(\bar{\eta} + h)} \qquad (2\text{-}17)$$

where A_3 is a (dimensional) friction coefficient.

Introduction of the depth integrated and time averaged vorticity equation will be convenient for later purposes. By Cross-differentiating with respect to x and y and subtracting Equations (2-8) and (2-9) yields

$$\frac{\partial \bar{\omega}}{\partial t} + U \frac{\partial \bar{\omega}}{\partial x} + V \frac{\partial \bar{\omega}}{\partial y} + \bar{\omega} \left(\frac{\partial V}{\partial x} + \frac{\partial U}{\partial y} \right) = \frac{\partial R_y}{\partial x} - \frac{\partial R_x}{\partial y} + \frac{\partial T_y}{\partial x} - \frac{\partial T_x}{\partial y} \qquad (2\text{-}18)$$

where $\bar{\omega}$, the mean vorticity is defined as

$$\bar{\omega} = \frac{\partial V}{\partial x} - \frac{\partial U}{\partial y} \qquad (2\text{-}19)$$

Vertical Vorticity Distribution

To facilitate later considerations of the vertical distribution of the horizontal vorticity component it is convenient to introduce the corresponding governing equation In boundary layer problems the equations of motion can be simplified by the fact that the largest changes in the velocity occur in the vertical direction.

If Equations (2-1) and (2-2) are cross-differentiated and subtracted and scaling arguments are considered, all the gradients of the stresses in the x and y directions are dropped when compared with those gradients in the z direction the equation of vorticity results

$$\frac{\partial \omega}{\partial t} + u \frac{\partial \omega}{\partial x} + v \frac{\partial \omega}{\partial y} = \nu \frac{\partial^2 \omega}{\partial z^2} \tag{2-20}$$

where the local vorticity is defined as

$$\omega = \frac{\partial v}{\partial x} - \frac{\partial u}{\partial y} \tag{2-21}$$

and ν is the kinematic viscosity. The shear stresses are represented by

$$\begin{aligned} \tau_{xz} &= \nu \frac{\partial u}{\partial z} \\ \tau_{yz} &= \nu \frac{\partial v}{\partial z} \end{aligned} \tag{2-22}$$

Comparison between the Applied Longshore Thrust and Applied Torque Inside the Surf Zone

It is well known that as waves propagate obliquely into the surf zone, breaking results in a reduction of the wave energy introducing a change in the radiation stress components S_{xx}, S_{yy} and S_{xy}. The force applied is related to the magnitudes of the gradients of those components as shown by Equations (2-8), (2-9) and (2-11). For a plane beach with no changes in the y-direction

$$\frac{\partial S_{xx}}{\partial y} = 0$$
$$\frac{\partial S_{yy}}{\partial y} = 0 \qquad (2\text{-}23)$$

and the change in the flux of momentum in the x-direction is balanced by the change in the mean water level, so, in the absence of inertia terms and friction,

$$-g\frac{\partial \bar{\eta}}{\partial x} - \frac{1}{\rho(\bar{\eta} + h)}\frac{\partial S_{xx}}{\partial x} = 0 \qquad (2\text{-}24)$$

In the y-direction, the change of S_{xy} is manifested as an applied longshore thrust on the surf zone

$$T_y = -\frac{1}{\rho(\bar{\eta} + h)}\frac{\partial S_{xy}}{\partial x} \qquad (2\text{-}25)$$

which in the absence of other external forces is balanced by the bottom friction. Thus, from Equations (2-25) and (2-17)

$$-A_3 V - \frac{\partial S_{xy}}{\partial x} = 0 \qquad (2\text{-}26)$$

which was introduced by Longuet-Higgins (1970) to represent longshore currents in the absence of lateral mixing.

For a beach with a periodic longshore variation the forces induced by breaking waves are interpreted as an applied torque and related to the mean vorticity as shown in Equation (2-18). If the inertia and external forces are negligible, the torque is balanced by friction as follows:

$$\frac{\partial R_y}{\partial x} - \frac{\partial R_x}{\partial y} + \frac{\partial T_y}{\partial x} - \frac{\partial T_x}{\partial y} = 0 \qquad (2\text{-}27)$$

This equation was considered by Bowen (1969a) to represent the simplest (linear) theoretical approach to the rip currents problem when a sinusoidal longshore variation of the wave height is assumed.

CHAPTER 3
MODEL DESIGN

A small scale physical model was designed and constructed to study the circulation pattern and flow properties over a simple bathymetry.

The bottom topography was configured to represent an alongshore periodic bar formation. In order to minimize the sidewall effects the model is symmetric about a line through the ridge center in the direction of the wave propagation so the wave energy converges toward the center of the test basin. The walls placed along the centerline of the troughs reorient streamlines for normal wave incidence and thus do not alter the flow pattern. The amplitude of the bar was small so as to be consistent with linear approximations and it was decided to construct the model with a uniform slope seaward of the bar region.

The model was constructed in the main wave basin of the Coastal and Oceanographic Engineering Laboratory of the University of Florida. The model was separated from the rest of the basin by two walls of 0.8 m height. This isolation avoided the contamination of the flow over the bar by the remainder of the basin.

The model was 14 m long and 3.12 m wide. From the shoreside it starts with 2.43 m of uniform slope area

followed by 3.65 m of wave-like bathymetry referred to as the "bar area" aud finally an 8.07 m section with straight and parallel bottom contours (Figure 3-1). The bottom slope is not uniform seaward of the "bar area," but followed the natural floor of the basin from the wavemaker uutil a depth of 24 cm is reached. Figures 3-1a and 3-1b show the lateral and top view of the model, Table 3-1 provides the actual depth distribution and Figure 3-2 displays coutours of equal depth.

The bottom was composed of metal sheets firmly affixed to a wooden forms with the wave-like shape. Minor irregularities, of the order of one-half cm, were noted after the first day of testiug, probably due to the swelling of the wood due to submergence in water. However, these irregularities were far offshore and no adjustments were made. During the rest of experiments no further changes were observed.

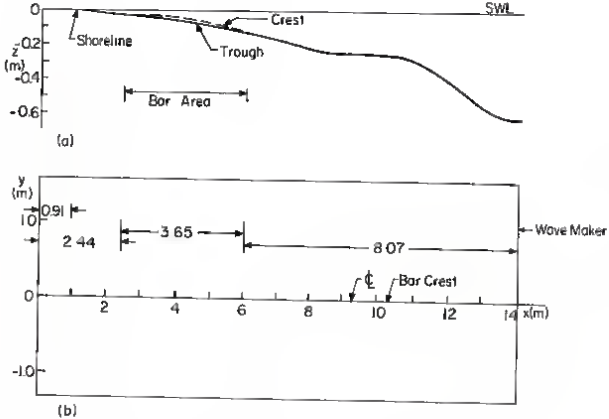

Figure 3-1. Lateral (a) and Top (b) View of the Model; Units in m

Table 3-1. Bathymetry of the Model

x(m) \ y(m)	-1.52	-1.22	-0.91	-0.61	-0.30	0.00
	depth h in cm					
0.91						0.0
1.22						0.5
1.52						1.0
1.83						1.6
2.13						2.2
2.44						2.8
2.74	3.8	3.6	3.6	3.4	3.0	2.8
3.05	4.4	4.4	4.2	3.7	3.1	2.9
3.35	5.2	5.0	4.7	3.9	3.2	3.0
3.66	5.8	5.5	5.2	4.2	3.3	3.1
3.96	6.6	6.3	6.0	5.3	4.4	4.0
4.27	7.6	7.2	7.1	6.2	5.4	4.9
4.57	8.7	8.3	8.1	7.2	6.5	6.1
4.88	9.7	9.4	9.0	8.2	7.3	7.2
5.18	10.5	10.4	10.1	9.5	9.0	8.3
5.49	12.0	11.5	11.3	11.2	10.7	9.8
5.78	12.8	12.5	12.3	12.3	12.1	11.8
6.10						13.6
6.40						14.8
6.71						16.2
7.01						17.4
7.32						18.7
7.62						20.1
7.92						21.2
8.23						22.6
8.53						23.8
8.84						24.8
9.14						25.9
9.45						26.0
9.75						26.0
10.06						26.2
10.36						26.5
10.67						28.0
10.97						30.3
11.28						33.2
11.58						35.9
11.89						40.4
12.19						43.9
12.50						48.4
12.80						52.5

Table 3-1. Continued

x(m) \ y(m)	-1.52	-1.22	-0.91	-0.61	-0.30	0.00
	depth h in cm					
13.11						56.5
13.41						60.0
13.72						63.2
14.00						64.5

NOTE: (1) Where entries are omitted the bathymetry is uniform in the y-direction with the depth in the last column.

(2) The bathymetry is symmetric about y = 0.

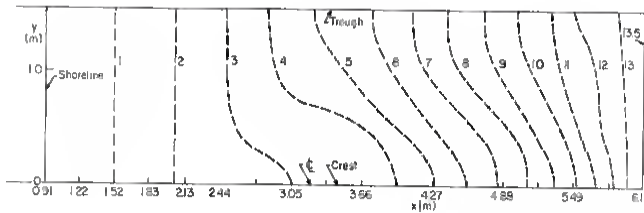

Figure 3-2. Bathymetry of the Model; Contours of Equal Depth in cm

CHAPTER 4
DATA ACQUISITION

Introduction

The data acquisition program comprised a series of tests in which wave height, vorticity and mean currents were measured. Wave heights were monitored with four wave gages and the data recorded on chart paper.

The vorticity data were inferred by the measurement of the angle of rotation produced by an eight vane "mill" placed parallel and close to the bottom and supported by a metal rod. The rotation of the mill was recorded on tape by a video camera above the mill. The wave-induced torque was estimated from measurements of the time dependent vorticity, through the measurements of the time dependent angle of rotation of the mill. Therefore, Equation (2-18) represents the basis for the measuring procedure. The simplest possible approach to estimate the torque assumed that the nonlinear terms were negligible so the measurements were restricted to early stages in time before the nonlinearities became significant. This consideration was satisfied by limiting the measurements to short times after commencement of the wavemaker.

The current measurements were obtained by observation of floating disk trajectories and in a limited number of locations by dye releases. The current and vorticity information was taken by a video camera placed above the model and recorded on tape. The camera and the video recorder used in the experiments were Sony Trinicon.

The symmetry of the bathymetry required measurements only in one half of the model.

Wave Height Measurements

The wave height information was obtained by four wave-meters, each supported by a metal tripod. The instruments were developed in the laboratory and they are of the "capacitance type." Briefly, the wave gage operates with an insulated wire at a frequency tunable in the range of one to two megahertz. The time varying height of the water column creates a varying capacitance which detunes the high frequency oscillator in an approximate linear fashion. The signal is converted to voltage which produces an analog output proportional to the water surface displacement. Once a wire type and length are tuned, no further adjustments are required; however, calibration of each instrument was done before and after each test and no changes were observed. The calibrations were performed using a calibration tank where the signal was compared with a graduated scale. Figure 4-1 displays the instrument and its metal support.

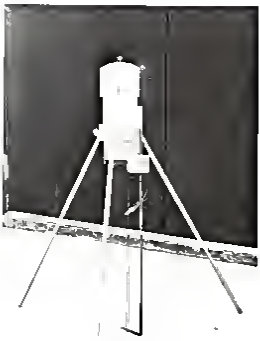

Figure 4-1 "Capacitance Type" Wave Gage and Tripod

The signal from the wave gage was recorded on chart paper. The size of the wave gage precluded measurements of the wave height where the depth was less than one centimeter.

Vorticity Measurements

The vorticity was determined by measuring the time dependent angle of rotation of an eight vane mill supported by a metal rod (Figure 4-2). Each vane was 3.8 cm long, 0.9 cm high and 0.1 cm thick. Built of rigid and light plastic, the vanes were attached to a center cylindrical hub of the same height and material. This hub is 1.2 cm in diameter and was provided with two steel ball bearings which reduce friction on the support rod. The base for the support rod is a 3.0 by 2.5 cm metal sheet on which a plastic protractor was glued to allow more accurate measurement. Figure 4-3 shows a top view of the instrument. In order to avoid instability of the device while measurmentes were taken, a weight was attached to the top of the rod. The top of the mill was located 1.5 cm above the bottom.

The motion of the mill was recorded on tape and taken by a camera placed 1 meter above the instrument supported by a tripod as illustrated by Figure 4-4. The angle of rotation and the time were recorded simultaneously on tape. The time provided by a digital clock appears superimposed with the view of the instruments. Both the angle of rotation and the time were read later on a television screen.

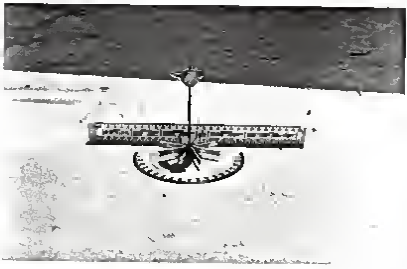

Figure 4-2. Lateral View of the Mill

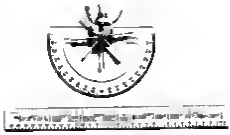

Figure 4-3: Top View of the Mill

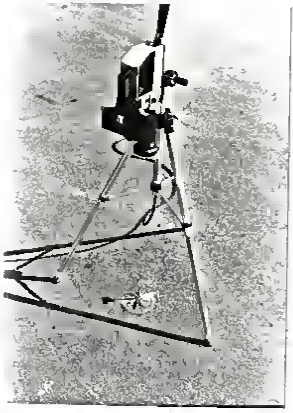

Figure 4-4. Video Camera, Tripod and Mill

Figure 4-5 shows a [illegible] the screen during the reading procedure.

In order to measure the change of the angle of rotation with time in a particular location, the following steps were carried out: first the instrument and the camera were placed in the location of interest and then the wavemaker was turned on, the actual interval of time during which the measurements were performed was from a minimum of 2 minutes to a maximum of 7 minutes. After each measurement, the wavemaker was stopped and the circulation allowed to cease before additional measurements were conducted.

Mean Current Measurements

The velocity field was determined by observing the trajectories of floating disks. The disks were designed to follow the mean currents and to avoid the surfing effect inside the breaker zone. They were built with a top layer of plastic to provide strength and with a painted surface for identification purposes and a lower layer of cork of the required thickness to keep the disk almost completely submerged. The drag was increased by eight plastic vanes beneath the cork layer.

The diameter of each disk was 8.5 cm and the vanes were 1.4 cm high. Figure 4-6 shows the top and lateral views of one of the disks used in the experiments.

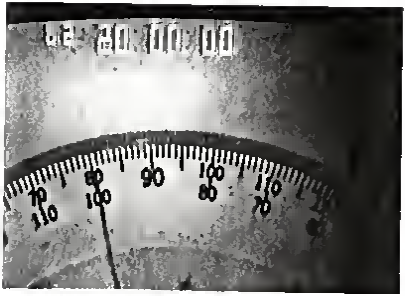

Figure 4-5. Television Screen View During Reading Procedure

Figure 4-5. Top and Lateral View of the Disks Used to Measure Mean Currents

The disk trajectories were taken by a video camera and recorded on tape. The camera was located 10 m above the modal

CHAPTER 5
DATA ANALYSIS AND DISCUSSION

The purpose of this chapter is, through the analysis and presentation of the data, to provide insight into the physics involved in the problem of mean vorticity generation inside the surf zone. In particular, the wave-induced applied torque is examined. A method of analysis of the vorticity-related data was developed and applied. Since the vorticity information was taken at early stages of wave development, the wave stabilization time was measured. However, after waves break the wave height distribution and consequently the wave-induced torque, inside the surf zone, depend primarily on the bathymetry. The wave height distribution and mean currents were measured inside and outside the breaker zone. All measurements were performed for three different wave periods.

Wave Height

Introduction

This section presents the results of the measurement program to determine the wave stabilization time (ts) and the distribution of the steady state wave height.

Wave Stabilization Time

Measurements of the wave stabilization time were performed as part of the program of measurements of wave and wave-induced properties. An example of the calculation of the wave stabilization time is shown in Figure 5-1. Two measurements of the wave height versus time were obtained for each wave period. Each experiment was commenced after it was observed that the currents from the preceding experiment had ceased. Figures 5-2, 5-3 and 5-4 showed the actual measurements (a) and the distribution of the wave height (b) over time. Table 5-1 summarizes the results.

Table 5-1. Wave Stabilization Time (ts)

Period (s)	Measurement 1			Measurement 2		
	Location		ts	Location		ts
	x (m)	y (m)	(s)	x (m)	y (m)	(s)
1.0	5.03	.00	6.0	5.03	.00	5.5
1.5	5.03	.00	3.5	5.03	.00	3.0
1.9	3.81	1.07	3.8	4.11	.00	2.8

Wave Height Distribution

Wave height measurements were performed at different locations and for three different wave periods over the "bar area." These measurements were obtained after the

Figure 5-1. Wave Stabilization Time (ta). Example of the Calculation
(a) Wave Record and (b) Wave Height Versus Time

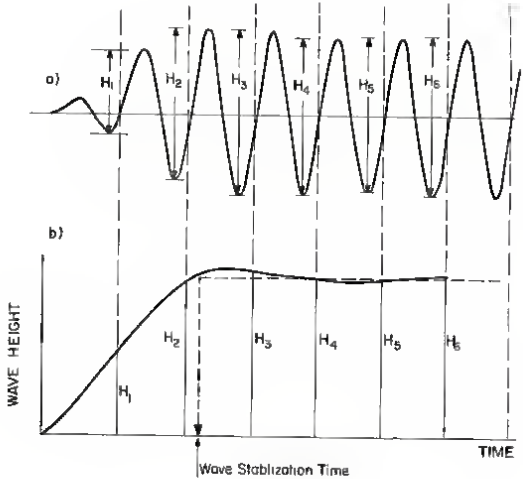
a)
H1
H2
H3
H4
H5
H6
b)
WAVE HEIGHT
H1
H2
H3
H4
H5
H6
TIME
Wave Stablization Time

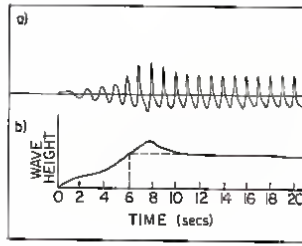

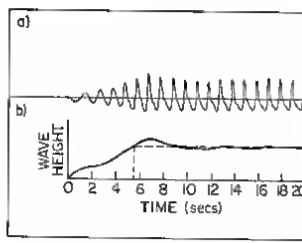

Figure 5-2. Wave Stabilization Time (ts): Period = 1.0 s, (a) Actual Record and (b) Wave Height Versus Time, Upper: Measurement No. 1 (x = 5.03 m, y = 0 m), ts = 6.0 s. Lower: Measurement No. 2 (x = 5.03 m, y = 0 m), ts = 5.5 s

Figure 5-3. Wave Stabilization Time (ts): Period = 1.5 s, (a) Actual Record and (b) Wave Height Versus Time; Upper: Measurement No. 1 (x = 5.03 m, y = 0 m), ts = 3.5 s; Lower: Measurement No. 2 (x = 5.03 m, y = 0 m), ts = 3.0 s

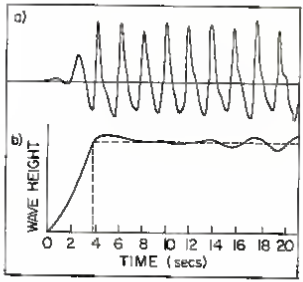
a)
b)
WAVE HEIGHT
0 2 4 6 8 10 12 14 16 18 20
TIME (secs)

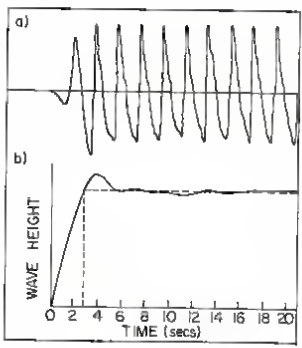
a)
b)
WAVE HEIGHT
0 2 4 6 8 10 12 14 16 18 20
TIME (secs)

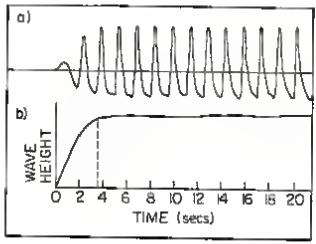

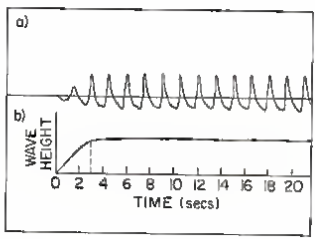

Figure 5-4. Wave Stabilization Time (ts): Period = 1.9 s: (a) Actual Record and (b) Wave Height Versus Time; Upper: Measurement No. 1 (x = 3.81 m, y = 1.07 m) ts = 3.4 s, Lower: Measurement No. 2 (x = 4.11 m, y = 0 m) ts = 2.8 s

waves had stabilized. However, these values are not truly steady state due to the unsteadiness of the current pattern.

Figures 5-5, 5-6 and 5-7 show the wave height distribution over the model for the different wave periods considered. The measurements are presented in tabular form in Appendix A.

A common assumption in problems of this type is that inside the surf zone the wave height is proportional to the local depth ($H = \gamma h$, where $\gamma = 0.78$). Figure 5-8 shows the relationship between wave height and local depth for the measurements obtained.

Vorticity

Introduction

This section addresses mean vorticity (depth integrated) and the downward diffusion of vorticity from the surface, inside the breaker zone. A series of measurements of the time-varying angle of rotation, θ_m (which is related to vorticity, $\bar{\omega}$) was performed inside the breaker zone using the mill to measure θ_m is described in Chapter 4. The measurements were taken at the water surface and close to the bottom. A simple analytical model is introduced for the representation of mean vorticity and the applied torque and in some cases the friction coefficients were calculated by the method of least squares. Also, a vorticity diffusion model is developed which represents the downward diffusion

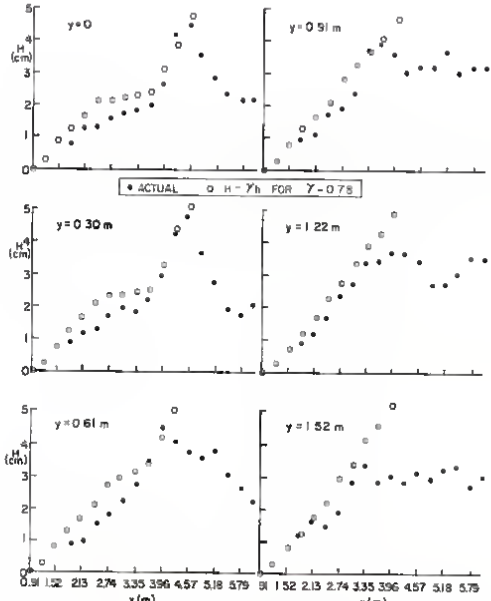

Figure 5-5. Wave Height Measurements; Period = 1.0 s, Actual (•), H = h (o) for γ = 0.78

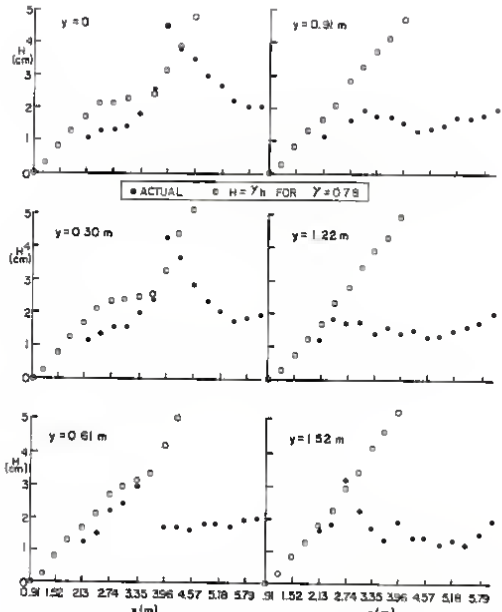

Figure 5-6. Wave Height Measurements; Period = 1.5 s, Actual (●), H = h (o) for γ = 0.78

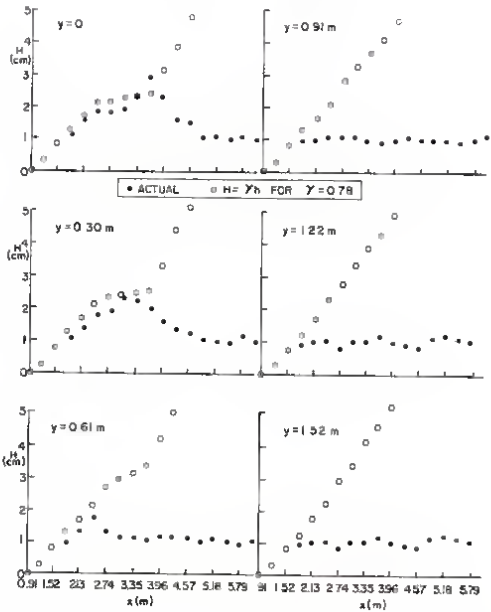

Figure 5-7. Wave Height Measurements; Period = 1.9 s, Actual (•), H = h (o) for γ = 0.78

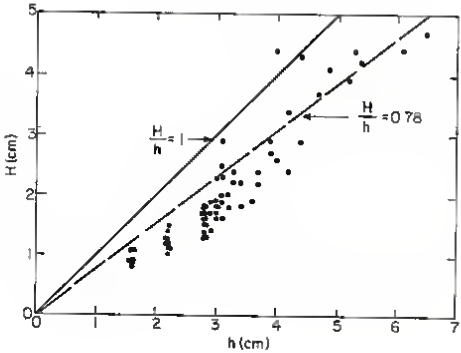

Figure 5-8. Measure Wave Height (H) Versus Local Water (h) Depth Inside the Surf Zone

of vorticity from the water surface under the assumption that the torque due to the wave breaking is totally applied at the water surface. Values of the applied torque and the effective viscosity were calculated by the least-squares method and are presented in tabular form.

General Description of the Data: Types of Curves, Classification and Associated Forces

Before the data analysis method is presented it is convenient to discuss the forms of the curves (angle of rotation versus time) that were obtained and also the most probable causes for those forms. The convention of signs adopted is shown in Figure 2-1 which indicates that negative values of $\bar{\omega}$ (and ϵ_m) are expected to be dominant given the bathymetry and the wave direction considered in that portions of the model where the measurements were conducted. To characterize the curves the following classification is proposed:

Type A. The slope of the curve remains essentially constant after the first few seconds.

Type B. The slope of the curve continues to increase after the first few seconds.

Type C. The slope of the curve decreases after the first few seconds.

Figure 5-9 illustrates these different types and Table 5-2 shows their frequency of occurrence based on the total number of curves analyzed.

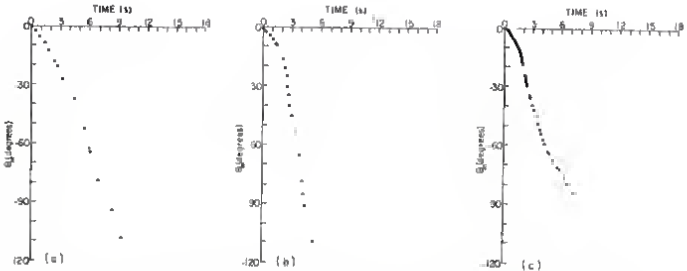

Figure 5-9. Angle of Rotation, ϕ_m, Versus Time; Types of Curves, (a) Type A: Run No. 99, Period = 1.0 s; Location. x = 4.42 m, y = 0 46 m; (b) Type B: Run No. 2; Period = 1.5 s, Location: x = 3 43 m, y = 0.15 m; (c) Type C: Run No. 15; Period = 1 9 s; Location. x = 2.59 m. y = 0.15 m

Table 5-2 Type of Curves, Frequency of Occurrence

Type	Frequency (%)
A	10.4
B	29.2
C	60.4

The physical interpretation of the different curves is difficult because of the nonlinearities and unsteadiness involved. The rotation of the mill and the associated vorticity in a particular place can be related to forces generated "in situ" and with forces generated in some other location which modify the local vorticity by advection processes. These forces are

(a) Local. radiation stress-related applied torque exerted by breaking waves, and

(b) Generated elsewhere: vorticity advection by the currents.

These factors have been identified as predominant for most of the data collected as causing or transforming the local mean vorticity. There are other factors that should be considered: the location where the measurements were taken (close to the bottom), the source of vorticity (mostly concentrated at the water surface, inside the breaker zone) and the response of the instrument under such hydraulic regimes.

Type A is associated with those cases where advection was not important and the applied torque was balanced by frictional forces at an early time. Type B represents the case where the local vorticity was increased by advection from areas of higher vorticity. In Type C the local vorticity was diminished by advection from areas of lower level of vorticity.

Mean Vorticity

A method is introduced below to estimate the wave-induced torque. The method is based on Equation (2-18) which can be written as

$$\underset{\text{(I)}}{\frac{\partial \bar{\omega}}{\partial t}} = \underset{\text{(II)}}{-\frac{A_3}{(\bar{\eta} + h)}\,\bar{\omega}} + \underset{\text{(III)}}{\left[\frac{A_3}{(\bar{\eta} + h)^2}\,\frac{\partial(\bar{\eta} + h)}{\partial x}\,v - \frac{\partial(\bar{\eta} + h)}{\partial y}\,u\right]} + \underset{\text{(IV)}}{A_2} \tag{5-1}$$

where the forcing term A_2 can be written:

$$A_2 = -\frac{1}{\rho(\bar{\eta} + h)}\left(\frac{\partial^2 S_{yy}}{\partial x \partial y} + \frac{\partial^2 S_{xy}}{\partial x^2} - \frac{\partial^2 S_{xx}}{\partial x \partial y} - \frac{\partial^2 S_{xy}}{\partial y^2}\right)$$
$$+ \frac{1}{\rho(\bar{\eta} + h)^2}\left[\frac{\partial(\bar{\eta} + h)}{\partial x}\left(\frac{\partial S_{yy}}{\partial y} + \frac{\partial S_{xy}}{\partial x}\right) - \frac{\partial(\bar{\eta} + h)}{\partial y}\left(\frac{\partial S_{xx}}{\partial x} + \frac{\partial S_{xy}}{\partial y}\right)\right] \tag{5-2}$$

In order to develop a method to determine the wave-induced applied torque (A_2) inside the surf zone the following assumptions have been made:

(1)--The forcing term A_2 is a function of the radiation stress tensor and its gradients as indicated in Equation (5-2). For computation purposes A_2 was considered independent of time although in reality it varies somewhat since some unsteadiness in the wave height data was observed. A_2 was estimated from early portions of the measurements of the time dependent angle of rotation of the mill described before.

(2)--The friction coefficient A_3 depends primarily on the Reynolds number. For computation purposes it was considered as a constant and calculated when the mean vorticity was approximately constant in the later portions of the data.

(3)--Since it is to be expected that the convective terms would be small in the early stages of vorticity development and to reduce the complexity due to these nonlinear terms, they were omitted from Equation (5-1) and in the corresponding analysis. This advantage is offset to some degree because of the need to deal with the unsteady phase of the vorticity equation.

(4)--The wave-induced vorticity depends on the local topographical characteristics. For a beach form of regular offshore sloping bottom with the superimposed mild periodic form parallel to the coast and assuming that the bathymetry

and the velocity field induced by breaking waves may be represented by

$$h = h_1 + \mu h_2 \phi \tag{5-3}$$

$$\begin{aligned} U &= U^{(1)} + \mu U^{(2)} \\ V &= V^{(1)} + \mu V^{(2)} \end{aligned} \tag{5-4}$$

where h_1 and h_2 are functions of x, ϕ is a function of y, $(U^{(1)}, V^{(1)})$ the mean velocities induced without the bottom undulations, $(U^{(2)}, V^{(2)})$ are the contribution to the velocity due to the effect of the undulations parallel to the coast and μ is a small parameter proportional to the amplitude of the bottom forms. As a consequence the mean vorticity results

$$\begin{aligned} \bar{\omega} &= \left(\frac{\partial V^{(1)}}{\partial x} - \frac{\partial U^{(1)}}{\partial y}\right) + \mu\left(\frac{\partial V^{(2)}}{\partial x} - \frac{\partial U^{(2)}}{\partial y}\right) \\ &= \bar{\omega}^{(1)} + \mu\, \bar{\omega}^{(2)} \end{aligned} \tag{5-5}$$

The first order mean velocities depend on the wave angle of incidence. For normal incidence the alongshore component of velocity $(V^{(1)})$ is zero and the onshore mean velocity $(U^{(1)})$ is also zero because the onshore transport is balanced by the return flow satisfying the conservation of mass requirement. As a consequence of the above, the first order mean vorticity $(\omega^{(1)})$ is zero. For waves with a different angle of incidence than normal the circulation (order μ) is affected by the presence of longshore currents. This case

has been investigated numerically by Sonu (1972). Dropping the superscript and recognizing that Term III in Equation (5-1) can be neglected because

(a) the product

$$\frac{\partial(\bar{\eta} + h)}{\partial y} u \tag{5-6}$$

is of higher order (u^2) and

(b) the mean velocity V is particularly small at early stages in time since at breaking the onshore component dominates. Finally, the remaining mean vorticity results

$$\frac{\partial \bar{\omega}}{\partial t} = - \frac{A_3}{(\bar{\eta} + h)} \bar{\omega} + A_2 \tag{5-7}$$

The vorticity can be related to the angle of rotation as follows

$$\bar{\omega} = 2 \frac{\partial \theta}{\partial t} \tag{5-8}$$

Where $\partial\theta/\partial t$ represents the angular velocity of the fluid. Integrating Equation (5-7) an expression for the mean vorticity is obtained

$$\bar{\omega} = \frac{A_2 h}{A_3} + (\omega_o + \frac{A_2 h}{A_3}) \text{ Exp } [- \frac{A_3}{h} (t - ta)] \tag{5-9}$$

and introducing Equation (5-8) and integrating again

$$\theta = A_1 + \frac{A_2 h}{2A_3}(t - ta) + \frac{h}{A_3}\left(\bar{\omega}_o - \frac{A_2 h}{2A_3}\right) \left\{1 - \mathrm{Exp}\left[-\frac{A_3}{h}(t - ta)\right]\right\} \tag{5-10}$$

where the following initial conditions were imposed

$$\bar{\omega} = \bar{\omega}_o \qquad \theta = A_1 \qquad t = ta \tag{5-11}$$

where ta is the arrival time of the first broken wave.

Based on Equation (5-10) the values of A_1, A_2 and A_3 were determined for each set by the nonlinear least squares method using the Newton-Raphson technique. The mean quadratic error was defined as follows

$$\overline{\varepsilon^2} = \frac{1}{N}\sum_{i=1}^{N}(\theta - \theta_m)^2 \tag{5-12}$$

where θ_m represents the measured value of θ and N the number of points considered. The error is minimum when the following conditions are met

$$\frac{\partial \overline{\varepsilon^2}}{\partial A_n} = 0 \qquad n = 1, 2, 3 \tag{5-13}$$

which represents a system of three equations and three unknowns. Due to the nonlinearity of these equations it was necessary to obtain convergence through iteration.

Before the calculations of A_1, A_2 and A_3 are described it is appropriate to mention some mechanical properties of the mill considered relevant at this point. This instrument responds to the velocity field in a manner which is not understood completely. The vanes of the mill may be considered as a quadratic drag device and it was found that when placed in an irrotational field, rotation did occur. Briefly, the instrument senses gradients in the wave height, which is equivalent to a gradient in the wave orbital velocities producing a net drag force which induces a rotation. This effect is particularly relevant in the absence of breaking waves. When waves break the wave-induced vorticity overcomes the effect of the drag force. Since the measurements of the angle of rotation were conducted from the starting of the wavemaker in order to evaluate the wave-induced applied torque, the wave height grows with time until reaching the steady state value. This is particularly important because the first incoming waves do not necessarily break, in which case the mill senses the wave height gradient initiating the rotation and introducing an extraneous force in the data. In order to remove this artificial contribution, the arrival time of the broken wave (ta) to the location of interest is necessary. Further details about the mechanics of the mill are presented in Appendix D.

To evaluate the effect of this artificial force consider the set of data corresponding to station No. 13 shown

in Figure 5-10. The arrival of the first broken wave was at ta = 0.8 s and the total interval of time considered for the analysis was approximately 7 s. To evaluate the results two different scenarios were considered:

(a) Friction was neglected ($A_3 = 0$) and the data were analyzed considering that the initiation of the motion coincided with the arrival of the first broken wave (ta = 0) and

(b) Friction was neglected ($A_3 = 0$) and the data were analyzed considering the actual arrival of the first broken wave (ta = 0.8 s).

Figure 5-11 shows the results for Cases a and b where friction has been omitted. It can be seen that at a time approximately equal to the wave stabilization time both A_2-curves are essentially the same indicating that, for reasonable values of ta, the artificial torque introduced by the wave-induced drag on the vanes of the mill, before any broken wave arrives, does not alter the estimation of A_2. Note also that the mean quadratic error ($\overline{\varepsilon^2}$) increases with time for both a and b cases. This effect can be associated with the fact that Equation (5-7), in the absence of friction, behaves well until currents (and friction) become significant. For run No. 13 a reasonable value for A_2 seems to be about -10 degrees/s^2 because the error is small and the length of time analyzed is large enough to balance the effect of the artificial force.

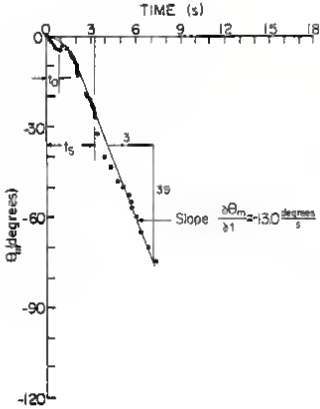

Figure 5-10. Angle of Rotation, θ_m, of the Mill Versus Time Corresponding to Run No. 13, Period = 1.5 s, Location: x = 3.20 m, y = 0.46 m, t_0 Indicates the Arrival Time of the First Broken Wave and t_s is the Wave Stabilization Time

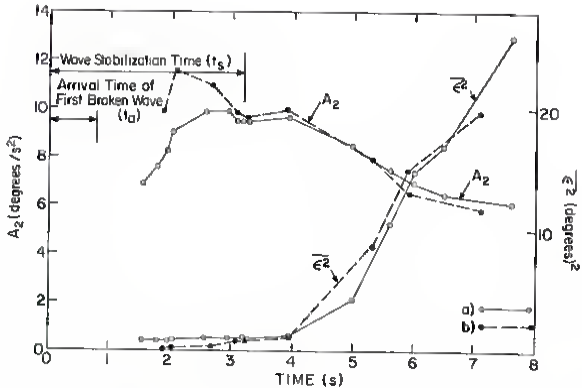

Figure 5-11. The Forcing Term, A_2, Versus Time and the Corresponding Mean Quadratic Error for Data Corresponding to Run No. 13; Period = 1.5 s; Location: x = 3.20 m, y = 0.46 m

When friction is considered, Equation (5-13) must be solved simultaneously. To illustrate this case consider Run No. 13 again. As mentioned before, the nonlinear character of the equations requires initial values for their numerical solution. These values should be as accurate as possible so the absolute minimum of the mean quadratic error can be obtained. To compute the initial friction coefficient the later portions of the data were considered. The method requires the absence of curvature in the measurements of the time dependent angle of rotation after few seconds the motion was initiated and on the previous known value of the forcing term A_2. For the data shown in Figure 5-10 and approximately constant mean vorticity is present after the first 3 s, so

$$\frac{\partial \bar{\omega}}{\partial t} = 0 \tag{5-14}$$

and from Equation 5-7 the friction coefficient A_3 is estimated provided that the steady state mean vorticity is known. This value can be calculated from the slope of the data presented in Figure 5-10, thus

$$A_3 = \frac{A_2 (\bar{\eta} + h)}{\frac{\partial \theta_m}{\partial t}} \tag{5-15}$$

Considering $(\bar{\eta} + h) \approx h = 3.5$ cm, the initial value of the angle of rotation $A_1 = 0$, the initial torque $A_2 = -10$ degrees/s^2 and $\partial\theta_m/\partial t = -13$ degrees/s the

[illegible] coefficient A_3 = 2.70 cm/s. The simultaneous solutions of Equations (5-13) are A_1 = 0.14 degrees, A_2 = -18.86 degrees/s^2, A_3 = 2.62 cm/s and the mean quadratic error $\overline{\varepsilon^2}$ = 4.07 degrees^2.

When this procedure was possible (data presented a curvature near zero after the first few seconds), A_3 was calculated; otherwise, the first few seconds were analyzed (ensuring that friction was not dominant) and only the torque A_2 was calculated.

The instrument was placed about 1.0 cm from the bottom for all measurements. Thus, when interpreting the data on a depth-averaged basis as has been discussed before the calculated torque represents a fraction of that applied at the water surface. The effect of the distribution over depth of the vorticity generated (applied torque) will be addressed in a later section of this chapter.

The time interval for which each set of data was analyzed depended on the arrival time of the first broken wave (ta) and the characteristics of the data. For those sets that were well-behaved the maximum time interval considered ranged up to 10.5 s (Run No. 14). However, some of the sets of data were analyzed for a small time interval (Run No. 157) because of the complicated behavior of the data and must be interpreted as an approximation. The time interval between the initiation of the motion of the mill and the arrival of the first broken wave (ta) was small,

ranging up to 1.2 s. Due to the smallness of t_a, its effect on the calculations of A_2 and A_3 is considered unimportant.

The bar area was gridded into 30 cm by 30 cm and one vorticity measurement inside the surf zone was performed in the center of each square in most of the cases. The resulting number of stations is presented in Table 5-3. Figure 5-12a, b, c indicates the actual locations of each station.

Table 5-3. Angle of Rotation θ_m Measurement Runs

Period (s)	Number of Runs
1.0	21
1.5	15
1.9	6

The results of the analyses are presented in Tables 5-4, 5-5 and 5-6. For those runs in which values of A_1, A_2 and A_3 are not included, the data are presented in Appendix B but a meaningful analysis was precluded due to the complexity of the data.

Diffusion of Vorticity Inside the Breaker Zone

Since the development presented in the preceding section relies on depth-integrated properties such as the radiation stress tensor and its gradients as derived by Longuet-Higgins and Stewart (1964), the results presented above have been obtained under the assumption that the

Figure 5-12 Angle of Rotation, θ_m, of the Mill Measurement Stations. (a) Period = 1.0 s, (b) Period = 1.5 s and (c) Period = 1.5 s Inside the Figures the Run Numbers Are Indicated

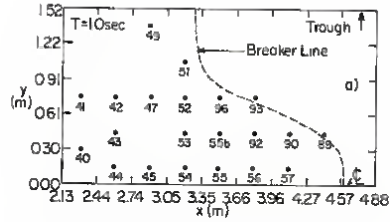
T=10sec
Trough
Breaker Line
a)
y (m)
x (m)
1.52
1.22
0.91
0.61
0.30
0.00
2.13 2.44 2.74 3.05 3.35 3.66 3.96 4.27 4.57 4.88
49
51
41 42 47 52 96 93
43 53 55b 92 90 89
40
44 45 54 55 56 57

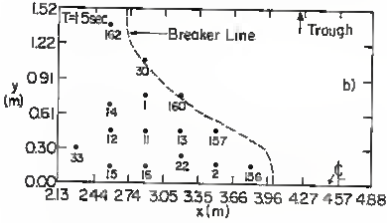
T=15sec
Trough
Breaker Line
b)
y (m)
x (m)
1.52
1.22
0.91
0.61
0.30
0.00
2.13 2.44 2.74 3.05 3.35 3.66 3.96 4.27 4.57 4.88
162
30
1
160
14
12 11 13 157
33
22
15 16 2 136

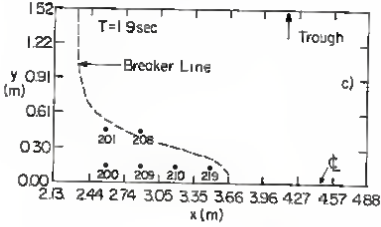
T=19sec
Trough
Breaker Line
c)
y (m)
x (m)
1.52
1.22
0.91
0.61
0.30
0.00
2.13 2.44 2.74 3.05 3.35 3.66 3.96 4.27 4.57 4.88
201
208
200 209 210 219

Table 5-4. Mean Vorticity Analysis Results for T = 1.0 s

Run (No.)	x (m)	y (m)	h (cm)	A_1 (degrees)	A_2 (degrees/s^2)	A_3 (cm/s)	$\overline{\varepsilon^2}$ (degrees)^2	time (s)
40	2.29	.30	2.5	-3.31	-9.18		5.71	2.9
41	2.29	.76						
44	2.59	.15	2.9	1.46	-2.64		1.21	4.3
43	2.59	.46	3.0	-1.34	-13.40		1.47	3.1
42	2.59	.76	3.2	1.29	-2.42		1.43	6.0
45	2.90	.15	3.0	.08	-2.80		1.53	4.3
47	2.90	.76	3.7	-3.53	-10.50		2.60	3.1
49	2.90	1.37	4.1	.44	1.32		3.58	7.5
54	3.20	.15	3.1	-1.78	-3.88		1.86	3.7
53	3.20	.46	3.5	-.62	-12.48		.39	2.5
52	3.20	.76	4.1	-.04	-3.40		.05	2.2
51	3.20	1.07	4.6	-1.67	-2.30		1.08	4.0
55	3.51	.15	3.1	-3.26	-12.18		6.07	4.2
55b	3.51	.46	3.7	1.27	-11.36		2.52	2.7
96	3.51	.76	4.5	-.29	-2.28		2.38	8.1
56	3.81	.15	3.7	-1.39	-3.06		.72	2.8
92	3.81	.46	4.3	-1.88	-12.24		1.84	3.6
93	3.81	.76	5.2	-1.83	-2.04		2.18	7.8
57	4.11	.15	4.7	.00	-6.76		.46	5.4
90	4.11	.46	5.3	-.86	-6.82		.48	4.2
89	4.42	.46	5.3	-2.76	-10.36		2.65	3.2

Table 5-5. Mean Vorticity Analysis Results for T = 1.5 s

Run (No.)	x (m)	y (m)	h (cm)	A_1 (degrees)	A_2 (degrees/s^2)	A_3 (cm/s)	$\overline{\varepsilon^2}$ (degrees)^2	time (s)
33	2.29	.30	2.5	.42	-16.90	1.44	1.44	6.6
15	2.59	.15	3.0	-.79	-20.54		.56	2.5
12	2.59	.45	2.9	1.00	-7.52	1.48	.82	5.8
14	2.59	.69	3.2	3.16	-13.14	2.14	2.85	10.5
162	2.59	1.37	3.3	.21	-.32		.02	3.4
1	2.82	.76	3.7	-1.21	-13.80		.48	2.1
16	2.80	.15	2.9	2.86	-4.52		2.15	3.3
11	2.80	.38	3.3	-.81	-4.86	1.21	7.30	6.9
30	2.80	1.07	4.0	-2.04	-9.26		.94	2.9
22	3.20	.23	3.1	-3.48	-11.74	1.08	7.18	5.9
13	3.20	.46	3.5	-.14	-18.46	2.64	4.07	7.6
160	3.20	.76	4.1	-2.19	-7.90		1.61	4.0
2	3.43	.15	3.1	.54	-17.28		5.57	3.9
157	3.51	.46	3.7	-.61	-15.22		.21	1.6
156	3.81	.15	3.7					

Table 5-6. Mean Vorticity Analysis Results for T = 1.9 s

Run (No.)	x (m)	y (m)	h (cm)	A_1 (degrees)	A_2 (degrees/s^2)	A_3 (cm/s)	$\overline{\epsilon^2}$ (degrees)^2	time (s)
200	2.59	.15	2.9	9.01	-7.92	.57	11.17	8.4
201	2.59	.46	3.0	-.35	-11.78		1.14	2.3
209	2.30	.15	3.0					
208	2.30	.46	3.3	-1.16	-5.42		1.01	4.2
210	3.20	.15	3.1					
219	3.51	.15	3.1					

torque is uniformly distributed over depth. However, these properties are truly depth-dependent as presented by Horecki (1981). It is not the objective of this work to develop the details of the problem but rather to justify the assumption that within the surf zone the torque is mostly applied at the water surface so values of the S_{xx} and S_{xy} components of the radiation stress tensor should be calculated as a function of the depth.

Under the considerations mentioned above, the vorticity is diffused to the bottom after a time interval inversely proportional to the viscosity in the water column. Because of the close proximity of the instrument to the bottom the torque calculated from the mean vorticity equation through the measurements should be smaller than the actual torque, located near the water surface.

In order to estimate the actual torque, consider an idealization of the problem assuming that the torque due to the wave breaking is located entirely at the surface so the process of diffusion is reduced to the boundary value problem sketched in Figure 5-13 where ν represents the viscosity and T_1 the wave-applied torque.

The solution of this problem can be found through the Laplace transform method and is

$$\omega_1 = \frac{T_1 h}{\nu} f_1 (z/h) \qquad (5\text{-}16)$$

where

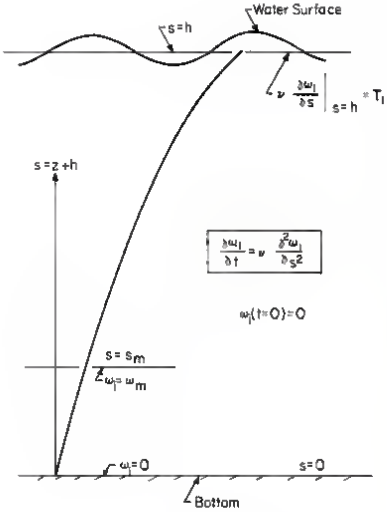

Figure 5-13. Diffusion of Vorticity Inside the Surf Zone, Boundary Value Problem Sketch

$$\Phi_1 = \frac{s}{h} - \frac{8}{\pi^2} \sum_{n=0}^{\infty} \frac{(-1)^n}{(2n+1)^2} \exp\left[- \frac{\nu(2n+1)^2\pi^2 t}{4h^2} \right] \sin\left[\frac{(2n+1)}{2} \frac{s}{h} \right] \tag{5-17}$$

and since

$$\omega_1 = 2 \frac{\partial \theta_1}{\partial t} \tag{5-18}$$

the angle of rotation θ_1 results

$$\theta_1 = \frac{T_1 h}{2} f_2 (s/h) \tag{5-19}$$

where

$$f_2 = \frac{s}{h} t + \frac{32h^2}{\nu\pi^4} \sum_{n=0}^{\infty} \frac{(-1)^n}{(2n+1)^4} \left\{ \exp\left[- \frac{(2n+1)^2\pi^2 t}{4h^2} \right] - 1 \right\} \sin\left[\frac{(2n+1)}{2} \frac{s}{h} \right] \tag{5-20}$$

Figure 5-14 shows the resulting nondimensional vorticity as a function of the nondimensional depth for different values of $\nu t/h^2$.

In order to estimate the applied torque (T_1) and the viscosity ν the least squares method was implemented and the mean quadratic error was defined in Equation (5-11) and becomes a minimum if

$$\frac{\partial \overline{\varepsilon^2}}{\partial T_1} = 0 \; ; \; \frac{\partial \overline{\varepsilon^2}}{\partial \nu} = 0 \tag{5-21}$$

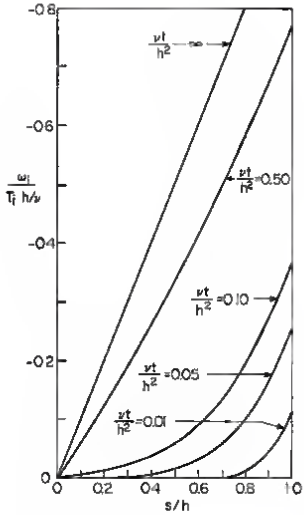

Figure 5-14: Nondimensional Vorticity Distribution Over Depth Inside the Surf Zone

which represents a system of two equations and two unknowns solved by the Newton-Raphson Method. To illustrate the procedure consider Run No. 13. The interval of time considered was 7.6 s (Table 5-5). Since the measurements were taken at a = 1.0 cm (from the bottom), this value was utilized in Equations (5-18) and (5-13). The results were Ti = 2.12 cm/s^2 and ν = 5.05 cm^2/s.

The results of the analysis for those runs inside the breaker zone are presented in Table 5-7. Figure 5-15 shows the correlation between the mean applied torque A_2 and the applied torque Ti for the same runs. For the comparison the applied torque A_2 was expressed in radians/s^2.

Estimation of the Vorticity at the Water Surface

A limited number of experiments were carried out in order to estimate the vorticity at the water surface and at the same time the vorticity close to the bottom inside the breaker zone. Two mills were considered, the mill at a fixed location was as described previously. The other was allowed to float freely in the water surface. Figure 5-16a and b show the area of measurement and the relative location of the mills

The rotations of the fixed and the free mill were recorded on video tape. The area of measurement was about 45 cm by 45 cm placed inside the breakers and the wave period was 1.5 s.

Table 5-7. Values of the Torque (Ti) and the Viscosity, ν, Determined from Measurements of the Angle of Rotation

Run (No.)	T (s)	x (m)	y (m)	h (cm)	ν (cm²/s)	Ti (cm/s²)	$\varepsilon^2 \times 10^{-3}$ (1/s²)
44	1.0	2.59	.15	2.9	.65	-.34	.24
43	1.0	2.59	.46	3.0	6.22	-2.30	.19
42	1.0	2.59	.76	3.2	5.65	-1.70	1.70
45	1.0	2.90	.15	3.0	.31	-.64	.28
54	1.0	3.20	.15	3.1	5.39	-.81	.31
53	1.0	3.20	.46	3.5	4.48	-2.22	.04
55	1.0	3.51	.15	3.1	2.10	-1.74	2.30
33	1.5	2.29	.30	2.5	2.00	-1.38	.17
15	1.5	2.59	.15	3.0	2.30	-2.52	.28
12	1.5	2.59	.46	3.0	2.33	-.58	.24
14	1.5	2.59	.69	3.2	3.60	-1.20	.82
11	1.5	2.90	.38	3.3	1.12	-.42	2.07
22	1.5	3.20	.23	3.1	3.65	-1.52	2.15
13	1.5	3.20	.46	3.5	5.05	-2.12	1.11
2	1.5	3.43	.15	3.1	1.41	-2.28	1.64
200	1.9	2.59	.15	2.9	1.06	-.66	2.77
201	1.9	2.59	.46	3.0	10.13	-2.50	.47
208	1.9	2.90	.46	3.3	2.15	-.35	.42

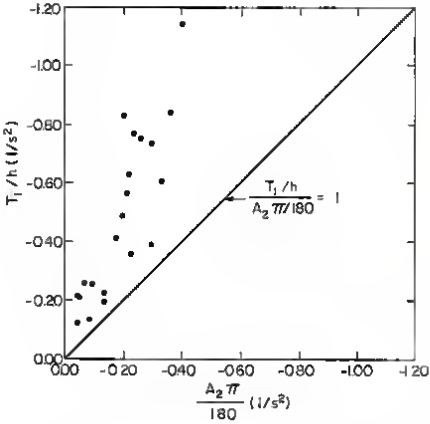

Figure 5-15. Correlation between the Mean Wave-Applied Torque, A_2, and the Wave-Applied Torque at the Water Surface, T_1

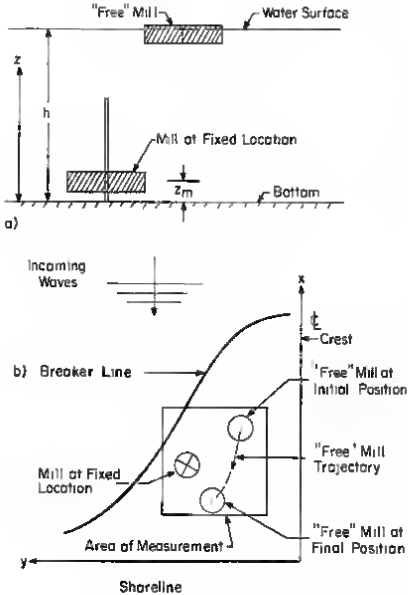

Figure 5-16. Measurements of the Angle of Rotation, θ_m. (a) Relative Position of the "Free" Mill (b) "Free" Mill Trajectory Inside the Surf Zone

Two experiments were carried out at two different locations as shown in Table 5-8.

Table 5-8. Measurements of the Angle of Rotation, θ_m, at the Water Surface. Location and Number of Runs Per Experiment

Experiment	x (m)	y (m)	h (cm)	Number of runs
A	2.74	.61	3.4	12
B	3.35	.46	4.3	3

Each run consisted of a measurement of the rotations of the mills at the bottom and at the free surface. The interval of time considered per run varies from 2 to 9 s. This time corresponds to the time that the mill is inside the area of measurement.

Except for experiment A (Run No. 1) in which the wave-maker was turned on at the beginning of the experiment the rest of the measurements are considered as representing steady state considerations. Since the vorticity is related to the angle of rotation by Equation (5-8), the following equation was used to calculate the vorticity at the water surface and at the bottom

$$\bar{\omega} = 2\,\frac{\Delta\theta}{\Delta t} \qquad (5\text{-}22)$$

Tables 5-9 and 5-10 present a summary of the results.

Table 5-9. Experiment A: Vorticity at the Surface (ω_s) and at the Bottom (ω_b) for x = 2.74 m, y = 0.61 m

Run (#)	ω_s (1/s)	ω_b (1/s)	ω_s/ω_b	Δt (s)
1	-1.000	-.322	3.11	4.50
2	-.590	-.270	2.19	3.00
3	-.952	-.884	1.08	6.00
4	-.780	-.838	.87	4.50
5	-.940	-.482	1.96	4.50
6	-.764	-.538	1.42	6.00
7	-.612	-.508	1.20	6.00
8	-.842	-.618	1.36	3.00
9	-1.304	-.768	1.70	4.50
10	-.786	-.628	1.25	4.50
11	-.962	-.532	1.81	2.00
12	-.260	-.394	.66	3.00

Table 5-10. Experiment B: Vorticity at the Surface (ω_s) and at the Bottom (ω_b) for x = 3.35 m, y = 0.46 m

Run (#)	ω_s (1/s)	ω_b (1/s)	ω_s/ω_b	Δt (s)
1	-.634	-.370	1.71	6.00
2	-.648	-.384	1.69	7.50
3	-.596	-.390	1.53	5.25

From these results it is possible to infer that the mean vorticity at the surface is about 50 percent larger than that sensed by the bottom-mounted mill. Run No. 1 (Experiment A) is considered as nonsteady state conditions so a much larger value of the vorticity (applied torque) at the water surface is expected.

Total Wave-Applied Torque Computed from Early Measurements of the Angle of Rotation of the Mill

Local values of the mean wave-induced torque, A_2, are presented in Tables 5-4, 5-5 and 5-6 for three different wave periods. Here, a numerical integration of A_2 is presented. The area of integration is limited to the zone of wave breaking. The method of integration used was the fourth order Simpson's Rule, which states that the value of integral (I) of a function f(x) in some specific interval (a, b) is approximated by

$$I = \frac{\Delta x}{3} \left(f_o + f_n + 4 \sum_{\substack{j=1 \\ j \text{ odd}}}^{n-1} f_j + 2 \sum_{\substack{j=2 \\ j \text{ even}}}^{n-2} f_j \right) - \frac{(\Delta x)^4}{180} (b - a) \frac{\partial^4 f}{\partial x^4} (\bar{x}) \qquad (5\text{-}23)$$

where Δx is the size of the partition, (n - 1) is the number of partitions and $\bar{x}$ is the mean value of x.

Equation (5-23) was applied in x and y and the results are presented in Table 5-11 for the wave periods investigated. The number of values of A_2, for the case where the period was equal to 1.5 s, was small; so, the resulting value of $(WT)_m$ is considered as approximate.

Table 5-11 Values of the Total Wave-Applied Torque, $(WT)_m$, from Measurements of the Angle of Rotation, θ_m, of the Mill

Period (s)	$(WT)_m$ (m^2/s^2)
1.0	-.30
1.5	-.34
1.9	-.14

Mean Currents

Introduction

The velocity fields were determined by a Lagrangian technique by monitoring the trajectories of floating disks. Their drifting characteristics were compared carefully with dye releases to ensure that they follow the mean current in particular inside the breakers, where no "surfing" tendency was seen. After several tests their behavior was considered representative for measurements purposes.

Initial coordinates for each disk release were selected in the vicinity of the "bar area." Each run consisted of the release of a number of disks, usually between seven and nine with the initial positions in a particular part of the "bar area" as indicated in Figures 5-17, 5-18 and 5-19. These figures show different groups of circles representing the corresponding runs. For instance, in Figure 5-17, Run No. 42 includes three disks represented by three

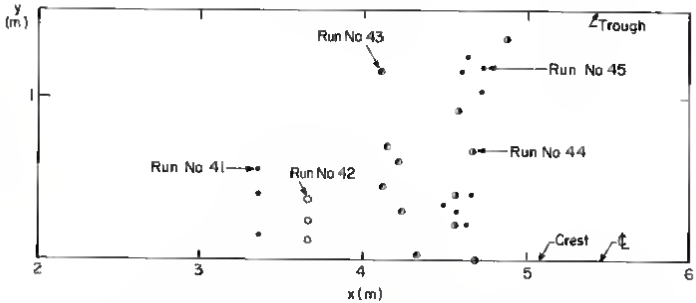

Figure 5-17. Mean Current Measurements: Initial Locations of the Floating Disks; Period = 1.0 s, Each Run Includes All Disks with Common Symbol

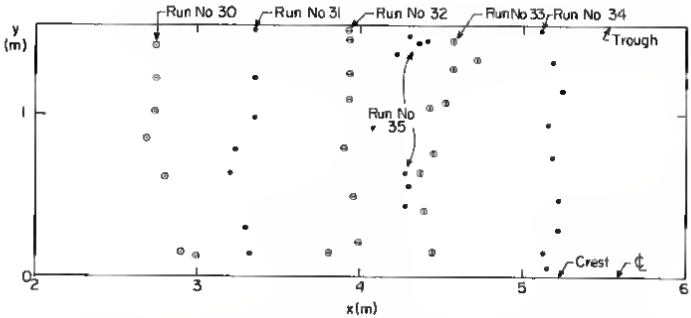

Figure 5-18 Mean Current Measurements. Initial Location of the Floating Disks; Period = 1.5 s, Run Includes All Disks with Each Common Symbol

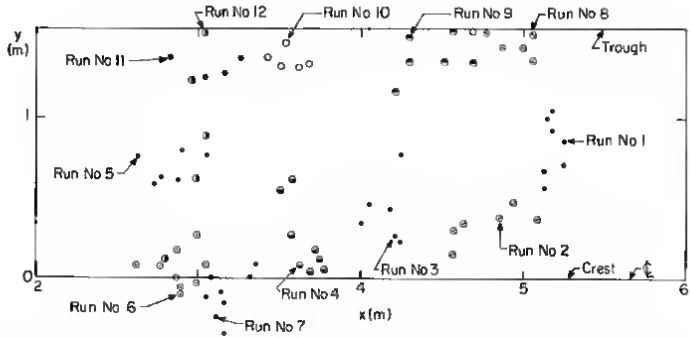

Figure 5-19. Mean Current Measurements: Initial Locations of the Floating Disks, Period = 1.9 s; Each Run Includes All Disks with Common Symbol

empty circles. The circle near the crest identifies Disk No. 01, so the corresponding information is found in Run No. 42/01. The disks are numbered in sequence from the crest to the trough.

The trajectory of each disk was observed from the arrival of the first wave to the location of interest.

The velocity field information was tabulated and is presented in Appendix C. In the heading of Table C-4 numbers separated by a bar (42/01) can be seen, the first indicates the run number and the second the disk number. The table also indicates the time when the wavemaker was turned on and the table itself contains the time, location and velocity components.

Table 5-11 summarizes the number of runs and the number of disks per run for the wave periods under study.

Table 5-11. Mean Currents: Runs and Number of Disks Per Run

Period (s)	Number of Runs	Number of Disks per Run
1.0	5	3 to 8
1.5	5	7 to 9
1.9	12	4 to 9

Each disk is 1.5 cm high so that measurements were terminated before that depth was reached by the disk.

Also, measurements for a particular disk were terminated if the disk was carried out of the field of view of the video camera. Complementary measurements of the velocity field were made through dye releases, to encompass the shallower area of the model where measurements by disks were not practical. Dye measurements are complicated by dispersion effects and thus are not of the same quality as those obtained with the disks. The dye results are also included in Appendix C.

Characteristics of the Mean Current Pattern

The circulation pattern for periods equal to 1.5 s and 1.5 s are shown in Figures 5-20 and 5-21. The velocities represent the average of all measurements made at the particular location. Those measurements indicated by dashed arrows correspond to dye releases and represent an approximate value of the mean velocity given the dispersion of the dye particles inside the surf zone.

Total Frictional Torque Applied to the Bottom Computed from Mean Current Measurements

The wave-induced circulation pattern about the surf zone can be approximate by the following transport stream function, ψ,

$$\psi = \psi_o \sin \frac{\pi(x - x_o)}{L_x} \sin \frac{\pi y}{L_y} \qquad (5\text{-}24)$$

Figure 5-20. Mean Current Measurements: Circulation Pattern; Period = 1.5 s; Floating Disk Trajectories (——) and Dye Releases (---)

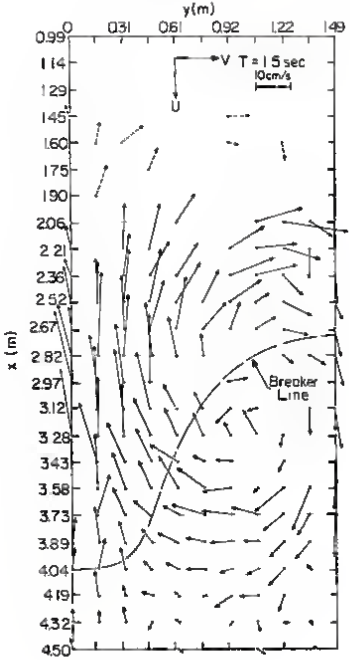
y(m)
0
0.31
0.61
0.92
1.22
1.49
x (m)
0.99
1.14
1.29
1.45
1.60
1.75
1.90
2.06
2.21
2.36
2.52
2.67
2.82
2.97
3.12
3.28
3.43
3.58
3.73
3.89
4.04
4.19
4.32
4.50
V
U
T = 1.5 sec
10cm/s
Breaker Line

Figure 5-21. Mean Current Measurements: Circulation Pattern; Period = 1.3 a; Floating Disk Trajectories (——) and Dye Releases (---)

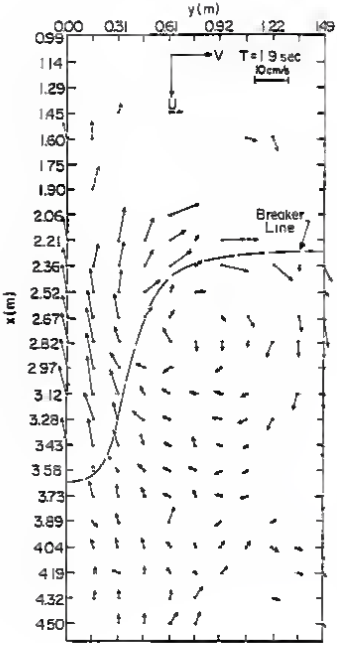
y (m)
0.00
0.31
0.61
0.92
1.22
1.49
x (m)
0.99
1.14
1.29
1.45
1.60
1.75
1.90
2.06
2.21
2.36
2.52
2.67
2.82
2.97
3.12
3.28
3.43
3.58
3.73
3.89
4.04
4.19
4.32
4.50
V
U
T = 1.9 sec
10cm/s
Breaker Line

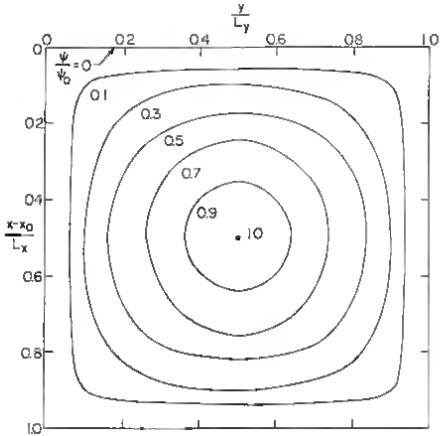

Figure 5-22. Nondimensional Transport Stream Function, ψ/ψ_o

where ψ_o represents the magnitude of the transport stream function, and L_x and L_y are the dimensions of the rectangle which encloses the significant current pattern measured in the model. In addition, the no flow condition is exactly satisfied for $y = 0$, $y = L_y$, $x = x_o + L_x$ and is approximately satisfied for $x = x_o$. This location was chosen instead of the shoreline ($x = x_1$) because computational reasons: The water depth equal to zero introduces an artificial singularity of the integrated wave-applied torque due to the simplicity of the representation of the transport stream function given by Equation (5-24). The transport between $x = x_1$ and $x = x_o$ is very small, so the approximation $x_1 = x_o$ does not introduce any significant error in the calculations. Figure 5-22 shows the ratio ψ/ψ_o for different values of $(x - x_o)/L_x$ and y/L_y.

The transport stream function is related to the currents by the following relationships

$$Uh = -\frac{\partial\psi}{\partial y}$$
$$Vh = \frac{\partial\psi}{\partial x} \tag{5-25}$$

Assuming a linear representation for the friction components (R_x, R_y)

$$R_x = -\frac{A_3 U}{h} = \frac{A_3}{h^2}\frac{\partial\psi}{\partial y}$$
$$R_y = -\frac{A_3 V}{h} = -\frac{A_3}{h^2}\frac{\partial\psi}{\partial x} \tag{5-26}$$

Integrating over the area limited by $x = x_o$, $x = x_o + L_x$, $y = 0$ and $y = L_y$, the steady state mean vorticity equation becomes

$$0 = \underbrace{\int_0^{L_y}\int_{x_o}^{x_o + L_x} A_2 \, dx \, dy}_{(WT)_m} + \underbrace{\int_x^{L_y}\int_{x_o}^{x_o + L_x} \left[\frac{\partial R_y}{\partial x} - \frac{\partial R_x}{\partial y} \right] dx \, dy}_{FT} \tag{5-27}$$

where the first term represents the total wave-applied torque computed from early measurements of the angle of rotation, ϕ_m, of the mill, and the second term represents the total frictional torque applied to the bottom and is computed from measurements of the mean currents.

The contribution of the nonlinear terms is identically zero since there is no flow through the sides of the area of integration. The friction components are

$$\begin{aligned} R_x &= \frac{A_3 \, \phi_o{}'}{h^2 L_y} \sin \frac{\pi(x - x_o)}{L_x} \cos \frac{\pi y}{L_y} \\ R_y &= -\frac{A_3 \, \phi_o{}'}{h^2 L_x} \cos \frac{\pi(x - x_o)}{L_x} \sin \frac{\pi y}{L_y} \end{aligned} \tag{5-28}$$

Integrating the second term of Equation (5-28) in x and y, the following expression is obtained

$$FT = -\int_0^{L_y} R_y \Big|_{x_o}^{x_o + L_y} dy - \int_{x_o}^{x_o + L_x} R_x \Big|_0^{L_y} d_x \tag{5-29}$$

Considering Equation (5-29), Equation (5-30) can be written

$$FT = -\frac{2A_3\,\psi_o\,L_y}{L_x}\left[\frac{1}{h^2(x_o + L_x)} + \frac{1}{h^2(x_o)}\right]$$

$$+ \frac{2A_3\,\psi_o\,\pi\ell}{h_o^2\,L_y}\left[\sin\frac{\pi(x - x_o)}{L_y}\,I_1 \right. \qquad (5\text{-}30)$$

$$\left. + \cos\frac{\pi(x - x_o)}{L_x}\,I_2\right]$$

where

$$I_1 = \sum_{j=0,2,4\ldots} \frac{\left(\frac{x - x_1}{\ell}\right)^{j+1-2m}}{(j+1-2m)} \Bigg|_{x_o}^{x_o + L_x} \qquad (5\text{-}31)$$

$$\frac{\left(\frac{\pi\ell}{L_x}\right)^{j}}{j!}$$

and

$$I_2 = \sum_{j=1,3,5\ldots} \frac{\left(\frac{x - x_1}{\ell}\right)^{j+1-2m}}{(j+1-2m)} \Bigg|_{x_o}^{x_o + L_x} \qquad (5\text{-}32)$$

$$\frac{\left(\frac{\pi\ell}{L_x}\right)^{j}}{j!}$$

To compute FT it is necessary to estimate ψ_o from current measurements. Considering Equation (5-25) and solving for ψ_o the following expressions are obtained.

$$\psi_o = -\frac{Uh\,L_y}{\pi \cos \frac{\pi(x - x_o)}{L_x} \cos \frac{\pi y}{L_y}} \tag{5-33}$$

or

$$\psi_o = \frac{Vh\,L_x}{\pi \cos \frac{\pi(x - x_o)}{L_x} \sin \frac{\pi y}{L_y}} \tag{5-34}$$

From Figure 5-21, for instance, values of U, h, x and y are obtained and ψ_o is calculated. Tables 5-13 and 5-14 show the values of ψ_o obtained.

Table 5-13: Values of ψ_o Obtained from Current Measurements Shown in Figure 5-20; Period = 1.5 s; L_x = 3.68 m and L_y = 1.52 m

x (m)	y (m)	h (cm)	U (cm/s)	$\psi_o \times 10^{-3}$ (cm²/s)
3.12			-21.0	3.20
3.12	.31	3.1	-19.0	3.60
3.12	.46	3.4	-18.0	5.10
3.12	.61	3.7	-8.0	4.70
3.12	1.07	4.4	2.0	.71
3.12	1.37	4.5	9.0	2.06
3.12	1.49	4.6	13.0	2.90
3.73	.15	3.3	-13.0	2.50
3.73	.31	3.6	-9.0	2.25
3.73	.46	4.0	-5.0	1.92
3.73	.61	4.5	-3.5	2.88
3.73	1.22	5.8	5.5	2.22
3.73	1.37	5.9	7.0	2.42
3.73	1.49	6.1	14.0	4.76
3.89	.31	3.6	-7.5	2.06

Table 5-14 Values of ψ_o Obtained from Current Measurements Shown in Figure 5-21; Period = 1.9 s; L_x = 3.36 m and L_y = 1.52 m

x (m)	y (m)	h (cm)	U (cm/s)	$\psi_o \times 10^{-3}$ (cm^3/s)
2.67	0.15	2.8	-8.5	1.21
2.67	0.31	2.8	-7.5	1.27
2.67	0.46	2.8	-4.0	.93
2.67	0.61	2.8	-2.0	.89
2.67	1.07	2.8	3.0	.68
2.67	1.37	2.8	5.0	.71
2.37	0.46	2.6	-5.0	1.13
2.37	0.61	2.6	-4.0	1.72
2.37	0.91	2.6	2.0	.81
2.37	1.22	2.6	4.5	.73
3.28	0.15	3.1	-8.0	1.50
3.28	0.31	3.2	-5.0	1.15
3.28	0.46	3.5	-2.5	.87
3.28	0.61	3.9	-1.0	.74
3.21	0.46	2.2	-6.5	1.31

For illustration purposes Figure 5-23 shows the computed mean velocity profile (x-component) for a period equal to 1.9 s at x = 2.67 m for $\psi_o = 1.04 \times 10^{-3}\ m^3/s$. Considering the values of ψ_o presented in Tables 5-13 and 5-14, and the values of the friction coefficient, A_3, presented in Tables 5-5 and 5-6 and applying Equation (5-30) values of FT were obtained and are shown in Table 5-15.

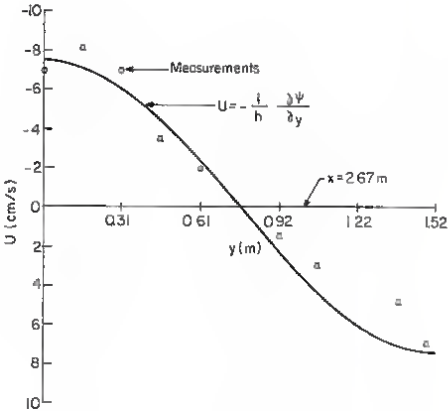

Figure 5-23. Mean Velocity Profile (x-component) at x = 2.67 m for a Period = 1.5 s; Theory Based on Equation (5-24) for $\psi_0 = 1.04 \times 10^{-3}$ cm^3/s and Measurement (o)

Table 5-15. Values of the Total Frictional Torque Applied to the Bottom, FT, Calculated from Current Measurements

Period (s)	A_3 (cm/s)	$\Psi_o \times 10^{-3}$ (cm^3/s)	FT (m^2/s^2)
1.5	1.67 (*)	2.39 (**)	.71
1.5	.57	1.04 (***)	.10

(*) Averaged value from Table 5-5.

(**) Averaged value from Table 5-13.

(***) Averaged value from Table 5-14.

Comparison Between the Steady State Vorticity Computed from Early Measurements of the Angle of Rotation, θ_m, of the Mill, and the Steady State Vorticity Computed from Measurements of the Mean Currents

Considering Equation (5-9) as time goes to infinity, the following expression is obtained

$$\bar{\omega}_s = \frac{A_2 h}{A_3} \tag{5-35}$$

where $\bar{\omega}_s$ is the steady state vorticity calculated from early measurements of the angle of rotation, θ_m, of the mill. Tables 5-5 and 5-6 contain the information needed in order to obtain values of $\bar{\omega}_s$ when A_2 and A_3 are known.

Expressing the mean vorticity as presented in Equation (2-19) and considering Equations (5-24), (5-25) and (5-26), it results

$$\bar{\omega}_f = \frac{\nabla^2\psi}{h} - \frac{1}{h^2}\left(\frac{\partial h}{\partial x}\frac{\partial\psi}{\partial x} + \frac{\partial h}{\partial y}\frac{\partial\psi}{\partial y}\right) \tag{5-36}$$

where $\bar{\omega}_f$ is the steady state mean vorticity computed from mean current measurements, consequently, $\bar{\omega}_f$ can be obtained from the values of ψ_o presented in Table 5-15 and the values of L_x and L_y shown in Tables 5-13 and 5-14. Also, the steady state mean vorticity can be calculated from Equation (5-18), and the data presented in Appendix B. For illustration purposes, consider Figure 5-10. Since $\partial\theta_m/\partial t$ = -13.0 degrees/s the mean vorticity calculated by Equation (5-18) is $\bar{\omega}_g$ = -26.0 (degrees/s) or $\bar{\omega}_g$ = 0.45 1/s. Table 5-16 shows the values obtained for $\bar{\omega}_a$, $\bar{\omega}_f$ and $\bar{\omega}_g$.

Table 5-15. Values of the Steady State Mean Vorticities, $\bar{\omega}_s$, $\bar{\omega}_f$ and $\bar{\omega}_g$ for Those Runs Where A_3 Was Calculated

Run (No.)	h (cm)	A_2 ($1/s^2$)	A_3 (cm/s)	$\psi_o \times 10^{-3}$ (cm^3/s)	$\bar{\omega}_s$ (1/s)	$\bar{\omega}_f$ (1/s)	$\bar{\omega}_g$ (1/s)
33	2.5	-.295	1.44	2.89	-.51	-.31	-.50
12	2.9	-.131	1.48	2.89	-.26	-.47	-.32
14	3.2	-.234	2.14	2.89	-.36	-.55	-.33
11	3.3	-.085	1.21	2.89	-.23	-.39	-.30
22	3.1	-.205	1.08	2.89	-.59	-.23	-.45
13	3.5	-.329	2.64	2.89	-.44	-.36	-.45
200	2.9	-.138	.57	1.04	-.70	-.07	-.52

CHAPTER 6
COMPARISON WITH THEORY

Introduction

In this chapter a comparison is made between the experimental and available mathematical representations of the physical processes, forming the focus of this study. In particular, an analytical representation of the bottom bathymetry and the refraction pattern is introduced considering the wave field to be represented by the shallow water wave case. Finally, a calculation of the predicted wave-induced applied torque and the wave set-up distribution are presented.

Analytical Representation of the Bathymetry

The bottom bathymetry represented in the model may be approximated by

$$h = h_1 + u\, h_2\, \phi \tag{6-1}$$

where

$$h_1 = h_o \left(\frac{x - x_1}{\ell} \right)^m$$

$$h_2 = h_o \left(\frac{x - x_2}{\ell} \right) \left(\frac{x - x_3}{\ell} \right) \tag{6-2}$$

$$\phi = (1 + \cos \lambda y)$$

and $h_0 = 13.6$ cm, $m = 1.25$, $x_1 = .91$ m, $x_2 = 2.44$ m, $x_3 = 6.10$ m, $\ell = 5.19$ m, $\lambda = 2\pi/L_b$ where $L_b = 3.04$ m is the wavelength of the bottom undulations along the shore and $\mu = .75$ is a dimensionless parameter. In spite of the rather large value of μ the second term in Equation (6-1) is small compared with the leading term. Figure 6-1 shows the theoretical and the actual bathymetry. Table 6-1 presents the depth as calculated by Equation (6-1).

Table 6-1. Idealized bathymetry

y(m) / x(m)	-1.52	-1.22	-0.91	-0.61	-0.30	0.00
0.91						0.0
1.22						0.4
1.52			(depth h in centimeters)			0.9
1.83						1.6
2.13						2.2
2.44						2.9
2.74	3.7	3.6	3.4	3.2	3.0	2.9
3.05	4.5	4.4	4.0	3.6	3.2	3.1
3.35	5.3	5.1	4.6	4.1	3.6	3.4
3.66	6.1	5.9	5.4	4.7	4.1	3.9
3.96	7.0	6.8	6.2	5.4	4.8	4.5
4.27	7.9	7.6	7.0	6.2	5.6	5.3
4.57	8.8	8.6	7.9	7.2	6.6	6.3
4.88	9.7	9.5	8.9	8.2	7.7	7.4
5.18	10.6	10.5	10.0	9.4	8.9	8.7
5.49	11.6	11.5	11.1	10.7	10.3	10.2
5.79	12.6	12.5	12.3	12.1	11.9	11.8
6.10						13.5

Refraction

The refraction pattern in the absence of currents is described by Equation (2-5). For shallow water waves

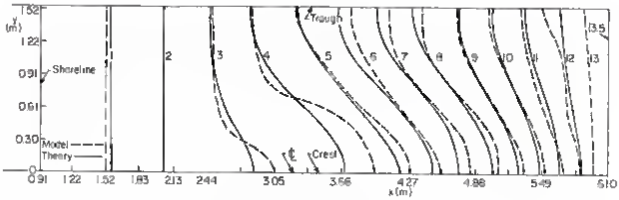

Figure 6-1. Idealized (——) and Actual (---) Bathymetry; Contours of Equal Depth in cm

$(k = \sigma/(gh)^{1/2})$ and for small local angle of incidence $(\cos\alpha \sim -1)$ the refraction equation can be written

$$\frac{\partial(k \sin\alpha)}{\partial x} = \frac{\sigma}{2g^{1/2}} \frac{h_2}{h_1^{3/2}} \frac{\partial\phi}{\partial y} \tag{6-3}$$

and the solution of the Equation (6-3) is expressed as

$$(k \sin\alpha) = (k \sin\alpha)^{(1)} + \mu (k \sin\alpha)^{(2)} \tag{6-4}$$

where the first term represents the solution for a regular sloping beach and the second term is the contribution to the solution due to the presence of alongshore bottom undulations. Substituting Equation (6-4) in Equation (6-5) and collecting terms by their order, the following differential equations were obtained:

$$\frac{\partial(k \sin\alpha)^{(1)}}{\partial x} \doteq 0 \tag{6-5}$$

$$\frac{\partial(k \sin\alpha)^{(2)}}{\partial x} = \frac{\sigma}{2g^{1/2}} \frac{h_2}{h_1^{3/2}} \frac{\partial\phi}{\partial y} \tag{6-6}$$

since the waves approached the model at normal incidence Equation (6-5) becomes

$$(k \sin\alpha)^{(1)} = (k_o \sin\alpha_o) = 0 \tag{6-6}$$

where the subscript (o) indicates deepwater conditions. Integrating Equation (6-6)

$$(k \sin \alpha)^{(2)} = \frac{\sigma}{2g^{1/2}} \frac{\partial \phi}{\partial y} \int \frac{h_2}{h_1^{3/2}} \, dx + \text{constant} \tag{6-8}$$

considering Equations (6-2) and the fact that

$$(k \sin \alpha)^{(2)} = 0 \quad \text{at} \quad X = \frac{x - x_1}{\ell} = 1 \tag{6-9}$$

results in

$$\sin \alpha = -\mu \frac{\lambda \ell}{2} f_3 \sin \lambda y \tag{6-10}$$

where

$$f_3 = X^{p_1} \left(\frac{X^{p_2} - 1}{p_2} + p_5 \frac{X^{p_3} - 1}{p_3} + p_6 \frac{X^{p_4} - 1}{p_4} \right) \tag{6-11}$$

and

$$\begin{aligned} p_1 &= m/2 \\ p_2 &= 3 - 3m/2 \\ p_3 &= 2 - 3m/2 \\ p_4 &= 1 - 3m/2 \\ p_5 &= \frac{2x_1 - x_2 - x_3}{\ell} \\ p_6 &= \frac{(x_1 - x_3)(x_1 - x_2)}{\ell^2} \end{aligned} \tag{6-12}$$

The local angle of incidence α is shown in Figure 6-2.

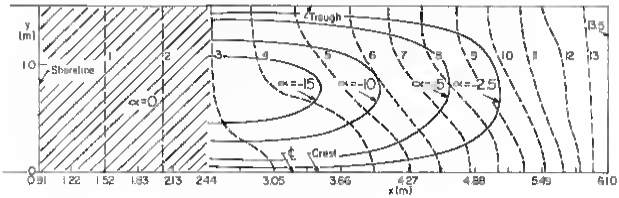

Figure 5-2. Theoretical Local Wave Angle of Incidence α in Degrees

Theoretical Wave-Applied Torque Inside the Surf Zone

The wave-applied torque A_2 is expressed as

$$A_2 = \frac{\partial T_y}{\partial x} - \frac{\partial T_x}{\partial y} \tag{6-13}$$

considering Equation (2-11) and assuming that Equation (5-13) becomes

$$\begin{aligned} A_2 = & -\frac{1}{\rho h^2}\frac{\partial h}{\partial y}\left(\frac{\partial S_{xx}}{\partial x} + \frac{\partial S_{xy}}{\partial y}\right) \\ & - \frac{\partial h}{\partial x}\left(\frac{\partial S_{yy}}{\partial y} + \frac{\partial S_{xy}}{\partial x}\right) \\ & - \frac{1}{\rho h}\left(\frac{\partial^2 S_{yy}}{\partial x \partial y} + \frac{\partial^2 S_{xy}}{\partial x^2} - \frac{\partial^2 S_{xx}}{\partial x \partial y} - \frac{\partial^2 S_{xy}}{\partial y^2}\right) \end{aligned} \tag{6-14}$$

Since the depth, sin α and wave height have been expanded in terms of the parameter μ, the terms of the applied torque will be examined in the same way. The order of the variables is

$$\begin{aligned} & \left(\frac{\partial S_{xx}}{\partial x};\ \frac{\partial h}{\partial x}\right) \longrightarrow (1) \\ & \left(\frac{\partial h}{\partial y};\ \frac{\partial S_{xy}}{\partial y};\ \frac{\partial S_{yy}}{\partial y},\ \frac{\partial S_{xy}}{\partial x};\ \frac{\partial^2 S_{yy}}{\partial x \partial y};\right. \\ & \left.\frac{\partial^2 S_{xy}}{\partial x^2};\ \frac{\partial^2 S_{xx}}{\partial x \partial y};\ \frac{\partial^2 S_{xy}}{\partial y^2}\right) \longrightarrow (\mu) \end{aligned} \tag{6-15}$$

which indicates that the wave-applied torque is of order μ. In other words, no torque is generated unless some alongshore variation of the bathymetry is present. The individual terms of Equation (6-14) (provided that the wave breaking height is assumed to be proportional to the local depth, $H = \gamma h$) are

$$I = -\frac{1}{\rho h^2}\frac{\partial h}{\partial y}\frac{\partial S_{xx}}{\partial x} = -\frac{3g\gamma^2}{8h}\frac{\partial h}{\partial x}\frac{\partial h}{\partial y} \tag{6-16}$$

$$II = -\frac{1}{\rho h^2}\frac{\partial h}{\partial x}\frac{\partial S_{yy}}{\partial y} = \frac{g\gamma^2}{8h}\frac{\partial h}{\partial x}\frac{\partial h}{\partial y} \tag{6-17}$$

$$\begin{aligned} III = {} & \frac{1}{\rho h^2}\frac{\partial h}{\partial x}\frac{\partial S_{xy}}{\partial x} \\ & - \frac{g\gamma^2}{8h}\frac{\partial h}{\partial x}\left(2\frac{\partial h}{\partial x}\sin\alpha + h\frac{\partial \sin\alpha}{\partial x}\right) \end{aligned} \tag{6-18}$$

$$IV = -\frac{1}{\rho h}\frac{\partial^2 S_{yy}}{\partial x \partial y} = -\frac{g\gamma^2}{8h}\left(\frac{\partial h}{\partial x}\frac{\partial h}{\partial y} + h\frac{\partial^2 h}{\partial x \partial y}\right) \tag{6-19}$$

$$\begin{aligned} V = {} & -\frac{1}{\rho h}\frac{\partial^2 S_{xx}}{\partial x^2} = -\frac{g\gamma^2}{8h}\left[2\left(\frac{\partial h}{\partial x}\right)^2 \sin\alpha \right. \\ & + 2h\frac{\partial^2 h}{\partial x^2}\sin\alpha + 4h\frac{\partial h}{\partial x}\frac{\partial \sin\alpha}{\partial x} \\ & \left. + h\frac{\partial^2 \sin\alpha}{\partial x^2}\right] \end{aligned} \tag{6-20}$$

$$VI = \frac{1}{\rho h}\frac{\partial^2 S_{xx}}{\partial x \partial y} = \frac{3g\gamma^2}{8h}\frac{\partial h}{\partial y}\frac{\partial h}{\partial x} + h\frac{\partial^2 h}{\partial x \partial y} \tag{6-21}$$

$$\text{VII} = \frac{1}{\rho h}\frac{\partial^2 S_{xy}}{\partial y^2} = -\frac{\gamma y^2}{2} h \frac{\partial^2 \sin}{\partial y^2} \qquad (6\text{-}22)$$

therefore, the wave-applied torque becomes

$$A_2 = \frac{\gamma y^2}{4}\left[\frac{\partial^2 h}{\partial x \partial y} + \frac{3}{2}\frac{\partial h}{\partial x}\frac{\partial \sin \alpha}{\partial x} + \frac{\partial^2 h}{\partial x^2}\sin\alpha + \frac{h}{2}\left(\frac{\partial^2 \sin \alpha}{\partial x^2}\frac{\partial^2 \sin \alpha}{\partial y^2}\right)\right] \qquad (6\text{-}23)$$

The individual terms in Equation (6-14) (Equations (6-16) to (6-22)) are presented in Figures 6-3 to 6-5 and the sum of those terms given by Equation (6-23) is presented in Figure 6-6. The term II has been omitted in these figures because it differs from term I by a constant.

The integration of Equation (6-23) using Simpson's Rule over the breaker zones indicated in Figure (5-12 gives the total wave-applied torque predicted by theory, $(WT)_p$, for the three periods investigated. These results and the values of $(WT)_m$ and FT are included in Table 6-2 for comparison purposes.

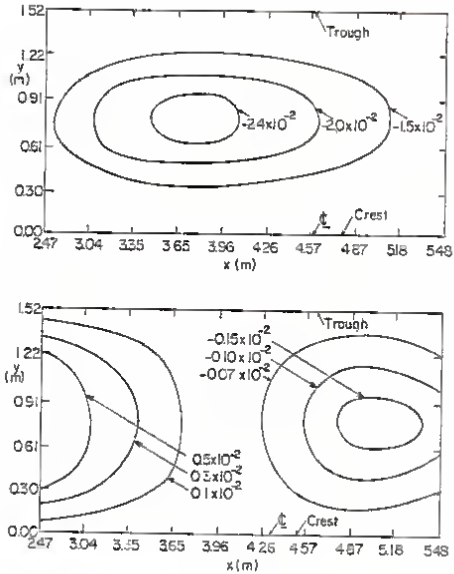

Figure 6-3. Values Inside the Figures Indicate I and III Assuming Breaking Wave Conditions; Upper: Distribution of I Given by Equation (6-16) in $1/s^2$; Lower: Distribution (6-18) in $1/s^2$

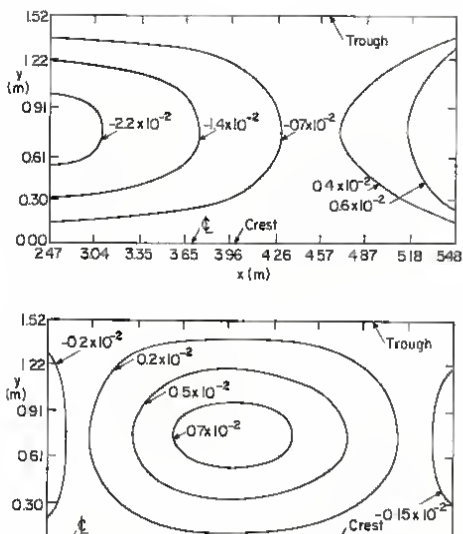

Figure 6-4. Values Inside the Figures Indicate IV and V Assuming Breaking Wave Conditions, Upper: Distribution of IV Given by Equation (6-19) in $1/s^2$; Lower: Distribution (6-20) in $1/s^2$

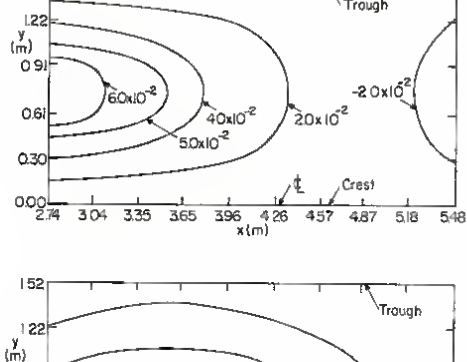

Figure 6-5. Values Inside the Figures Indicate V1 and VII Assuming Breaking Wave Conditions; Upper: Distribution of VI Given by Equation (6-21) in $1/s^2$; Lower: Distribution (6-22) in $1/s^2$

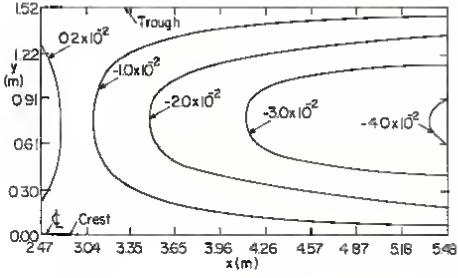

Figure 6-6. Distribution of the Wave-Applied Torque (I + II + III + IV + V + VII) or Equation (6-23), Values Inside Indicate A_2 in l/s^2, Assuming Breaking Wave Condition

Table 6-2 Values of $(WT)_m$, FT and $(WT)_p$ for the Periods Considered

Period (s)	$(WT)_m$ (m^2/s^2)	FT (m^2/s^2)	$(WT)_p$ (m^2/s^2)
1.0	-.30	--	-.07
1.5	-.34	-.71	-.05
1.9	-.14	-.10	-.02

NOTE: FT for T = 1.0 s was not calculated due to the complexity of the warrant period.

Wave Set-Up Distribution

In this section a qualitative distribution of the wave set-up over the "bar area" is developed. The analysis is based on Equations (2-8) and (2-9) when the inertia terms are neglected, so

$$0 = -g \frac{\partial \bar{\eta}}{\partial x} + R_x + T_x \tag{6-24}$$

$$0 = -g \frac{\partial \bar{\eta}}{\partial y} + R_y + T_y \tag{6-25}$$

where the friction terms (R_x, R_y) and the forcing terms (T_x, T_y) are given by Equations (2-17) and (2-11), respectively Assuming that all variables involved in the problem can be represented by expanding in terms of the parameter μ, it follows

$$\bar{\eta} = \bar{\eta}^{(1)} + \mu \bar{\eta}^{(2)} \tag{6-26}$$

$$(R_x, R_y) = (R_x^{(1)}, R_y^{(1)}) + \mu\ (R_x^{(2)}, R_y^{(2)}) \qquad (6\text{-}27)$$

$$(T_x, T_y) = (T_x^{(1)}, T_y^{(1)}) + \mu\ (T_x^{(2)}, T_y^{(2)}) \qquad (6\text{-}28)$$

where the superscript (2) is associated with the contribution to the set-up due to the bottom undulations.

Since in the absence of y-related variations in the bathymetry, the x-component of the mean velocity, $U^{(1)}$ is zero, and, for normally incident waves the y-component of the mean velocity is zero, it follows from Equation (2-17)

$$(R_x^{(1)}, R_y^{(1)}) = 0 \qquad (6\text{-}29)$$

Substitution Equations (6-26), (6-27) and (6-28) in Equations (6-24) and (6-25) and considering Equation (6-29), the following results are obtained after separating by order

$$0 = -g\ \frac{\partial \bar{\eta}^{(1)}}{\partial x} + T_x^{(1)} \qquad (6\text{-}30)$$

$$0 = -g\ \frac{\partial \bar{\eta}^{(2)}}{\partial x} + R_x^{(2)} + T_x^{(2)} \qquad (6\text{-}31)$$

$$0 = -g\ \frac{\partial \bar{\eta}^{(2)}}{\partial y} + R_y^{(2)} + T_y^{(2)} \qquad (6\text{-}32)$$

Recalling the water depth as

$$h = h^{(1)} + \mu\ h^{(2)} \qquad (6\text{-}33)$$

where

$$h^{(1)} = h_o h_1$$
$$h^{(2)} = h_o h_2 \phi \tag{6-34}$$

And considering first the forcing term $T_x^{(1)}$ from Equation (2-12), the following expression is obtained

$$T_x^{(1)} = -\frac{3g\gamma^2}{8} \frac{(\bar{\eta}^{(1)} + h^{(1)})}{\partial x} \tag{6-35}$$

combining the above equation and Equation (6-30) and integrating

$$\bar{\eta}^{(1)} = -\beta h^{(1)} + \bar{\eta}_o \tag{6-36}$$

where

$$\beta = \frac{3\gamma^2}{8(1 + \frac{3\gamma^2}{8})} \tag{6-37}$$

$\bar{\eta}_o$ is a constant of integration which can be evaluated at the breaking point where the wave height is expressed as

$$H_b = \gamma(\bar{\eta}_b^{(1)} + h_b) \tag{6-38}$$

where the subscript (b) indicates breaking conditions. Substituting Equation (6-37) in Equation (6-36) the constant $\bar{\eta}_o$ results

$$\bar{\eta}_o = \beta h_b - \frac{\gamma^2}{16} h_b \tag{6-39}$$

Finally, Equation (6-36) becomes

$$\bar{\eta}^{(1)} = \xi (h_b - h^{(1)}) - \frac{\gamma^2 h_b}{16} \tag{6-40}$$

which represents the well known set-up distribution over a sloping beach.

Considering first the forcing term in the y-direction and recalling Equations (2-11) and (2-12), it follows

$$\tau_y^{(2)} = - \frac{1}{\rho(\bar{\eta}^{(1)} + h^{(1)})} \left(\frac{\partial S_{yy}^{(2)}}{\partial y} \quad \frac{\partial S_{xy}^{(2)}}{\partial x} \right) \tag{6-41}$$

where

$$\frac{\partial S_{xx}^{(2)}}{\partial y} = \frac{\rho g \gamma^2}{8} \left[(\bar{\eta}^{(1)} + h^{(1)}) \frac{\partial \bar{\eta}^{(2)}}{\partial y} + h^{(1)} \frac{\partial h^{(2)}}{\partial y} \right] \tag{6-42}$$

and from Equation (6-10)

$$\frac{\partial S_{xy}^{(2)}}{\partial x} = \frac{\rho g \gamma^2}{16} \lambda \ell \sin \lambda y \frac{\partial}{\partial x} \left[(\bar{\eta}^{(1)} + h^{(1)}) f_3 \right] \tag{6-43}$$

Substituting Equation (6-41), considering Equations (6-42) and (6-43), recalling Equation (6-10) and operating, Equation (6-32) can be written as

$$\frac{\partial \bar{\eta}^{(2)}}{\partial y} = \frac{\sin \lambda y}{g(1 + \frac{\gamma^2}{8})} f_4 \tag{6-44}$$

where

$$f_4 = \frac{A_3\ \psi_o\ \pi}{(\bar{\eta}^{(1)} + h^{(1)})^2\ L_x} \cos \frac{\pi(x - x_o)}{L_x}$$

$$+ \frac{\lambda\ h_2\ h_o\ g\gamma^2\ h^{(1)}}{8(\bar{\eta}^{(1)} + h^{(1)})} \tag{6-45}$$

$$- \frac{g\gamma^2\ \lambda\ell}{16(\bar{\eta}^{(1)} + h^{(1)})} \frac{\partial}{\partial x} [(\bar{\eta}^{(1)} + h^{(1)})^2\ f_3]$$

integrating Equation (6-44)

$$\bar{\eta}^{(2)} = - \frac{\cos \lambda y}{\lambda g(1 + \frac{\gamma^2}{8})} f_4 + B \tag{6-46}$$

where B results to be zero or a constant as will be demonstrated. As Equation (6-46) is substituted in Equation (6-31) and integrated between y = 0 and y = L_y

In order to illustrate this result, Figure 6-7 shows the first order set up, $\bar{\eta}^{(1)}$, and the total set-up, $\bar{\eta}^{(1)} + \mu\ \bar{\eta}^{(2)}$, for an arbitrary location of the breaker line and for the following parameters

$$L_x = 3.36\ m$$

$$L_y = 1.52\ m$$

$$h_b = 5.3\ cm$$

$$A_3 = 10^{-2}\ m/s$$

$$\psi_o = 10^{-3}\ m^3/s$$

Figure 6-7. Wave Set-Up Distribution: A Qualitative Description, the Superscript (1) Indicates a First Order Set-Up, Only a Function of x, the Superscript (2) Indicates the Contribution Due to the Bottom Undulations; Values of the Set-Up in m

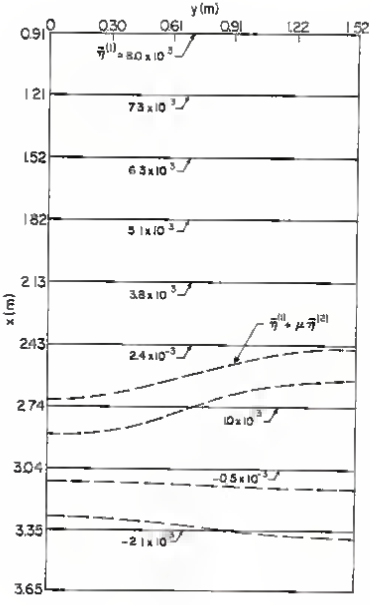
y (m)
0
0.30
0.61
0.91
1.22
1.52
x (m)
0.91
1.21
1.52
1.82
2.13
2.43
2.74
3.04
3.35
3.65
$\bar{\eta}^{(1)} = 8.0 \times 10^{-3}$
7.3×10^{-3}
6.3×10^{-3}
5.1×10^{-3}
3.8×10^{-3}
$\bar{\eta}^{(1)} + \mu\bar{\eta}^{(2)}$
2.4×10^{-3}
1.0×10^{-3}
-0.5×10^{-3}
-2.1×10^{-3}

Computed and Predicted Friction Coefficient

The average value of the friction coefficient A_3 resulted equal to 1.62 cm/s. In order to evaluate the representativity of that value consider Laminar flow which is appropriate for the conditions given in the model. The linearization of the bottom shear stresses presented in Chapter 2 implies that

$$A_3 = \frac{\bar{f}}{8} u \tag{6-47}$$

where $\bar{f}$ is the Darcy friction factor and the wave orbital velocity. For laminar flow $\bar{f}$ can be expressed as

$$\bar{f} = \frac{8}{\sqrt{R_e}} \tag{6-48}$$

where R_e represents the Reynolds number given by

$$R_e = \frac{u^2}{\sigma \nu} \tag{6-49}$$

where u/σ represents the excursion of the water particles. Substituting Equation (6-49) in Equation (6-48) the friction coefficient, A_3, becomes

$$A_3 = \sqrt{\sigma \nu} \tag{6-50}$$

Considering the kinematic viscosity ranging from 0.01 cm^2/s to 1 cm^2/s and assuming a wave period equal to 1.5 s, A_3 becomes

$$2.0 \frac{cm}{s} > A_3 > 0.2 \frac{cm}{s}$$

which is within the range of the computed values of A_3 presented in Tables 5-5 and 5-6.

CHAPTER 7
CONCLUSIONS AND RECOMMENDATIONS

A number of conclusions and recommendations are warranted as a result of this investigation. Conclusions drawn from this study must be interpreted with a view toward the effects of a more general type of bottom bathymetry in spite of the fact that the experimental data were acquired for only one topography. The conclusions and recommendations of this investigation are enumerated below.

The general circulation pattern is in qualitative agreement with the expected model based on the gradients of the radiation stress tensor. This includes a shoreward-directed flow over the bar crest and a return flow from the trough regions. The theoretical results presented in this study and those obtained by Mei and Liu (1977) predicted a counter-circulation within a small region near the shoreline which was not observed in the model data. This effect might be due to the absence of lateral mixing in the theoretical considerations.

Measured values of the wave height are in good agreement with prediction, based on the simple spilling breaking assumption. The proportionality factor γ between the wave height and the local water depth varies from .6 to 1.0. The smaller values corresponded to regions of mild bottom slope

and the larger values corresponded to regions of steep bottom slope, which is in agreement with the results obtained by Dally et al. (1985).

The local wave-induced torque computed from measurements of the angle of rotation of the mill indicate an overall mean value of $A_2 = -.15\ 1/s^2$. Maximum values of A_2 were obtained between the crest (centerline) of the "bar" and the midpoint between the crest and trough. Theory predicts maximum values of A_2 at the midpoint between crest and trough.

Values of the friction (dimensional) coefficient, A_3, from measurements of the angle of rotation of the mill, yield an average value of $A_3 - 1.5$ cm/s, which is within the expected range based on Reynolds Number characteristic of the model and bottom texture.

Based on the transient vorticity diffusion model the wave-applied torque T_1/h located at the water surface is about two times larger than the wave-applied torque, A_2, considered to be uniformly distributed over depth.

Measurements (steady state) of the angle of rotation of the mill at the water surface ("free" mill) and at mid-depth ("fixed" mill) indicate that the vorticity at the water surface is about two times larger than that at mid-depth, which is consistent with that mentioned above.

The total (integrated over the surf zone) wave-induced torque was computed from two independent data sources and compared with the theory of Mei and Liu.

The total (transient) wave-induced torque, $(WT)_m$, was computed from the transient phase of the measurements of the angle of rotation of the mill based on the mean (depth integrated and time averaged, over one wave period) vorticity equation in the absence of nonlinear terms.

The total (steady state) frictional torque applied to the bottom, FT, was computed from mean current measurements based on the mean vorticity equation and assuming an approximate form of the transport stream function in accord with observations of the circulation pattern.

Since $(WT)_m$ and FT should be equal from theory, the resulting values were compared along with the predicted total wave-induced torque $(WT)_p$, for the three periods investigated. The results indicate that $(WT)_m$ and FT (which are calculated from independent data sources) are in reasonable agreement. However, the predicted values of $(WT)_p$ are smaller by a factor of five to ten than $(WT)_m$ and FT. No explanation has been found for the disagreement and future efforts should be concentrated on resolving the discrepancy between theory and measurements.

The steady state mean vorticity was computed in the following three ways:

(a) by measurements of the angle of rotation of the mill and the computations based on the mean vorticity equations,

(b) by mean current measurements and the computations based on the relationship between vorticity and the mean current components, and

(c) by measurements of the angle of rotation of the mill and the computations based on the relationship between vorticity and angular velocity.

The results from these three approaches were in general agreement.

The floating disks used to measure mean currents did not experience any rotation outside the surf zone; however, rotation started as soon as the disks entered the surf zone. This observation agrees with the theoretical considerations that mean vorticity is only generated as a result of energy dissipation.

The mechanics of the mill used to "measure" vorticity are not completely understood in spite of the fact that the results inferred are reasonable when compared with an independent data source such as mean current measurements. Further studies are needed for a better understanding of the mechanics of the mill under the effect of the wave field.

Future studies should include testing with floating mills and "fixed" mills. Also, a larger scale model would be desirable, as a larger surf zone would allow a more detailed and smoother hydraulic regime; consequently, better measurements would be obtained. The mill should occupy a larger portion of the total water depth but avoid contact with the bottom during the passage of the trough. Also,

measurements of the mean water level are suggested because currents inside the surf zone are driven by water slopes. Finally, an automated way to analyze the data should be developed.

The primary purpose of this work was not to study sediment transport; however, the following comments can be made based on hydrodynamic consideration.

(a) As a result of the refraction process, convergence of waves over the crest of the bar occur. Waves break first over the crest and later over the trough inducing a set-up responsible for the generation of currents over the crest of the bar to shore and back through the trough. This circulation associated with the bar might be interpreted as a self-maintenance mechanism for these sand features as indicated by Niedoroda (1972) after a qualitative analysis of natural and laboratory-made bars. The present study seems to agree with Niedoroda's observations, for those bars confined to the surf zone.

(b) Since these circulations have a scale proportional to the width of the surf zone, no conclusions about large scale bars (also called "sand ridges" which have a length 50 to 100 times the size of the surf zone) can be drawn from this study.

APPENDICES

APPENDIX A
WAVE HEIGHT DATA

Table A-1. Wave Height Distribution in cm; Wave Period = 1.0 s

x(m) \ y(m)	-1.52	-1.22	-0.91	-0.61	-0.30	0.[illegible]
1.83	1.2	0.9	0.9	0.9	0.9	0.[illegible]
2.13	1.6	1.2	1.1	1.0	1.2	1.3
2.44	1.5	1.7	1.7	1.5	1.3	1.3
2.74	1.9	2.4	1.9	1.8	1.7	1.6
3.05	2.8	2.7	2.4	2.2	1.9	1.7
3.35	3.3	3.4	3.7	2.7	1.8	1.8
3.66	2.8	3.4	3.9	3.4	2.2	2.0
3.96	3.0	3.7	3.6	4.4	2.9	2.6
4.27	2.8	3.7	3.0	4.0	4.2	4.1
4.57	3.1	3.4	3.2	3.7	4.7	4.4
4.88	2.9	2.7	3.2	3.5	3.6	3.5
5.18	3.2	2.7	3.7	3.7	2.7	2.8
5.48	3.3	3.0	3.0	3.0	1.9	2.3
5.79	2.7	3.5	3.2	2.6	1.7	2.1
6.10	3.0	3.5	3.2	2.2	2.0	2.1

Table B-3. Wave Height Distribution in cm, Wave Period [illegible] s

x(m) \ y(m)	-1.52	-1.22	-0.91	-0.61	-0.30	0.00
1.83						
2.13	1.6	1.2	1.1	1.2	1.2	1.1
2.44	1.8	1.8	1.8	1.5	1.4	1.3
2.74	3.1	1.7	1.6	2.2	1.6	1.3
3.05	2.2	1.7	1.9	2.4	1.6	1.4
3.35	1.7	1.4	1.7	2.9	2.0	1.8
3.66	1.3	1.6	1.7	2.0	2.4	2.5
3.96	1.9	1.4	1.5	1.7	4.3	4.4
4.27	1.4	1.5	1.3	1.7	3.7	3.7
4.57	1.4	1.3	1.4	1.6	2.9	3.4
4.88	1.2	1.3	1.5	1.8	2.4	2.3
5.18	1.3	1.5	1.7	1.8	2.1	2.6
5.49	1.2	1.6	1.7	1.7	1.8	2.2
5.79	1.5	1.7	1.8	1.9	1.9	2.0
6.10	1.9	2.0	2.0	2.0	2.0	2.0

Table A-3. Wave Height Distribution in cm, Wave Period = 1.9 s

y(m) / x(m)	-1.52	-1.22	-0.91	-0.61	-0.30	0.00
1.83	0.9	1.1	1.0	0.9	1.1	1.1
2.13	1.0	1.1	1.0	1.3	1.4	1.5
2.44	1.0	0.9	1.1	1.7	1.8	1.8
2.74	0.8	0.9	1.1	1.3	1.9	1.8
3.05	1.0	0.9	1.1	1.1	2.3	1.9
3.35	1.0	0.9	1.0	1.1	2.2	2.3
3.66	1.1	0.9	0.9	1.0	2.0	2.3
3.96	1.0	1.1	1.0	1.1	1.6	2.3
4.27	0.9	1.0	1.1	1.1	1.4	1.6
4.57	0.8	1.0	1.0	1.1	1.3	1.5
4.88	1.1	1.0	1.0	1.0	1.1	1.1
5.18	1.2	1.1	1.0	1.1	1.0	1.1
5.49	1.1	1.1	0.9	1.0	1.0	1.0
5.79	1.0	0.9	1.0	0.9	1.2	1.1
6.10	1.1		1.1	1.0	1.0	1.0

APPENDIX B
VORTICITY DATA

TABLE [illegible] Angle of Rotation θ_m Versus Time; Run No. 40; Depth = 2.5 cm; Period = 1.0 sec; Location X = 2.25 m, Y = 0.30 m

time (s)	θ_m (deg)	time (s)	θ_m (deg)	time (s)	θ_m (deg)	time (s)	θ_m (deg)
0.00	0.0	0.15	-1.0	0.25	-2.0	0.41	-4.0
0.61	-5.0	1.11	-9.0	1.45	-11.0	1.98	-15.0
2.52	-20.0	4.80	-21.0	5.22	-25.0	5.45	-30.0
6.00	-38.0	6.29	-43.0	6.50	-48.0	7.25	-57.0
7.80	-62.0	8.20	-67.0	8.50	-72.0	8.80	-76.0
9.46	-81.0	10.16	-86.0	10.69	-91.0	11.40	-97.0
12.20	-107.0	12.73	-116.0	13.36	-126.0		

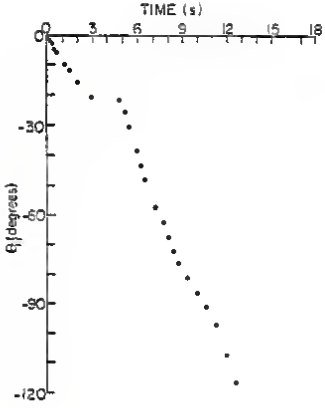

Table B-2. Angle of Rotation θ_m Versus Time, Run No. 41; Depth = 2.5 cm; Period = 1.0 s; Location X = 2.29 m, Y = 0.76 m

time (s)	θ_m (deg)	time (s)	θ_m (deg)	time (s)	θ_m (deg)	time (s)	θ_m (deg)
0.00	0.0	0.86	-1.0	3.85	-5.0	4.27	-17.0
4.45	-22.0	5.00	-32.0	5.20	-37.0	5.43	-42.0
5.67	-47.0	6.03	-52.0	6.50	-57.0	7.07	-62.0
8.47	-60.0	8.70	-57.0	9.74	-51.0	10.34	-47.0
10.70	-41.0	11.24	-32.0	11.67	-27.0	11.91	-22.0
12.63	-9.0	13.00	-2.0	13.74	9.0	14.44	18.0
15.18	23.0	15.91	28.0	17.75	35.0	18.68	38.0

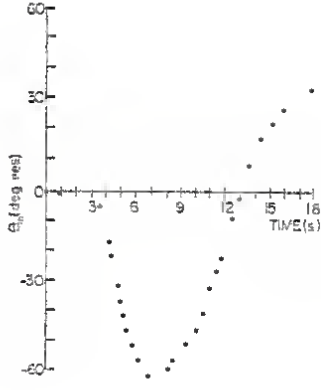

Table B-3. Angle of Rotation θ_m Versus Time; Run No. 044, Depth = 2.9 cm; Period = 1.0 s; Location X = 2.59 m, Y = 0.15 m

time (s)	θ_m (deg)	time (s)	θ_m (deg)	time (s)	θ_m (deg)	time (s)	θ_m (deg)
0.00	0.0	2.54	-1.0	2.67	-2.0	2.94	-4.0
3.20	-6.0	3.60	-8.0	4.27	-11.0	4.61	-8.0
6.07	-10.0	6.21	-12.0	6.67	-17.0	7.61	-22.0
7.88	-24.0	8.08	-27.0	8.34	-31.0	8.81	-35.0
9.74	-39.0	9.88	-41.0	10.14	-46.0	10.34	-49.0
10.61	-54.0	11.08	-60.0	11.35	-64.0	11.95	-67.0

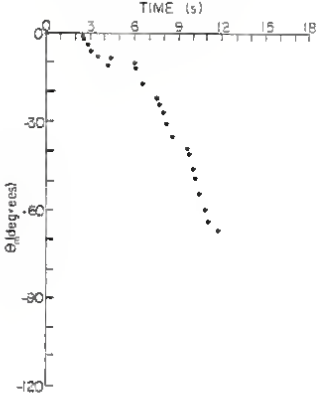

Table B-4. Angle of Rotation θ_m Versus Time; Run No. 043; Depth = 3.0 cm; Period = 1.0 s; Location X = 2.59 m, Y = 0.46 m

time (s)	θ_m (deg)	time (s)	θ_m (deg)	time (s)	θ_m (deg)	time (s)	θ_m (deg)
0.00	0.0	0.00	0.0	0.38	-1.0	0.58	-3.0
0.84	-5.0	1.24	-8.0	1.65	-11.0	1.98	-16.0
2.51	-21.0	3.05	-26.0	3.38	-28.0	3.85	-31.0
4.38	-34.0	5.12	-37.0	5.32	-39.0	5.65	-42.0
5.98	-46.0	6.32	-49.0	7.25	-52.0	8.45	-46.0
9.19	-47.0	10.19	-50.0	10.72	-53.0		

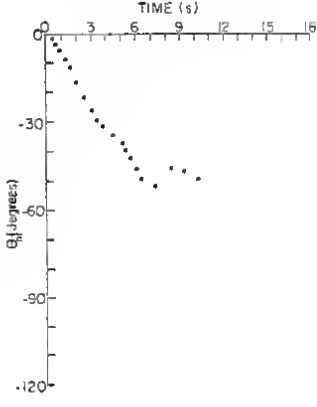

Table B-5. Angle of Rotation θ_m Versus Time; Run No 042, Depth = 3.2 cm; Period = 1.5 s; Location X = 2.59 m, Y = 0.76 m

time (s)	θ_m (deg)	time (s)	θ_m (deg)	time (s)	θ_m (deg)	time (s)	θ_m (deg)
0.00	0.0	1.90	-1.0	2.23	-2.0	2.77	-3.0
3.37	-5.0	3.57	-6.0	3.90	-7.0	4.64	-11.0
5.04	-14.0	5.70	-19.0	5.97	-21.0	6.90	-19.0
7.77	-11.0	8.04	-6.0	8.64	6.0	9.77	9.0
8.97	14.0						

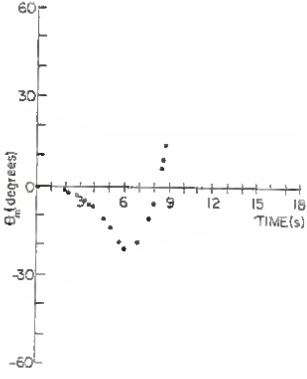

Table B-6. Angle of Rotation θ_m Versus Time [illegible]
Depth = 3.0 cm; Period = 1.8 [illegible]
X = 2.90 m, Y = 0.15 m

time (s)	θ_m (deg)	time (s)	θ_m (deg)	time (s)	θ_m (deg)	time (s)	θ_m (deg)
0.00	0.0	0.87	-1.0	1.21	-2.0	2.74	-4.0
3.34	-6.0	3.81	-9.0	4.08	-12.0	4.28	-15.0
4.54	-19.0	4.81	-24.0	5.14	-29.0	5.34	-34.0
5.61	-39.0	5.88	-44.0	6.21	-49.0	6.75	-56.0
7.21	-63.0	7.55	-69.0	7.95	-74.0	8.28	-79.0
9.35	-84.0	10.02	-89.0	10.55	-99.0	11.02	-106.0
11.35	-111.0	11.88	-116.0	12.28	-122.0	12.55	-126.0
12.82	-136.0						

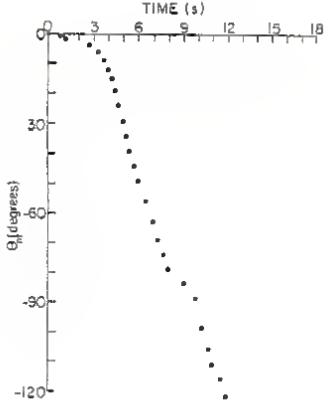

Table B-7. Angle of Rotation θ_m Versus Time; Run No. 47; Depth - 3.7 cm; Period - 1.0 s, Location X = 2.90 m, Y - 0.78 m

time (s)	θ_m (deg)	time (s)	θ_m (deg)	time (s)	θ_m (deg)	time (s)	θ_m (deg)
0.00	0.0	0.34	-3.0	0.81	-6.0	1.14	-8.0
1.47	-10.0	1.74	-13.0	2.07	-16.0	2.41	-20.0
2.81	-24.0	3.07	-26.0	3.54	-30.0	4.01	-34.0
4.54	-36.0	5.81	-36.0	7.14	-31.0	8.68	-16.0
9.75	-1.0						

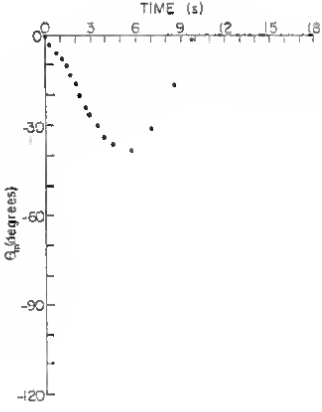

Table B-8. Angle of Rotation θ_m Versus Time; Run No. 49; Depth = 4.1 cm; Period = 1.0 s; Location X = 2.90 m, Y = 1.37 m

time (s)	θ_m (deg)	time (s)	θ_m (deg)	time (s)	θ_m (deg)	time (s)	θ_m (deg)
0.00	0.0	0.92	1.0	2.60	4.0	4.12	8.0
4.57	5.0	5.73	8.0	6.74	18.0	7.49	19.0
8.73	36.0	9.73	59.0	10.70	79.0	11.86	79.0
12.87	74.0	13.77	64.0	14.47	57.0	15.77	64.0
16.77	66.0						

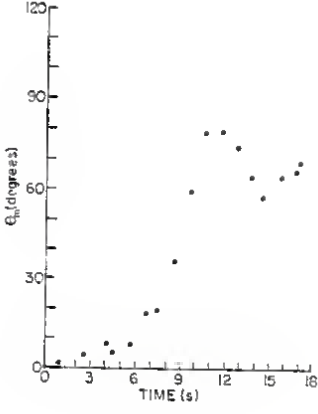

Table B-9. Angle of Rotation θ_m Versus Time, Run No. 54, Depth = 3.1 cm, Period = 1.0 s, Location X = 3.20 m, Y = 0.15 m

time (s)	θ_m (deg)	time (s)	θ_m (deg)	time (s)	θ_m (deg)	time (s)	θ_m (deg)
0.00	0.0	0.80	-1.0	1.20	-5.0	1.80	-6.0
2.47	-8.0	2.87	-11.0	3.74	-14.0	4.54	-18.0
6.14	-20.0	7.08	-27.0	7.48	-33.0	7.81	-37.0
8.41	-45.0	9.21	-46.0	9.61	-50.0	9.95	-57.0
10.61	-62.0						

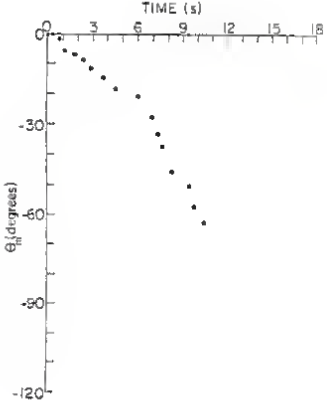

Table B-10. Angle of Rotation θ_m Versus Time, Run No. 053, Depth - 3.5 cm; Period - 1.0 s; Location X = 3.20 m, Y - 0.45 m

time (s)	θ_m (deg)	time (s)	θ_m (deg)	time (s)	θ_m (deg)	time (s)	θ_m (deg)
0.00	0.0	0.80	-1.0	0.87	-3.0	1.07	-4.0
1.47	-8.0	1.67	-10.0	1.74	-11.0	1.94	-13.0
2.14	-15.0	2.41	-18.0	2.54	-20.0	3.14	-25.0
3.41	-30.0	3.87	-35.0	4.61	-38.0	5.74	-43.0
8.74	-48.0						

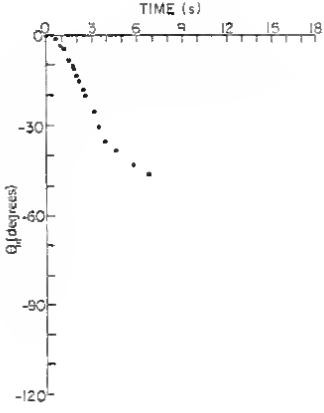

Table B-11 Angle of Rotation θ_m Versus Time, Run No. 52; Depth = 4.1 cm, Period = 1.0 s; Location X = 3.20 m, Y = 0.76 m

time (s)	θ_m (deg)	time (s)	θ_m (deg)	time (s)	θ_m (deg)	time (s)	θ_m (deg)
0.00	0.0	1.14	-1.0	1.74	-3.0	2.21	-4.0
3.74	-3.0	4.14	-1.0	4.87	3.0	5.27	4.0
5.54	9.0	6.01	14.0	6.41	20.0	6.74	29.0
7.01	34.0	7.88	44.0	9.35	54.0	9.95	59.0

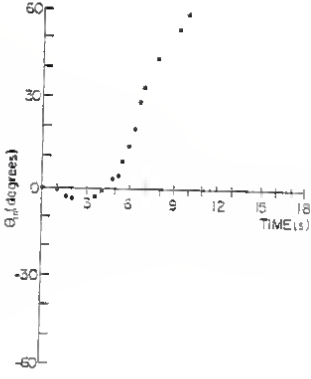

Table B-12. Angle of Rotation θ_m Versus Time; Run No 51; Depth = 4.6 cm, Period = 1.0 s; Location X = 3.20 m, Y = 1.07 m

time (s)	θ_m (deg)	time (s)	θ_m (deg)	time (s)	θ_m (deg)	time (s)	θ_m (deg)
0.00	0.0	0.30	-1.0	0.63	-2.0	1.06	-3.0
1.77	-5.0	2.80	-7.0	4.00	-10.0	5.64	-15.0
6.17	-20.0	6.87	-24.0	7.80	-19.0	8.21	-15.0
8.81	-5.0	9.74	0.0	10.67	11.0	10.87	15.0
11.74	25.0	12.58	30.0	12.84	35.0	13.27	30.0
14.24	35.0	14.68	45.0	15.18	45.0		

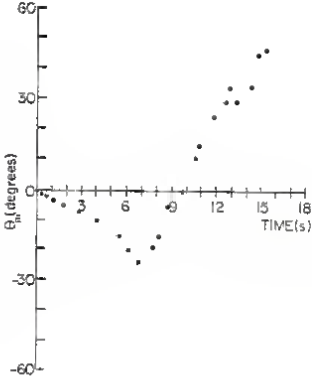

Table B-13 Angle of Rotation θ_m Versus Time; Run No. 055; Depth = 3.1 cm; Period = 1.0 s; Location X = 3.51 m, Y = 0.15 m

time (s)	θ_m (deg)	time (s)	θ_m (deg)	time (s)	θ_m (deg)	time (s)	θ_m (deg)
0.00	0.0	0.21	-1.0	0.48	-2.0	0.61	-3.0
0.88	-6.0	1.21	-10.0	1.34	-11.0	1.81	-17.0
2.01	-20.0	2.61	-25.0	3.88	-27.0	3.14	-31.0
3.54	-38.0	3.75	-45.0	3.95	-52.0	4.21	-60.0
4.41	-70.0	4.61	-75.0	4.75	-80.0	5.01	-86.0
5.35	-101.0	5.55	-110.0	5.68	-114.0	5.81	-118.0
6.01	-124.0	6.21	-128.0				

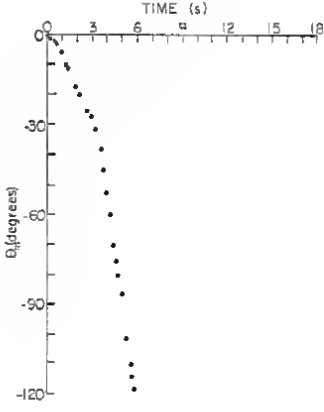

Table B-14. Angle of Rotation θ_m Versus Time; Run No. 55b, Depth = 3.7 cm; Period = 1.0 s; Location X = 3.51 m, Y = 0.46 m

time (s)	θ_m (deg)	time (s)	θ_m (deg)	time (s)	θ_m (deg)	time (s)	θ_m (deg)
0.00	0.0	1.08	1.0	1.41	-4.0	1.68	-8.0
2.08	-13.0	2.48	-16.0	2.74	-19.0	3.01	-23.0
3.48	-28.0	3.81	-31.0	4.28	-34.0	5.88	-29.0
6.41	-24.0	6.88	-17.0	8.48	-7.0		

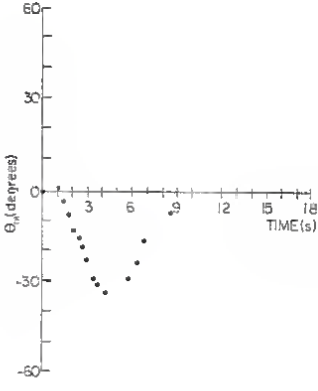

Table B-15. Angle of Rotation θ_m Versus Time; Run No. 96; Depth = 4.5 cm; Period = 1.0 s; Location X = 3.51 m, Y = 0.76 m

time (s)	θ_m (deg)	time (s)	θ_m (deg)	time (s)	θ_m (deg)	time (s)	θ_m (deg)
0.00	0.0	2.82	-3.0	3.29	+5.0	3.65	-7.0
4.12	-11.0	4.56	-14.0	5.37	-19.0	6.49	-26.0
7.46	-31.0	8.13	-36.0	9.69	+38.0	10.78	-31.0
12.63	-26.0	14.06	-25.0	15.33	-29.0	16.36	-26.0

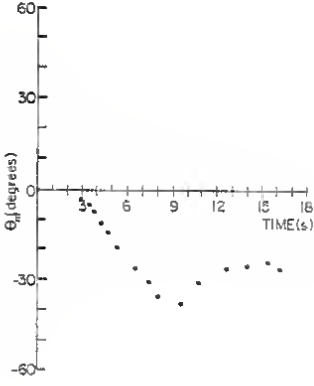

Table B-16. Angle of Rotation θ_m Versus Time; Run No. 56; Depth = 3.7 cm, Period = 1.0 s, Location X = 3.81 m, Y = 0.15 m

time (s)	θ_m (deg)	time (s)	θ_m (deg)	time (s)	θ_m (deg)	time (s)	θ_m (deg)
0.00	0.0	0.35	-1.0	0.62	-2.0	0.89	-3.0
1.49	-4.0	2.82	-7.0	3.82	-9.0	4.16	-7.0
5.09	3.0	5.43	7.0	7.16	-11.0	7.23	-14.0
8.03	-29.0	8.30	-34.0	8.56	-40.0	9.23	-56.0
10.03	-92.0	10.16	-102.0				

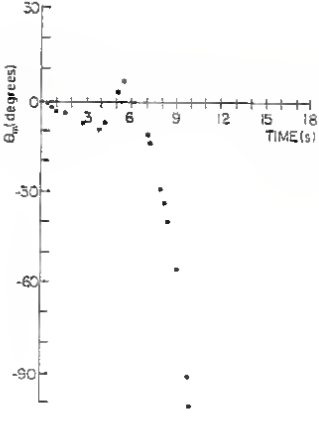

Table B-17. Angle of Rotation θ_m Versus Time; Run No 92; Depth = 4.3 cm; Period = 1.0 s; Location X = 3.81 m, Y = 0.46 m

time (s)	θ_m (deg)	time (s)	θ_m (deg)	time (s)	θ_m (deg)	time (s)	θ_m (deg)
0.00	0.0	0.48	-1.0	0.63	-2.0	0.97	-5.0
1.13	-7.0	1.40	-9.0	1.80	-14.0	2.27	-19.0
3.03	-29.0	3.57	-40.0	4.58	-49.0	5.40	-46.0
6.17	-39.0	8.11	-44.0	9.21	-39.0	10.78	-36.0
11.36	-34.0	12.41	-29.0	12.74	-24.0	13.55	-14.0
14.41	1.0	15.27	17.0	15.77	29.0	16.31	42.0
16.61	52.0						

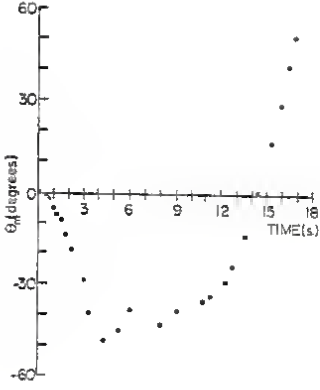

Table B-18. Angle of Rotation ϕ_m Versus Time; Run No. 93; Depth = 5.2 cm; Period = 1.0 s; Location X = 3.81 m, Y = 0.76 m

time (s)	ϕ_m (deg)	time (s)	ϕ_m (deg)	time (s)	ϕ_m (deg)	time (s)	ϕ_m (deg)
0.00	0.0	0.79	-2.0	1.10	-4.0	2.12	-7.0
3.46	-8.0	4.29	-9.0	5.06	-14.0	5.74	-18.0
6.69	-25.0	7.79	-34.0	8.58	-39.0	9.12	-41.0
10.00	-49.0	10.80	-54.0	11.53	-64.0	12.10	-74.0
12.60	-80.0	12.97	-91.0	13.44	-99.0	14.13	-111.0
15.04	-124.0	15.70	-132.0	16.20	-141.0	17.14	-154.0

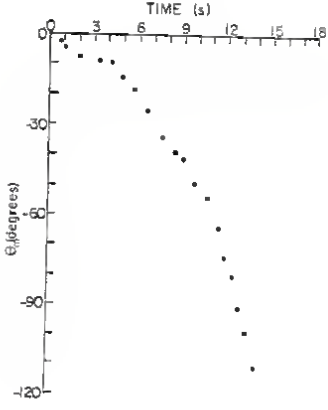

Table B-19. Angle of Rotation θ_m Versus Time; Run No 57, Depth = 4.7 cm, Period = 1.0 s; Location X = 4.11 m, Y = 0.15 m

time (s)	θ_m (deg)	time (s)	θ_m (deg)	time (s)	θ_m (deg)	time (s)	θ_m (deg)
0.00	0.0	0.97	-1.0	1.17	-2.0	1.30	-3.0
1.50	-4.0	1.83	-6.0	2.37	-9.0	2.90	-14.0
3.17	-19.0	3.84	-24.0	4.17	-29.0	4.44	-34.0
4.84	-39.0	5.10	-44.0	5.37	-49.0	5.97	-53.0
6.84	-56.0	7.71	-53.0	8.44	-57.0	9.57	-58.0

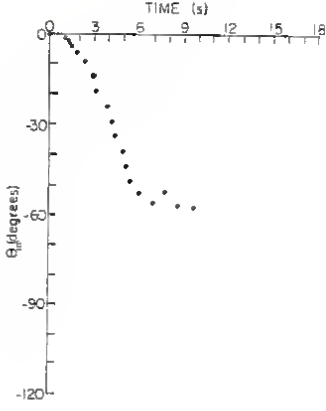

Table B-20 Angle of Rotation θ_m Versus Time; Run No. 90, Depth = 5.3 cm, Period = 1.0 s; Location X - 4.11 m, Y - 0.46 m

time (s)	θ_m (deg)	time (s)	θ_m (deg)	time (s)	θ_m (deg)	time (s)	θ_m (deg)
0.00	0.0	0.37	-1.0	1.10	-3.0	1.49	-6.0
2.46	-11.0	2.96	-16.0	3.52	-21.0	4.17	-31.0
5.03	-41.0	6.84	-51.0	7.54	-59.0	8.40	-70.0
9.40	-80.0	10.31	-90.0	11.89	-95.0	13.51	-93.0
14.03	-85.0	14.51	-85.0	15.39	-82.0	15.91	-80.0
17.65	-75.0	19.12	-72.0				

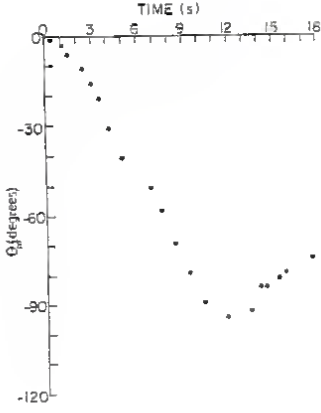

Table B-21. Angle of Rotation θ_m Versus Time; Run No. 89; Depth = 6.3 cm; Period - 1.0 s; Location X - 4.42 m, Y = 0.46 m

time (s)	θ_m (deg)	time (s)	θ_m (deg)	time (s)	θ_m (deg)	time (s)	θ_m (deg)
0.00	0.0	0.37	-2.0	0.76	-5.0	1.27	-8.0
1.67	-12.0	2.29	-18.0	2.58	-20.0	3.18	-27.0
4.35	-37.0	5.46	-52.0	5.94	-62.0	6.09	-64.0
6.91	-79.0	8.37	-94.0	9.41	-109.0	10.78	-126.0
12.04	-141.0	13.20	-154.0	14.33	-168.0	15.85	-185.0
16.89	-195.0	18.38	-205.0				

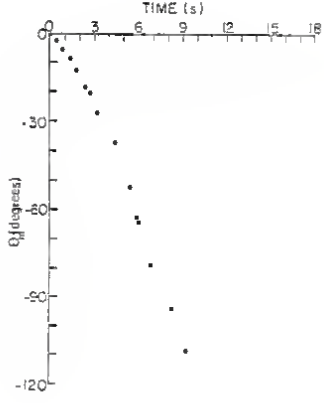

Table B-22. Angle of Rotation θ_m Versus Time; Run No. 033, Depth = 2.5 cm, Period = 1.5 s, Location X = 2.29 m, Y = 0.30 m

time (s)	θ_m (deg)	time (s)	θ_m (deg)	time (s)	θ_m (deg)	time (s)	θ_m (deg)
0.00	0.0	0.14	-0.5	0.47	-1.0	0.80	-2.0
1.00	-3.0	1.14	-4.0	1.34	-5.0	1.67	-7.0
1.80	-8.0	1.94	-9.0	2.00	-10.0	2.40	-16.0
2.47	-17.0	2.54	-18.0	2.60	-19.0	3.14	-26.0
3.27	-27.0	3.47	-29.0	3.74	-32.0	3.85	-35.0
4.01	-36.0	4.14	-38.0	4.67	-45.0	4.74	-45.5
4.87	-46.5	5.21	-51.5	5.27	-52.5	5.34	-53.5
5.41	-54.5	5.47	-55.5	5.54	-56.5	6.01	-63.5
6.28	-65.5	6.61	-72.5	6.81	-70.5	7.01	-72.5
7.08	-73.5	8.38	-80.5	8.64	-81.5	9.18	-84.5
9.98	-85.5	10.31	-87.5	10.58	-88.5	11.25	-89.5
11.58	-93.0	12.18	-95.5	12.51	-94.5	13.05	-97.5

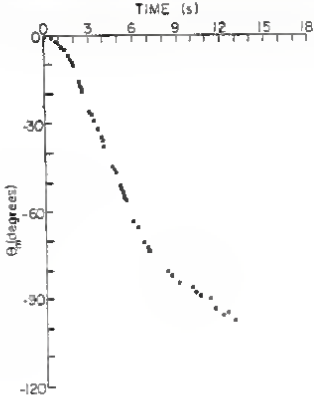

Table B-23. Angle of Rotation θ_m Versus Time; Run No 15; Depth = 3.0 cm; Period = 1.5 s; Location X = 2.59 m, Y = 0.15 m

time (s)	θ_m (deg)	time (s)	θ_m (deg)	time (s)	θ_m (deg)	time (s)	θ_m (deg)
0.00	0.0	0.17	-0.5	0.31	-1.0	0.33	-1.5
0.43	-2.5	0.61	-3.5	0.75	-4.5	0.89	-5.5
1.01	-6.5	1.08	-7.5	1.18	-8.5	1.28	-9.5
1.38	-10.5	1.47	-11.5	1.54	-12.5	1.61	-13.5
1.68	-14.5	1.77	-15.5	1.83	-16.5	1.88	-17.5
1.92	-18.5	2.12	-24.5	2.16	-25.5	2.21	-26.5
2.24	-27.5	2.29	-28.5	2.34	-29.5	2.44	-31.5
2.48	-32.5	2.58	-34.5	2.65	-35.5	2.92	-39.5
2.97	-40.5	3.12	-42.5	3.33	-45.5	3.61	-49.5
3.78	-52.5	3.88	-54.5	4.08	-57.5	4.23	-59.5
4.60	-63.5	4.72	-64.5	5.08	-68.5	5.62	-71.5
5.82	-72.5	6.03	-74.5	6.29	-76.5	6.70	-80.0
7.45	-84.5						

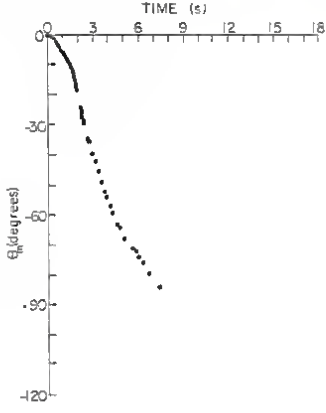

Table B-24- Angle of Rotation θ_m Versus Time; Run No. 012; Depth = 3.0 cm; Period - 1.5 s; Location X - 2.53 m, Y = 0.46 m

time (s)	θ_m (deg)	time (s)	θ_m (deg)	time (s)	θ_m (deg)	time (s)	θ_m (deg)
0.00	0.0	0.41	-075	0.71	-1.0	1.89	-2.0
1.98	-3.0	2.10	-4.0	2.28	-5.0	2.43	-6.0
2.59	-7.0	2.71	-8.0	2.78	-9.0	2.88	-10.0
2.98	-11.0	3.08	-12.0	3.86	-14.0	4.05	-15.0
4.12	-16.0	4.22	-17.0	4.31	-18.0	4.44	-19.0
4.79	-21.0	5.07	-22.0	5.16	-23.0	5.28	-24.0
5.40	-25.0	5.51	-26.0	5.62	-27.0	5.72	-28.0
5.81	-29.0	7.00	-29.0	7.36	-30.0	9.44	-36.0
10.00	-41.0	10.79	-50.0	11.30	-55.0	11.79	-59.0
13.90	-70.0						

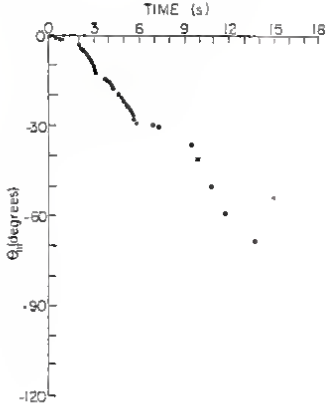

Table B-25 Angle of Rotation θ_m Versus Time. Run No 014; Depth = 3.2 cm; Period = 1.5 s; Location X = 2.59 m, Y = 0.69 m

time (s)	θ_m (deg)	time (s)	θ_m (deg)	time (s)	θ_m (deg)	time (s)	θ_m (deg)
0.00	0.0	0.29	1.0	1.15	0.5	1.27	0.0
1.38	-0.5	1.40	-1.0	1.61	-2.0	1.74	-3.0
1.88	-4.0	1.98	-5.0	2.56	-7.0	2.72	-8.0
2.61	-9.0	2.88	-10.0	2.96	-11.0	3.02	-12.0
3.07	-13.0	3.12	-14.0	3.17	-15.0	3.22	-16.0
3.27	-17.0	3.37	-18.0	3.72	-21.0	3.79	-22.0
3.90	-23.0	3.97	-24.0	4.11	-25.0	4.23	-26.0
4.32	-27.0	4.42	-28.0	4.51	-29.0	4.58	-30.0
4.79	-33.0	5.42	-35.0	5.93	-39.0	6.11	-41.0
6.26	-43.0	6.32	-44.0	7.06	-49.0	8.00	-59.0
9.00	-71.0	10.80	-82.5				

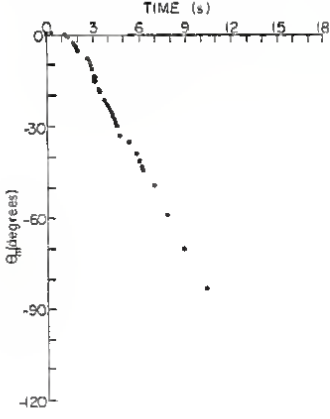

Table B-26. Angle of Rotation θ_m Versus Time; Run No. 162, Depth - 3.3 cm; Period - 1.5 s; Location X = 2.59 m, Y = 1.37 m

time (s)	θ_m (deg)	time (s)	θ_m (deg)	time (s)	θ_m (deg)	time (s)	θ_m (deg)
0.00	0.0	1.00	-0.5	2.00	-0.5	2.90	-1.0
3.41	-1.0	4.96	4.0	5.16	6.0	5.48	9.0
6.35	11.0	6.75	16.0	7.35	21.0	8.15	26.0
8.68	32.0	9.08	37.0	9.88	42.0	10.28	47.0
10.88	52.0	11.35	57.0	11.89	62.0	12.42	67.0

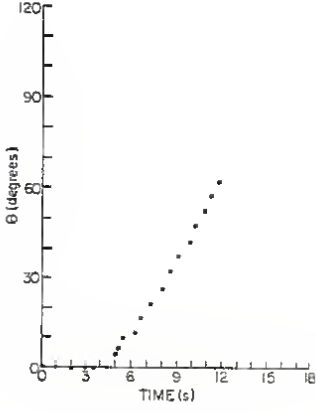

Table B-27 Angle of Rotation θ_m Versus Time; Run No. 001; Depth = 3.7 cm; Period = 1.5 s, Location X = 2.82 m, Y = 0.76 m

time (s)	θ_m (deg)	time (s)	θ_m (deg)	time (s)	θ_m (deg)	time (s)	θ_m (deg)
0.00	0.0	0.53	-3.0	1.20	-7.0	1.60	-10.0
1.87	-13.0	2.07	-16.0	2.54	-15.0	4.67	-15.0
4.87	-17.0	5.67	-18.0	5.94	-20.0	6.14	-22.0
6.21	-23.0	6.41	-26.0	7.14	-30.0	7.34	-32.0
7.54	-36.0	7.61	-38.0	7.81	-43.0	9.08	-49.0
9.28	-53.0	9.76	-58.0	10.21	-64.0		

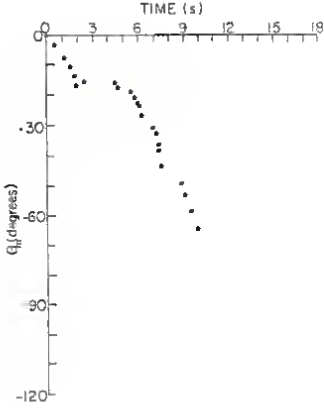

Table B-28. Angle of Rotation θ_m Versus Time; Run No. 018, Depth = 2.9 cm; Period = 1.5 s; Location X = 2.90 m, Y = 0.15 m

time (s)	θ_m (deg)	time (s)	θ_m (deg)	time (s)	θ_m (deg)	time (s)	θ_m (deg)
0.00	0.0	0.40	1.0	0.71	2.0	1.74	1.5
1.95	1.0	2.08	0.0	2.38	-3.0	2.62	-4.0
2.75	-5.0	2.85	-6.0	2.92	-7.0	3.02	-8.0
3.11	-9.0	3.22	-10.0	3.29	-11.0	3.42	-12.0
3.54	-13.0	3.71	-14.0	5.68	-14.0	6.17	-13.0
6.56	-12.0	6.72	-11.0	6.82	-10.0	6.98	-9.0
7.18	-8.0	7.61	-8.0	7.74	-9.0	7.84	-8.0
8.09	-8.0	8.18	-7.0	8.43	-6.0	8.55	-5.0
8.68	-4.0	8.85	-3.0	8.94	-4.0	9.05	-5.0
9.17	-6.0	9.35	-5.0	9.46	-5.0	9.53	-4.0
9.61	-3.0	9.68	-2.0	9.78	-1.0	9.92	0.0
10.07	1.0	10.20	2.0				

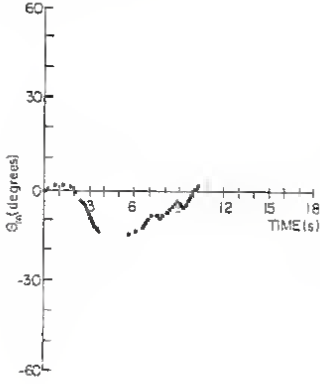

Table B-29. Angle of Rotation θ_m Versus Time; Run No. 11, Depth = 3.3 cm; Period = 1.5 s; Location X = 2.90 m, Y = 0.38 m

time (s)	θ_m (deg)	time (s)	θ_m (deg)	time (s)	θ_m (deg)	time (s)	θ_m (deg)
0.00	0.0	0.21	-0.5	0.51	-1.0	1.04	-1.5
1.15	-2.5	1.25	-3.5	1.33	-4.5	1.39	-5.5
1.49	-6.5	1.59	-7.5	2.12	-8.5	2.71	-7.5
2.81	-8.5	2.89	-9.5	3.02	-10.5	3.45	-10.0
4.08	-10.0	4.15	-10.5	4.24	-11.0	4.31	-11.5
4.45	-12.5	4.85	-14.5	4.98	-15.5	5.08	-16.5
5.15	-17.5	5.29	-18.5	5.39	-19.5	5.49	-20.5
5.55	-21.5	5.60	-22.5	6.00	-25.5	6.50	-32.5
6.88	-37.5	7.89	-42.5	9.26	-52.5	10.59	-54.5
12.79	-48.5						

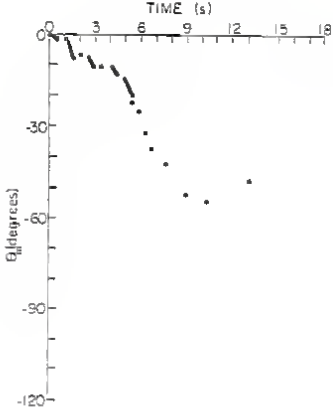

Table B-30. Angle of Rotation θ_m Versus Time; Run No. 30; Depth = 4.0 cm; Period = 1.5 s, Location X = 2.50 m, Y = 1.07 m

time (s)	θ_m (deg)	time (s)	θ_m (deg)	time (s)	θ_m (deg)	time (s)	θ_m (deg)
0.00	0.0	0.07	-0.3	0.14	-0.7	0.21	-1.0
0.31	-1.3	0.37	-1.8	0.44	-2.0	0.51	+2.5
0.57	+3.0	0.64	-3.5	0.71	+3.8	0.77	-4.0
0.84	-4.5	0.91	+5.0	1.11	-6.0	1.31	-7.0
1.45	-8.0	1.63	-9.0	1.71	+9.5	1.77	-10.0
1.91	-11.2	1.97	-12.0	2.11	-13.0	2.24	-14.0
2.31	-14.5	2.44	-15.5	2.51	-16.0	2.64	+17.0
2.84	-18.0	2.91	-19.3	3.04	-20.5	3.24	-22.0
3.38	-24.0	3.44	+25.0	3.51	-26.2	3.58	-27.0
3.78	-29.0	3.84	-30.0	3.98	+32.0	4.24	-34.0
4.91	-35.0	5.04	-36.2	5.18	-37.0	5.38	-38.0
5.44	+39.0	5.58	-40.0	5.64	-40.5	5.78	-41.0
5.88	-42.0	6.21	-43.0	7.08	-45.0	7.81	-44.0
7.95	-43.0	8.91	-38.0	9.77	-29.0	10.47	+24.0
10.92	-19.0						

Table B-30. Continued

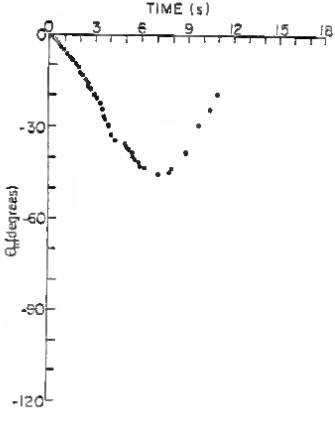

Table B-31. Angle of Rotation θ_m Versus Time; Run No. 022; Depth = 3.1 cm; Period = 1.5 s; Location X = 3.20 m, Y = 0.23 m

time (s)	θ_m (deg)	time (s)	θ_m (deg)	time (s)	θ_m (deg)	time (s)	θ_m (deg)
0.00	0.0	0.35	-1.0	0.62	-2.0	0.82	-3.0
1.02	-5.0	1.09	-6.0	1.15	-7.0	1.35	-11.0
1.42	-12.0	1.55	-14.0	2.16	-17.0	2.62	-20.0
2.76	-22.0	3.02	-27.0	3.62	-30.0	4.16	-31.0
4.36	-36.0	5.09	-47.0	5.36	-52.0	5.63	-57.0
5.89	-62.0	6.69	-85.0	6.83	-90.0	6.96	-95.0
7.09	-100.0	7.29	-105.0	7.49	-110.0	8.76	-115.0
8.96	-122.0						

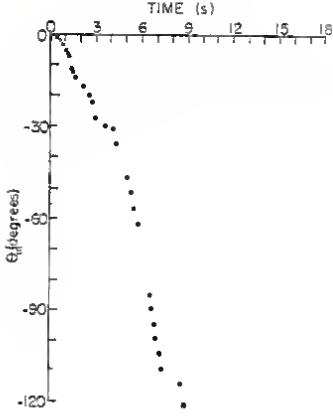

Table B-32. Angle of Rotation θ_m Versus Time: Run No. 013; Depth = 3.5 cm; Period = 1.5 s; Location X = 3.20 m, Y = 0.46 m

time (s)	θ_m (deg)	time (s)	θ_m (deg)	time (s)	θ_m (deg)	time (s)	θ_m (deg)
0.00	0.0	0.13	-0.5	0.16	-1.0	0.27	-1.5
0.32	-2.0	0.48	-3.0	0.62	-4.0	1.01	-3.0
1.36	-4.0	1.47	-5.0	1.57	-6.0	1.67	-7.0
1.78	-8.0	1.88	-9.0	1.95	-10.0	1.97	-11.0
2.05	-12.0	2.10	-13.0	2.59	-18.5	2.72	-20.0
2.95	-21.0	3.03	-22.0	3.09	-23.0	3.15	-24.0
3.19	-25.0	3.25	-26.0	3.29	-27.0	3.40	-32.0
3.95	-40.0	4.38	-43.0	4.94	-48.0	5.31	-50.0
5.62	-53.0	5.86	-55.0	5.91	-57.0	6.17	-60.0
6.47	-65.0	7.09	-70.0	7.61	-75.0		

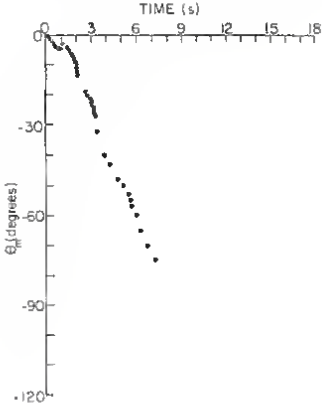

TABLE B-33. Angle of Rotation θ_M Versus Time; Run No. 180, Depth = 4.1 cm; Period = 1.5 s; Location X = 3.20 m, Y = 0.76 m

time (s)	θ_m (deg)	time (s)	θ_m (deg)	time (s)	θ_m (deg)	time (s)	θ_m (deg)
0.00	0.0	0.44	-2.0	1.04	-4.0	1.24	-5.0
1.57	-7.0	1.77	-10.0	2.04	-12.0	2.51	-17.0
3.17	-21.0	3.51	-26.0	3.71	-29.0	3.97	-32.0
5.04	-38.0	5.57	-38.0	5.98	-35.0	6.78	-38.0
7.44	-32.0	8.24	-35.0	9.51	-41.0	9.85	-45.0
10.11	-48.0	10.71	-53.0	10.98	-58.0	11.18	-63.0
11.51	-68.0	12.18	-72.0	12.52	-78.0	12.78	-83.0
13.12	-88.0						

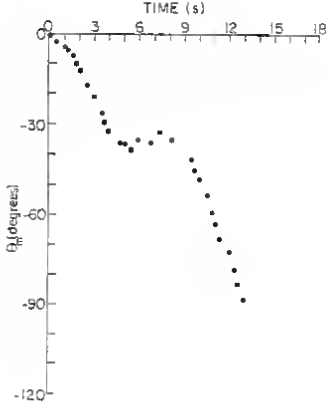

Table 8-34 Angle of Rotation θ_m Versus Time, Run No. 002
Depth = 3.1 cm, Period = 1.5 s, Location
X = 3.43 m, Y = 0.15 m

time (s)	θ_m (deg)	time (s)	θ_m (deg)	time (s)	θ_m (deg)	time (s)	θ_m (deg)
0.00	0.0	0.14	-1.0	0.41	-2.0	0.81	-4.0
1.14	-6.0	1.47	-8.0	1.61	-9.0	2.27	-16.0
2.41	-21.0	2.54	-25.0	2.68	-30.0	2.81	-35.0
2.94	-40.0	3.14	-45.0	3.54	-55.0	3.94	-65.0
4.21	-78.0	4.34	-85.0	4.48	-91.0	5.28	-109.0

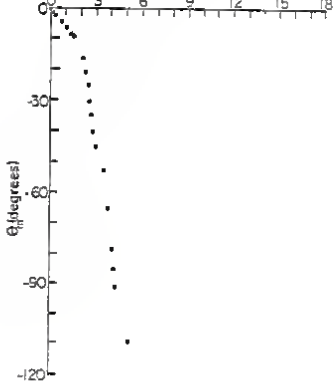

Table B-35. Angle of Rotation θ_m Versus Time; Run No. 157; Depth = 3.7 cm; Period = 1.5 s, Location X = 3.51 m, Y = 0.46 m

time (s)	θ_m (deg)	time (s)	θ_m (deg)	time (s)	θ_m (deg)	time (s)	θ_m (deg)
0.00	0.0	0.08	-1.0	0.68	-2.0	0.88	-4.0
1.15	-6.0	1.35	-8.0	1.61	-10.0	1.88	-12.0
1.95	-16.0	2.68	-7.0	2.81	-5.0	3.01	-2.0
3.28	0.0	3.75	5.0	3.95	10.0	4.62	22.0
5.35	25.0	5.68	28.0	6.42	24.0	6.55	20.0
6.68	17.0	8.15	5.0	8.23	7.0	9.96	5.0
10.82	10.0	11.36	14.0	11.76	19.0	12.16	25.0
12.96	35.0	13.23	41.0				

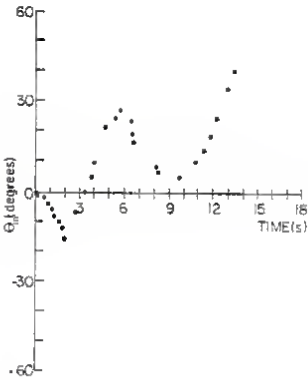

Table B-36 Angle of Rotation θ_m Versus Time; Run No. 156; Depth = 3.7 cm; Period = 1.5 s; Location X = 3.01 m, Y = 0.15 m

time (s)	θ_m (deg)	time (s)	θ_m (deg)	time (s)	θ_m (deg)	time (s)	θ_m (deg)
0.00	0.0	0.33	-1.0	0.53	-2.0	1.00	-3.0
1.07	-4.0	1.20	-5.0	1.27	-6.0	1.47	-7.0
2.21	-5.0	3.74	-1.0	3.87	0.0	4.20	0.0
4.34	1.0	5.27	-15.0	5.40	-18.0	5.54	-22.0
5.60	-24.0	5.74	-26.0	5.87	-28.0	6.41	-29.0
6.61	-30.0	6.81	-31.0	6.94	-32.0	7.21	-34.0
8.01	-32.0	8.54	-31.0	8.81	-29.0	9.61	-22.0
10.01	-26.0	11.88	-29.0				

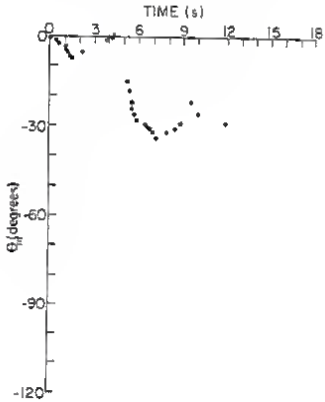

Table B-37. Angle of Rotation θ_m Versus Time; Run No 200, Depth = 2.8 cm; Period - 1.9 s; Location X = 2.59 m, Y - 0.15 m

time (s)	θ_m (deg)	time (s)	θ_m (deg)	time (s)	θ_m (deg)	time (s)	θ_m (deg)
0.00	0.0	0.80	4.0	1.00	6.0	2.73	2.0
2.87	1.0	3.07	-2.0	3.53	-9.0	3.87	-13.0
4.00	-15.0	4.40	-20.0	4.67	-23.0	5.07	-27.0
5.20	-29.0	5.47	-33.0	5.80	-39.0	6.27	-49.0
6.67	-54.0	7.27	-59.0	7.65	-65.0	7.81	-69.0
8.41	-74.0	8.87	-83.0	9.14	-89.0	9.34	-94.0
10.01	-113.0	10.41	-119.0	10.87	-129.0	11.21	-134.0
11.87	-139.0	12.81	-149.0	14.94	-157.0		

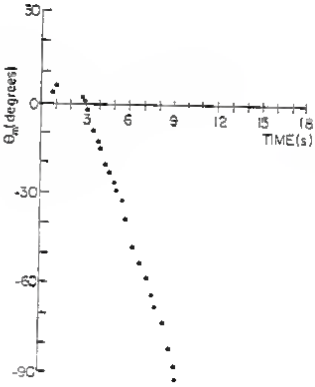

Table B-38. Angle of Rotation θ_m Versus Time; Run No. 201; Depth = 3.0 cm; Period = 1.9 s; Location X = 2.59 m, Y = 0.46 m

time (s)	θ_m (deg)	time (s)	θ_m (deg)	time (s)	θ_m (deg)	time (s)	θ_m (deg)
0.00	0.0	0.65	-1.0	1.25	-5.0	1.72	-11.0
2.32	-15.0	3.39	-20.0	5.06	-21.0	5.59	-25.0
6.72	-25.0	7.72	-30.0	8.93	-25.0	11.13	-25.0
13.06	-21.0	13.93	-25.0				

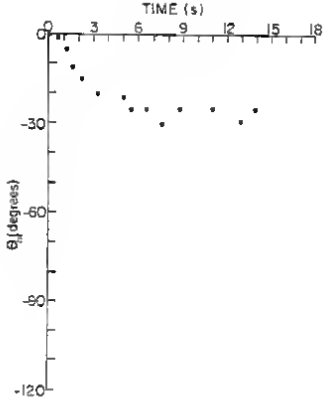

Table B-39. Angle of Rotation θ_m Versus Time; Run No. 203; Depth = 3.0 cm; Period = 1.9 s, Location X = 2.90 m, Y = 0.15 m

time (s)	θ_m (deg)	time (s)	θ_m (deg)	time (s)	θ_m (deg)	time (s)	θ_m (deg)
0.00	0.0	0.34	1.0	0.61	2.0	1.28	3.0
1.54	2.0	2.54	3.0	3.28	-2.0	4.08	-3.0
4.81	-5.0	5.41	-8.0	7.01	-8.0	7.28	-3.0
7.55	3.0	7.82	7.0	9.35	7.0	9.95	1.0
10.15	-3.0	10.55	-15.0	10.82	-23.0	11.22	-31.0
11.55	-35.0	11.89	-40.0	12.22	-45.0	12.49	-50.0
12.69	-53.0	13.82	-62.0	14.89	-74.0	15.96	-78.0
16.49	-80.0	16.82	-85.0	17.29	-91.0	17.96	-97.0
17.35	-101.0	19.29	-106.0	20.76	-111.0	21.30	-116.0

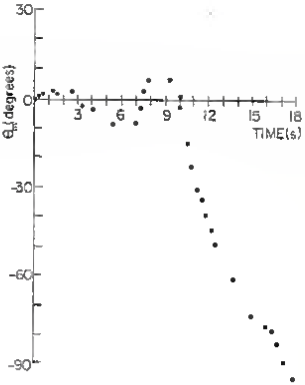

Table B-40. Angle of Rotation θ_m Versus Time, Run No 208; Depth - 3.3 cm, Period - 1.9 s; Location X - 2.90 m, Y - 0.46 m

time (s)	θ_m (deg)	time (s)	θ_m (deg)	time (s)	θ_m (deg)	time (s)	θ_m (deg)
0.00	0.0	0.27	-1.0	0.61	-2.0	1.01	-3.0
1.94	-8.0	3.01	-12.0	4.15	-25.0	5.81	-25.0
6.41	-15.0	6.81	-9.0	7.68	-7.0	8.22	-5.0
9.15	1.0	10.08	4.0	11.89	4.0	13.89	8.0

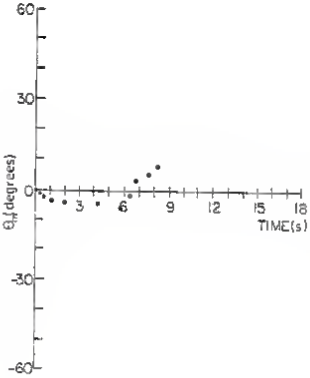

Table B-41. Angle of Rotation θ_m Versus Time; Run No. 210, Depth = 3.1 cm; Period = 1.3 s; Location X = 3.20 m, Y = 0.15 m

time (s)	θ_m (deg)	time (s)	θ_m (deg)	time (s)	θ_m (deg)	time (s)	θ_m (deg)
0.00	0.0	0.26	2.0	0.66	3.0	0.86	1.0
1.06	-1.0	2.26	-4.0	2.86	-9.0	3.33	-8.0
3.67	-4.0	3.87	-2.0	4.20	-1.0	4.40	-3.0
5.00	-6.0	5.40	-3.0	6.27	-6.0	7.74	-10.0
8.00	-12.0	8.60	-21.0	8.87	-25.0	9.40	-30.0
10.20	-35.0	10.81	-40.0	11.41	-45.0	12.37	-48.0
13.58	-51.0	13.78	-50.0	14.84	-52.0	15.64	-50.0
17.50	-51.0						

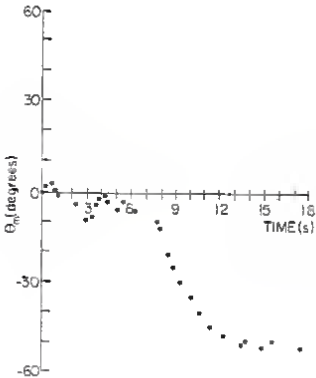

Table B-42 Angle of Rotation θ_m Versus Time; Run No. 219; Depth = 3.1 cm; Period = 1.9 s; Location X = 3.51 m, Y = 0.15 m

time (s)	θ_m (deg)	time (s)	θ_m (deg)	time (s)	θ_m (deg)	time (s)	θ_m (deg)
0.00	0.0	2.08	5.0	3.02	4.0	3.22	2.0
4.16	-11.0	4.43	-16.0	4.76	-20.0	4.96	-22.0
5.09	-23.0	6.23	-16.0	7.90	-23.0	8.16	-28.0
8.50	-33.0	8.83	-38.0	9.56	-58.0	9.83	-67.0
10.16	-77.0	10.37	-81.0	10.63	-86.0		

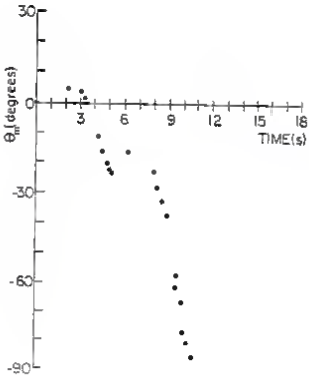

APPENDIX C
MEAN CURRENT DATA

Table C-1 Mean Current Measurements by Floating Disk Trajectories; Run No. 41/01; Wave Period = 1 s; Wavemaker Starting Time = 10-5

Time (s)	x (m)	y (m)	U (cm/s)	V (cm/s)
35.00	3.35	0.55		
40.24	3.08	0.64	-5.2	1.7
44.73	2.96	0.82	-2.7	4.1
49.27	3.05	1.13	2.0	6.7

The first time in the table indicates the time when the motion becomes perceptible.

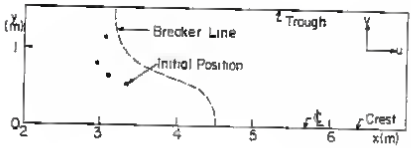

Table C-2. Mean Current Measurements by Floating Disk Trajectories; Run No. 41/02; Wave Period = 1 s; Wavemaker Starting Time = 10.0 s

Time (s)	x (m)	y (m)	U (cm/s)	V (cm/s)
33.22	3.35	0.41		
35.49	3.26	0.41	-4.0	0.0
38.70	3.14	0.44	-3.8	0.9
42.04	2.93	0.58	-6.4	4.1
45.20	2.74	0.73	-5.8	4.8
51.89	2.74	1.19	0.0	6.8

The first time in the table indicates the time when the motion becomes perceptible.

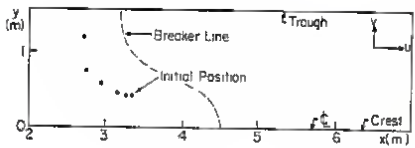

Table C-3. Mean Current Measurements by Floating Disk Trajectories; Run No. 41/01, Wave Period = 1 s; Wavemaker Starting Time = 10.5 s

Time (s)	x (m)	y (m)	U (cm/s)	V (cm/s)
31.97	3.35	0.15		
34.50	3.17	0.15	-7.2	0.0
36.07	3.05	0.18	-7.8	1.9
37.62	2.83	0.21	-13.8	2.0
39.94	2.62	0.27	-9.2	2.6
42.58	2.44	0.34	-6.3	2.3
46.05	2.26	0.43	-5.3	4.4
48.82	2.13	0.61	-4.4	4.4

The first time in the table indicates the time when the motion becomes perceptible.

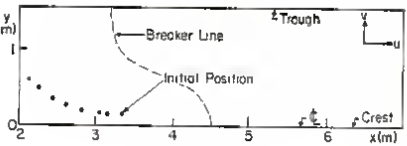

Table C-4. Mean Current Measurements by Floating Disk Trajectories; Run No. 42/01; Wave Period ~ 1 s; Wavemaker Starting Time = 23.0 s

Time (s)	x (m)	y (m)	U (cm/s)	V (cm/s)
38.67	3.66	0.37		
41.70	3.35	0.43	-6.1	1.2
43.81	3.20	0.58	-7.2	7.2
48.19	3.08	0.82	-2.8	5.6
55.60	3.08	1.22	0.0	5.3

The first time in the table indicates the time when the motion becomes perceptible.

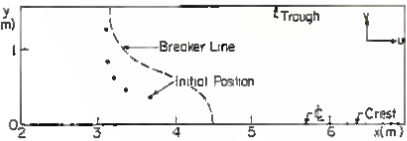

Table C-5. Mean Current Measurements by Floating Disk Trajectories* Run No. 42/02; Wave Period = 1 s; Wavemaker Starting Time = 23.0 s

Time (s)	x (m)	y (m)	U (cm/s)	V (cm/s)
35.23	3.66	0.24		
38.98	3.32	0.24	-8.9	0.0
42.25	2.99	0.27	-10.3	0.9
45.31	2.74	0.34	-8.0	2.0
46.86	2.62	0.40	-7.9	3.9
50.24	2.50	0.61	-3.6	6.3
56.22	2.44	0.94	-1.0	5.6

The first time in the table indicates the time when the motion becomes perceptible.

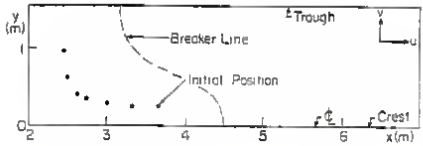

Table C-6. Mean Current Measurements by Floating Disk Trajectories; Run No. 42/03; Wave Period = 1 s; Wavemaker Starting Time - 23.0 s

Time (s)	x (m)	y (m)	U (cm/s)	V (cm/s)
35.55	3.66	0.12		
37.48	3.35	0.12	-15.8	0.0
40.77	3.11	0.15	-7.4	0.9
42.75	2.87	0.27	-12.3	6.2
47.28	2.50	0.37	-8.1	2.0

The first time in the table indicates the time when the motion becomes perceptible.

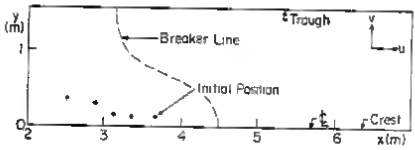

Table C-7. Mean Current Measurements by Floating Disk Trajectories; Run No. 43/01. Wave Period = 1 s. Wavemaker Starting Time = 16 2 s

Time (s)	x (m)	y (m)	U (cm/s)	V (cm/s)
34.18	4.11	1.16		
43.80	3.75	0.91	-3.8	-2.5
46.87	3.69	0.82	-2.0	-3.0
50.38	3.54	0.61	-4.3	-6.1
53.48	3.20	0.46	-10.8	-4.5
59.43	2.74	0.58	-7.7	2.0

The first time in the table indicates the time when the motion becomes perceptible.

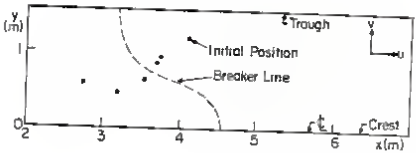

Table C-8 Mean Current Measurements by Floating Disk Trajectories; Run No. 43/02; Wave Period = 1 s; Wavemaker Starting Time - 16.2 s

Time (s)	x (m)	y (m)	U (cm/s)	V (cm/s)
34.31	4.15	0.70		
44.10	3.60	0.34	-5.6	-3.7
47.92	3.05	0.30	-14.4	-0.8
50.86	2.74	0.37	-10.4	2.1
55.00	2.50	0.61	-5.9	5.9

The first time in the table indicates the time when the motion becomes perceptible.

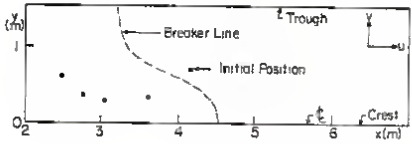

Table C-9: Mean Current Measurements by Floating Disk Trajectories: Run No. 43/03; Wave Period = 1 s; Wavemaker Starting Time - 16.2 s

Time (s)	x (m)	y (m)	U (cm/s)	V (cm/s)
33.69	4.21	0.61		
38.70	3.96	0.43	-4.9	-3.7
42.82	3.66	0.27	-7.4	-3.7
45.92	3.20	0.21	-14.7	-2.0
48.49	2.74	0.30	-17.8	3.6
50.88	2.50	0.38	-10.2	3.2
53.78	2.32	0.61	-6.3	7.9
61.14	2.59	1.07	3.7	6.2
65.09	2.68	1.22	2.3	3.9

The first time in the table indicates the time when the motion becomes perceptible.

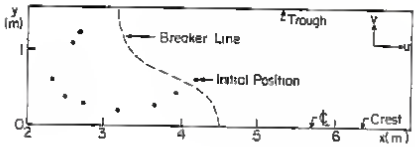

Table C-10. Mean Current Measurements by Floating Disk Trajectories; Run No. 43/04; Wave Period = 1 s; Wavemaker Starting Time = 16.2 s

Time (s)	x (m)	y (m)	U (cm/s)	V (cm/s)
33.24	4.11	0.45		
37.68	3.93	0.30	-4.1	-3.4
40.50	3.66	0.18	-9.7	-4.3
42.60	3.26	0.18	-18.9	0.0
45.55	2.83	0.37	-14.5	6.2
48.55	2.65	0.55	-6.1	6.1
51.74	2.65	0.82	0.0	8.6
58.57	2.74	1.22	1.3	5.8

The first time in the table indicates the time when the motion becomes perceptible.

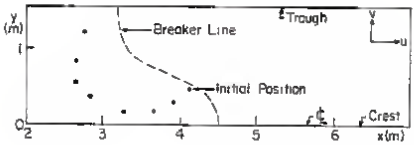

Table C-11. Mean Current Measurements by Floating Disk Trajectories, Run No. 43/05. Wave Period = 1 s; Wavemaker Starting Time = 16.2 s

Time (s)	x (m)	y (m)	U (cm/s)	V (cm/s)
30.04	4.24	0.30		
33.64	3.96	0.21	-7.5	-2.5
36.18	3.60	0.15	-14.4	-2.4
37.68	3.35	0.18	-16.3	2.0
40.55	2.90	0.37	-15.9	6.4
42.23	2.80	0.49	-5.4	7.3
47.08	2.62	0.82	-3.9	6.9
53.86	2.71	1.22	1.4	5.3

The first time in the table indicates the time when the motion becomes perceptible.

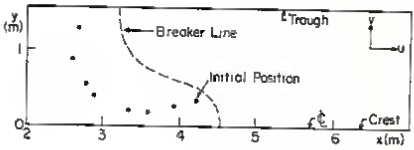

Table C-12. Mean Current Measurements by Floating Disk Trajectories, Run No. 43/06, Wave Period = 1 s; Wavemaker Starting Time = 16.2 s

Time (s)	x (m)	y (m)	U (cm/s)	V (cm/s)
28.59	4.33	0.03		
32.64	3.81	0.03	-12.8	0.0
35.14	3.41	0.00	-15.8	-1.2
38.06	3.02	0.00	-13.6	0.0
42.59	2.53	0.21	-10.8	4.7
46.29	2.35	0.40	-4.9	4.9

The first time in the table indicates the time when the motion becomes perceptible.

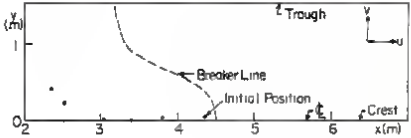

Table C-13. Mean Current Measurements by Floating Disk Trajectories, Run No. 44/01; Wave Period = 1 s; Wavemaker Starting Time = 29.5 s

Time (s)	x (m)	y (m)	U (cm/s)	V (cm/s)
52.00	4.88	1.37		
66.85	4.72	1.37	-1.0	0.0
76.64	4.57	1.37	-1.6	0.0
96.73	4.72	1.43	0.8	0.3
108.77	4.79	1.22	0.5	-1.8
113.29	4.85	0.91	1.3	-6.7
118.26	4.88	0.61	0.6	-6.1
129.45	4.88	0.30	0.0	-2.7
134.78	4.82	0.27	-1.1	-0.6
139.84	4.57	0.21	-4.8	-1.2
144.64	4.21	0.24	-7.6	0.6
146.63	3.96	0.27	-12.3	1.5
147.95	3.72	0.34	-18.5	4.6
150.55	3.23	0.49	-18.8	5.9
152.42	2.99	0.58	-13.0	4.9

The first time in the table indicates the time when the motion becomes perceptible.

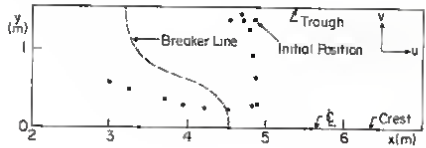

Table C-14 Mean Current Measurements by Floating Disk Trajectories; Run No. 44/02; Wave Period = 1 s, Wavemaker Starting Time = 29.5 s

Time (s)	x (m)	y (m)	U (cm/s)	V (cm/s)
48.21	4.57	0.91		
59.24	4.27	0.73	-2.8	-1.7
62.48	4.05	0.61	-6.6	-3.8
67.80	3.66	0.40	-7.4	-4.0
69.84	3.38	0.37	-13.4	-1.5
71.85	3.20	0.34	-9.1	-1.5
73.89	2.99	0.30	-10.5	-1.5
76.09	2.74	0.30	-11.1	0.0

The first time in the table indicates the time when the motion becomes perceptible.

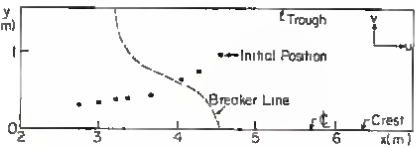

Table C-15. Mean Current Measurements by Floating Disk Trajectories, Run No. 44/03; Wave Period = 1 s; Wavemaker Starting Time = 29.5 s

Time (s)	x (m)	y (m)	U (cm/s)	V (cm/s)
47.23	4.66	0.67		
54.15	4.42	0.61	-3.5	-0.9
56.87	4.30	0.55	-4.5	-2.2
58.77	4.27	0.55	-1.6	0.0
61.24	4.05	0.46	-8.6	-3.7
63.90	3.81	0.30	-9.2	-5.7
64.85	3.72	0.27	-9.6	-3.2
65.76	3.66	0.27	-6.7	0.0
66.42	3.44	0.24	-32.3	-4.6
68.05	3.17	0.21	-16.8	-1.9
69.94	2.83	0.24	-17.7	1.6
70.75	2.74	0.27	-11.3	3.8
72.02	2.56	0.30	-14.4	2.4

The first time in the table indicates the time when the motion becomes perceptible.

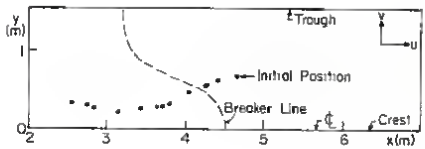

Table C-16. Mean Current Measurements by Floating Disk Trajectories; Run No. 44/04: Wave Period = 1 s; Wavemaker Starting Time = 29.5 s

Time (s)	x (m)	y (m)	U (cm/s)	V (cm/s)
43.88	4.57	0.40		
48.05	4.35	0.37	-4.4	-0.7
49.90	4.27	0.30	-6.6	-3.3
53.80	3.81	0.18	-11.7	-3.1
55.05	3.66	0.17	-12.2	-1.2
56.36	3.41	0.14	-18.6	-2.3
58.18	3.11	0.17	-16.7	-2.3
59.57	2.87	0.24	-17.5	1.7
60.55	2.71	0.27	-15.6	3.1
61.81	2.56	0.30	-12.1	2.4

The first time in the table indicates the time when the motion becomes perceptible.

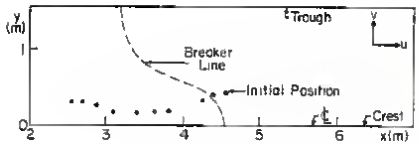

Table C-17. Mean Current Measurements by Floating Disk Trajectories, Run No. 44/05; Wave Period = 1 s, Wavemaker Starting Time = 29.5 s

Time (s)	x (m)	y (m)	U (cm/s)	V (cm/s)
43.09	4.57	0.21		
46.25	4.33	0.18	-7.7	-1.0
48.47	4.11	0.15	-9.6	-1.4
50.05	3.81	0.12	-19.3	-1.9
50.85	3.63	0.09	-22.9	-3.8
52.28	3.38	0.09	-17.1	0.0
53.15	3.19	0.12	-22.8	3.5
54.05	3.02	0.12	-18.6	0.0
56.74	2.74	0.24	-10.2	4.5
59.14	2.50	0.34	-10.2	3.8

The first time in the table indicates the time when the motion becomes perceptible.

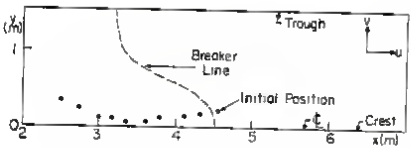

Table C-18. Mean Current Measurements by Floating Disk Trajectories; Run No. 44/06, Wave Period = 1 m Wavemaker Starting Time = 29.5 s

Time (s)	x (m)	y (m)	U (cm/s)	V (cm/s)
41.81	4.69	0.00		
48.25	4.42	0.00	-4.3	0.0
52.50	4.08	0.00	-7.5	0.0
54.12	4.08	0.00	-18.8	0.0
55.74	3.41	0.00	-22.5	0.0
57.14	3.11	0.03	-21.8	2.2
59.37	2.71	0.06	-17.8	1.4
61.16	2.53	0.09	-10.2	1.7

The first time in the table indicates the time when the motion becomes perceptible.

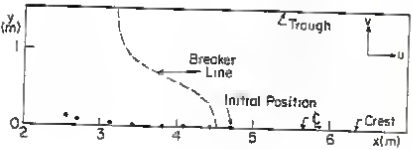

TABLE C-19. Mean Current Measurements by Floating Disk Trajectories, Run No. 45/01; Wave Period = 1 s; Wavemaker Starting Time = 15.4 s

Time (s)	x (m)	y (m)	U (cm/s)	V (cm/s)
33.90	4.63	1.25		
38.05	4.51	1.25	-2.9	0.0
43.51	4.45	1.22	-1.1	-0.6
50.43	4.27	1.16	-2.6	-0.9
54.82	3.96	0.94	-6.9	-4.9
59.04	3.57	0.85	-9.4	-2.2
60.66	3.35	0.85	-13.2	0.0
62.67	3.11	0.94	-12.1	4.5
64.24	3.05	1.10	-3.9	9.7

The first time in the table indicates the time when the motion becomes perceptible.

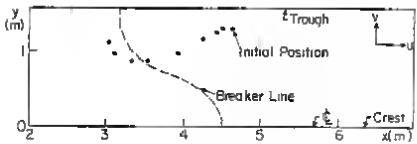

Table C-20. Mean Current Measurements by Floating Disk Trajectories; Run No. 45/02; Wave Period = 1 s; Wavemaker Starting Time = 15.4 s

Time (s)	x (m)	y (m)	U (cm/s)	V (cm/s)
35.05	4.72	1.19		
41.14	4.57	1.19	-2.5	0.0
50.98	4.27	1.07	-3.1	-1.2
55.85	3.96	0.88	-6.3	-3.8
57.55	3.78	0.79	-10.8	-5.4
59.27	3.54	0.76	-14.2	-1.8
61.67	3.26	0.76	-11.4	0.0
63.63	3.05	0.91	-10.9	7.8
66.56	2.90	1.22	-5.2	10.4

The first time in the table indicates the time when the motion becomes perceptible.

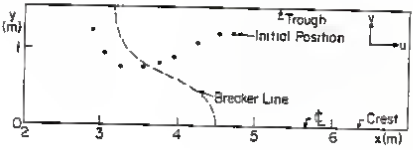

Table C-21 Mean Current Measurements by Floating Disk Trajectories; Run No. 45/03; Wave Period = 1 s; Wavemaker Starting Time = 15.4 s

Time (s)	x (m)	y (m)	U (cm/s)	V (cm/s)
33.78	4.60	1.16		
38.40	4.48	1.16	-2.6	0.0
44.22	4.27	1.10	-3.7	-1.0
52.05	3.96	0.88	-3.9	-2.7
54.87	3.63	0.76	-11.9	-4.3
57.42	3.35	0.73	-10.8	-1.2
59.72	3.08	0.79	-11.9	2.7
62.06	2.90	0.91	-7.8	5.2
64.39	2.77	1.10	-5.2	7.8
66.25	2.71	1.22	-3.3	6.6

The first time in the table indicates the time when the motion becomes perceptible.

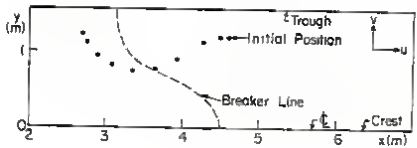

Table C-22. Mean Current Measurements by Floating Disk Trajectories; Run No. 45/04. Wave Period = 1 s; Wavemaker Starting Time = 15.4 s

Time (s)	x (m)	y (m)	U (cm/s)	V (cm/s)
34.60	4.72	1.04		
39.60	4.57	1.04	-3.0	0.0
43.43	4.42	1.01	-4.0	-0.8
47.58	4.27	0.91	-3.7	-2.2
53.23	3.96	0.79	-5.4	-2.2
56.20	3.66	0.64	-10.3	-5.1
58.55	3.35	0.58	-13.0	-2.6
60.87	3.05	0.61	-13.1	1.3
64.83	2.74	0.67	-7.7	1.5

The first time in the table indicates the time when the motion becomes perceptible.

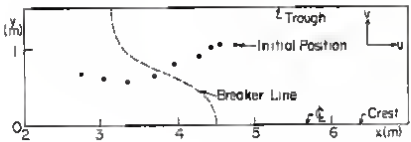

Table C-23. Mean Current Measurements by Floating Disk Trajectories, Run No. 45/05; Wave Period = 1 s; Wavemaker Starting Time = 15.4 s

Time (s)	x (m)	y (m)	U (cm/s)	V (cm/s)
28.36	4.56	0.40		
31.26	4.54	0.40	-4.2	0.0
33.60	4.36	0.34	-7.8	-2.6
35.76	3.84	0.27	-24.0	-2.8
38.30	3.81	0.15	-1.2	-4.8
39.45	3.54	0.15	-23.9	0.0
40.25	3.41	0.18	-15.2	3.8
40.80	3.29	0.18	-22.2	0.0
41.80	3.08	0.21	-21.3	3.0
43.19	2.90	0.30	-13.2	5.6
45.92	2.68	0.46	-7.8	5.6
47.38	2.62	0.61	-4.2	10.4
49.08	2.65	0.75	1.8	8.1

The first time in the table indicates the time when the motion becomes perceptible.

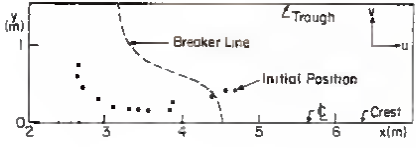

Table C-24. Mean Current Measurements by Floating Disk Trajectories; Run No. 45/06; Wave Period = 1 s, Wavemaker Starting Time = 15.4 s

Time (s)	x (m)	y (m)	U (cm/s)	V (cm/s)
27.91	4.48	0.34		
30.73	4.39	0.34	-3.2	0.0
31.93	4.30	0.30	-7.6	-2.5
33.85	4.08	0.27	-11.1	-1.6
35.16	3.93	0.24	-11.6	-2.3
36.56	3.78	0.20	-10.9	-3.3
38.07	3.51	0.18	-18.2	-1.0
39.22	3.32	0.21	-15.9	2.7
40.38	3.11	0.21	-18.2	0.0
41.64	2.99	0.24	-9.8	2.4
43.54	2.74	0.30	-12.8	3.2
45.51	2.56	0.40	-8.3	4.6
48.11	2.38	0.46	-7.0	2.3

The first time in the table indicates the time when the motion becomes perceptible.

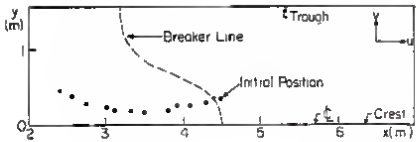

Table C-25. Mean Current Measurements by Floating Disk Trajectories; Run No. 45/07, Wave Period = 1 s; Wavemaker Starting Time = 15.4 s

Time (s)	x (m)	y (m)	U (cm/s)	V (cm/s)
27.86	4.57	0.30		
30.43	4.46	0.30	-3.6	0.0
32.78	4.27	0.27	-9.1	-1.3
33.73	4.21	0.24	-6.4	-3.2
34.73	4.21	0.24	-12.2	-3.0
35.06	3.90	0.15	-13.5	-4.5
37.72	3.63	0.12	-16.7	-1.9
38.50	3.35	0.09	-23.2	-2.6
40.50	3.05	0.15	-19.1	3.8
42.17	2.60	0.21	-14.6	3.7
44.07	2.59	0.27	-11.2	3.2
46.55	2.44	0.37	-6.1	3.7
49.88	2.32	0.61	-3.7	7.3

The first time in the table indicates the time when the motion becomes perceptible.

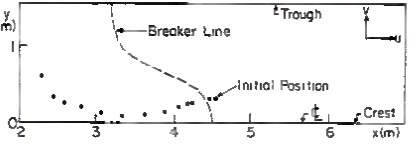

Table C-26. Mean Current Measurements by Floating Disk Trajectories; Run No 45/08; Wave Period = 1 s; Wavemaker Starting Time - 15.4 s

Time (s)	x (m)	y (m)	U (cm/s)	V (cm/s)
28.66	4.63	0.21		
30.74	4.56	0.21	-3.7	0.0
32.25	4.33	0.18	-15.1	-2.0
33.55	4.24	0.15	-7.0	-2.3
34.96	4.08	0.12	-10.8	-2.2
35.90	3.78	0.06	-32.4	-6.5
37.08	3.51	0.03	-23.2	-2.6
38.32	3.23	0.03	-22.1	0.0
39.74	2.96	0.05	-19.3	1.1
40.58	2.77	0.06	-21.5	1.8
41.52	2.62	0.06	-16.4	0.0
43.23	2.44	0.12	-10.3	3.4
44.34	2.28	0.24	-9.2	7.4

The first time in the table indicates the time when the motion becomes perceptible.

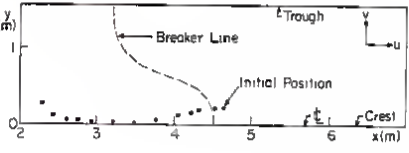

Table C-27. Mean Current Measurements by Floating Disk Trajectories: Run No. 30/01; Wave Period = 1.5 s; Wavemaker Starting Time = 23.2 s

Time (s)	x (m)	y (m)	U (cm/s)	V (cm/s)
34.65	2.74	1.43		
40.12	3.05	1.37	5.6	-1.1
47.93	3.35	1.16	3.9	-2.7
52.90	3.35	0.91	0.0	-4.5
57.80	3.05	0.61	-6.2	-6.2
61.51	2.74	0.61	-8.2	0.0
64.88	2.44	0.76	-9.0	4.5
68.32	2.29	1.22	-4.4	13.3
72.92	2.44	1.52	3.3	6.6
75.19	2.74	1.52	13.4	0.0
76.89	3.05	1.52	17.9	0.0
78.79	3.35	1.52	16.0	0.0
81.10	3.66	1.46	13.2	-2.6
84.07	3.96	1.22	10.3	-8.2
89.87	3.96	0.76	0.0	-7.9
97.11	3.20	0.85	-10.5	1.3
100.08	2.74	0.61	-15.4	-8.2
105.72	2.29	1.22	-8.1	10.8
110.69	2.44	1.52	3.1	6.1
115.16	3.05	1.52	13.6	0.0
123.57	3.81	1.22	9.1	-3.6
125.87	3.81	0.91	0.0	-13.3
132.35	3.20	0.76	-9.4	-2.4
135.12	2.74	0.46	-16.5	-11.0
136.85	2.44	0.49	-17.6	1.8
138.62	2.13	0.61	-17.2	6.9

The first time in the table indicates the time when the motion becomes perceptible.

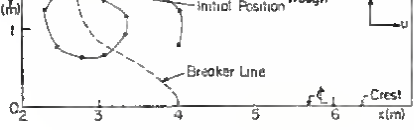

Table C-28. Mean Current Measurements by Floating Disk Trajectories; Run No. 30/02, Wave Period = 1.5 s; Wavemaker Starting Time = 23.2 s

Time (s)	x (m)	y (m)	U (cm/s)	V (cm/s)
36.00	2.74	1.22		
41.86	3.05	1.22	5.2	0.0
47.83	3.20	0.91	2.6	-5.1
53.34	2.87	0.61	-6.1	-5.5
58.60	2.44	0.85	-8.1	4.6
62.04	2.19	1.22	-7.1	10.6
69.65	2.74	1.52	7.2	4.0
73.52	3.35	1.52	15.8	0.0
75.62	3.66	1.52	14.5	0.0
91.81	4.11	1.22	2.8	-1.9
116.36	3.96	0.76	-0.6	-1.9
122.00	3.66	0.46	-5.4	-5.4
124.20	3.35	0.46	-13.9	0.0
124.94	3.11	0.40	-33.0	-8.2
127.51	2.68	0.37	-16.6	-1.2
128.91	2.44	0.40	-17.4	2.2
131.48	2.13	0.55	-11.9	5.9

The first time in the table indicates the time when the motion becomes perceptible.

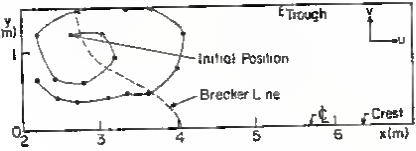

Table C-29. Mean Current Measurements by Floating Disk Trajectories; Run No. 30/03; Wave Period = 1.5 s; Wavemaker Starting Time = 23.2 s

Time (s)	x (m)	y (m)	U (cm/s)	V (cm/s)
29.50	2.74	1.01		
39.13	2.96	1.22	2.2	2.2
42.59	3.05	1.01	2.7	-6.3
44.73	3.14	0.91	4.3	-4.3
46.96	3.05	0.76	-4.1	-6.8
50.83	2.74	0.61	-7.9	-3.9
53.80	2.44	0.76	-10.3	5.1
57.44	2.23	1.22	-5.9	12.6
62.24	2.44	1.52	4.4	6.3
65.18	2.74	1.52	10.4	0.0
69.50	3.35	1.52	14.1	0.0
75.19	3.66	1.34	5.4	-3.2
79.56	3.72	0.85	1.3	-10.2
81.76	3.66	0.67	-3.4	-10.2
84.03	3.41	0.46	-10.7	-9.4
87.07	3.02	0.30	-13.0	-5.0
88.74	2.74	0.27	-16.4	-1.8
90.81	2.44	0.27	-14.7	0.0
93.17	2.13	0.24	-12.9	-1.3

The first time in the table indicates the time when the motion becomes perceptible.

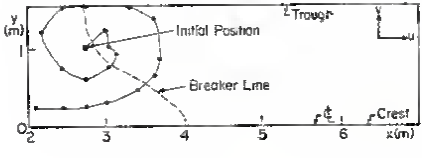

Table C-30. Mean Current Measurements by Floating Disk Trajectories; Run No. 30/04; Wave Period = 1.5 s; Wavemaker Starting Time = 23.2 s

Time (s)	x (m)	y (m)	U (cm/s)	V (cm/s)
22.81	2.68	0.85		
25.07	2.59	0.85	-4.0	0.0
33.58	2.56	1.04	-0.3	2.1
39.46	2.74	1.22	3.3	3.3
46.50	3.05	1.07	4.3	-2.2
50.67	2.99	0.85	-1.5	-5.1
54.27	2.80	0.79	-5.1	-1.7
57.47	2.62	0.88	-5.7	2.9
61.44	2.44	1.13	-4.6	6.1
65.01	2.44	1.28	0.0	4.3
69.42	2.59	1.52	3.5	5.5
72.32	2.90	1.52	10.5	0.0
73.79	3.05	1.55	10.4	2.1
77.23	3.44	1.52	11.5	-0.9
79.53	3.72	1.34	11.9	-8.0
81.50	3.81	1.22	4.6	-6.2
85.80	3.87	0.91	1.4	-7.1
89.60	3.60	0.73	-7.2	-4.8
91.71	3.35	0.61	-11.6	-5.8
94.38	3.05	0.58	-11.4	-1.1
96.71	2.68	0.61	-15.7	1.3
98.78	2.44	0.67	-11.8	2.9
101.12	2.26	0.98	-7.8	13.0
103.12	2.13	1.22	-6.1	12.2
113.80	3.14	1.52	9.4	2.9
120.50	3.81	1.22	10.0	-4.5
127.61	3.87	0.61	0.9	-8.6
132.95	3.51	0.43	-6.8	-3.4
134.45	3.14	0.37	-24.4	-4.1
136.65	2.68	0.40	-20.8	1.4
140.05	2.13	0.46	-16.1	1.8

The first time in the table indicates the time when the motion becomes perceptible

Table C-30. Continued

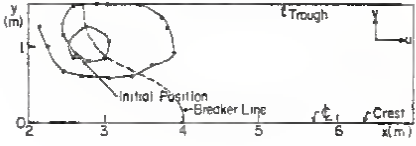

Table C-31 Mean Current Measurements by Floating Disk Trajectories, Run No. 30/05· Wave Period(s), 1.5, Wavemaker Starting Time(s), 23.2 seconds

Time (s)	x (m)	y (m)	U (cm/s)	V (cm/s)
24.00	2.80	0.61		
31.38	2.41	0.79	-5.4	2.5
33.78	2.19	1.01	-8.3	8.9
37.48	2.04	1.22	-4.1	5.8

The first time in the table indicates the time when the motion becomes perceptible.

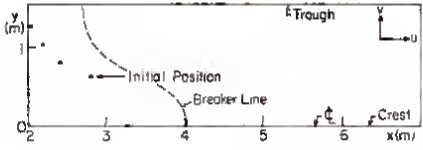

Table C-32. Mean Current Measurements by Floating Disk Trajectories; Run No. 30/06· Wave Period = 1.5 s; Wavemaker Starting Time = 23.2 s

Time (s)	x (m)	y (m)	U (cm/s)	V (cm/s)
23.50	2.90	0.15		
25.37	2.68	0.15	-11.4	0.0
27.11	2.56	0.15	-7.0	0.0
30.85	2.38	0.12	-4.9	-0.8
38.82	2.13	0.00	-4.2	-2.1

The first time in the table indicates the time when the motion becomes perceptible.

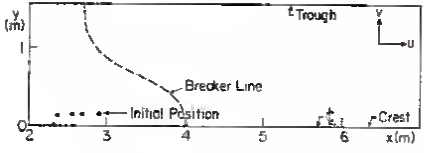

Table C-33 Mean Current Measurements by Floating Disk Trajectories; Run No. 30/07, Wave Period = 1 s; Wavemaker Starting Time = 23.2 s

Time (s)	x (m)	y (m)	U (cm/s)	V (cm/s)
22.94	2.99	0.12		
27.98	2.71	0.09	-5.4	-0.6
30.31	2.59	0.06	-5.2	-1.3
33.28	2.44	0.03	-5.1	-1.0
40.12	2.13	-0.09	-4.5	-1.8

The first time in the table indicates the time when the motion becomes perceptible.

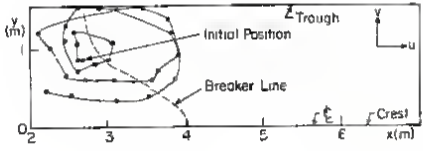

Table F-34. Mean Current Measurements by Floating Disk Trajectories; Run No. 31/01; Wave Period = 1.5 s, Wavemaker Starting Time = 28.4 s

time (s)	x (m)	y (m)	U (cm/s)	V (cm/s)
36.71	3.35	1.52		
44.18	3.63	1.49	3.7	-0.4
55.30	3.78	1.34	1.4	-1.4
59.73	3.81	1.22	0.7	-2.8
67.14	3.81	0.91	0.0	-4.1
73.28	3.66	0.61	-2.5	-5.0
75.75	3.51	0.49	-6.2	-4.9
77.48	3.29	0.43	-12.3	-3.5
78.92	2.99	0.43	-21.2	0.0
80.49	2.74	0.47	-15.5	2.9
82.32	2.50	0.61	-13.3	7.5
84.86	2.26	0.85	-8.6	9.6
86.79	2.23	1.13	-1.6	14.2
88.26	2.23	1.28	0.0	10.4
93.53	2.65	1.52	8.1	4.6
95.87	3.05	1.52	16.5	0.0
98.27	3.38	1.52	14.0	0.0
100.74	3.66	1.49	11.1	-1.2
103.58	3.90	1.37	8.6	-4.3
107.48	3.81	1.16	-2.3	-5.5
109.78	3.84	0.94	1.3	-9.3
111.12	3.84	0.76	0.0	-13.6
113.72	3.78	0.43	-2.3	-12.9
115.45	3.63	0.30	-8.8	-7.0
116.92	3.38	0.09	-16.6	-14.5
117.82	3.20	0.06	-20.3	-3.4
119.06	2.93	0.00	-22.1	-4.9
120.23	2.74	-0.03	-15.6	-2.6
122.06	2.44	-0.06	-16.7	-1.7

The first time in the table indicates the time when the motion becomes perceptible

Table C-34. Continued

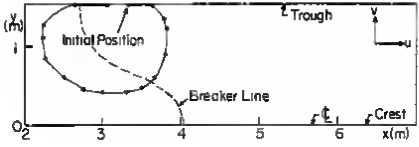

Table C-35. Mean Current Measurements by Floating Disk Trajectories; Run No. 31/02. Wave Period = 1.5 s; Wavemaker Starting Time - 28.4 s

Time (s)	x (m)	y (m)	U (cm/s)	V (cm/s)
37.00	3.35	1.22		
40.15	3.44	1.16	2.9	-1.9
45.25	3.51	1.07	1.2	-1.8
48.06	3.51	0.91	0.0	-5.4
52.23	3.44	0.76	-1.5	-3.7
55.93	3.26	0.61	-4.9	-4.1
57.66	3.05	0.55	-12.3	-3.5
59.37	2.83	0.55	-12.5	0.0
61.07	2.59	0.58	-14.3	1.8
62.67	2.41	0.64	-11.4	3.8
65.31	2.13	0.91	-10.4	10.4
67.07	2.10	1.22	-1.7	17.3
69.48	2.10	1.40	0.0	7.6
75.32	2.74	1.52	11.0	2.1
76.98	3.02	1.52	16.5	0.0
79.05	3.35	1.52	16.2	0.0
81.15	3.66	1.52	14.5	0.0
82.69	3.90	1.40	15.8	-7.9
86.73	4.21	1.28	7.5	-3.0
96.00	4.11	1.22	-1.0	-0.7
98.84	4.11	1.07	0.0	-5.4
102.11	4.11	0.85	0.0	-6.5
106.25	4.02	0.67	-2.2	-4.4
109.22	3.96	0.52	-2.1	-5.1
111.28	3.87	0.40	-4.4	-5.9
113.15	3.66	0.18	-11.4	-11.4
114.32	3.35	0.15	-26.1	-2.6
115.63	3.08	0.09	-20.0	-4.4
116.66	2.83	0.06	-25.1	-3.1
118.46	2.53	0.00	-16.9	-3.4
120.86	2.19	0.00	-14.0	0.0

The first time in the table indicates the time when the motion becomes perceptible.

Table C-3b. Continued

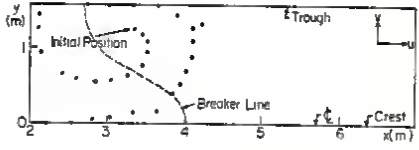

Table C-36. Mean Current Measurements by Floating Disk Trajectories; Run No. 31/03; Wave Period = 1.5 s; Wavemaker Starting Time = 28.4 s

Time (s)	x (m)	y (m)	U (cm/s)	V (cm/s)
37.00	3.35	0.98		
39.28	3.38	0.91	1.3	-2.7
46.30	3.35	0.61	-0.4	-4.3
47.39	3.23	0.58	-11.2	-2.8
48.56	3.08	0.52	-13.0	-5.2
50.22	2.87	0.46	-12.9	-3.7
52.13	2.56	0.55	-16.0	4.8
54.63	2.19	0.67	-14.6	4.9
56.80	2.13	0.91	-2.8	11.2
58.30	2.07	1.13	-4.1	14.2
60.27	2.13	1.34	3.1	10.8
65.67	2.44	1.52	5.6	3.4
68.14	2.74	1.52	12.3	0.0
69.91	3.08	1.52	18.9	0.0
71.81	3.35	1.52	14.4	0.0
74.38	3.66	1.52	11.9	0.0
77.05	3.81	1.34	5.6	-6.8
80.59	3.81	1.07	0.0	-7.8
82.56	3.75	0.91	-3.1	-7.7
84.69	3.69	0.70	-2.9	-10.0
86.23	3.54	0.61	-9.9	-5.9
87.83	3.35	0.49	-11.4	-7.6
89.26	3.05	0.46	-21.3	-2.1
90.93	2.77	0.43	-16.4	-1.8
92.27	2.59	0.49	-13.6	4.5
94.47	2.32	0.64	-12.5	6.9
96.70	2.13	0.91	-8.2	12.3
98.40	2.10	1.19	-1.8	16.1
105.95	2.47	1.52	4.8	4.4
108.61	2.90	1.52	16.0	0.0
110.58	3.23	1.52	17.0	0.0
114.69	3.66	1.37	10.4	-3.7
116.49	3.69	1.22	1.7	-8.5
119.16	3.69	0.91	0.0	-11.4
121.79	3.47	0.61	-8.1	-11.6
123.63	3.23	0.46	-13.3	-8.3
125.40	2.93	0.34	-17.2	-6.9
127.47	2.59	0.27	-16.2	-2.9
129.44	2.38	0.27	-10.8	0.0
135.37	1.98	0.61	-6.7	5.7

The first time in the table indicates the time when the motion becomes perceptible.

Table C-36. Continued

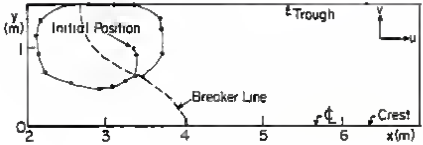

Table C-37. Mean Current Measurements by Floating Disk Trajectories; Run No. 31/04; Wave Period = 1.5 s; Wavemaker Starting Time = 26.4 s

Time (s)	x (m)	y (m)	U (cm/s)	V (cm/s)
36.40	3.23	0.79		
37.55	3.29	0.73	5.3	-5.3
38.89	3.35	0.64	4.8	-6.9
40.54	3.23	0.52	-7.3	-7.3
41.75	3.08	0.46	-12.6	-5.0
42.82	2.87	0.43	-19.9	-2.8
43.92	2.74	0.40	-11.1	-2.8
46.10	2.50	0.64	-11.2	11.2
48.19	2.38	0.91	-5.8	13.1
50.19	2.41	1.22	1.5	15.2
54.90	2.59	1.52	3.9	6.5
57.03	2.93	1.52	15.7	0.0
59.43	3.23	1.52	12.7	0.0
62.04	3.57	1.37	12.8	-5.8
64.37	3.75	1.25	7.8	-5.2
68.78	4.15	1.19	9.0	-1.4
83.22	4.33	1.34	1.3	1.1
88.50	4.33	1.52	0.0	3.5
115.89	3.81	1.37	-1.9	-0.6
121.43	3.72	1.22	-1.7	-2.8
124.36	3.66	1.01	-2.1	-7.3
126.63	3.57	0.76	-4.0	-10.7
128.13	3.41	0.61	-10.2	-10.2
130.30	3.20	0.46	-9.8	-7.0
133.21	2.68	0.30	-17.8	-5.2
135.81	2.35	0.37	-12.9	2.3
137.81	2.13	0.46	-10.7	4.6

The first time in the table indicates the time when the motion becomes perceptible.

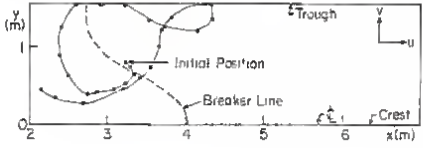

Table C-38. Mean Current Measurements by Floating Disk Trajectories: Run No. 31/04; Wave Period = 1.5 s, Wavemaker Starting Time = 28.4 s

Time (s)	x (m)	y (m)	U (cm/s)	V (cm/s)
28.97	3.20	0.64		
32.20	3.08	0.64	-3.8	0.0
35.44	3.05	0.70	-0.9	1.9
38.58	3.17	0.61	2.9	-2.2
41.72	3.05	0.52	-5.7	-4.3
43.05	2.83	0.55	-16.0	2.3
45.80	2.62	0.73	-7.8	6.7
47.12	2.56	0.91	-4.6	13.9
48.89	2.56	1.16	0.0	13.8
54.36	2.74	1.43	3.3	5.0
58.03	3.05	1.43	8.3	0.0
62.80	3.32	1.25	5.8	-3.8
66.74	3.29	1.10	-0.8	-3.9
69.58	3.17	1.07	-4.3	-1.1
77.52	3.29	1.22	1.5	1.9
82.82	3.44	1.16	2.9	-1.2
89.33	3.41	0.91	-0.5	-3.7
92.40	3.29	0.82	-4.0	-3.0
95.13	3.05	0.76	-8.9	-2.2
98.77	2.74	0.79	-8.4	0.8
102.41	2.62	1.01	-3.3	5.9
105.38	2.59	1.22	-1.0	7.2
110.05	2.74	1.46	3.3	5.2
112.55	3.05	1.52	12.2	2.4
115.69	3.35	1.52	9.7	0.0
118.62	3.57	1.25	7.3	-9.4
121.63	3.60	0.91	1.0	-11.1
123.30	3.51	0.76	-5.5	-9.1
125.00	3.38	0.58	-7.2	-10.8
127.33	3.05	0.37	-14.4	-9.2
128.47	2.74	0.34	-26.7	-2.7
131.04	2.44	0.34	-11.9	0.0
135.27	2.13	0.61	-7.2	6.5

The first time in the table indicates the time when the motion becomes perceptible.

Table 38. Continued

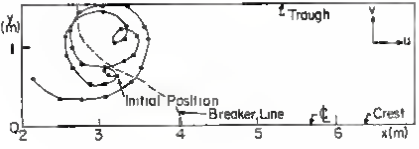

Table C-39. Mean Current Measurements by Floating Disk Trajectories; Run No. 31/06; Wave Period = 1.5 s; Wavemaker Starting Time = 28.4 s

Time (s)	x (m)	y (m)	U (cm/s)	V (cm/s)
28.70	3.29	0.30		
32.81	2.83	0.27	-11.1	-0.7
36.18	2.59	0.30	-7.2	0.9
38.58	2.41	0.49	-6.5	6.5
41.48	2.32	0.61	-3.7	4.9
45.22	2.13	0.94	-4.9	9.0

The first time in the table indicates the time when the motion becomes perceptible.

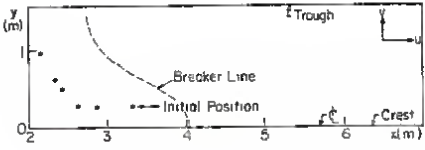

Table C-40. Mean Current Measurements by Floating Disk Trajectories; Run No. 31/07; Wave Period = 1.5 s; Wavemaker Starting Time = 28.4 s

Time (s)	x (m)	y (m)	U (cm/s)	V (cm/s)
27.67	3.32	0.15		
32.87	2.87	0.12	-8.8	-0.6
34.28	2.74	0.06	-8.6	-4.3
36.14	2.56	0.06	-9.8	0.0
39.58	2.35	0.00	-6.2	-1.8
42.92	2.13	-0.06	-6.4	-1.8

The first time in the table indicates the time when the motion becomes perceptible.

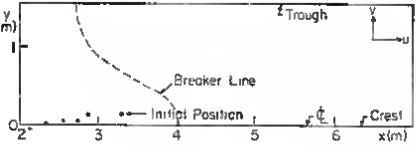

Table C-41. Mean Current Measurements by Floating Disk Trajectories; Run No. 32/01; Wave Period = 1.5 s; Wavemaker Starting Time = 22 s

Time (s)	x (m)	y (m)	U (cm/s)	V (cm/s)
42.20	3.93	1.52		
52.12	4.02	1.28	0.9	-2.5
60.79	4.02	1.07	0.0	-2.5
67.03	4.05	0.85	0.5	-3.4
81.71	4.11	0.73	0.4	-0.8
86.65	3.96	0.61	-3.1	-2.4
89.92	3.78	0.46	-5.7	-4.7
92.92	3.41	0.30	-12.2	-5.1
95.06	3.02	0.24	-18.5	-2.8
97.73	2.59	0.27	-16.0	1.1
99.10	2.41	0.30	-13.3	2.2
102.67	2.13	0.55	-7.7	6.8

The first time in the table indicates the time when the motion becomes perceptible.

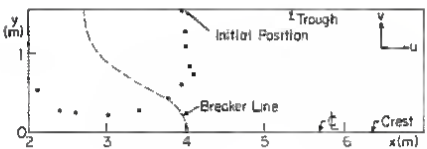

Table C-42. Mean Current Measurements by Floating Disk Trajectories. Run No. 32/02, Wave Period = 1.5 s; Wavemaker Starting Time - 22 s

Time (s)	x (m)	y (m)	U (cm/s)	V (cm/s)
36.50	3.93	1.46		
42.88	3.99	1.22	1.0	-3.8
53.39	3.96	1.07	-0.3	-1.5
58.22	3.93	0.91	-0.6	-3.2
64.36	3.75	0.67	-3.0	-4.0
66.60	3.69	0.61	-2.7	-2.7
69.07	3.35	0.49	-13.6	-4.5
70.90	3.08	0.46	-15.0	-1.7
72.54	2.77	0.49	-17.5	1.8

The first time in the table indicates the time when the motion becomes perceptible.

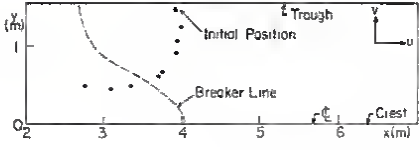

Table 13 Mean Current Measurements by Floating Disk Trajectories; Run No 32/03; Wave Period = 1.5 s; Wavemaker Starting Time = 22 s

Time (s)	x (m)	y (m)	U (cm/s)	V (cm/s)
31.03	3.96	1.25		
35.37	3.93	1.16	-0.7	-2.1
41.61	3.93	1.07	0.0	-1.5
50.28	3.93	0.91	0.0	-1.8
56.62	3.81	0.76	-1.9	-2.4
59.96	3.69	0.61	-3.7	-4.6
62.89	3.44	0.49	-8.3	-4.2
64.73	3.20	0.46	-13.3	-1.7
66.97	2.87	0.46	-15.0	0.0

The first time in the table indicates the time when the motion becomes perceptible.

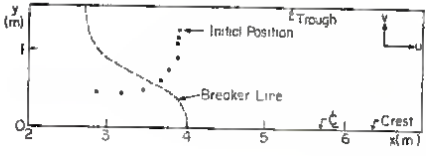

Table C-44. Mean Current Measurements by Floating Disk Trajectories; Run No. 32/04; Wave Period = 1.5 s; Wavemaker Starting Time = 22 s

Time (s)	x (m)	y (m)	U (cm/s)	V (cm/s)
26.45	3.93	1.10		
34.60	3.90	0.98	-0.4	-1.5
38.60	3.87	0.91	-0.8	-1.6
44.61	3.81	0.76	-1.0	-2.5
51.02	3.66	0.55	-2.4	-3.3
53.92	3.38	0.46	-9.5	-3.2
55.79	3.11	0.40	-14.7	-3.3
57.66	2.83	0.46	-14.7	3.3

The first time in the table indicates the time when the motion becomes perceptible.

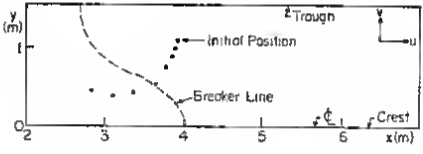

Table C-45 Mean Current Measurements by Floating Disk Trajectories, Run No. 32/05; Wave Period = 1.5 s; Wavemaker Starting Time = 22.0 s

Time (s)	x (m)	y (m)	U (cm/s)	V (cm/s)
25.00	3.90	0.79		
32.70	3.75	0.64	-2.0	-2.0
35.80	3.69	0.55	-2.0	-2.9
38.97	3.47	0.43	-6.7	-3.8
41.34	3.17	0.37	-12.9	-2.6
43.01	2.87	0.37	-18.3	0.0
44.84	2.56	0.40	-16.7	1.7
46.71	2.35	0.52	-11.4	6.5

The first time in the table indicates the time when the motion becomes perceptible

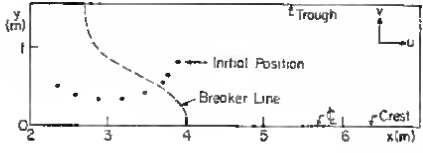

Table C-46. Mean Current Measurement by Floating Disk Trajectories; Run No. 32/06; Wave Period = 1.5 s; Wavemaker Starting Time - 22.0 s

Time (s)	x (m)	y (m)	U (cm/s)	V (cm/s)
23.50	3.96	0.49		
28.06	3.72	0.40	-5.3	-2.0
30.06	3.60	0.34	-6.1	-3.0
32.16	3.29	0.27	-14.5	-2.9
33.50	2.99	0.27	-22.7	0.0
34.63	2.80	0.30	-16.2	2.7
35.90	2.62	0.34	-18.9	3.1
37.30	2.44	0.46	-10.8	7.2
38.94	2.38	0.61	-3.7	9.3
40.87	2.29	0.88	-4.7	14.2
42.71	2.26	1.10	-1.7	11.6
46.51	2.13	1.37	-3.2	7.2
56.86	3.08	1.52	9.1	1.5
58.36	3.35	1.52	18.3	0.0
60.79	3.66	1.37	12.5	-6.3
63.00	3.90	1.16	11.0	-9.7
68.43	4.15	0.94	4.5	-3.9
81.08	4.27	1.07	1.0	1.0
91.76	4.27	1.22	0.0	1.4
104.17	4.11	1.46	-1.2	2.0
120.95	3.90	1.52	-1.3	0.4
138.74	3.96	1.31	0.3	-1.2

The first time in the table indicates the time when the motion becomes perceptible.

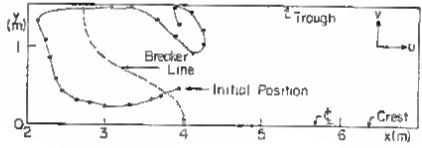

Table C-47. Mean Current Measurements by Floating Disk Trajectories, Run No. 32/07; Wave Period ~ 1.5 s; Wavemaker Starting Time - 22.0 s

Time (s)	x (m)	y (m)	U (cm/s)	V (cm/s)
22.89	3.99	0.21		
24.99	3.72	0.21	-13.1	0.0
26.73	3.44	0.15	-15.8	-3.5
28.69	3.11	0.12	-17.1	-1.6
31.00	2.77	0.24	-14.5	5.3
33.60	2.59	0.40	-7.0	5.9
36.17	2.44	0.61	-5.9	8.3
40.27	2.32	1.13	-3.0	12.6
54.22	3.05	1.52	5.2	2.8
56.52	3.35	1.52	12.7	0.0
59.38	3.66	1.25	11.0	-8.8
61.59	3.90	1.19	11.1	-4.2
65.53	4.11	0.98	5.4	-5.4
71.07	4.33	1.01	3.9	0.6
77.84	4.45	1.10	1.8	1.4
85.38	4.48	1.22	0.4	1.6
96.16	4.42	1.40	-0.6	1.7
123.32	4.42	1.52	0.0	0.4

The first time in the table indicates the time when the motion becomes perceptible.

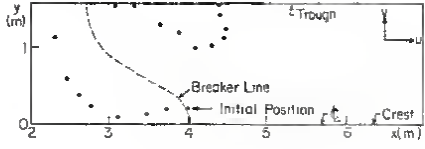

Table C-48: Mean Current Measurements by Floating Disk Trajectories. Run No. 32/08. Wave Period = 1.5 s; Wavemaker Starting Time = 22.0

Time (s)	x (m)	y (m)	U (cm/s)	V (cm/s)
22.00	3.81	0.15		
23.56	3.66	0.15	-9.8	0.0
25.83	3.35	0.12	-13.4	-1.3
27.86	3.11	0.12	-12.0	0.0
29.43	2.90	0.09	-13.6	-1.9
31.86	2.58	0.06	-8.8	-1.3
33.50	2.53	0.00	-9.3	-3.7
36.94	2.38	-0.09	-4.4	-2.7
38.34	2.29	-0.34	-3.6	-10.2
40.87	2.29	-0.55	0.0	-13.8
45.54	2.26	-1.07	-0.7	-11.1

The first time in the table indicates the time when the motion becomes perceptible.

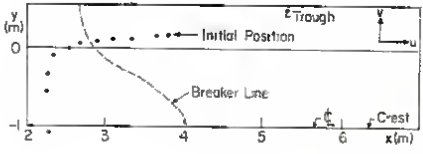

Table G-19. Mean Current Measurements by Floating Disk Trajectories; Run No. 33/01; Wave Period = 1.5 s; Wavemaker Starting Time = 24.0 s

Time (s)	x (m)	y (m)	U (cm/s)	V (cm/s)
36.23	4.57	1.46		
43.47	4.57	1.34	0.0	-1.7
76.50	4.57	1.52	0.0	0.6
103.36	4.27	1.52	-1.1	0.0
113.34	3.96	1.52	-3.1	0.0
132.49	3.51	1.52	-2.4	0.0
153.31	3.81	1.22	1.5	-1.5
156.68	4.02	1.01	6.3	-6.3
161.05	4.33	0.98	7.0	-0.7
173.93	4.57	1.10	1.9	0.9
180.14	4.88	1.22	4.9	2.0

The first time in the table indicates the time when the motion becomes perceptible.

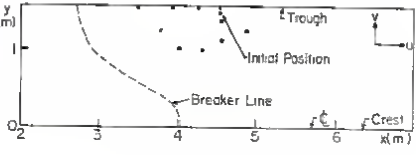

Table C-50. Mean Current Measurements by Floating Disk Trajectories, Run No. 33/02, Wave Period = 1.5 s; Wavemaker Starting Time = 24.0 s

Time (s)	x (m)	y (m)	U (cm/s)	V (cm/s)
37.00	4.72	1.34		
86.61	4.72	1.52	0.0	0.4
117.71	4.88	1.52	0.5	0.0
122.25	5.03	1.52	3.4	0.0
125.98	5.18	1.52	4.1	0.0
129.38	5.33	1.52	4.5	0.0
133.26	5.49	1.52	3.8	0.0
142.20	5.79	1.37	3.4	-1.7
149.24	5.85	1.22	0.5	-2.2
156.95	5.85	1.07	0.0	-2.0
166.86	5.79	0.91	-0.6	-1.5
182.11	5.70	0.85	-0.6	-0.4

The first time in the table indicates the time when the motion becomes perceptible.

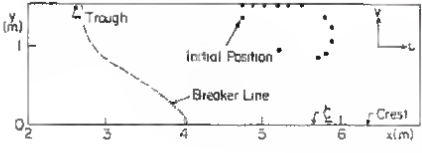

Table [illegible]. Mean Current Measurements by Floating Disk Trajectories; Run No. 33/03, Wave Period = 1.5 s, Wavemaker Starting Time = 24.0 s

Time (s)	x (m)	y (m)	U (cm/s)	V (cm/s)
36.00	4.57	1.28		
45.40	4.57	1.22	0.0	-0.6
73.23	4.57	1.28	0.0	0.2
87.05	4.60	1.37	0.2	0.7
96.39	4.51	1.49	-1.0	1.3
109.80	4.27	1.52	-1.8	0.2
122.01	4.08	1.52	-1.5	0.0
132.76	3.96	1.52	-1.1	0.0
146.67	3.75	1.40	-1.5	-0.9
152.24	3.96	1.22	3.8	-3.3
163.85	4.05	1.10	0.8	-1.1
167.96	4.05	0.79	0.0	-7.4
173.96	4.15	0.49	1.5	-5.1

The first time in the table indicates the time when the motion becomes perceptible.

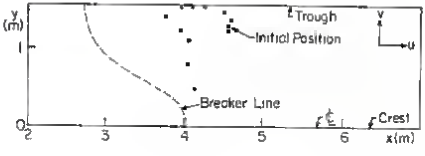

Table G-52. Mean Current Measurements by Floating Disk Trajectories; Run No. 33/04; Wave Period - 1.5 s, Wavemaker Starting Time - 24.0 s

Time (s)	x (m)	y (m)	U (cm/s)	V (cm/s)
35.63	4.51	1.07		
44.34	4.42	1.07	-1.0	0.0
53.21	4.33	0.94	-1.0	-1.4
65.26	4.27	0.85	-0.5	-0.8
83.44	4.15	0.82	-0.7	-0.2
88.21	4.02	0.67	-2.6	-3.2
89.75	3.96	0.61	-4.0	-4.0
91.48	3.84	0.55	-7.0	-3.5
93.69	3.72	0.46	-5.5	-4.1

The first time in the table indicates the time when the motion becomes perceptible.

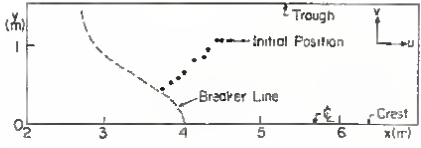

Table C-53. Mean Current Measurements by Floating Disk Trajectories; Run No. 33/05; Wave Period = 1.5 s; Wavemaker Starting Time = 24.0 s

Time (s)	x (m)	y (m)	U (cm/s)	V (cm/s)
33.00	4.42	1.04		
35.09	4.33	0.98	-4.4	-2.8
47.04	4.27	0.85	-0.5	-1.0
57.85	4.08	0.76	-1.7	-0.8
64.06	3.86	0.61	-2.0	-2.5
68.73	3.75	0.52	-4.6	-2.0
71.73	3.51	0.46	-8.1	-2.0
73.47	3.29	0.40	-12.3	-3.5

The first time in the table indicates the time when the motion becomes perceptible.

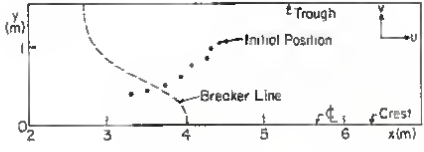

Table C-54. Mean Current Measurements by Floating Disk Trajectories; Run No. 33/06; Wave Period = 1.5 s, Wavemaker Starting Time = 24.0 s

Time (s)	x (m)	y (m)	U (cm/s)	V (cm/s)
28.42	4.45	0.76		
36.63	4.30	0.70	-1.8	-0.7
43.60	4.27	0.61	-0.4	-1.3
48.81	4.08	0.55	-3.5	-1.2
53.48	3.93	0.52	-3.3	-0.7
57.65	3.72	0.40	-5.1	-2.8
58.12	3.54	0.34	-12.4	-4.1
60.95	3.23	0.34	-16.7	0.0
62.29	2.99	0.37	-18.2	2.3
63.83	2.71	0.43	-17.1	3.8

The first time in the table indicates the time when the motion becomes perceptible.

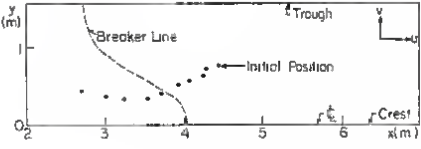

Table C-55. Mean Current Measurements by Floating Disk Trajectories, Run No. 33/07; Wave Period = 1.5 s; Wavemaker Starting Time = 24.0 s

Time (s)	x (m)	y (m)	U (cm/s)	V (cm/s)
25.86	4.36	0.64		
32.36	4.24	0.61	-1.3	-0.5
35.53	4.21	0.58	-1.0	-1.0
38.43	4.11	0.52	-3.2	-2.1
41.73	4.08	0.46	-0.9	-1.8
44.97	3.56	0.43	-3.8	-0.9
48.31	3.72	0.30	-7.3	-3.7
49.54	3.54	0.27	-14.9	-2.5
51.21	3.26	0.27	-16.4	0.0
52.48	3.08	0.27	-14.4	0.0
53.51	2.80	0.30	-26.6	3.0
55.28	2.53	0.37	-15.5	3.4
57.35	2.29	0.43	-11.8	2.9
60.79	1.98	0.61	-8.9	5.3

The first time in the table indicates the time when the motion becomes perceptible.

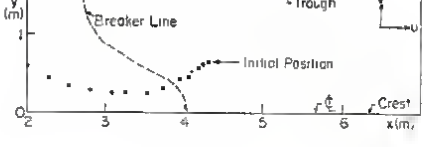

Table C-58. Mean Current Measurements by Floating Disk Trajectories; Run No. 33/08; Wave Period = 1.5 s, Wavemaker Starting Time = 24.0 s

Time (s)	x (m)	y (m)	U (cm/s)	V (cm/s)
24.75	4.39	0.40		
27.75	4.30	0.37	-3.0	-1.0
30.66	4.18	0.34	-4.2	-1.0
32.83	4.11	0.34	-2.8	0.0
36.70	3.87	0.30	-6.3	-0.8
38.90	3.80	0.27	-12.5	-1.4
41.50	3.14	0.21	-17.6	-2.3
42.84	2.80	0.21	-25.0	0.0
44.60	2.50	0.21	-17.3	0.0
46.51	2.23	0.24	-14.4	1.6

The first time in the table indicates the time when the motion becomes perceptible.

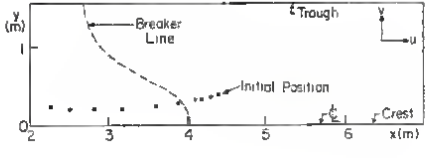

Table C-57. Mean Current Measurements by Floating Disk Trajectories; Run No. 33/03; Wave Period = 1.5 s; Wavemaker Starting Time = 24.0 s

Time (s)	x (m)	y (m)	U (cm/s)	V (cm/s)
24.59	4.45	0.15		
26.09	4.33	0.12	-8.1	-2.0
28.19	4.27	0.12	-2.9	0.0
29.32	4.11	0.12	-13.5	0.0
30.92	3.96	0.15	-9.5	1.9
32.73	3.72	0.12	-13.5	-1.7
34.03	3.51	0.12	-16.4	0.0
35.46	3.05	0.18	-32.0	4.3

The first time in the table indicates the time when the motion becomes perceptible.

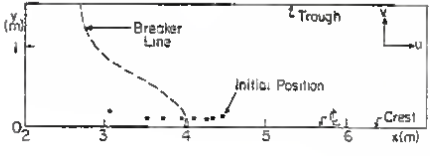

Table C-58. Mean Current Measurements by Floating Disk Trajectories, Run No. 34/01, Wave Period = 1.5 s, Wavemaker Starting Time = 25.8 s

Time (s)	x (m)	y (m)	U (cm/s)	V (cm/s)
49.00	5.12	1.52		
54.96	5.06	1.52	-1.0	0.0
68.47	4.94	1.49	-0.9	-0.2
91.90	5.03	1.52	0.4	0.1
102.07	5.12	1.52	0.9	0.0
113.05	5.18	1.49	0.6	-0.3
121.49	5.30	1.37	1.4	-1.4
129.57	5.43	1.22	1.5	-1.9
136.57	5.49	1.07	0.9	-2.2
141.48	5.46	0.91	-0.6	-3.1
152.09	5.33	0.67	-1.1	-2.3
161.53	5.18	0.55	-1.6	-1.3
169.14	5.03	0.46	-2.0	-1.2
175.21	4.88	0.43	-2.5	-0.5
181.45	4.72	0.37	-2.4	-1.0
187.56	4.57	0.30	-2.5	-1.0
192.16	4.39	0.23	-4.0	-1.7
195.33	4.24	0.15	-4.8	-2.4
198.70	3.87	0.12	-10.9	-0.9

The first time in the table indicates the time when the motion becomes perceptible.

Table C-58. Continued

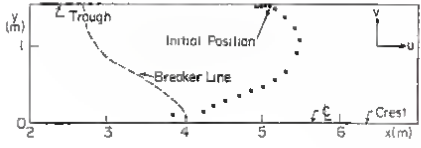

Table C-59. Mean Current Measurements by Floating Disk Trajectories: Run No. 34/02; Wave Period = 1.5 s, Wavemaker Starting Time = 25.8 s

Time (s)	x (m)	y (m)	U (cm/s)	V (cm/s)
35.00	5.18	1.31		
39.24	5.18	1.22	0.0	-2.2
51.69	5.12	1.13	-0.5	-0.7
62.70	5.03	1.07	-0.8	-0.6
85.79	5.15	1.10	0.5	0.1
93.13	5.30	1.07	2.1	-0.4
99.84	5.33	0.91	0.5	-2.3
105.54	5.30	0.76	-0.5	-2.7
112.05	5.18	0.70	-1.9	-0.9
116.39	5.03	0.67	-3.5	-0.7
121.29	4.88	0.73	-3.1	1.2
125.96	4.82	0.82	-1.3	2.0
129.87	4.82	0.91	0.0	2.3
133.87	4.75	1.07	-1.5	3.8
138.74	4.79	1.22	0.6	3.1
143.45	4.88	1.37	1.9	3.2
148.85	5.03	1.52	2.8	2.8
152.86	5.18	1.52	3.8	0.0
161.90	5.58	1.52	4.4	0.0
165.77	5.79	1.52	5.5	0.0
169.34	5.94	1.52	4.3	0.0
172.94	6.10	1.52	4.2	0.0

The first time in the table indicates the time when the motion becomes perceptible.

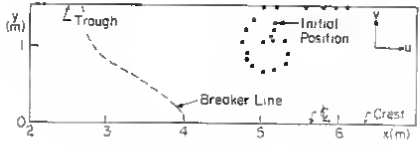

Table C-60. Mean Current Measurements by Floating Disk Trajectories, Run No. 34/03; Wave Period = 1.5 s; Wavemaker Starting Time = 25.8 s

Time (s)	x (m)	y (m)	U (cm/s)	V (cm/s)
33.77	5.24	1.14		
40.55	5.24	1.07	0.0	-1.1
56.43	5.18	0.98	-0.4	-0.6
77.92	5.24	0.98	0.3	0.0
88.13	5.49	0.88	2.4	-0.9
93.83	5.52	0.76	0.5	-2.1
98.34	5.44	0.61	-1.7	-3.4
102.81	5.24	0.55	-4.4	-1.4
106.28	5.11	0.53	-4.0	-0.4
110.78	4.88	0.61	-5.1	1.7
115.42	4.75	0.76	-2.6	3.3
119.32	4.63	0.91	-3.1	3.9
124.03	4.57	1.13	-1.3	4.5
127.30	4.57	1.22	0.0	2.8
137.51	4.63	1.52	0.6	3.0
151.79	4.88	1.52	1.7	0.0
162.30	5.18	1.52	2.9	0.0
168.87	5.45	1.52	4.6	0.0
174.61	5.79	1.52	5.3	0.0
180.75	6.10	1.52	5.0	0.0
195.83	6.40	1.22	2.0	-2.0

The first time in the table indicates the time when the motion becomes perceptible.

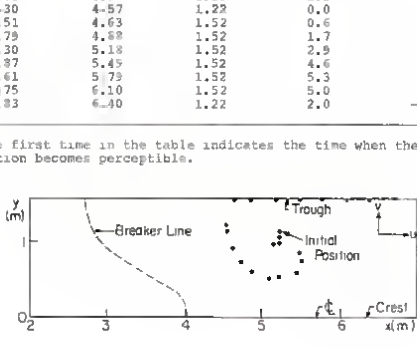

Table C-61. Mean Current Measurements by Floating Disk Trajectories; Run No 34/04, Wave Period = 1.5 s; Wavemaker Starting Time = 25.0 s

Time (s)	x (m)	y (m)	U (cm/s)	V (cm/s)
33.00	5.15	0.94		
38.58	5.12	0.91	-0.5	-0.5
44.75	5.12	0.88	0.0	-0.5
53.32	5.03	0.85	-1.1	-0.4
65.00	4.88	0.82	-1.3	-0.3
80.42	4.82	0.91	-0.4	0.6
89.09	4.88	1.01	0.7	1.1
95.10	4.94	1.10	1.0	1.5
114.02	5.18	1.13	1.3	0.2
123.33	5.24	0.91	0.7	-2.3
130.07	5.18	0.79	-0.9	-1.8
142.25	5.03	0.76	-1.3	-0.3
155.19	5.00	0.91	-0.2	1.2
166.54	5.18	1.07	1.6	1.3
175.28	5.33	1.22	1.7	1.7
189.56	5.64	1.43	2.1	1.5
194.90	5.79	1.46	2.5	0.6

The first time in the table indicates the time when the motion becomes perceptible.

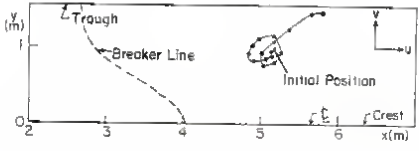

Table C-62. Mean Current Measurements by Floating Disk Trajectories; Run No. 34/05, Wave Period = 1.5 s; Wavemaker Starting Time = 25.8 s

Time (s)	x (m)	y (m)	U (cm/s)	V (cm/s)
30.00	5.18	0.73		
35.47	5.12	0.67	-1.1	-1.1
43.21	5.03	0.61	-1.2	-0.8
53.52	4.88	0.58	-1.5	-0.3
62.13	4.72	0.55	-1.8	-0.4
65.83	4.57	0.55	-4.1	0.0
81.12	4.27	0.46	-2.0	-0.6
87.59	4.08	0.40	-2.8	-0.9
91.29	3.90	0.37	-4.9	-0.8
93.16	3.69	0.27	-11.4	-4.9

The first time in the table indicates the time when the motion becomes perceptible.

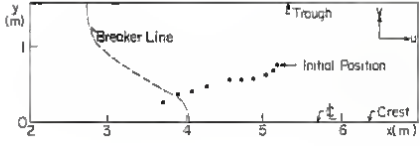

Table C-63. Mean Current Measurements by Floating Disk Trajectories; Run No. 34/06; Wave Period = 1.5 s; Wavemaker Starting Time = 25.8 s

Time (s)	x (m)	y (m)	U (cm/s)	V (cm/s)
28.60	5.21	0.46		
34.17	5.15	0.44	-1.1	-0.3
38.64	5.12	0.43	-0.7	-0.3
43.11	5.03	0.43	-2.0	0.0
50.82	4.88	0.40	-2.0	-0.4
57.33	4.72	0.37	-2.3	-0.5
61.70	4.57	0.37	-3.5	0.0
66.20	4.39	0.34	-4.1	-0.7
72.44	4.15	0.30	-3.9	-0.5
75.85	3.93	0.30	-6.3	0.0
77.55	3.75	0.24	-10.8	-3.6

The first time in the table indicates the time when the motion becomes perceptible.

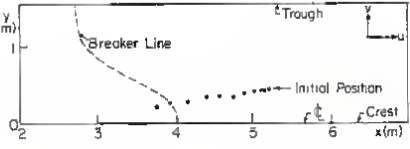

Table C-64. Mean Current Measurements by Floating Disk Trajectories: Run No. 34/07 Wave Period = 1.5 s, Wavemaker Starting Time = 25.8 s

Time (s)	x (m)	y (m)	U (cm/s)	V (cm/s)
26.50	5.21	0.25		
34.04	5.14	0.27	-1.0	-0.2
38.84	5.06	0.27	-1.6	0.0
46.28	4.85	0.24	-2.5	-0.4
52.09	4.69	0.24	-3.1	0.0
55.26	4.57	0.24	-3.8	0.0
59.00	4.40	0.24	-4.5	0.0
61.80	4.22	0.24	-6.5	0.0
63.77	4.02	0.24	-10.1	0.0
65.20	3.87	0.23	-10.7	-1.1
67.30	3.51	0.21	-17.4	-0.7
69.04	3.11	0.21	-22.8	0.0
71.51	2.56	0.24	-22.2	1.2

The first time in the table indicates the time when the motion becomes perceptible.

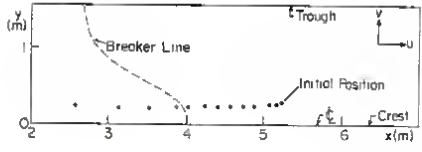

Table C-65. Mean Current Measurements by Floating Disk Trajectories; Run No. 34/08; Wave Period = 1.5 s; Wavemaker Starting Time = 25.8 s

Time (s)	x (m)	y (m)	U (cm/s)	V (cm/s)
27.00	5.12	0.15		
34.07	5.00	0.15	-1.7	0.0
38.51	4.89	0.12	-2.3	-0.6
43.38	4.79	0.12	-2.3	0.0
47.95	4.63	0.09	-3.3	-0.7
52.69	4.40	0.09	-4.5	0.0
56.23	4.19	0.09	-6.0	0.0
58.26	3.99	0.11	-9.8	0.8

The first time in the table indicates the time when the motion becomes perceptible

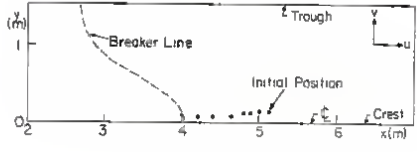

Table C-66. Mean Current Measurements by Floating Disk Trajectories; Run No. 34/09; Wave Period = 1.5 s; Wavemaker Starting Time = 25.8 s

Time (s)	x (m)	y (m)	U (cm/s)	V (cm/s)
26.90	5.15	0.06		
27.87	5.11	0.06	-4.7	0.0
34.04	5.00	0.06	-1.7	0.0
38.51	4.91	0.03	-2.0	-0.7
41.91	4.85	0.00	-1.8	-0.9
46.35	4.69	0.00	-3.4	0.0
50.93	4.54	-0.03	-3.3	-0.7
54.23	4.33	-0.03	-4.6	0.0
58.86	4.08	0.00	-6.7	0.7
60.73	3.93	0.03	-6.1	1.6
62.80	3.66	0.09	-13.3	2.9

The first time in the table indicates the time when the motion becomes perceptible.

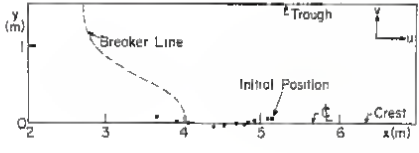

Table C-67. Mean Current Measurements by Floating Disk Trajectories; Run No. 35/01; Wave Period = 1.5 s; Wavemaker Starting Time = 31.4 s

Time (s)	x (m)	y (m)	U (cm/s)	V (cm/s)
37.70	4.30	1.49		
48.95	4.42	1.37	1.1	-1.1
80.28	4.39	1.34	-0.1	-0.1
98.57	4.27	1.52	-0.7	1.0
110.98	3.96	1.52	-2.5	0.0
117.48	3.81	1.37	-2.3	-2.3
119.95	3.81	1.22	0.0	-6.2
123.56	3.75	0.88	-1.7	-8.3
126.96	3.66	0.58	-2.7	-9.0
130.73	3.20	0.46	-12.1	-3.2

The first time in the table indicates the time when the motion becomes perceptible.

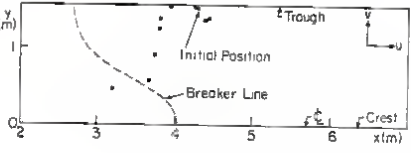

Table C-68. Mean Current Measurements by Floating Disk Trajectories, Run No. 35/02; Wave Period - 1.5 s; Wavemaker Starting Time = 31.4 s

Time (s)	x (m)	y (m)	U (cm/s)	V (cm/s)
36.50	4.42	1.46		
44.01	4.54	1.37	1.6	-1.2
61.76	4.57	1.31	0.2	-0.3
82.35	4.42	1.43	-0.7	0.6
95.83	4.24	1.52	-1.4	0.7
100.43	4.11	1.52	-2.7	0.0
108.44	3.90	1.52	-2.7	0.0
116.15	3.87	1.28	-0.4	-3.2
118.72	3.90	0.98	1.2	-11.9
120.79	3.96	0.76	2.9	-10.3
124.36	4.08	0.55	3.4	-6.0
133.17	4.27	0.46	2.1	-1.0
140.91	4.45	0.67	2.4	2.8
146.15	4.60	0.85	2.9	3.5
152.87	4.88	1.22	4.1	5.4

The first time in the table indicates the time when the motion becomes perceptible.

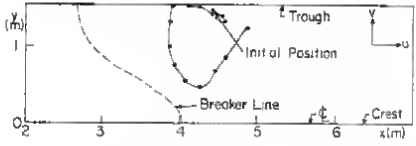

Table C-69 Mean Currant Measurements by Floating Disk Trajectories; Run No. 35/03; Wave Period = 1.5 s; Wavemaker Starting Time = 31.4 s

Time (s)	x (m)	y (m)	U (cm/s)	V (cm/s)
36.80	4.21	1.37		
59.09	4.27	1.22	0.3	-0.7
90.77	4.42	1.22	0.5	0.0
98.90	4.42	1.43	0.0	2.6
103.47	4.27	1.46	-3.3	0.7
110.11	1.05	1.31	-3.2	-2.3
115.12	4.05	1.07	0.0	-4.9
118.29	4.05	0.79	0.0	-8.7
122.02	4.02	0.55	-0.8	-6.5
126.69	3.87	0.34	-3.3	-4.6
129.00	3.66	0.24	-9.2	-4.0
131.00	3.14	0.27	-25.5	1.5

The first time in the table indicates the time when the motion becomas parcaptible.

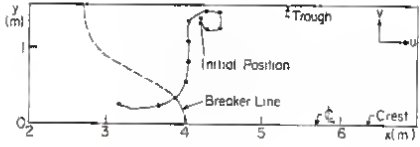

Table C-70. Mean Current Measurements by Floating Disk Trajectories; Run No. 35/04, Wave Period = 1.5 s; Wavemaker Starting Time = 31.4 s

Time (s)	x (m)	y (m)	U (cm/s)	V (cm/s)
37.17	4.36	1.34		
49.38	4.48	1.28	1.0	-0.5
61.63	4.42	1.22	-0.5	-0.5
79.21	4.45	1.31	0.2	0.5
99.83	4.36	1.52	-0.4	1.0
108.38	4.11	1.52	-2.9	0.0
117.12	3.96	1.49	-1.7	-0.3
123.46	3.96	1.25	0.0	-3.8
129.36	3.90	0.85	-1.0	-6.7
132.90	3.84	0.61	-1.7	-6.9
135.90	3.72	0.55	-4.1	-2.0
137.64	3.51	0.46	-12.3	-5.3
139.54	3.14	0.43	-19.3	-1.6
141.14	2.80	0.49	-21.0	3.8
143.01	2.50	0.61	-16.3	6.5
146.41	2.26	0.94	-7.2	9.9

The first time in the table indicates the time when the motion becomes perceptible.

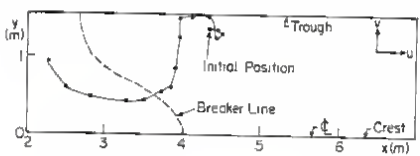

Table C-71. Mean Current Measurements by Floating Disk Trajectories, Run No. 35/05, Wave Period = 1.5 s; Wavemaker Starting Time = 31.4 s

Time (s)	x (m)	y (m)	U (cm/s)	V (cm/s)
33.00	4.27	0.64		
39.34	4.21	0.59	-1.0	-0.7
45.68	3.96	0.40	-2.4	-1.9
52.07	3.81	0.30	-6.4	-3.8
56.16	3.20	0.30	-14.9	0.0
58.69	2.68	0.37	-20.5	2.4
61.20	2.28	0.55	-15.8	7.3

The first time in the table indicates the time when the motion becomes perceptible.

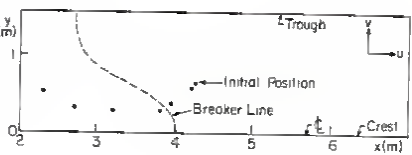

Table C-72. Mean Current Measurements by Floating Disk Trajectories; Run No. 35/06; Wave Period = 1.5 s; Wavemaker Starting Time = 31.4 s

Time (s)	x (m)	y (m)	U (cm/s)	V (cm/s)
32.50	4.30	0.55		
39.41	4.21	0.49	-1.3	-0.9
42.34	4.15	0.43	-2.1	-2.1
47.25	3.99	0.30	-3.1	-2.5
48.78	3.87	0.30	-8.0	0.0
55.99	2.77	0.34	-15.2	0.4
57.66	2.50	0.37	-16.4	1.8
60.13	2.23	0.55	-11.1	7.4

The first time in the table indicates the time when the motion becomes perceptible.

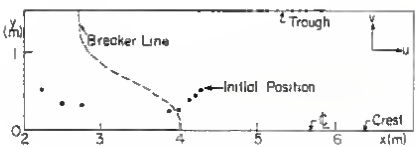

Table [illegible]-73. Mean Current Measurements by Floating Disk Trajectories; Run No. 01/01; Wave Period = 1.9 s; Wavemaker Starting Time = 20.9 s

Time (s)	x (m)	y (m)	U (cm/s)	V (cm/s)
34.39	5.18	1.04		
40.68	4.18	1.07	0.0	0.5
53.48	5.12	1.16	-0.5	0.7
66.66	5.03	1.22	-0.7	0.5
78.55	5.03	1.31	0.0	0.8
94.32	5.18	1.40	1.0	0.6
113.69	5.33	1.49	0.8	0.5
144.58	5.55	1.37	0.7	-0.4
154.55	5.64	1.22	0.9	-1.5
162.92	5.64	1.07	0.0	-1.8
169.13	5.58	0.91	-1.0	-2.5
184.39	5.49	0.61	-0.6	-2.0
199.30	5.18	0.49	-2.0	-0.8
215.17	4.88	0.58	-1.9	0.6
242.58	4.60	0.91	-1.0	1.2
266.00	4.72	1.13	0.5	0.9
278.94	4.88	1.22	1.2	0.7
293.90	5.18	1.25	2.0	0.2
310.73	5.64	1.25	2.7	0.0
327.18	6.10	1.13	2.8	-0.7
342.70	6.40	0.91	2.0	-1.4
362.62	6.46	0.61	0.3	-1.5
398.45	6.10	0.46	-1.0	-0.4
411.33	6.00	0.61	-0.7	1.2
430.59	5.97	0.91	-0.2	1.6

The first time in the table indicates the time when the motion becomes perceptible.

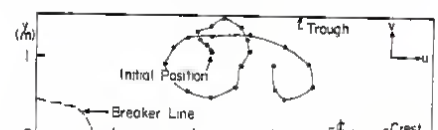

Table C-74. Mean Current Measurements by Floating Disk Trajectories; Run No. 01/02; Wave Period = 1.9, Wavemaker Starting Time = 20.9 s

Time (s)	x (m)	y (m)	U (cm/s)	V (cm/s)
34.00	5.15	0.98		
47.74	5.06	1.01	-0.7	0.2
59.58	5.03	1.07	-0.3	0.5
74.43	4.94	1.22	-0.6	1.0
100.03	5.18	1.34	1.0	0.5
115.34	5.33	1.37	1.0	0.2
126.38	5.49	1.31	1.4	-0.6
146.13	5.64	1.07	0.8	-1.2
153.83	5.64	0.91	0.0	-2.0
161.50	5.64	0.76	0.0	-2.0
171.03	5.55	0.61	-1.0	-1.6
180.40	5.49	0.49	-0.7	-1.3
188.31	5.24	0.43	-3.1	-0.8
192.52	5.00	0.40	-5.8	-0.7
196.08	4.88	0.40	-3.4	0.0
198.85	4.72	0.43	-5.5	1.1
205.93	4.48	0.61	-3.4	2.6
212.10	4.27	0.79	-3.5	3.0
218.58	4.11	0.91	-2.4	1.9
229.72	3.96	1.16	-1.4	2.2
235.79	4.08	1.22	2.0	1.0
250.93	4.15	1.37	0.4	1.0
255.50	4.27	1.40	2.7	0.7
264.35	4.57	1.46	3.4	0.7
271.53	4.88	1.52	4.2	0.8
278.64	5.18	1.52	4.3	0.0
285.31	5.49	1.52	4.6	0.0
294.80	5.94	1.52	4.8	0.0
301.98	6.25	1.46	4.2	-0.8
314.10	6.71	1.22	3.8	-2.0
323.85	6.86	0.91	1.6	-3.1
333.36	6.96	0.61	0.0	-3.2
344.08	6.77	0.30	-0.9	-2.8
361.12	6.55	0.03	-1.3	-1.6
379.38	6.10	-0.03	-2.5	-0.3
404.23	5.79	0.15	-1.2	0.7
415.79	5.79	0.30	-0.3	1.3
432.19	5.79	0.46	0.2	0.9

Table C-74. Continued

Time (s)	x (m)	y (m)	U (cm/s)	V (cm/s)
438.59	5.79	0.76	0.0	4.8
457.06	5.82	1.16	0.2	2.1
469.80	5.94	1.22	1.0	0.5

The first time in the table indicates the time when the motion becomes perceptible.

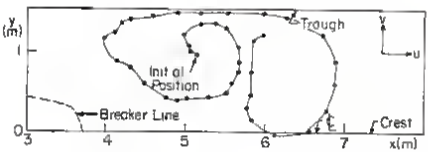

Table (-[illegible]) Mean Current Measurements by Floating Disk Trajectories, Run No. 01/03; Wave Period = 1.9 s; Wavemaker Starting Time = 20.9 s

Time (s)	x (m)	y (m)	U (cm/s)	V (cm/s)
33.69	5.18	0.91		
48.42	5.15	0.94	-0.2	0.2
57.62	5.03	1.01	-1.3	0.7
75.83	4.94	1.13	-0.5	0.7
87.81	4.94	1.22	0.0	0.8
96.09	5.03	1.28	1.1	0.7
107.49	5.18	1.28	1.3	0.0
119.44	5.46	1.19	2.3	-0.8
128.45	5.55	1.01	1.0	-2.0
143.27	5.58	0.67	0.2	-2.3
148.67	5.55	0.61	-0.6	-1.1
160.38	5.33	0.49	-1.8	-1.0
169.53	5.03	0.46	-3.3	-0.3
179.24	4.72	0.55	-3.1	0.9
189.31	4.42	0.70	-3.0	1.5
204.79	4.11	0.91	-2.0	1.4
216.34	3.96	1.07	-1.3	1.3
230.59	3.90	1.22	-0.4	1.1
244.77	3.96	1.34	0.4	0.9
253.18	4.11	1.46	1.8	1.4
265.72	4.57	1.52	3.6	0.5
280.54	5.33	1.52	5.1	0.0
288.35	5.79	1.52	5.9	0.0
294.60	6.10	1.52	4.9	0.0
302.29	6.40	1.37	4.0	-2.0
309.50	6.61	1.22	3.0	-2.1
318.12	6.71	0.91	1.1	-3.5
327.18	6.71	0.61	0.0	-3.4
338.86	6.64	0.30	-0.5	-2.6
348.74	6.40	0.18	-2.5	-1.2
361.78	6.10	0.06	-2.3	-0.9
379.79	5.79	0.12	-1.7	0.3
404.13	5.73	0.30	-0.3	0.8
425.98	5.55	0.61	-0.8	1.4
432.49	5.55	-0.91	0.0	4.7
440.30	5.55	1.22	0.0	3.9
445.90	5.61	1.37	1.1	2.7
450.74	5.70	1.52	1.9	3.1

The first time in the table indicates the time when the motion becomes perceptible.

Table C-75 Continued

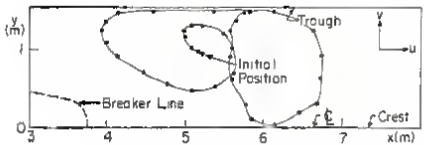

Table C-76. Mean Current Measurements by Floating Disk Trajectories; Run No. 01/04 Wave Period = 1.9 s; Wavemaker Starting Time - 20.9 s

Time (s)	x (m)	y (m)	U (cm/s)	V (cm/s)
35.00	5.24	0.85		
46.38	5.12	0.85	-1.1	0.0
59.89	5.03	0.91	-0.7	0.5
80.25	4.91	1.07	-0.6	0.7
95.02	5.03	1.22	0.6	1.0
104.50	5.18	1.25	1.6	0.3
114.02	5.33	1.19	1.6	-0.6
130.79	5.58	0.91	1.5	-1.6
145.25	5.43	0.61	-1.1	-2.1
154.81	5.18	0.49	-2.6	-1.3
162.29	4.85	0.43	-4.5	-0.8
168.54	4.54	0.46	-4.9	0.5
176.98	4.27	0.55	-3.3	1.1
184.58	3.87	0.67	-5.2	1.6
190.88	3.66	0.73	-3.4	1.0
200.22	3.35	0.70	-3.3	-0.3
208.88	3.05	0.64	-3.5	-0.7
218.12	2.74	0.55	-3.3	-1.0

The first time in the table indicates the time when the motion becomes perceptible.

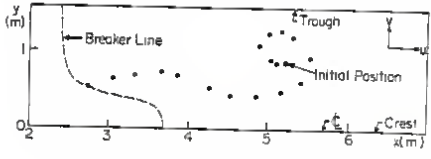

Table C-77 Mean Current Measurements by Floating Disk Trajectories; Run No 01/05; Wave Period = 1.9, Wavemaker Starting Time = 20.9 s

Time (s)	x (m)	y (m)	U (cm/s)	V (cm/s)
34.58	5.24	0.70		
41.62	5.18	0.73	-0.9	0.4
61.33	5.03	0.85	-0.8	0.6
79.29	4.91	0.94	-0.7	0.5
95.79	5.03	1.10	0.7	0.9
116.39	5.43	1.07	1.9	-0.1
126.32	5.49	0.88	0.6	-1.8
144.82	5.30	0.61	-1.0	-1.5
163.42	4.88	0.55	-2.3	-0.3
173.78	4.57	0.61	-2.9	0.6
183.39	4.27	0.76	-3.2	1.6
198.86	3.96	0.91	-2.0	1.0
213.87	3.66	0.94	-2.0	0.2
229.40	3.35	0.94	-2.0	0.0
235.24	3.20	0.91	-2.6	-0.5
240.40	3.05	0.85	-3.0	-1.2
253.09	2.71	0.64	-2.6	-1.7

The first time in the table indicates the time when the motion becomes perceptible.

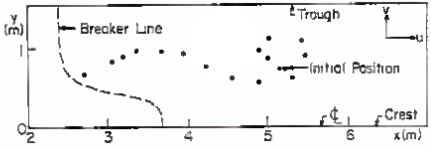

Table C-78. Mean Current Measurements by Floating Disk Trajectories, Run No. 01/06, Wave Period = 1.9, Wavemaker Starting Time = 20.9 s

Time (s)	x (m)	y (m)	U (cm/s)	V (cm/s)
33.00	5.12	0.67		
41.02	5.03	0.64	-1.1	-0.4
59.32	4.88	0.73	-0.8	0.5
73.18	4.72	0.82	-1.1	0.7
84.84	4.60	0.91	-1.0	0.8
105.06	4.57	1.13	-0.2	1.1
117.68	4.63	1.25	0.5	1.0
131.38	5.03	1.28	2.9	0.2
143.80	5.33	1.10	2.5	-1.5
153.31	5.43	0.91	1.0	-1.9
169.34	5.18	0.64	-1.5	-1.7
179.71	4.97	0.67	-2.1	0.3
192.92	4.72	0.73	-1.8	0.5
206.66	4.63	0.91	-0.7	1.3
235.21	4.88	1.13	0.9	0.7
255.50	5.18	1.16	1.5	0.2
269.88	5.49	1.16	2.1	0.0
286.28	5.79	1.07	1.9	-0.6
301.37	6.00	0.94	1.4	-0.8
324.80	5.91	0.64	-0.4	-1.3
334.42	5.79	0.61	-1.3	-0.3
356.78	5.49	0.91	-1.4	1.4
370.88	5.43	1.22	-0.4	2.2
388.78	5.79	1.37	2.0	0.9
418.06	6.71	1.22	3.1	-0.5
436.85	6.80	0.91	0.5	-1.6
463.42	6.55	0.30	-0.9	-2.3
489.00	6.10	0.09	-1.8	-0.8

The first time in the table indicates the time when the motion becomes perceptible.

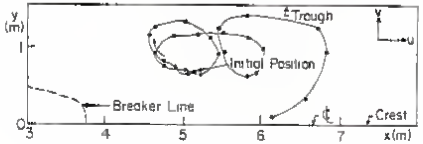

Table C-79 Mean Current Measurements by Floating Disk Trajectories; Run No. 01/07, Wave Period - 1.9; Wavemaker Starting Time = 20.9 s

Time (s)	x (m)	y (m)	U (cm/s)	V (cm/s)
31.00	5.12	0.55		
36.39	5.03	0.55	-1.7	0.0
55.26	4.88	0.55	-0.8	0.0
65.98	4.72	0.55	-1.4	0.0
75.22	4.57	0.61	-1.5	0.7
93.08	4.27	0.61	-1.7	0.0
101.64	4.11	0.55	-1.8	-0.7
106.55	3.96	0.55	-3.1	0.0
116.00	3.66	0.46	-3.2	-1.0
124.39	3.47	0.34	-2.2	-1.5
126.85	3.35	0.27	-5.0	-2.5
130.94	2.98	0.15	-8.9	-3.0

The first time in the table indicates the time when the motion becomes perceptible.

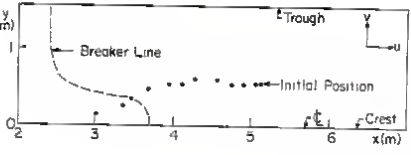

Table C-80. Mean Current Measurements by Floating Disk Trajectories; Run No. 02/01; Wave Period = 1.3, Wavemaker Starting Time ~ 7.4 s

Time (s)	x (m)	y (m)	U (cm/s)	V (cm/s)
25.29	4.94	0.46		
32.04	4.88	0.46	-0.9	0.0
42.05	4.72	0.46	-1.5	0.0
53.29	4.57	0.46	-1.4	0.0
63.04	4.42	0.43	-1.6	-0.3
78.40	4.11	0.37	-2.0	-0.4
84.76	3.96	0.34	-2.4	-0.5
92.20	3.66	0.27	-4.1	-0.8
96.26	3.29	0.18	-9.0	-2.3
98.76	2.98	0.12	-12.2	-2.4
100.34	2.80	0.09	-11.6	-1.9
101.50	2.56	0.06	-21.0	-2.6
103.21	2.44	0.03	-7.1	-1.8

The first time in the table indicates the time when the motion becomes perceptible.

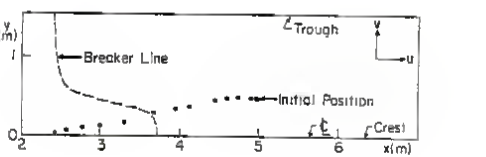

Table C-81. Mean Current Measurements by Floating Disk Trajectories; Run No. 02/02, Wave Period = 1.9 Wavemaker Starting Time 7.4 s

Time (s)	x (m)	y (m)	U (cm/s)	V (cm/s)
20.38	5.09	0.37		
37.10	4.97	0.37	-0.7	0.0
53.35	4.72	0.46	-1.5	0.6
68.18	4.48	0.43	-1.6	-0.2
78.17	4.24	0.43	-2.4	0.0
84.58	4.11	0.43	-1.9	0.0
89.88	3.96	0.40	-2.9	-0.6
96.41	3.66	0.30	-4.7	-1.4
101.08	3.41	0.24	-5.2	-1.3
105.72	2.99	0.09	-9.2	-3.3
107.03	2.74	0.00	-18.6	-7.0
109.28	2.44	0.00	-13.5	0.0
112.24	2.13	-0.03	-10.3	-1.0

The first time in the table indicates the time when the motion becomes perceptible.

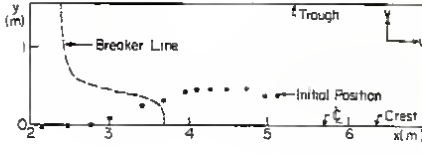

Table C-82. Mean Current Measurements by Floating Disk Trajectories; Run No. 02/03; Wave Period = 1.9 s; Wavemaker Starting Time = 7.4 s

Time (s)	x (m)	y (m)	U (cm/s)	V (cm/s)
21.07	4.85	0.37		
30.58	4.75	0.34	-1.0	-0.3
44.10	4.60	0.34	-1.1	0.0
51.76	4.45	0.34	-2.0	0.0
61.61	4.27	0.34	-1.9	0.0
68.50	4.05	0.30	-3.1	-0.4
77.42	3.81	0.27	-2.7	-0.3
80.39	3.60	0.24	-7.2	-1.0
83.59	3.35	0.18	-7.6	-1.9
85.86	3.11	0.12	-11.8	-2.9

The first time in the table indicates the time when the motion becomes perceptible.

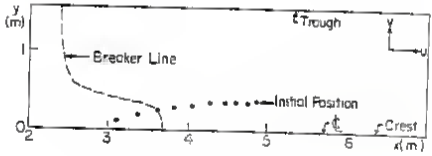

Table C-83. Mean Current Measurements by Floating Disk Trajectories; Run No. 02/04. Wave Period = 1.9 s Wavemaker Starting Time = 7.4 s

Time (s)	x (m)	y (m)	U (cm/s)	V (cm/s)
21.33	4.63	0.34		
34.68	4.51	0.34	-0.9	0.0
38.42	4.42	0.34	-2.4	0.0
46.31	4.27	0.34	-1.9	0.0
57.08	4.02	0.34	-2.3	0.0
63.69	3.81	0.30	-3.2	-0.5
72.43	3.41	0.24	-4.5	-0.7
74.42	3.17	0.18	-12.3	-3.1
76.67	2.87	0.12	-13.5	-2.7

The first time in the table indicates the time when the motion becomes perceptible.

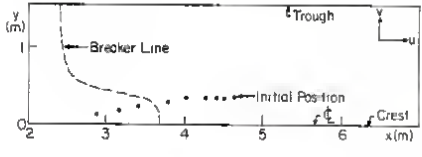

Table C-84. Mean Current Measurements by Floating Disk Trajectories; Run No. 02/05; Wave Period = 1.9; Wavemaker Starting Time = 7.4 s

Time (s)	x (m)	y (m)	U (cm/s)	V (cm/s)
20.35	4.57	0.30		
32.53	4.42	0.27	-1.3	-0.3
40.15	4.27	0.27	-2.0	0.0
44.62	4.11	0.24	-3.4	-0.7
54.42	3.84	0.24	-2.8	0.0
58.34	3.66	0.24	-4.7	0.0
62.27	3.44	0.21	-5.4	-0.8
64.59	3.17	0.15	-11.8	-2.6
66.39	2.93	0.12	-10.2	-1.7
68.20	2.80	0.09	-10.1	-1.7

The first time in the table indicates the time when the motion becomes perceptible.

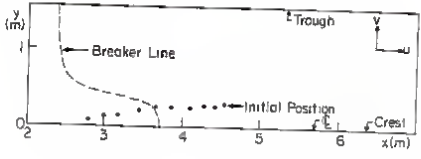

Table C-85. Mean Current Measurements by Floating Disk Trajectories: Run No. 02/06; Wave Period = 1.9, Wavemaker Starting Time - 7 4 s

Time (s)	x (m)	y (m)	U (cm/s)	V (cm/s)
20.72	4.57	0.15		
32.83	4.48	0.15	-0.8	0.0
42.32	4.27	0.18	-2.2	0.3
50.70	4.11	0.21	-1.8	0.4
56.05	3.96	0.24	-2.6	0.6
62.12	3.75	0.24	-3.5	0.0
66.10	3.60	0.24	-3.8	0.0
69.28	3.41	0.18	-5.8	-1.9
70.71	3.17	0.15	-17.1	-2.1
72.98	2.80	0.08	-16.1	-2.7
75.15	2.50	0.06	-14.0	-1.4

The first time in the table indicates the time when the motion becomes perceptible.

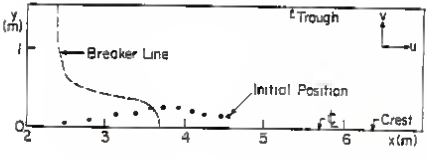

Table C-86. Mean Current Measurements by Floating Disk Trajectories, Run No. 03/01, Wave Period = 1.9, Wavemaker Starting Time = 11.0 s

Time (s)	x (m)	y (m)	U (cm/s)	V (cm/s)
24.00	4.24	0.76		
31.50	4.18	0.73	-0.8	-0.4
41.20	4.02	0.73	-1.6	0.0
48.31	3.96	0.61	-0.8	-1.6
60.52	3.75	0.49	-1.8	-1.0
66.59	3.63	0.43	-2.0	-1.0
70.85	3.57	0.30	-1.4	-2.9
75.06	3.26	0.18	-7.2	-2.5
76.91	3.02	0.15	-13.2	-1.6
78.58	2.74	0.12	-16.4	-1.8
81.50	2.44	0.06	-10.4	-2.1

The first time in the table indicates the time when the motion becomes perceptible.

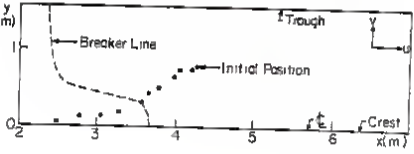

Table C-87. Mean Current Measurements by Floating Disk Trajectories; Run No. 03/02, Wave Period = 1.9, Wavemaker Starting Time = 11.0 s

Time (s)	x (m)	y (m)	U (cm/s)	V (cm/s)
24.22	4.05	0.46		
35.41	3.90	0.37	-1.4	-0.8
38.79	3.65	0.34	-5.3	-0.9
43.77	3.44	0.27	-4.3	-1.2
45.64	3.25	0.18	-8.1	-4.9
47.54	3.02	0.15	-14.4	-1.6
48.55	2.74	0.12	-19.5	-2.2

The first time in the table indicates the time when the motion becomes perceptible.

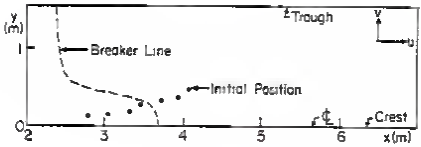

Table C-88. Mean Current Measurements by Floating Disk Trajectories, Run No. 03/03; Wave Period = 1.9; Wavemaker Starting Time = 11.0 s

Time (s)	x (m)	y (m)	U (cm/s)	V (cm/s)
25.12	4.18	0.43		
33.80	4.02	0.37	-1.8	-0.7
35.88	3.96	0.34	-2.9	-1.5
43.12	3.72	0.30	-3.4	-0.4
45.73	3.66	0.30	-2.3	0.0
47.73	3.51	0.27	-7.6	-1.5
49.75	3.32	0.21	-9.1	-3.0
51.62	3.11	0.18	-11.4	-1.6
53.65	2.87	0.12	-12.0	-3.0
54.97	2.69	0.09	-13.9	-2.3

The first time in the table indicates the time when the motion becomes perceptible.

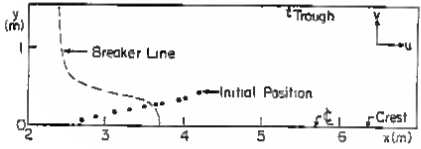

Table C-89. Mean Current Measurements by Floating Disk Trajectories; Run No. 03/04, Wave Period = 1.9; Wavemaker Starting Time = 11.0 s

Time (s)	x (m)	y (m)	U (cm/s)	V (cm/s)
23.72	3.99	0.34		
27.84	3.90	0.27	-2.2	-1.5
30.58	3.81	0.24	-3.3	-1.1
33.69	3.66	0.21	-4.9	-1.0
36.12	3.35	0.15	-12.5	-2.5
38.48	3.11	0.12	-10.3	-1.3
40.27	2.87	0.09	-13.6	-1.7

The first time in the table indicates the time when the motion becomes perceptible.

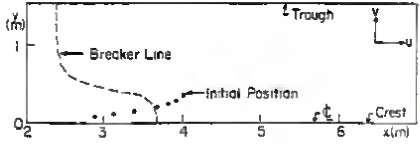

Table C-90. Mean Current Measurements by Floating Disk Trajectories; Run No. 03/05; Wave Period = 1.9, Wavemaker Starting Time = 11.0 s

Time (s)	x (m)	y (m)	U (cm/s)	V (cm/s)
23.80	4.21	0.27		
26.12	4.11	0.24	-3.9	-1.3
31.76	3.99	0.21	-2.2	-0.5
36.02	3.87	0.21	-2.9	0.0
39.80	3.66	0.18	-5.6	-0.8
43.80	3.35	0.12	-7.6	-1.5
46.04	3.05	0.06	-13.6	-2.7
47.53	2.90	0.00	-10.2	-4.1

The first time in the table indicates the time when the motion becomes perceptible.

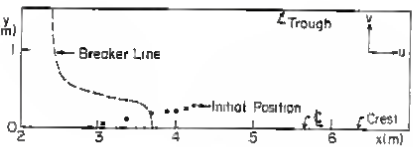

Table C-91. Mean Current Measurements by Floating Disk Trajectories, Run No. 03/06; Wave Period = 1.9; Wavemaker Starting Time = 11.0 s

Time (s)	x (m)	y (m)	U (cm/s)	V (cm/s)
22.15	4.24	0.24		
28.80	4.15	0.21	-1.4	-0.5
24.18	3.93	0.15	4.6	1.3
39.40	3.63	0.12	-2.0	-0.2
41.99	3.35	0.09	-10.6	-1.2
44.18	3.02	0.03	-15.3	-2.8

The first time in the table indicates the time when the motion becomes perceptible.

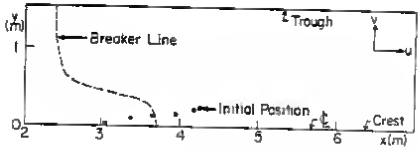

Table C-92. Mean Current Measurements by Floating Disk Trajectories; Run No. 04/01, Wave Period = 1.9; Wavemaker Starting Time = 12.9 s

Time (s)	x (m)	y (m)	U (cm/s)	V (cm/s)
24.99	3.57	0.61		
33.89	3.60	0.46	0.3	-1.7
35.40	3.51	0.34	-6.1	-8.1
37.06	3.38	0.27	-7.3	-3.7
38.82	3.26	0.24	-6.9	-1.7
41.10	2.99	0.18	-12.0	-2.7
42.42	2.80	0.15	-13.9	-2.3
43.60	2.59	0.12	-18.1	-2.6
46.13	2.29	0.12	-12.0	0.0

The first time in the table indicates the time when the motion becomes perceptible.

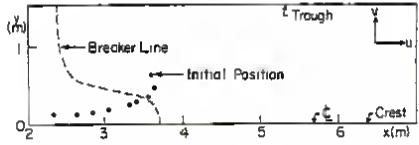

Table C-93 Mean Current Measurements by Floating Disk Trajectories; Run No 04/02; Wave Period = 1.9; Wavemaker Starting Time = 12.9 s

Time (s)	x (m)	y (m)	U (cm/s)	V (cm/s)
24.58	3.51	0.55		
28.89	3.47	0.46	-0.7	-2.1
32.46	3.38	0.34	-2.6	-3.8
33.73	3.29	0.30	-7.2	-2.4
35.95	3.05	0.24	-11.0	-2.7
37.73	2.80	0.24	-13.7	0.0
39.95	2.53	0.27	-12.4	1.4
41.94	2.41	0.37	-6.1	4.6
44.87	2.29	0.61	-4.2	8.3
48.69	2.38	0.91	2.4	8.0

The first time in the table indicates the time when the motion becomes perceptible.

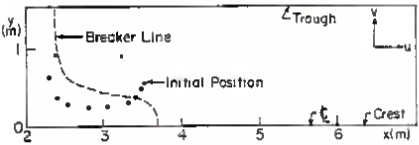

Table D-4. Mean Current Measurements by Floating Disk Trajectories; Run No. 04/03; Wave Period = 1.9, Wavemaker Starting Time = 12.9

Time (s)	x (m)	y (m)	U (cm/s)	V (cm/s)
22.98	3.57	0.27		
25.09	3.44	0.27	-5.8	0.0
27.27	3.29	0.34	-7.0	2.8
31.59	3.11	0.40	-4.2	1.4
33.64	3.05	0.43	-3.0	1.5
42.08	2.83	0.40	-2.5	-0.4
43.34	2.69	0.34	-12.1	-4.8
45.52	2.53	0.37	-7.0	1.4
47.58	2.41	0.46	-5.9	4.4
50.51	2.29	0.61	-4.2	5.2
53.93	2.35	0.91	1.8	8.9

The first time in the table indicates the time when the motion becomes perceptible.

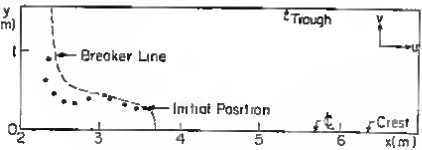

Table C-95. Mean Current Measurements by Floating Disk Trajectories; Run No. 04/04; Wave Period = 1.9; Wavemaker Starting Time = 12.9 s

Time (s)	x (m)	y (m)	U (cm/s)	V (cm/s)
23.08	3.72	0.18		
25.32	3.54	0.21	-8.2	1.4
27.09	3.38	0.27	-8.6	3.4
29.39	3.26	0.30	-5.3	1.3
33.58	3.05	0.40	-5.1	2.2
37.98	2.80	0.40	-5.5	0.0
42.01	2.68	0.43	-3.0	0.8
45.92	2.59	0.49	-2.4	1.6
50.74	2.50	0.61	-1.9	2.5
55.95	2.50	0.76	0.0	2.9
65.13	2.71	1.07	2.3	3.3
72.85	2.83	1.07	2.3	0.0
80.99	2.96	0.91	1.5	-1.9
88.90	2.90	0.73	-0.8	-2.3
96.29	2.74	0.61	-2.1	-1.6
108.19	2.44	0.55	-2.6	-0.5
118.75	2.29	0.76	-1.4	2.0

The first time in thm table indicates the time when the motion becomes perceptible.

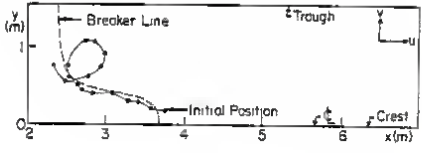

Table C-96. Mean Current Measurements by Floating Disk Trajectories; Run No. 04/05; Wave Period = 1.9; Wavemaker Starting Time = 12.9 s

Time (s)	x (m)	y (m)	U (cm/s)	V (cm/s)
22.90	3.75	0.12		
25.05	3.60	0.12	-7.1	0.0
27.89	3.35	0.12	-8.6	0.0
31.54	2.99	0.15	-10.0	0.8
34.20	2.77	0.30	-8.0	5.7
36.80	2.68	0.43	-3.5	4.7
41.07	2.59	0.61	-2.1	4.3

The first time in the table indicates the time when the motion becomes perceptible.

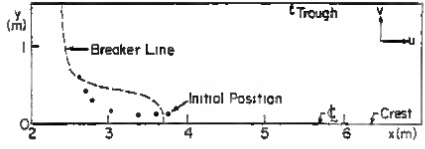

Table C-97. Mean Current Measurements by Floating Disk Trajectories; Run No. 04/06, Wave Period = 1.5, Wavemaker Starting Time = 12.9 s

Time (s)	x (m)	y (m)	u (cm/s)	v (cm/s)
22.89	3.63	0.09		
25.45	3.47	0.09	-6.0	0.0
27.36	3.26	0.12	-11.2	1.6
29.32	3.08	0.15	-9.3	1.6
32.03	2.83	0.18	-9.0	1.1
34.45	2.59	0.21	-10.1	1.3
37.83	2.41	0.30	-5.4	2.7
41.97	2.16	0.46	-5.5	3.7
45.32	2.13	0.61	-0.9	4.5

The first time in the table indicates the time when the motion becomes perceptible.

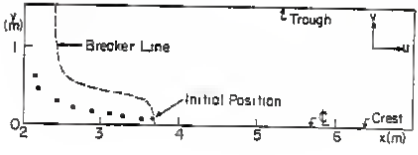

Table C-98. Mean Current Measurements by Floating Disk Trajectories; Run No. 04/07; Wave Period = 1.9; Wavemaker Starting Time = 12.9 s

Time (s)	x (m)	y (m)	U (cm/s)	V (cm/s)
22.42	3.78	0.06		
25.37	3.60	0.03	-6.2	-1.0
27.69	3.38	0.00	-9.2	-1.3
29.74	3.17	-0.06	-10.4	-3.0
33.51	2.93	-0.18	-6.5	-3.2

The first time in the table indicates the time when the motion becomes perceptible.

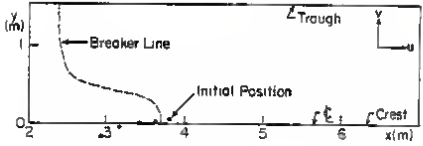

Table C-99. Mean Current Measurements by Floating Disk Trajectories, Run No. 05/01; Wave Period - 1.9; Wavemaker Starting Time - 10.5 s

Time (s)	x (m)	y (m)	U (cm/s)	V (cm/s)
22.52	2.90	0.79		
34.23	3.05	0.82	1.3	0.3
40.77	3.11	0.73	0.9	-1.4
45.28	3.11	0.61	0.0	-2.7
50.72	2.96	0.43	-2.8	-3.4
53.32	2.87	0.37	-3.5	-2.3
55.47	2.74	0.30	-5.7	-2.8
57.32	2.62	0.30	-6.6	0.0
58.93	2.44	0.34	-7.0	1.2
63.13	2.19	0.40	-7.6	1.9

The first time in the table indicates the time when the motion becomes perceptible.

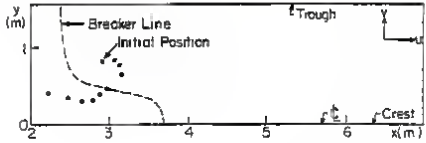

Table C-100. Mean Current Measurements by Floating Disk Trajectories; Run No. 05/02; Wave Period = 1.9; Wavemaker Starting Time = 10.5 s

Time (s)	x (m)	y (m)	U (cm/s)	V (cm/s)
22.76	3.05	0.76		
33.82	3.17	0.67	1.1	-0.8
38.69	3.17	0.49	0.0	-3.8
44.93	2.93	0.27	-3.9	-3.4
47.48	2.74	0.15	-7.2	-4.8
49.58	2.50	0.18	-11.6	1.5
51.70	2.50	0.18	-10.1	1.4

The first time in the table indicates the time when the motion becomes perceptible.

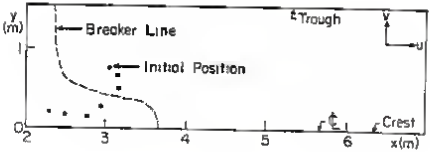

Table C-101. Mean Current Measurements by Floating Disk Trajectories; Run No. 05/03, Wave Period = 1.91 Wavemaker Starting Time = 10.5 s

Time (s)	x (m)	y (m)	U (cm/s)	V (cm/s)
22.32	2.62	0.76		
25.06	2.59	0.79	-1.1	1.1
33.68	2.68	0.85	1.1	0.7
36.95	2.77	0.85	2.8	0.0
40.92	2.83	0.79	1.5	-1.5
44.14	2.93	0.70	2.8	-2.8
46.35	2.87	0.61	-2.8	-4.1
48.85	2.80	0.52	-2.4	-3.7
51.03	2.74	0.43	-2.8	-4.2
54.99	2.50	0.37	-6.2	-1.5
58.38	2.38	0.40	-3.6	0.9
61.33	2.13	0.46	-8.3	2.1

The first time in the table indicates the time when the motion becomes perceptible.

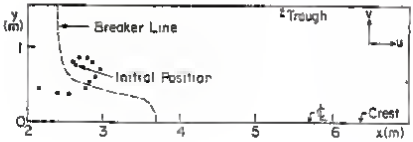

Table C-102 Mean Current Measurements by Floating Disk Trajectories; Run No. 05/04; Wave Period = 1.9; Wavemaker Starting Time = 10.5 s

Time (s)	x (m)	y (m)	U (cm/s)	V (cm/s)
22.16	2.77	0.64		
32.28	2.99	0.61	2.1	-0.3
36.25	3.05	0.49	1.5	-3.1
39.21	2.96	0.37	-3.1	-4.1
41.16	2.83	0.34	-6.3	-1.6
43.29	2.65	0.27	-8.6	-2.9
44.76	2.53	0.30	-8.3	2.1
46.35	2.35	0.34	-11.5	1.9
48.07	2.16	0.37	-10.6	1.8
50.12	2.10	0.55	-3.0	8.9

The first time in the table indicates the time when the motion becomes perceptible.

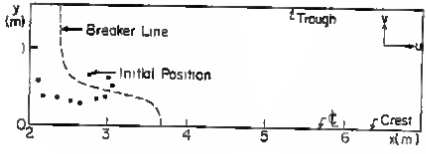

Table C-103. Mean Current Measurements by Floating Disk Trajectories; Run No. 05/05; Wave Period = 1.9; Wavemaker Starting Time = 10.5 s

Time (s)	x (m)	y (m)	U (cm/s)	V (cm/s)
21.99	2.87	0.61		
30.90	3.02	0.55	1.7	-0.7
33.65	3.02	0.46	0.0	-3.3
36.31	2.96	0.37	-2.6	-3.8
38.37	2.77	0.30	-7.8	-2.6
40.12	2.59	0.30	-10.5	0.0
42.48	2.38	0.37	-9.0	2.6
44.90	2.19	0.49	-7.6	5.0
47.46	2.16	0.64	-1.2	6.0
51.09	2.16	0.91	0.0	7.6
53.59	2.29	1.07	4.9	6.1
65.13	2.29	1.28	0.0	1.8
67.89	2.41	1.34	4.4	2.2
72.76	2.62	1.37	4.4	0.6
76.08	2.77	1.37	4.6	0.0
81.37	3.05	1.31	5.2	-1.2
87.02	3.20	1.22	2.7	-1.6
95.25	3.26	1.07	0.7	-1.9
105.22	3.14	0.85	-1.2	-2.1
111.69	3.05	0.76	-1.4	-1.4
120.95	2.90	0.73	-1.6	-0.3
132.33	2.71	0.67	-1.6	-0.5
151.95	2.44	0.64	-1.4	-0.2
173.24	2.19	0.79	-1.1	0.7
182.85	2.19	1.07	0.0	2.9
203.94	2.44	1.43	1.2	2.0
211.34	2.74	1.52	4.1	0.4
218.15	3.05	1.52	4.5	0.0
227.58	3.38	1.52	3.6	0.0
234.37	3.66	1.52	4.0	0.0

The first time in the table indicates the time when the motion becomes perceptible.

Table C-103. Continued

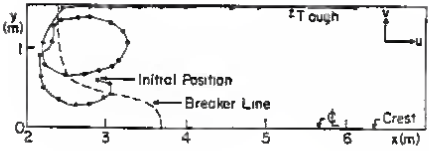

Table C-104. Mean Current Measurements by Floating Disk Trajectories: Run No. 05/06; Wave Period = 1.3; Wavemaker Starting Time = 10.5 s

Time (s)	x (m)	y (m)	U (cm/s)	V (cm/s)
22.16	2.74	0.58		
29.56	2.71	0.67	-0.4	1.2
33.15	2.83	0.73	3.4	1.7
38.22	2.90	0.61	1.2	-2.4
42.88	2.83	0.49	-1.3	-2.6
44.94	2.74	0.40	-4.4	-4.4
47.62	2.53	0.37	-8.0	-1.1
48.69	2.38	0.37	-14.2	0.0
51.85	2.13	0.46	-7.7	2.9

The first time in the table indicates the time when the motion becomes perceptible.

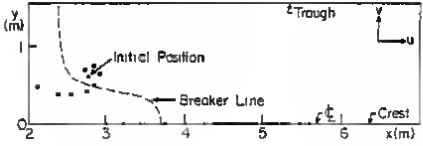

Table C-105. Mean Current Measurements by Floating Disk Trajectories. Run No. 06/01; Wave Period = 1.9; Wavemaker Starting Time = 19.1 s

Time (s)	x (m)	y (m)	U (cm/s)	V (cm/s)
31.90	2.99	0.27		
33.41	2.87	0.27	-8.1	0.0
35.93	2.77	0.30	-3.6	1.2
37.64	2.62	0.30	-8.9	0.0
39.73	2.53	0.37	-4.4	2.9
42.39	2.44	0.49	-3.4	4.6
44.85	2.29	0.58	-6.2	3.7
46.62	2.23	0.67	-3.1	4.6
50.22	2.29	0.91	1.8	7.2

The first time in the table indicates the time when the motion becomes perceptible.

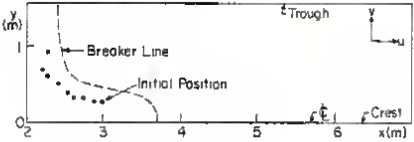

Table C-106. Mean Current Measurements by Floating Disk Trajectories; Run No. 06/02; Wave Period = 1.5; Wavemaker Starting Time = 19.1 s

Time (s)	x (m)	y (m)	U (cm/s)	V (cm/s)
31.17	2.87	0.18		
33.67	2.77	0.18	-3.7	0.0
35.58	2.68	0.15	-4.8	-1.6
37.28	2.56	0.15	-7.2	0.0
40.00	2.44	0.18	-4.5	1.1
42.15	2.38	0.24	-2.8	2.8
44.63	2.26	0.30	-4.9	2.5

The first time in the table indicates the time when the motion becomes perceptible.

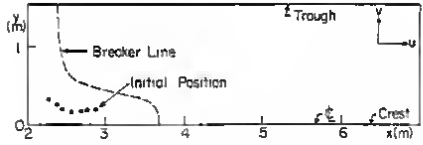

Table C-107. Mean Current Measurements by Floating Disk Trajectories; Run No. 06/03 Wave Period - 1.3; Wavemaker Starting Time = 19.1 s

Time (s)	x (m)	y (m)	U (cm/s)	V (cm/s)
32.08	3.05	0.09		
33.08	2.96	0.09	-9.1	0.0
35.44	2.80	0.09	-6.5	0.0
37.63	2.71	0.09	-4.2	0.0
39.36	2.58	0.06	-7.9	-1.6
41.68	2.44	0.03	-5.9	-1.3
46.04	2.19	-0.06	-5.6	-2.1

The first time in the table indicates the time when the motion becomes perceptible.

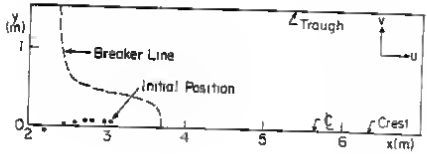

Table C-108. Mean Current Measurements by Floating Disk Trajectories; Run No. 06/04; Wave Period = 1.9; Wavemaker Starting Time = 19.1 s

Time (s)	x (m)	y (m)	U (cm/s)	V (cm/s)
31.27	2.77	0.09		
34.56	2.68	0.06	-2.8	-0.9
36.39	2.56	0.06	-6.7	0.0
37.86	2.50	0.06	-4.1	0.0
40.55	2.44	0.03	-2.0	-1.0
42.97	2.32	0.00	-6.0	-1.5
44.55	2.23	-0.03	-5.8	-1.9

The first time in the table indicates the time when the motion becomes perceptible.

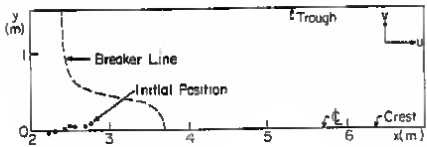

Table C-109. Mean Current Measurements by Floating Disk Trajectories: Run No. 06/05; Wave Period = 1.9; Wavemaker Starting Time = 19.1 s

Time (s)	x (m)	y (m)	U (cm/s)	V (cm/s)
31.92	2.62	0.09		
34.07	2.55	0.09	-2.8	0.0
36.14	2.50	0.12	-2.9	1.5
37.88	2.44	0.12	-3.5	0.0
40.20	2.35	0.15	-3.9	1.3

The first time in the table indicates the time when the motion becomes perceptible.

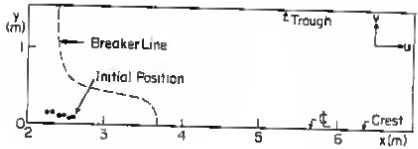

Table C-110. Mean Current Measurements by Floating Disk Trajectories, Run No. 06/06; Wave Period = 1.9; Wavemaker Starting Time = 19.1 s

Time (s)	x (m)	y (m)	U (cm/s)	V (cm/s)
31.08	2.87	0.00		
33.78	2.74	0.00	-4.5	0.0
36.16	2.68	0.00	-2.6	0.0
38.08	2.56	-0.03	-6.4	-1.6
40.60	2.50	-0.06	-2.4	-1.2
42.37	2.38	-0.09	-6.9	-1.7
44.50	2.29	-0.15	-4.3	-2.9

The first time in the table indicates the time when the motion becomes perceptible.

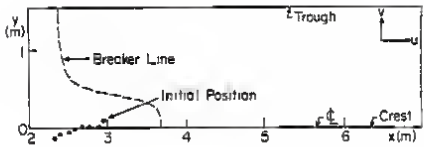

Table C-111. Mean Current Measurements by Floating Disk Trajectories: Run No. 06/07, Wave Period = 1.9; Wavemaker Starting Time = 19.1 s

Time (s)	x (m)	y (m)	U (cm/s)	V (cm/s)
31.29	2.99	-0.03		
34.16	2.97	-0.05	-0.5	-0.5
35.31	2.83	-0.06	-11.5	-1.3
37.09	2.71	-0.06	-6.8	-1.7
39.09	2.56	-0.15	-7.6	-3.0
41.40	2.41	-0.21	-7.6	-3.0

The first time in the table indicates the time when the motion becomes perceptible.

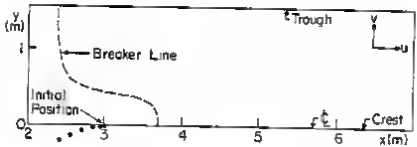

Table C-112. Mean Current Measurements by Floating Disk Trajectories; Run No. 06/08; Wave Period = 1.9; Wavemaker Starting Time = 19.1 s

Time (s)	x (m)	y (m)	U (cm/s)	V (cm/s)
30.85	2.80	-0.06		
33.60	2.80	-0.09	-3.3	-1.1
35.41	2.71	-0.12	-5.1	-1.7
37.46	2.56	-0.14	-7.4	-0.7
39.53	2.42	-0.15	-6.6	-0.7
41.20	2.35	-0.18	-4.6	-1.8

The first time in the table indicates the time when the motion becomes perceptible.

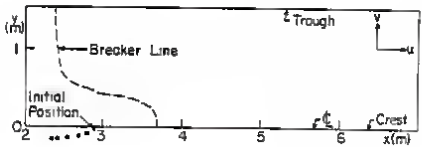

Table C-113. Mean Current Measurements by Floating Disk Trajectories; Run No. 06/09; Wave Period = 1.90 Wavemaker Starting Time = 19.1 s

Time (s)	x (m)	y (m)	u (cm/s)	v (cm/s)
31.20	2.90	-0.08		
35.78	2.68	-0.11	-4.7	-0.7
37.28	2.56	-0.12	-8.1	-1.0
39.06	2.50	-0.15	-3.4	-1.7
41.38	2.32	-0.18	-7.9	-1.3
44.07	2.10	-0.21	-7.9	-1.1

The first time in the table indicates the time when the motion becomes perceptible.

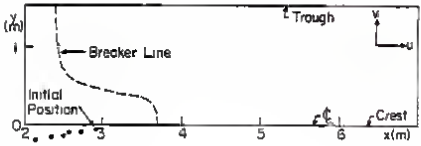

Table C-114. Mean Current Measurements by Floating Disk Trajectories; Run No. 07/01, Wave Period = 1.9; Wavemaker Starting Time = 25.8 s

Time (s)	x (m)	y (m)	U (cm/s)	V (cm/s)
36.55	3.35	0.09		
38.89	3.23	0.09	-5.2	0.0
40.86	3.08	0.06	-7.7	-1.5
42.83	2.93	0.03	-7.7	-1.5
44.85	2.77	0.03	-7.5	0.0
47.50	2.59	0.03	-6.9	0.0
49.57	2.47	0.00	-5.9	-1.5
51.55	2.35	0.00	-6.2	0.0
53.42	2.23	0.00	-6.5	0.0

The first time in the table indicates the time when the motion becomes perceptible.

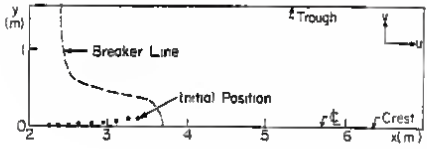

Table C-115. Mean Current Measurements by Floating Disk Trajectories; Run No. 07/02; Wave Period = 1.9; Wavemaker Starting Time = 25.8 s

Time (s)	x (m)	y (m)	U (cm/s)	V (cm/s)
36.57	3.32	0.00		
38.64	3.17	0.00	-7.4	0.0
40.98	3.08	-0.03	-3.9	-1.3
42.82	2.94	-0.09	-7.5	-3.3
44.68	2.80	-0.15	-7.4	-3.3
46.78	2.68	-0.24	-5.8	-4.4
48.70	2.53	-0.27	-7.9	-1.6
50.43	2.44	-0.27	-5.3	-5.3

The first time in the table indicates the time when the motion becomes perceptible.

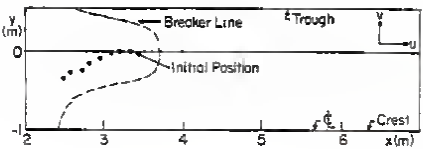

Table C-116. Mean Current Measurements by Floating Disk Trajectories; Run No. 07/03; Wave Period = 1.5; Wavemaker Starting Time = 25.8 s

Time (s)	x (m)	y (m)	U (cm/s)	V (cm/s)
36.55	3.08	0.00		
38.88	2.99	0.00	-3.9	0.0
41.26	2.83	0.00	-6.4	0.0
43.74	2.74	0.00	-3.7	0.0
47.33	2.50	-0.03	-6.8	-0.8
49.72	2.35	-0.06	-6.4	-1.3
52.35	2.19	-0.11	-5.8	-1.7

The first time in the table indicates the time when the motion becomes perceptible.

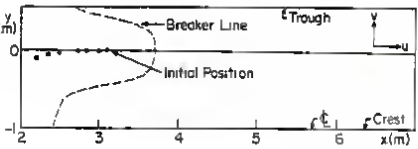

Table C-117. Mean Current Measurements by Floating Disk Trajectories, Run No. 07/04; Wave Period = 1.9; Wavemaker Starting Time = 25.8 s

Time (s)	x (m)	y (m)	U (cm/s)	V (cm/s)
37.05	3.14	-0.09		
38.80	3.05	-0.09	-5.2	0.0
41.02	2.90	-0.15	-6.9	-2.7
44.00	2.77	-0.18	-4.1	-1.0
45.85	2.62	-0.18	-8.2	0.0
47.80	2.50	-0.21	-6.3	-1.6
50.22	2.38	-0.24	-5.0	-1.3
52.24	2.16	-0.27	-10.6	-1.5

The first time in the table indicates the time when the motion becomes perceptible.

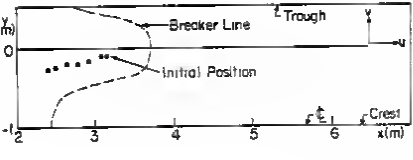

Table C-118. Mean Current Measurements by Floating Disk Trajectories: Run No. 07/05; Wave Period = 1.9; Wavemaker Starting Time = 25.8 s

Time (s)	x (m)	y (m)	U (cm/s)	V (cm/s)
36.73	3.05	-0.12		
37.77	3.00	-0.12	-4.4	0.0
39.36	2.90	-0.15	-6.7	-1.9
41.88	2.77	-0.18	-5.3	-1.3
43.40	2.65	-0.21	-7.1	-1.8
45.56	2.50	-0.21	-7.1	0.0
47.85	2.38	-0.24	-5.3	-1.3

The first time in the table indicates the time when the motion becomes perceptible.

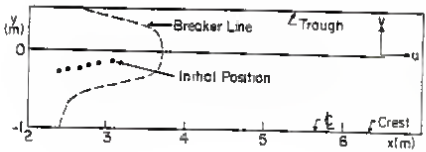

Table C-119. Mean Current Measurements by Floating Disk Trajectories; Run No. 07/06; Wave Period = 1.9; Wavemaker Starting Time = 25.8 s

Time (s)	x (m)	y (m)	U (cm/s)	V (cm/s)
37.50	3.17	-0.15		
40.04	3.05	-0.21	-4.2	-2.1
42.40	2.90	-0.24	-7.6	-1.5
44.08	2.80	-0.30	-5.4	-3.6
45.43	2.65	-0.34	-11.3	-2.3
47.05	2.53	-0.34	-7.5	0.0
48.95	2.41	-0.37	-6.4	-1.6

The first time in the table indicates the time when the motion becomes perceptible.

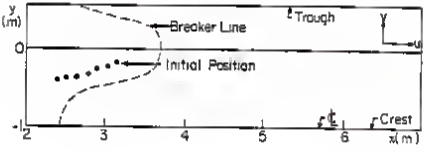

Table C-120. Mean Current Measurements by Floating Disk Trajectories; Run No. 07/07; Wave Period = 1.9; Wavemaker Starting Time = 25.8 s

Time (s)	x (m)	y (m)	U (cm/s)	V (cm/s)
37.05	3.17	-0.34		
40.14	3.14	-0.35	-1.0	-0.5
53.09	2.71	-0.18	-3.3	1.3
54.92	2.50	-0.27	-11.7	-5.0
56.38	2.41	-0.34	-6.3	-4.2
57.87	2.32	-0.46	-5.1	-8.2
59.34	2.23	-0.58	-6.2	-8.3
62.20	2.26	-0.70	1.1	-4.3
66.23	2.32	-0.94	1.5	-6.1
70.63	2.44	-1.13	2.8	-4.2

The first time in the table indicates the time when the motion becomes perceptible.

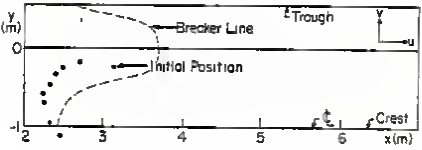

Table C-121. Mean Current Measurements by Floating Disk Trajectories, Run No. 08/01; Wave Period = 1.9, Wavemaker Starting Time = 21.8 s

Time (s)	x (m)	y (m)	U (cm/s)	V (cm/s)
104.10	5.06	1.52		
122.08	5.18	1.52	0.7	0.0
140.33	5.33	1.37	0.8	-0.8
152.66	5.44	1.22	0.9	-1.2
170.34	5.46	0.91	0.1	-1.7
179.82	5.33	0.76	-1.3	-1.6
193.38	5.18	0.70	-1.1	-0.4
225.30	5.09	0.79	-0.3	0.3
268.02	5.03	0.91	-0.1	0.3
281.33	5.12	1.04	0.7	0.9
301.46	5.49	1.16	1.8	0.6
312.65	5.79	1.13	2.7	-0.3
328.77	6.10	0.91	1.9	-1.3
353.49	6.13	0.61	0.1	-1.2
394.23	6.10	0.76	-0.1	0.4
408.15	6.10	0.91	0.0	1.1
427.96	6.28	0.91	0.9	0.0
449.80	6.25	0.76	-0.1	-0.7
479.18	6.10	0.76	-0.5	0.0

The first time in the table indicates the time when the motion becomes perceptible.

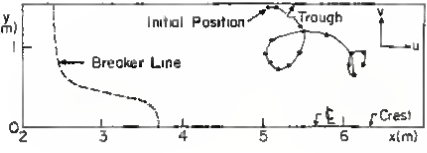

Table C-122. Mean Current Measurements by Floating Disk Trajectories; Run No. 08/02; Wave Period = 1.9, Wavemaker Starting Time - 21.8 s

Time (s)	x (m)	y (m)	U (cm/s)	V (cm/s)
101.96	4.79	1.52		
113.39	4.88	1.52	0.8	0.0
128.12	5.03	1.51	1.0	-0.1
135.21	5.18	1.49	2.1	-0.2
146.43	5.33	1.37	1.4	-1.1
157.45	5.49	1.22	1.4	-1.4
175.96	5.49	0.91	0.0	-1.6
192.83	5.33	0.67	-0.9	-1.4
208.28	5.18	0.61	-1.0	-0.4
225.28	5.00	0.64	-1.1	0.2
236.98	4.88	0.67	-1.0	0.3
246.99	4.82	0.76	-0.6	0.9
259.80	4.72	0.91	-0.7	1.2
279.12	4.88	1.22	0.8	1.6
290.60	5.18	1.28	2.7	0.5
299.42	5.49	1.37	3.5	1.0
307.06	5.79	1.37	4.0	0.0
314.22	6.10	1.37	4.3	0.0
325.63	6.40	1.28	2.7	-0.8
339.93	6.71	1.22	2.1	-0.4
354.58	6.86	0.91	1.0	-2.1
364.89	6.92	0.61	0.6	-3.0
388.23	6.91	0.00	-1.3	-2.6
404.68	6.10	-0.06	-3.1	-0.4
421.73	5.79	0.06	-1.8	0.7
441.19	5.64	0.30	-0.8	1.3
464.62	5.73	0.61	0.4	1.3
472.17	5.79	0.91	0.8	4.0
481.94	5.94	1.22	1.6	3.1

The first time in the table indicates the time when the motion becomes perceptible.

Table C-122. Continued

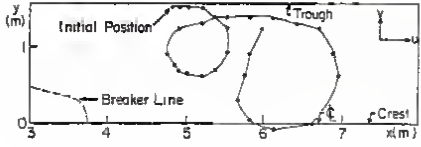

Table C-123. Mean Current Measurements by Floating Disk Trajectories, Run No. 08/03; Wave Period = 1.9; Wavemaker Starting Time - 21.8 s

Time (s)	x (m)	y (m)	U (cm/s)	V (cm/s)
101.39	5.00	1.43		
118.44	5.14	1.40	0.8	-0.2
139.70	5.33	1.22	0.9	-0.9
156.93	5.36	0.91	0.2	-1.8
172.60	5.18	0.67	-1.2	-1.6
188.11	4.88	0.64	-2.0	-0.2
201.78	4.72	0.85	-1.1	1.6
214.32	4.79	1.07	0.5	1.7
222.55	4.97	1.22	2.2	1.9
230.05	5.18	1.25	2.8	0.4
241.33	5.49	1.31	2.7	0.5
256.51	5.79	1.28	2.0	-0.2
270.89	6.10	1.22	2.2	-0.4
274.73	6.40	0.91	7.9	-7.9
307.53	6.40	0.61	0.0	-0.9
333.72	6.10	0.30	-1.2	-1.2
353.12	5.88	0.61	-1.1	1.6
368.86	5.64	0.94	-1.5	2.1
381.73	5.67	1.22	0.2	2.1
388.48	5.79	1.31	1.8	1.4
419.47	6.46	1.22	2.2	-0.3
449.80	6.74	0.76	0.9	-1.5
474.38	6.40	0.30	-1.4	-1.9
490.28	6.10	0.15	-1.9	-1.0

The first time in the table indicates the time when the motion becomes perceptible.

Table C-123. Continued

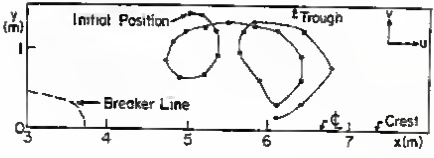

Table C-124. Mean Current Measurements by Floating Disk Trajectories; Run No. 08/04; Wave Period = 1.9; Wavemaker Starting Time = 21.8 s

Time (s)	x (m)	y (m)	U (cm/s)	V (cm/s)
102.50	4.88	1.43		
111.09	4.94	1.43	0.7	0.0
131.22	5.18	1.34	1.2	-0.5
143.92	5.38	1.22	1.4	-1.0
161.44	5.36	0.91	0.0	-1.7
179.15	5.18	0.70	-1.0	-1.2
197.22	4.88	0.78	-1.7	0.3
215.67	4.94	0.98	0.3	1.2
232.09	5.18	1.07	1.5	0.8
254.81	5.49	1.07	1.3	0.0
281.29	5.79	0.96	1.2	-0.4
310.45	5.94	0.76	0.5	-0.7
336.89	5.85	0.64	-0.3	-0.5
359.06	5.49	0.91	-1.6	1.2
388.94	5.39	1.22	-0.9	3.1
376.80	5.49	1.46	1.2	3.1
391.85	6.10	1.52	4.1	0.4
404.43	8.71	1.52	4.8	0.0
414.15	7.01	1.22	3.1	-3.1
422.18	7.01	0.91	0.0	-3.8
440.29	8.71	0.15	-1.7	-4.2
455.68	6.10	0.00	-4.0	-1.0
471.09	5.79	-0.03	-4.0	-0.2

The first time in the table indicates the time when the motion becomes perceptible.

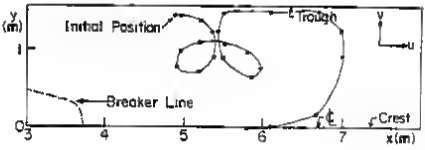

Teble C-125. Mean Current Measurements by Floating Disk Trejectories; Run No. 08/05, Wave Period = 1.9; Wavemaker Sterting Time = 12.8 s

Time (s)	x (m)	y (m)	U (cm/s)	V (cm/s)
103.96	5.06	1.34		
120.00	5.18	1.31	0.8	-0.2
132.42	5.27	1.22	0.7	-0.7
153.26	5.33	0.91	0.3	-1.5
166.52	5.18	0.73	-1.1	-1.4
181.82	4.88	0.67	-2.0	-0.4
193.66	4.66	0.76	-1.8	0.8
207.16	4.60	0.91	-0.5	1.1
224.56	4.91	1.25	1.8	1.9
234.46	5.21	1.37	3.1	1.2
242.35	5.49	1.37	3.5	0.0
252.22	5.79	1.37	3.1	0.0
265.19	6.10	1.28	2.4	-0.7
281.58	6.40	1.07	1.9	-1.3
316.43	6.40	0.30	0.0	-2.2
330.75	6.10	0.24	-2.1	-0.4
349.14	5.88	0.46	-1.2	1.2
359.10	5.67	0.76	-2.1	3.1
380.65	5.79	1.22	0.6	2.1
403.18	6.10	1.25	1.4	0.1
417.49	6.40	1.22	2.1	-0.2
435.82	6.68	1.07	1.5	-0.8
446.35	6.64	-0.91	-0.3	-1.4
462.98	6.61	0.61	-0.2	-1.8
482.77	6.45	0.30	-0.6	-1.5

The first time in the teble indicates the time when the motion becomes perceptible.

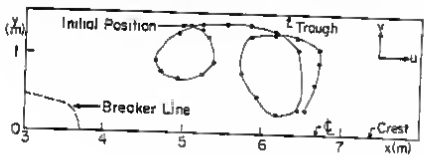

Table C-126. Mean Current Measurements by Floating Disk Trajectories. Run No. 09/01; Wave Period = 1.9· Wavemaker Starting Time = 15.7 s

Time (s)	x (m)	y (m)	U (cm/s)	V (cm/s)
84.23	4.69	1.52		
107.40	4.88	1.52	0.8	0.0
122.14	5.18	1.52	2.1	0.0
141.36	5.64	1.43	2.4	-0.5
153.79	5.79	1.22	1.2	-1.7
164.97	5.79	0.91	0.0	-2.7
182.45	5.64	0.55	-0.9	-2.1
196.08	5.33	0.50	-2.2	-0.3
205.92	5.03	0.70	-3.1	2.0
218.47	4.66	1.07	-2.9	2.9
222.49	4.57	1.22	-2.3	3.8
237.42	4.27	1.49	-2.0	1.8
260.97	3.96	1.52	-1.3	0.1

The first time in the table indicates the time when the motion becomes perceptible.

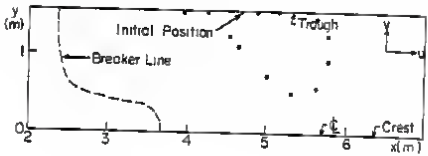

Table C-127. Mean Current Measurements by Floating Disk Trajectories; Run No. 09/02; Wave Period = 1.9; Wavemaker Starting Time - 15.7 s

Time (s)	x (m)	y (m)	U (cm/s)	V (cm/s)
82.00	4.57	1.52		
120.47	4.88	1.52	0.8	0.0
133.50	5.18	1.52	2.3	0.0
144.50	5.49	1.52	2.8	0.0
159.08	5.79	1.31	2.1	-1.5
177.36	5.85	0.98	0.3	-1.8
210.26	5.49	0.61	-1.1	-1.1
233.12	5.30	0.70	-0.8	0.4
259.79	5.18	0.91	-0.5	0.8

The first time in the table indicates the time when the motion becomes perceptible

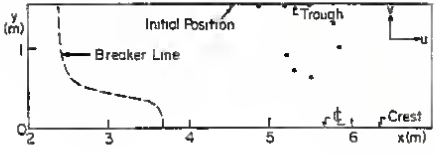

Table 128 Mean Current Measurements by Floating Disk Trajectories; Run No. 09/03; Wave Period = 1.9; Wavemaker Starting Time = 15.7 s

Time (s)	x (m)	y (m)	U (cm/s)	V (cm/s)
78.85	4.30	1.49		
118.40	4.42	1.52	0.3	0.1
138.04	4.57	1.52	0.8	0.0
152.52	4.88	1.52	2.1	0.0
167.69	5.49	1.52	4.0	0.0
182.38	5.94	1.37	3.1	-1.0
194.94	6.13	1.22	1.5	-1.2

The first time in the table indicates the time when the motion becomes perceptible.

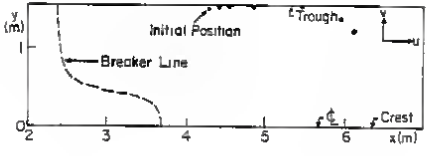

Table C-129. Mean Current Measurements by Floating Disk Trajectories; Run No. 09/04; Wave Period = 1.9, Wavemaker Starting Time - 15.7 s

Time (s)	x (m)	y (m)	U (cm/s)	V (cm/s)
85.84	4.69	1.34		
111.59	4.48	1.43	0.7	0.4
125.31	5.18	1.46	2.2	0.2
146.83	5.64	1.22	2.1	-1.1
161.00	5.64	0.91	0.0	-2.2
190.34	5.33	0.70	-1.0	-0.7
208.75	5.00	0.85	-1.8	0.8
224.98	4.79	1.22	-1.3	2.3

The first time in the table indicates the time when the motion becomes perceptible.

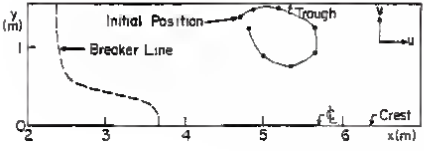

Table C-130. Mean Current Measurements by Floating Disk Trajectories; Run No. 09/05, Wave Period = 1.9; Wavemaker Starting Time - 15[illegible]7 s

Time (s)	x (m)	y (m)	U (cm/s)	V (cm/s)
82.85	4.51	1.34		
122.17	4.88	1.46	0.9	0.3
135.54	5.18	1.49	2.3	0.2
143.30	5.52	1.37	4.3	-1.6
157.54	5.73	1.22	1.5	-1.1
170.36	5.73	0.91	0.0	-2.4
189.44	5.49	0.61	-1.3	-1.6
212.60	5.03	0.79	-2.0	0.8
223.92	4.88	1.07	-1.3	2.4
237.47	4.72	1.37	-1.1	2.2

The first time in the table indicates the time when the motion becomes perceptible.

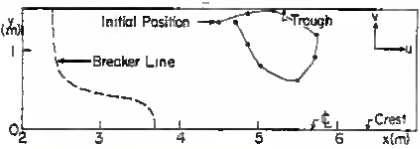

Table C-131. Mean Current Measurements by Floating Disk Trajectories; Run No. 09/06; Wave Period = 1.9; Wavemaker Starting Time = 15.7 s

Time (s)	x (m)	y (m)	U (cm/s)	V (cm/s)
82.25	4.30	1.34		
114.79	4.57	1.52	0.8	0.6
138.16	4.88	1.52	1.3	0.0
147.88	5.18	1.52	3.1	0.0
156.39	5.49	1.49	3.6	-1.4
170.88	5.79	1.22	2.1	-1.9
182.46	5.79	0.91	0.0	-2.6
204.39	5.49	0.61	-1.4	-1.4
230.18	5.30	0.76	-0.7	0.6
250.23	5.33	0.88	0.2	0.6
267.67	5.18	0.91	-0.9	0.2

The first time in the table indicates the time when the motion becomes perceptible.

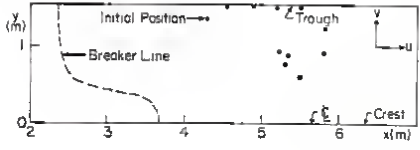

Table C-132. Mean Current Measurements by Floating Disk Trajectories; Run No. 09/07; Wave Period = 1.9; Wavemaker Starting Time = 15.7 s

Time (s)	x (m)	y (m)	U (cm/s)	V (cm/s)
78.50	4.21	1.16		
107.49	4.21	1.04	0.0	-0.4
120.00	4.24	1.10	0.2	0.5
126.55	4.27	1.22	0.5	1.9
133.33	4.30	1.37	0.4	2.2
153.77	4.42	1.52	0.6	0.7
170.98	4.72	1.52	1.8	0.0
182.78	5.18	1.52	3.8	0.0
197.15	5.78	1.52	4.2	0.0
214.35	6.40	1.37	3.5	-0.9

The first time in the table indicates the time when the motion becomes perceptible.

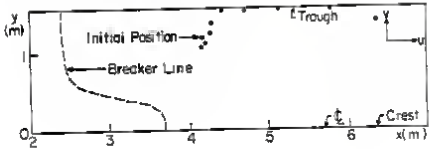

Table C-133. Mean Current Measurements by Floating Disk Trajectories; Run No. 10/01; Wave Period = 1.3; Wavemaker Starting Time - 8.1 s

Time (s)	x (m)	y (m)	U (cm/s)	V (cm/s)
32.84	3.54	1.46		
85.46	3.88	1.22	0.4	-0.7
78.58	3.72	1.07	0.5	-1.4
88.58	3.81	0.91	0.9	-1.5
110.10	3.72	0.61	-0.4	-1.3
119.50	3.54	0.30	-1.9	-3.2
123.88	3.28	0.18	-6.3	-2.8
127.77	2.87	0.06	-10.2	-3.1
129.84	2.62	-0.03	-11.8	-4.4

The first time in the table indicates the time when the motion becomes perceptible.

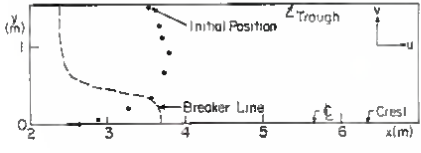

Table C-134. Mean Current Measurements by Floating Disk Trajectories; Run No. 10/02; Wave Period = 1.9; Wavemaker Starting Time = 8.1 s

Time (s)	x (m)	y (m)	U (cm/s)	V (cm/s)
33.80	3.44	1.37		
61.62	3.54	1.22	0.3	-0.5
76.85	3.66	1.07	0.8	-1.0
101.89	3.44	0.61	-0.9	-1.8
112.18	2.96	0.30	-4.7	-3.0
116.44	2.68	0.18	-6.4	-2.9
116.44	2.68	0.15	-6.2	-0.9

The first time in the table indicates the time when the motion becomes perceptible.

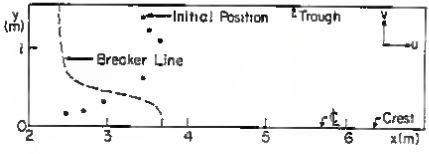

Table C-135. Mean Current Measurements by Floating Disk Trajectories, Run No. 10/03, Wave Period = 1.9; Wavemaker Starting Time = 8.1 s

Time (s)	x (m)	y (m)	U (cm/s)	V (cm/s)
33.42	3.69	1.34		
53.06	3.72	1.22	0.2	-0.6
69.34	3.72	1.04	0.0	-1.1
84.98	3.69	0.76	-0.2	-1.8
94.08	3.54	0.61	-1.7	-1.7
100.81	3.35	0.46	-2.7	-2.3
106.73	3.08	0.30	-4.6	-2.6
112.15	2.74	0.15	-6.2	-2.8
116.52	2.44	0.09	-7.0	-1.4

The first time in the table indicates the time when the motion becomes perceptible.

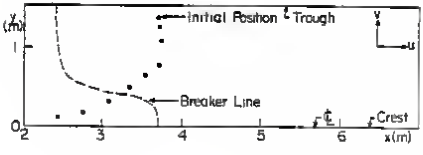

Table C-136. Mean Current Measurements by Floating Disk Trajectories, Run No. 10/04; Wave Period = 1.9; Wavemaker Starting Time = 8.1 s

Time (s)	x (m)	y (m)	U (cm/s)	V (cm/s)
30.61	3.63	1.31		
45.10	3.63	1.22	0.0	-0.6
75.22	3.63	0.85	0.0	-1.2
86.18	3.60	0.61	-0.3	-2.2
92.12	3.44	0.46	-2.6	-2.6
97.97	3.20	0.30	-4.2	-2.6
104.60	2.77	0.24	-6.4	-0.9
107.75	2.53	0.15	-7.7	-2.9

The first time in the table indicates the time when the motion becomes perceptible.

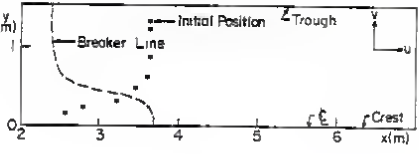

Table C-1.37. Mean Current Measurements by Floating Disk Trajectories; Run No. 10/05, Wave Period = 1.8; Wavemaker Starting Time = 8.1 s

Time (s)	x (m)	y (m)	u (cm/s)	v (cm/s)
32.57	3.51	1.31		
55.48	3.60	1.22	0.4	-0.4
71.70	3.66	1.07	0.4	-0.9
82.84	3.72	0.91	0.5	-1.4
96.22	3.66	0.67	-0.5	-1.8
102.18	3.54	0.52	-2.0	-2.6
108.90	3.35	0.40	-2.7	-1.8
114.02	3.02	0.27	-6.5	-2.4
118.84	2.65	0.15	-7.6	-2.5
121.16	2.44	0.09	-9.2	-2.6

The first time in the table indicates the time when the motion becomes perceptible.

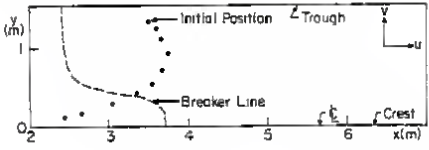

Table C-138. Mean Current Measurements by Floating Disk Trajectories; Run No. 11/01, Wave Period = 1.9; Wavemaker Starting Time = 15.5 s

Time (s)	x (m)	y (m)	U (cm/s)	V (cm/s)
32.28	3.28	1.37		
50.39	3.47	1.22	0.8	-0.6
73.32	3.54	1.07	0.4	-1.0
83.59	3.63	0.91	0.9	-1.5
92.46	3.57	0.73	-0.7	-2.1
106.88	3.26	0.30	-2.1	-3.0
112.25	2.87	0.15	-7.4	-2.8
116.28	2.56	0.09	-7.6	-1.5

The first time in the table indicates the time when the motion becomes perceptible.

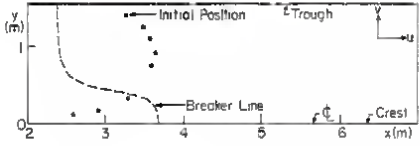

Table C-139. Mean Current Measurements by Floating Disk Trajectories; Run No. 11/02; Wave Period = 1.9; Wavemaker Starting Time = 15.5 s

Time (s)	x (m)	y (m)	U (cm/s)	V (cm/s)
33.65	2.83	1.37		
56.67	3.05	1.22	0.8	-0.7
67.75	3.14	1.07	0.8	-1.4
74.04	3.11	0.91	-0.5	-2.4
86.12	3.05	0.61	-0.5	-2.5
93.36	2.87	0.46	-2.5	-2.1
97.38	2.68	0.37	-4.5	-2.3
101.82	2.50	0.34	-4.1	-0.7

The first time in the table indicates the time when the motion becomes perceptible.

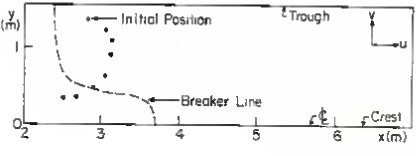

Table C-140. Mean Current Measurements by Floating Disk Trajectories; Run No. 11/03; Wave Period = 1.3. Wavemaker Starting Time = 15.5 s

Time (s)	x (m)	y (m)	U (cm/s)	V (cm/s)
31.93	3.17	1.28		
53.76	3.35	1.16	0.8	-0.6
65.80	3.41	1.07	0.5	-0.8
77.53	3.44	0.91	0.3	-1.3
92.91	3.35	0.67	-0.6	-1.6
98.52	3.20	0.49	-2.7	-3.3
105.49	2.90	0.34	-4.4	-2.2
109.54	2.82	0.27	-6.8	-1.5

The first time in the table indicates the time when the motion becomes perceptible.

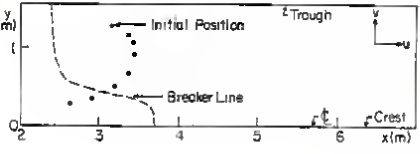

Table C-141. Mean Current Measurements by Floating Disk Trajectories, Run No. 11/04; Wave Period = 1.9; Wavemaker Starting Time = 15.5 s

Time (s)	x (m)	y (m)	U (cm/s)	V (cm/s)
34.00	3.05	1.25		
62.46	3.29	1.07	0.9	-0.6
74.16	3.35	0.91	0.5	-1.3
89.32	3.29	0.61	-0.4	-2.0
96.08	3.08	0.40	-3.2	-3.2
99.33	2.90	0.30	-5.6	-2.8
104.89	2.50	0.18	-7.1	-2.2

The first time in the table indicates the time when the motion becomes perceptible

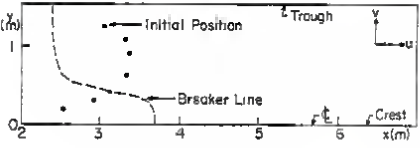

Table C-142. Mean Current Measurements by Floating Disk Trajectories, Run No. 12/01; Wave Period = 1.0; Wavemaker Starting Time - 11.0 s

Time (s)	x (m)	y (m)	U (cm/s)	V (cm/s)
36.28	3.11	1.52		
52.52	3.25	1.37	0.8	-0.9
68.23	3.51	1.22	1.6	-1.0
84.86	3.72	1.07	1.3	-0.9
96.57	3.78	0.91	0.5	-1.3

The first time in the table indicates the time when the motion becomes perceptible.

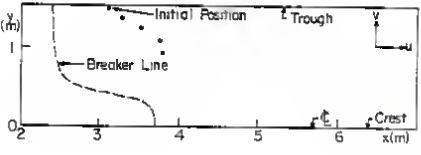

Table C-143. Mean Current Measurements by Floating Disk Trajectories; Run No. 12/02; Wave Period = 1.9; Wavemaker Starting Time = 11.0 s

Time (s)	x (m)	y (m)	U (cm/s)	V (cm/s)
32.65	2.96	1.22		
47.58	3.08	1.07	0.8	-1.0
56.55	3.11	0.91	0.3	-1.7
64.18	3.14	0.76	0.4	-2.0
69.93	3.05	0.61	-1.6	-2.7
76.42	2.96	0.46	-1.4	-2.3
80.18	2.83	0.40	-3.2	-1.6
84.27	2.65	0.34	-4.5	-1.5
86.62	2.51	0.30	-5.8	-1.3
89.95	2.36	0.30	-4.6	0.0

The first time in the table indicates the time when the motion becomes perceptible.

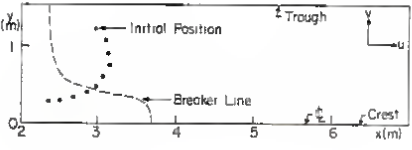

Table C-144. Mean Current Measurements by Floating Disk Trajectories; Run No. 12/03; Wave Period - 1.9; Wavemaker Starting Time - 11.0 s

Time (s)	x (m)	y (m)	U (cm/s)	V (cm/s)
31.69	3.05	0.38		
37.69	3.11	0.76	1.0	-2.0
46.08	3.08	0.61	-0.4	-1.8
51.78	2.99	0.46	-1.6	-2.7
57.89	2.80	0.30	-3.0	-2.5
61.88	2.59	0.26	-5.3	-1.1
65.28	2.38	0.24	-6.3	-0.4

The first time in the table indicates the time when the motion becomes perceptible.

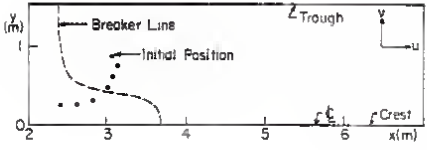

Table C-145. Mean Current Measurements by Floating Disk Trajectories; Run No. 12/04; Wave Period = 1.9, Wavemaker Starting Time = 11.0 s

Time (s)	x (m)	y (m)	U (cm/s)	V (cm/s)
22.89	2.99	0.62		
34.18	2.99	0.46	0.0	-1.5
37.93	2.87	0.34	-3.3	-3.3
40.06	2.74	0.27	-5.7	-2.8
42.42	2.50	0.18	-10.4	-3.9

The first time in the table indicates the time when the motion becomes perceptible.

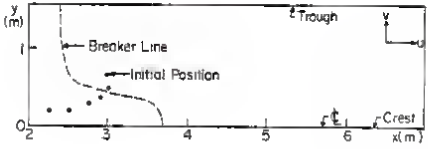

Table C-146. Mean Current Measurements by Floating Disk Trajectories; Run No. 12/05; Wave Period = 1.9; Wavemaker Starting Time = 11.0 s

Time (s)	x (m)	y (m)	U (cm/s)	V (cm/s)
22.80	2.80	0.12		
25.71	2.71	0.12	-3.1	0.0
28.98	2.65	0.09	-4.8	-2.4
29.15	2.53	0.09	-5.6	0.0
31.28	2.41	0.06	-5.7	-1.4
33.51	2.28	0.03	-6.8	-1.4

The first time in the table indicates the time when the motion becomes perceptible.

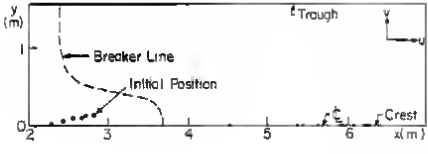

Table C-147. Mean Current Measurements by Dye Releases, Period = 1.5 s

Location		Mean Velocity	
x (m)	y (m)	U (cm/s)	V (cm/s)
1.45	0.00	-3.5	-1.5
1.60	0.15	-7.0	1.5
1.90	0.15	-10.0	4.0
1.60	0.31	-6.0	7.0
1.75	0.46	-7.0	3.0
1.45	0.91	0.0	7.0
1.60	0.91	1.0	3.0
1.60	1.22	5.0	1.0

Table C-14*. Mean Current Measurements by Dye Releases; Period ~ 1.5 s

Location		Mean Velocity	
x (m)	y (m)	U (cm/s)	V (cm/s)
1.60	0.00	-6.0	-1.5
1.60	0.15	-6.0	0.0
1.45	0.31	-3.0	1.0
1.45	0.61	0.0	4.0
1.60	1.07	1.0	3.5
1.60	1.22	4.0	1.5

APPENDIX D
"VORTICITY METER" THEORETICAL AND EXPERIMENTAL CONSIDERATIONS

Introduction

In order to understand the response of the mill better, a set of experiments was carried out in a two-dimensional wave tank with the axis of the mill in a horizontal orientation. Each test consisted of a different combination of wave height and wave period for the same depth and two different positions of the mill, one close to the water surface and the other close to the bottom of the wave tank. The rotation of the mill and the actual waves were recorded on video tape. This information was read later on a television screen. The observations in the wave tank indicated that the mill starts its rotation when some combination of wave height and period occurs. In any case the total motion is characterized by the superposition of an oscillatory component, of small amplitude, and a net rotation with the top of the mill moving in the direction of wave propagation. Before presenting the analysis of the data three possible scenarios occur:

1. The wave field is not strong enough to drive any net rotation.

2. The wave field is strong enough to drive some rotation which balances the gravitational torque of the mill (due to imperfect balance). In this case the mean angle of rotation becomes constant at large times.

3. The drag due to the wave field is enough to drive a continuous rotation on the mill. The angle of rotation tends to infinity as time tends to infinity.

The imbalance of the mill is due to a slight asymmetrical distribution of its weight that produces a natural moment which requires a minimum wave-induced torque in order to force any continuous rotation. The following experiment was carried out in order to determine the natural moment of the mill.

Net Rotation of the Mill under a Static Load: An Experiment

This experiment was carried out in order to determine the imbalance of the mill. In other words, what is the torque needed to rotate the mill some angle, say θ_E. The tests were performed inside a small glass water tank where the mill was introduced and supported from its axis by a metal rod as indicated in Figure D-1. In order to illustrate the procedure consider Figure D-2 which shows the mill with its unknown net weight (F) pointing downwards, the different vanes are indicated by F_n where n ranges from 2 to 8. The procedure was as follows:

1. A known weight W_s was placed at the extreme of one of the vanes, F_8 for instance.

2. The mill was freed and the position of equilibrium changed to some other location. The net displacement (between the original and the new location) was measured in degrees and called θ_E as shown in Figure D-3.

The weight W_s was located at some other vane and the procedure was repeated again. The experiments were performed with three different weights Ws1 = 32.16 dynes, We2 = 64.33 dynes and We3 = 96.50 dynes and each test

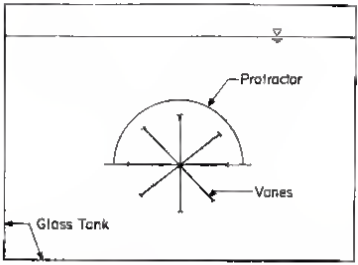

FRONT VIEW

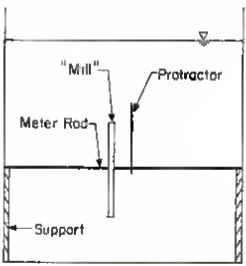

LATERAL VIEW

Figure D-1. Sketch of the Mill Inside the Glass Water Tank

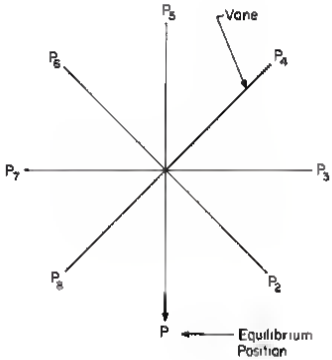

Figure D-2. Mill in Its Natural (No Extra Load) Position of Equilibrium; P Represents the Net Weight of the Mill

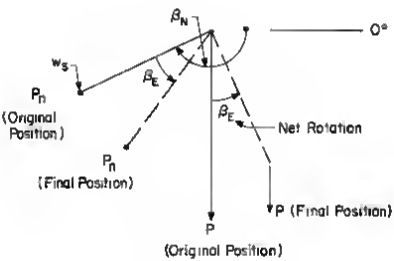

Figure D-3. Mill in Its Equilibrium Position When Loaded with a Weight W_s

consisted of a combination of weight and location. Table D-1 summarizes the results of each experiment where P_n was the original position of the load Ws. As an example, consider the first case where a weight We1 was located on vane P8. After being freed the mill rotated 20 degrees so the new position of the net weight P was 70 degrees.

Table D-1. Net Rotation of the Mill under a Static Load

Test	Load	Original Position of the Load (P_n)	New Position of P (degrees)	Net Rotation (θ_E) (degrees)
1	We1	P8	70	20
2	We1	P7	58	32
3	We1	P6	52	38
4	We2	P8	60	30
5	We2	P7	36	54
6	We2	P6	7	83
7	We3	P8	56	34
8	We3	P7	30	60
9	We3	P6	342	108

NOTE: The original position of P was at 90 degrees.

In equilibrium the sum of the moments with respect to mill axis (line P5-P) must be zero so

$$MW_S = MP \qquad \text{(D-1)}$$

where

$$MW_S = W_e R \sin [\theta_N - (\theta_S + 90)] \qquad \text{(D-2)}$$

$$MP = P R \sin \theta_E = M_O \sin \theta_Z \qquad \text{(D-3)}$$

and then

$$\left(\frac{W_s}{P}\right)_N = \frac{\sin \beta_E}{\sin\left[\beta_N - (\beta_E + 90)\right]}$$

where the angle β_N corresponded to the vane Pn at the position of equilibrium. In this way it was possible to calculate the ratios of Ws and P and, therefore, the potential imbalance moment, Mo, for all the cases. The results are presented in Table D-2.

Table D-2. Values of Ws/Pe and Mo

Test (No.)	Load (Ws)	Ws/Pe	Mo (dyn.cm)
1	Ws1	.556	248.72
2	Ws1	.572	241.76
3	Ws1	.647	213.74
4	Ws2	1.065	259.70
5	Ws2	1.125	245.85
6	Ws2	1.114	248.27
7	Ws3	1.375	301.72
8	Ws3	1.347	307.99
9	Ws3	1.545	268.52

From Table D-2 an average value of Mo = 259.59 dyn.cm resulted. Therefore, in order to induce a continuous rotation an applied torque larger than Mo is needed.

Some Dynamical Considerations about the Mill

In order to gain some insight about the dynamical behavior of the mill a limited number of tests was conducted. The objective was to determine the angle of rotation versus time as the mill was recovering its natural position of equilibrium after being perturbated. In other words, the position of equilibrium characterized by P at 90 degrees was altered by an angle equal to 80 degrees and the mill was freed. During its trajectory towards equilibrium the local angle β_ℓ and the corresponding time were measured. Table D-3 summarizes the results.

Table D-3. Angle of Rotation β_ℓ of the Mill Versus Time as it Recovers Its Natural Position of Equilibrium

Angle of Rotation from the Perturbed Position (β_ℓ) (Degrees)	Time Taken by the Mill from Perturbed Position (s) (*)
10	.84
20	1.25
30	1.50
40	1.80
50	2.37
60	3.01
70	3.43
80	4.31

(*) Averaged over three measurements.

NOTE: The angle where all measurement started was 10 degrees; thus the angle of 80 degrees in this table corresponds to the equilibrium position. Figure D-4 illustrates the results.

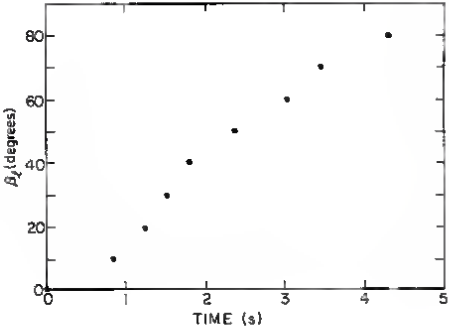

Figure D-4 Angle of Rotation, β_g, Versus Time as the Mill Recovers Its Position of Equilibrium

Estimation of the Angle of Rotation of the Mill under a Wave Field

A limited number of tests was carried out in order to calculate the rotation of the mill under different wave conditions. The experiments were performed at two different depths of measurement, wave heights and periods. The angle of rotation was recorded on video tape. As an example, Test No. 2 was performed (location of the mill) 15 cm from the water surface, the steady state wave height was 0.6 cm, the wave period 1.3 s and no continuous rotation was observed. Table D-4 shows the results.

The angle of rotation versus time for each of these experiments are presented in Tables D-6, D-7 and D-8. Figure D-6 shows the angle of rotation of the mill versus time for tests No. 3 and No. 13. It can be seen that for the first 180 degrees of rotation the natural torque of the mill opposes the wave-induced torque and for the next 180 degrees of rotation it works in favor of the wave-induce torque increasing the angular velocity, represented by the slope of the curves.

Table D-4. Angle of Rotation of the Mill, θ, under a Wave Field, Water Depth = 48 cm

Test No.	Depth of Measurement (cm)	Wave Height (cm)	Period (s)	Angle of Rotation (θ) (degrees)
1	-15	4.0	1.3	65 (*)
2	-15	.6	1.3	0
3	-15	5.5	1.0	-- (**)
4	-15	.9	2.0	0
5	-15	1.4	2.0	3
6	-15	1.7	2.0	6
7	-15	2.1	2.0	10
8	-15	2.3	2.0	13
9	-15	3.1	2.0	20
10	-15	4.9	2.0	-- (**)
11	-36	5.0	2.0	40
12	-36	5.6	1.5	40
13	-36	12.0	1.1	-- (**)

(*) For illustration purposes the angle of rotation versus time is presented in Table D-5 and Figure D-5 shows the results in graphical form.

(**) In this case the angle of rotation does not reach a constant value rather tends to infinity as time tends to infinity.

Table D-5. Angle of Rotation of the Mill, θ_m, Versus Time, Test No. 1

Time (s)	Angle of Rotation (θ) (degrees)
0.0	0
2.0	5
3.6	10
8.9	25
11.5	35
13.2	40
15.4	45
18.7	50
22.0	55
30.0	55
39.0	60
53.0	65
79	65

Table D-6. Angle of Rotation of the Mill, θ_m, Versus Time, Test No. 3

Time (s)	Angle of Rotation (θ) (degrees)
0.0	0
1.0	5
1.9	8
3.0	30
3.9	42
5.0	50
6.1	70
7.9	90
15.8	180
22.0	360

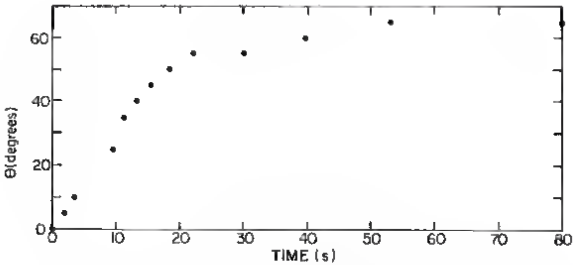

Figure D-5. Angle of Rotation of the Mill, θ, Versus Time under the Effect of a Wave Field; Test No. 1; Wave Height = 4.0 cm; Period = 1.3 s; Depth = 48.0 cm; Depth of Measure = -15.0 cm

Table D-7. Angle of Rotation of the Mill, θ_m, Versus Time, Test No. 10

Time (s)	Angle of Rotation (θ) (degrees)
0.0	0
4.5	45
9.5	90
16.1	140

Table D-8. Angle of Rotation of the Mill, θ_m, Versus Time, Test No. 13

Time (s)	Angle of Rotation (θ) (degrees)
0.0	0
3.0	20
4.7	38
5.9	60
7.2	80
8.3	90
15.2	180
21.6	360

For those cases in Table D-4 in which a continuous rotation was not observed, the limited rotation was in static equilibrium with the wave-induced kinematics. In order to compute the wave-induced torque for those cases, the known natural moment of the mill was used. As an example, consider Test No. 1. The mill rotated 65 degrees before reaching equilibrium with the wave field, therefore the averaged wave-induced torque is

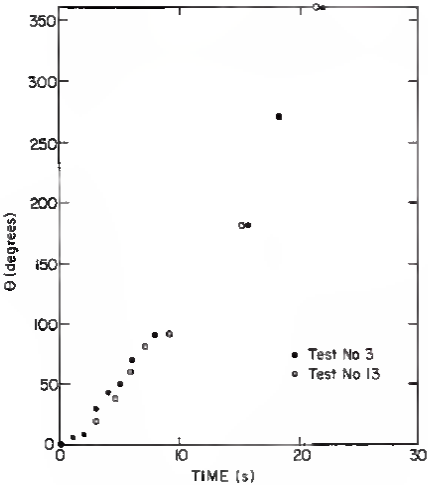

Figure D-6. Angle of Rotation of the Mill, θ, Versus Time under the Effect of a Wave Field; Test No. 3; Wave Height = 5.5 cm; Period = 1.0 s; Depth = 48.0 cm; Depth of Measure = -15.0 cm, Test No. 13; Wave Height = 12.0 cm, Period = 1.1 s, Depth = 48.0 cm; Depth of Measure = -36.0 cm

$$T_g = Mo \sin \theta = (259.59 \text{ dynes.cm}) \sin (65)$$
$$= 235.27 \text{ dynes.cm}$$

Table D-9 summarizes the results.

Table D-9. Wave-Induced Torque for Cases Where No Continuous Rotation of the Mill Was Observed

Test No.	Wave-Induced Torque (dynes.cm)
1	239.59
2	.00
4	.00
5	13.59
6	27.13
7	45.06
8	58.40
9	88.79
11	166.86
12	166.86

The experiments have established some static and dynamical characteristics of the mill. The potential imbalance moment Mo (due to the design) was established, therefore, the minimum wave-applied torque necessary to induce a continuous rotation was calculated. The measurements of the angle of rotation under a wave field permitted to estimation the wave-induced torque for the particular set of tests where the mill was in static equilibrium with the wave field.

The next section will present an analytical treatment of the wave-induced torque based on the assumption that

the rotation of the mill is due to the wave orbital velocities-induced drag on the vanes of the mill.

Theoretical Considerations

Introduction

In this section the wave-induced forces on the mill are discussed and a theoretical approach is described to predict the motion of the mill if the wave characteristics are known. The wave-induced torque due to gradients of the wave orbital velocities over the vanes of the mill is examined. Figure D-7 shows the position of the mill inside the wave tank and the coordinate system adopted.

Wave Orbital Velocities-Induced Torque

The instantaneous net drag force (Fdn) is assumed to be generated by the difference in the instantaneous drag forces induced by the wave orbital velocities over the vanes of the mill (Figure D-8) expressed in the following differential form

$$d(Fdn) = d(Fun) - d(Fwn) \qquad \text{(D-5)}$$

where

$$\begin{aligned} d(Fun) &= d(Fu_+) - d(Fu_-) \\ d(Fwn) &= d(Fw_+) - d(Fw_-) \end{aligned} \qquad \text{(D-6)}$$

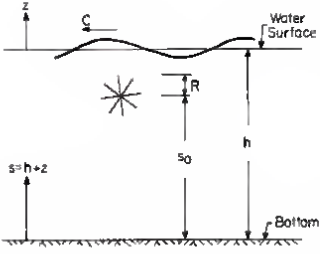

Figure D-7. Position on the Mill Inside the Wave Tank and Coordinate System Adopted

Figure D-8. Wave Orbital Velocities and Drag Forces Applied on the Mill

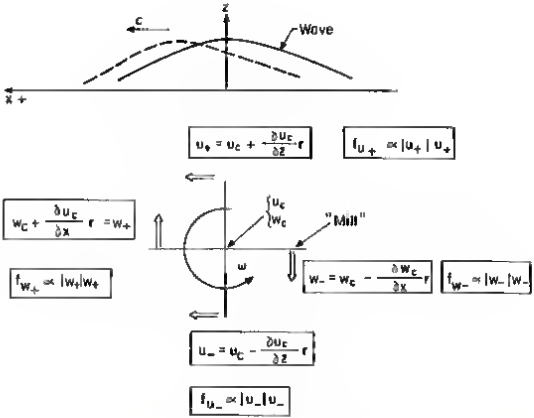
c
z
Wave
x +
$u_+ = u_c + \frac{\partial u_c}{\partial z} r$
$f_{u_+} \propto |u_+| u_+$
$w_c + \frac{\partial u_c}{\partial x} r = w_+$
$f_{w_+} \propto |w_+| w_+$
u_c
w_c
"Mill"
ω
$w_- = w_c - \frac{\partial w_c}{\partial x} r$
$f_{w_-} \propto |w_-| w_-$
$u_- = u_c - \frac{\partial u_c}{\partial z} r$
$f_{u_-} \propto |u_-| u_-$

(Fu_+, Fu_-) represent the x-components of the drag force on the upper and lower vanes, respectively, and (Fw_+, Fw_-) represent the z-components of the drag force on the left and right side vanes, respectively. The differential form of the drag force can be written

$$
\begin{aligned}
d(Fu_+) &= \frac{C_D \rho b}{2} dr\ u_+ \ |u_+| \\
d(Fu_-) &= \frac{C_D \rho b}{2} dr\ u_- \ |u_-| \\
d(Fw_+) &= \frac{C_D \rho b}{2} dr\ w_+ \ |w_+| \\
d(Fw_-) & \quad \frac{C_D \rho b}{2} dr\ w_- \ |w_-|
\end{aligned}
\tag{D-7}
$$

where C_D is the drag coefficient, ρ the water density, b the width of the vane and dr represents a differntial length along the vane, (u_+, u_-) the local horizontal velocities on the upper and the lower vanes and (w_+, w_-) the local vertical velocities on the left and the right vanes under the assumption that the mill does not rotate. The instantaneous torque (Tq), in its differential form, is defined

$$d(T_q) = r\ d(F_{\theta n}) \tag{D-8}$$

or

$$
\begin{aligned}
d(T_q) = \frac{C_D \rho b}{2} r\ dr\ (& u_+ \ |u_+| - u_- \ |u_-| \\
& + w_- \ |w_-| - w_+ \ |w_+|)
\end{aligned}
\tag{D-9}
$$

the velocities can be expressed

$$
\begin{aligned}
u_+ &= u_c + \frac{\partial u_c}{\partial s} r \\
u_- &= u_c - \frac{\partial u_c}{\partial s} r \\
w_+ &= w_c + \frac{\partial u_c}{\partial x} r \\
w_- &= w_c - \frac{\partial u_c}{\partial x} r
\end{aligned}
\tag{D-10}
$$

where (u_c, w_c) represent the velocity component at $s = s_o$. Substituting the above in Equation (D-9), integrating in r and time averaging over one wave period the net torque becomes

$$
\begin{aligned}
T_q = \frac{C_D \rho b}{2T} \int_0^T \int_0^R r \, [& (u_c + \frac{\partial u_c}{\partial s} r) \, |u_c + \frac{\partial u_c}{\partial s} r| \\
& - (u_c - \frac{\partial u_c}{\partial s} r) \, |u_c - \frac{\partial u_c}{\partial s} r| \\
& + (w_c + \frac{\partial w_c}{\partial x} r) \, |w_c + \frac{\partial w_c}{\partial x} r| \\
& - (w_c - \frac{\partial w_c}{\partial x} r) \, |w_c + \frac{\partial w_c}{\partial x} r| \,] \, dr \, dt
\end{aligned}
\tag{D-11}
$$

Before proceeding further, consider as a simplified example, the instantaneous applied torque under the crest of the wave. The integrand of Equation (D-11) can be written

$$
4 \, u_c \frac{\partial u_c}{\partial x} r^2 \tag{D-12}
$$

and the instantaneous torque becomes

$$T_q = \frac{2C_D \sigma b}{3} R^3 u_c \frac{\partial u_c}{\partial a} \tag{D-13}$$

Based on linear wave theory the wave orbital velocities are

$$\begin{aligned} u_c &= U_1 \text{ ch } (k\, a_o) \cos (kx - \sigma t) \\ w_c &= W_1 \text{ sh } (k\, a_o) \sin (kx - \sigma t) \end{aligned} \tag{D-14}$$

where

$$U_1 = W_1 = \frac{g \pi k}{2\sigma \text{ ch } (kh)} \tag{D-15}$$

and the gradients

$$\begin{aligned} \frac{\partial u_c}{\partial w} &= U_1\, k \text{ sh } (k\, s_o) \cos (kx - \sigma t) \\ \frac{\partial u_c}{\partial x} &= W_1\, k \text{ ch } (k\, a_o) \sin (kx - \sigma t) \end{aligned} \tag{D-16}$$

Substituting in Equation (D-12) and considering Equation (D-15) the instantaneous torque under the crest of the wave becomes

$$T_q = \frac{2C_D \sigma b}{3} R^3 \sigma^2 g \left(\frac{H}{L}\right)^2 \frac{\text{ch } (2k\, s_o)}{\text{ch } (2k\, s)} \tag{D-17}$$

where the dispersion relationship

$$\sigma^2 = gk \text{ th } (k\, h) \tag{D-18}$$

has been considered. Figure D-9 displays the nondimensional wave-applied torque under the crest of the wave (assuming that the mill does not rotate) for different values of h/L.

Consider now the net applied torque (averaged over one wave period). From Equations (D-14) and (D-16) the integrand in Equation (D-11) results proportional to

$$\cos(kx - \sigma t)\,|\cos(kx - \sigma t)| + \sin(kx - \sigma t)\,|\sin(kx - \sigma t)| \tag{D-18}$$

which is identically equal to zero when averaged over one wave period. Therefore, linear waves do not contribute to the net torque and only induce an oscillatory torque which has a value under the crest of the wave given by Equation (D-17).

Consider now, the effect of the nonlinearities on the net torque assuming a wave field represented by a second order Stokes wave. Under this wave the orbital velocities are

$$u_o = U_1 \operatorname{ch}(k s_o) \cos(kx - \sigma t) + U_2 \operatorname{ch}(2k s_o) \cos 2(kx - \sigma t)$$

$$w_o = W_1 \operatorname{sh}(k s_o) \sin(kx - \sigma t) + W_2 \operatorname{sh}(2k s_o) \sin 2(kx - \sigma t)$$

where

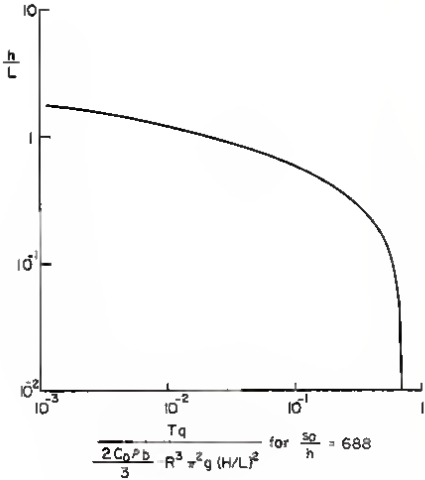

Figure D-9. Nondimensional Wave-Applied Torque on the Mill under the Crest of the Wave as a Function of (h/L), for s_o/h = 0.688

$$U_2 = W_2 = \frac{3}{16} \frac{H^2 k}{sh^4 (kh)} \tag{D-21}$$

and the gradients are

$$\begin{aligned} \frac{\partial u_c}{\partial x} &= U_1 k \, sh (k z_o) \cos (kx - \sigma t) \\ &\quad + U_2 2k \, sh (2k z_o) \cos 2(kx - \sigma t) \\ \frac{\partial w_c}{\partial x} &= W_1 k \, sh (k z_o) \cos (kx - \sigma t) \\ &\quad + W_2 2k \, sh (k z_o) \cos (kx - \sigma t) \end{aligned} \tag{D-22}$$

Before Equation (D-11) is integrated consider the following approximation. Suppose that the velocity field is known at the extremes of the vanes. The horizontal and vertical velocities at the center of the mill can be expressed as

$$\begin{aligned} u_c &= \frac{(u_1 + u_2)}{2} \\ w_c &= \frac{(w_1 + w_2)}{2} \end{aligned} \tag{D-23}$$

where u_1 and u_2 represent the horizontal velocities at the top of the upper vane and at the bottom of the lower vane, respectively, and w_1 and w_2 represent the vertical velocities at the extreme of the left vane and at the extreme of the right vane, respectively, and their gradients can be expressed as

$$\frac{\partial u_c}{\partial \theta} = \frac{(u_1 - u_2)}{2R}$$

$$\frac{\partial w_c}{\partial x} = \frac{(w_1 - w_2)}{2R} \tag{D-24}$$

Replacing Equations (D-23) and (D-24) in Equation (D-11) for the terms of the integrand become

$$\left(u_c + \frac{\partial u_c}{\partial \theta} r\right) \left| u_c + \frac{\partial u_c}{\partial \theta} r \right| \sim \left(\frac{3u_1 + u_2}{4}\right)^2 \cdot$$

$$\text{sign}\left(\frac{3u_1 + u_2}{4}\right) = \text{I}$$

$$\left(u_c - \frac{\partial u_c}{\partial \theta} r\right) \left| u_c - \frac{\partial u_c}{\partial \theta} r \right| \sim \left(\frac{u_1 + 3u_2}{4}\right)^2 \cdot$$

$$\text{sign}\left(\frac{u_1 + 3u_2}{4}\right) = \text{II}$$

$$\left(w_c + \frac{\partial w_c}{\partial x} r\right) \left| w_c + \frac{\partial w_c}{\partial x} r \right| \sim \left(\frac{3w_1 + w_2}{4}\right)^2 \cdot \tag{D-25}$$

$$\text{sign}\left(\frac{3w_1 + w_2}{4}\right) = \text{III}$$

$$\left(w_c - \frac{\partial w_c}{\partial x} r\right) \left| w_c - \frac{\partial w_c}{\partial x} r \right| \sim \left(\frac{w_1 + 3w_2}{4}\right)^2 \cdot$$

$$\text{sign}\left(\frac{w_1 + 3w_2}{4}\right) = \text{IV}$$

which are only a function of time so, integrating in r Equation (D-11) results

$$\overline{T_q} = \frac{C_D \rho b}{2} \frac{R^2}{2} \int_0^T (\text{I} - \text{II} + \text{III} - \text{IV})\, dt \tag{D-26}$$

As a numerical example consider Test No. 13 shown in Table D-4. The wave characteristics were

wave height (H)	:	12.0 cm
wave period (T)	:	1.1 s
water depth (h)	:	48.0 cm
wave length (L)	:	150.5 cm
depth of measure (zm)	:	-36.0 cm
H/L	:	.0797
h/L	:	.3190

and the other parameters used in the calculations were

drag coefficient (C_D)	:	1.0
water density (ρ)	:	1.0 gram/cm
width of the vane (b)	:	.8 cm
length of the vane (R)	:	4.3 cm

The resulting maximum velocities were

u_1	:	14.2 cm/s
u_2	:	12.0 cm/s
w_1	:	6.0 cm/s
w_2	:	6.0 cm/s

the strength of the nonlinearities can be expressed by the ratio between the velocity component amplitude of the linear components to those of second order Stokes wave

$$\frac{U_1 \text{ ch } (k\, z_o)}{U_2 \text{ ch } (2k\, z_o)} = 14.2$$

$$\frac{W_1 \text{ sh } (k\, z_o)}{W_2 \text{ sh } (k\, z_o)} = 5.0$$

Figure D-10 shows the velocity components as a function of time. To calculate the integral, the fourth order Simpson's rule was applied. The results are summarized below

net torque on the upper vane :	1.47 dyn.cm
net torque on the lower vane :	1.04 dyn.cm
net torque on the left vane :	.0011 dyn.cm
net torque on the right vane :	-.0011 dyn.cm
net total torque	.434 dyn.cm

The net torque obtained is two orders of magnitude smaller than the minimum torque needed to induce a continuous rotation. As a consequence, based on this analysis it is not possible to explain the rotation of the mill under the wave field. However, since the mill senses gradients in the wave height, the following considerations are necessary. before a broken wave arrives to the place where the mill is located, the wave height gradient (in the y-direction) is negative, so larger wave heights are on the crest of the "bar" due to refraction, inducing a clockwise rotation (negative vorticity). When waves break the wave height gradient becomes positive because the wave height, inside the breaker zone, is proportional to the local water

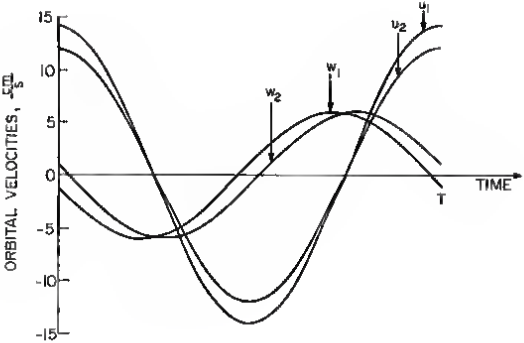

Figure D-10. Wave Orbital Velocities at the Extremes of the Waves Versus Time

depth, consequently induces a positive rotation. Measurements of the angle of rotation of the mill indicate negative values. Therefore, it is clear that the wave-induced vorticity overcomes the extraneous effect introduced by the gradient of the wave height.

BIBLIOGRAPHY

Borecki, D.S. 1982. Distribution of Wave-Induced Momentum Fluxes Over Depth and Application within the Surf Zone. Doctoral Dissertation, University of Delaware.

Bowen, A.J. 1969a. Rip Currents 1. Journal of Geophysical Research 74:5467-5478.

Bowen, A.J. 1969b. Rip Currents 2. Journal of Geophysical Research 74:5479-5490.

Bowen, A.J. 1967. Rip Currents. Doctoral Dissertation, University of California, San Diego.

Dally, W.R., Dean, R.G., and Dalrymple, R.A. 1985. Wave Height Variation Across Beaches of Arbitrary Profile. Journal of Geophysical Research 90:11917-11927.

Ebersole, B.A., and Dalrymple, R.A. 1979. A Numberical Model for Nearshore Circulation Including Convective Accelerations and Lateral Mixing. Technical Report No. 4. Ocean Engineering Report No. 21, University of Delaware.

Komar, P.D. 1971. Nearshore Circulation Cells and the Formation of Giant WSPS. Bulletin of the Geology Society of America, pp. 2643-2650.

Longuet-Higgins, M.S. 1970. Longshore Currents Generated by Obliquely Incident Sea Waves, 1. Journal of Geophysical Research 75:6778-6789.

Longuet-Higgins, M.S., and Stewart, R.W. 1962. Radiation Stress and Mass Transport in Gravity Waves. Journal of Fluid Mechanics 13:481-504.

Longuet-Higgins, M.S., and Stewart, R.W. 1964. Radiation Stress in Water Waves: A Physical Discussion, with Applications. Deep Sea Research 11:529-562.

Mei, C.C., and Liu, P.L.F. 1977. Effect of Topography on the Circulation in and Near the Surf Zone. Linear Theory. Estuarine and Coastal Marine Science 5:25-37.

Niedoroda, A.W. 1968. Preliminary Study of Transverse Bars. Master's Thesis, Florida State University, Tallahassee.

Niedoroda, A.W. 1972. The Generation of Currents Associated with Transverse Bars. Doctoral Dissertation, Florida State University, Tallahassee.

Noda, E.E. 1974. Wave-Induced Nearshore Circulation. Journal of Geophysical Research 79:4097-4106.

Phillips, O.M. 1966. Dynamics of the Upper Ocean. Cambridge University Press, Cambridge, 261 pp.

Sonu, C.J. 1972. Field Observation of Nearshore Circulation and Meandering Currents. Journal of Geophysical Research 77:3232-3247.

Walker, J.R. 1974. Wave Transformations over a Sloping Bottom and over a Three-Dimensional Shoal. Doctoral Dissertation, University of Hawaii.

Whalin, R.W. 1971. The Limit of Applicability of Linear Wave Refraction Theory in a Convergence Zone. U.S. Army Engineer Waterways Experiment Station. Research Report H-71-3. Vicksburg, Mississippi.

BIOGRAPHICAL SKETCH

Sergio Alejandro Schmidt was born October 25, 1949, in Argentina. He is married and lives at Salguero 1921, Capital Federal (1425), Buenos Aires, Argentina.

Mr. Schmidt was Assistant Professor in Oceanography at the University of La Plata. In the Argentine Navy (Naval Hydrographic Service), he specialized in research in the field of coastal engineering. He received his degree in physical oceanography from Buenos Aires Institute of Technology. He spent several years in the Argentine Navy and he was awarded a National Council of Scientific and Technical Sciences postgraduate fellowship at the University of Delaware. Mr. Schmidt was visiting Professor at the Naval Academy of Colombia, and he is author of several coastal engineering publications.

I certify that I have read this study and that in my opinion it conforms to acceptable standards of scholarly presentation and is fully adequate, in scope and quality, as a dissertation for the degree of Doctor of Philosophy.

Robert G. Dean, Chairman
Graduate Research Professor of
Engineering Sciences and Coastal and
Oceanographic Engineering

I certify that I have read this study and that in my opinion it conforms to acceptable standards of scholarly presentation and is fully adequate, in scope and quality, as a dissertation for the degree of Doctor of Philosophy.

Thomas T. Bowman
Associate Professor of Mathematics

I certify that I have read this study and that in my opinion it conforms to acceptable standards of scholarly presentation and is fully adequate, in scope and quality, as a dissertation for the degree of Doctor of Philosophy.

Joseph L. Hammack
Professor of Engineering Sciences

I certify that I have read this study and that in my opinion it conforms to acceptable standards of scholarly presentation and is fully adequate, in scope and quality, as a dissertation for the degree of Doctor of Philosophy.

Ulrich H. Kurzweg
Professor of Engineering Sciences

I certify that I have read this study and that in my opinion it conforms to acceptable standards of scholarly presentation and is fully adequate, in scope and quality, as a dissertation for the degree of Doctor of Philosophy.

Hsiang Wang
Professor of Coastal and
Oceanographic Engineering

This dissertation was submitted to the Graduate Faculty of the College of Engineering and to the Graduate School and was accepted as partial fulfillment of the requirements for the degree of Doctor of Philosophy.

December 1986

Dean, College of Engineering

Dean, Graduate School